National Library
of Canada

Acquisitions and
Bibliographic Services Branch

395 Wellington Street
Ottawa, Ontario
K1A 0N4

Bibliothèque nationale
du Canada

Direction des acquisitions et
des services bibliographiques

395, rue Wellington
Ottawa (Ontario)
K1A 0N4

Your file Votre référence

Our file Notre référence

NOTICE

The quality of this microform is heavily dependent upon the quality of the original thesis submitted for microfilming. Every effort has been made to ensure the highest quality of reproduction possibie.

If pages are missing, contact the university which granted the degree.

Some pages may have indistinct print especially if the original pages were typed with a poor typewriter ribbon or if the university sent us an inferior photocopy.

AVIS

La qualité de cette microforme dépend grandement de la qualité de la thèse soumise au microfilmage. Nous avons tout fait pour assurer une qualité supérieure de reproduction.

S'il manque des pages, veuillez communiquer avec l'université qui a conféré le grade.

La qualité d'impression de certaines pages peut laisser à désirer, surtout si les pages originales ont été dactylographiées à l'aide d'un ruban usé ou si l'université nous a fait parvenir une photocopie de qualité inférieure.

Canada

STRATIGRAPHY, STRUCTURE AND METAMORPHIC PETROLOGY OF THE TURNER LAKE AREA, ARCHEAN SLAVE PROVINCE, NORTHWEST TERRITORIES

by

Susan Elizabeth Schaan

A thesis submitted to the School of Graduate
Studies in partial fulfillment of the requirements
for the degree of M.Sc. in Geology

UNIVERSITY OF OTTAWA
OTTAWA, CANADA, 1993

ISBN 0-315-96014-0

UNIVERSITÉ D'OTTAWA
UNIVERSITY OF OTTAWA

Abstract

Lithological, metamorphic and structural relationships are established in the Turner Lake area of the Archean Hood River supracrustal domain. Four map units define a stratigraphic sequence of subvertical beds that appears to young eastward. Metamorphosed greywacke to mudstone turbidites (Unit 1) are overlain with local discordance by polymict conglomerate (Unit 2, James Falls Conglomerate) with clasts mainly of diorite, volcanic and sedimentary rocks interpreted to be of local origin. An intercalated metamorphosed sequence (Unit 3) of arenite, layered volcaniclastic rocks, breccia and conglomerate (including tonalite cobbles), pyroxenite and dioritic to gabbroic intrusions, is apparently overlain further east by a second sequence (Unit 4) of greywacke-mudstones. Sheet-like trondhjemitic to tonalitic intrusions, one with a U-Pb zircon age of 2607 ± 1.3 Ma, are common within Unit 3; minor tonalitic sheets intrude Unit 1. Larger plutons include the (2600 ± 2 Ma, U-Pb zircon) Pistol Lake granodiorite to tonalite in the south and the Fish-hook Lake monzogranite in the west. Proterozoic diabase dykes of at least three ages cross-cut the Archean rocks.

Metagreywacke-mudstones of Units 1 and 4 have similar rare earth element signatures and may be derived from a similar source terrane. The signatures resemble those of Yellowknife Supergroup metasedimentary rocks in the Yellowknife area. Trace element signatures of epiclastic amphibolites and mafic tuffs suggest mixed ultramafic and felsic sources. They may be consanguineous with the metapyroxenite. Highly foliated tonalite sheets and less deformed trondhjemite sheets have similar whole rock and rare earth element signatures to the Pistol Lake pluton. The lack of negative europium anomalies in the rare

earth element signatures of the plutonic rocks is comparable to synkinematic granites in the Yellowknife area.

The supracrustal succession, apparently 5 km thick, is metamorphosed to regional amphibolite grade defined by the assemblage quartz + plagioclase + biotite + muscovite + cordierite + andalusite ± fibrolite. A slight increase in grade within metagreywacke-mudstones to the northwest is indicated by abundant prismatic sillimanite and lack of cordierite. Pressure- temperature conditions constrained by this assemblage are less than 3.5 kb and between 550 and 600°C respectively. The metamorphism is typical of low pressure assemblages common elsewhere in the Slave Province.

Structures record three and possibly four phases of deformation associated with the metamorphism. Complex isoclinal folds, the geometry of which is obscure, are interpreted to be either first or second generation (D_1 or D_2) and appear to have been accompanied by the formation at low metamorphic grades of a steep axial planar fabric (S_1 or S_2). D_3 deformation is marked by a steeply dipping, regional S_3 schistosity that developed during the growth of peak metamorphic minerals. Overall, S_3 strikes northeasterly, which is clockwise from the steeply dipping, more northerly striking bedding; however a north to northwest striking oblique fabric best observed in Unit 2 conglomerate is in the opposite sense to bedding and could be an earlier sub-phase of S_3. The relative timing of these two directional sets of foliation is ambiguous. The S_3 schistosity is oriented east-northeasterly near the Pistol Lake pluton, suggesting influence by intrusion of the pluton during late stages of deformation. D_4 disharmonic folds and crenulations of S_3 are developed best in pelitic units where S_3 is

locally at a low angle to bedding. S_4 axial planes are parallel to S_3 in the psammites in most places.

A zone of highly strained rocks characterized by intense foliation and interfingering and truncation of sub-units transects the map area from north to south within the Unit 3 complex. Kinematic indicators are not definitive.

Table of Contents

Chapter 4
Structural Geology

Chapter 5
Metamorphic Petrology

List of Tables

List of Figures

Maps

Appendices

Chapter 1
Introduction

1.1 Location, size of study area and access

The rocks studied for this thesis are located in the northern Slave Structural Province (Figure 1-1) and comprise mainly Archean supracrustal rocks within the Turner Lake-Pistol Lake area (Figure 1-2) of the Hood River Belt (Jefferson et al., 1990, 1992). The map area lies above the Arctic Circle nearly 380 km north of the tree line and approximately 590 km northeast of Yellowknife. It covers about 60 km^2 between latitudes 67^{0}15' and 67^{0}09' and longitudes 109^{0}02' and 108^{0}53', west of Bathurst Inlet. The area lies within topographic map sheet 76N/2 with parts extending into the 76N/3. Bathurst Inlet lodge is the closest settlement, some 58 km to the southeast. Access is by float plane to Turner Lake during the summer months (late June to mid-late September). Turner Lake is large enough to accommodate Hercules aircraft in the winter months.

1.2 Weather conditions and wildlife

Turner Lake is ice-free for most of the summer. Air temperatures range from 0^{0}C to 25^{0}C from June to September with the highest temperatures recorded in July and early August. From mid August to freeze up the weather is typically poor and unpredictable with rain, fog and occasional snow flurries impairing air access. Similar conditions prevail in the spring. Turner Lake is relatively shallow and tends to have an earlier breakup than other lakes in the region. There is no permanent snow in the area and the ground may be free of

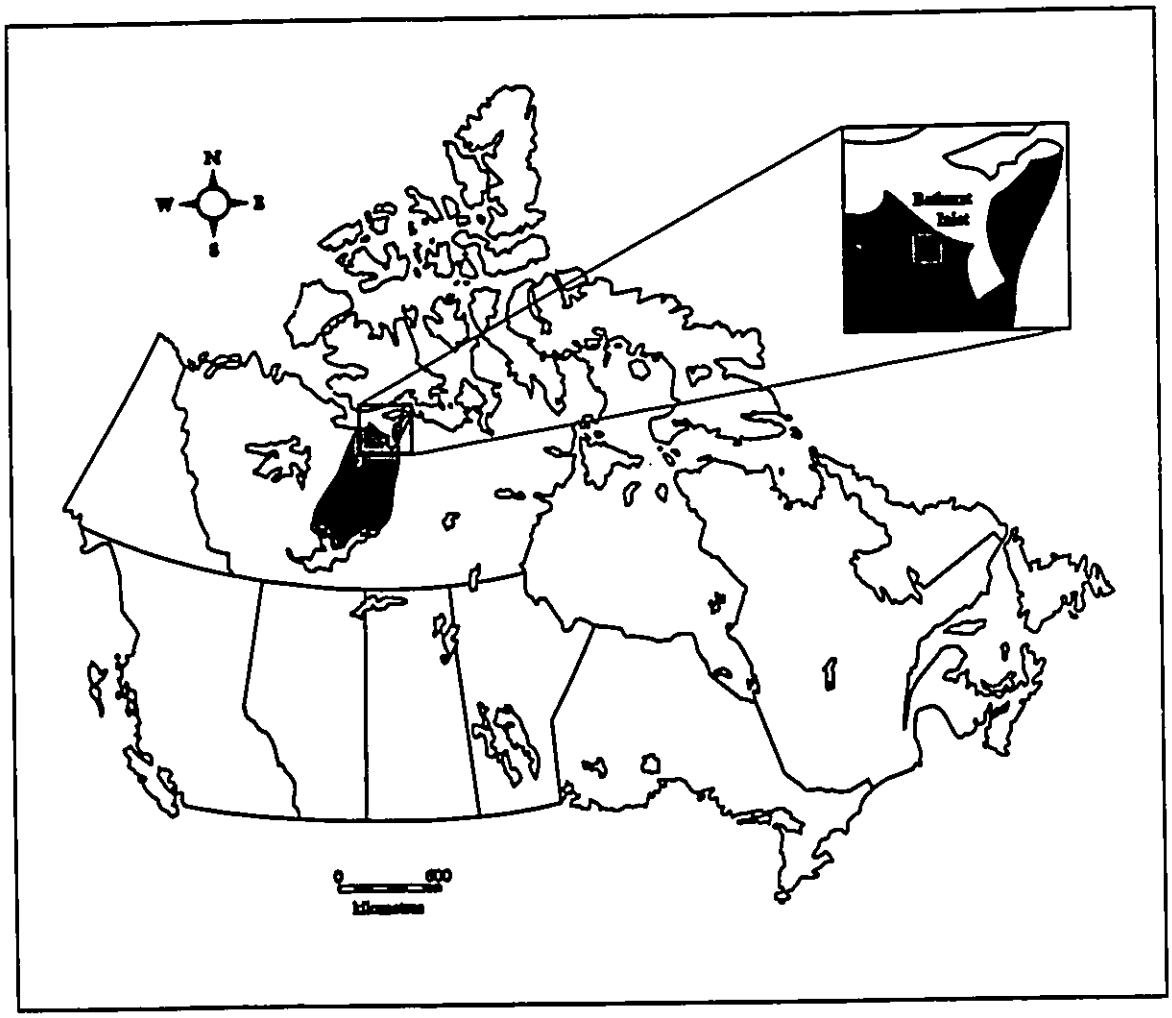

Figure 1-1. Location of the Archean Slave Province in Canada. Yellowknife indicated with star, study area indicated with black square.

Figure 1-2. Geological map of the Slave Province (modified from Padgham and Fyson, 1992). The map area of this project is outlined within the Turner Lake - Pistol Lake domain of the Hood River Belt (HRB). The Torp Lake domain of the Hood River Belt is the extension of supracrustal rocks to the north of the study area.

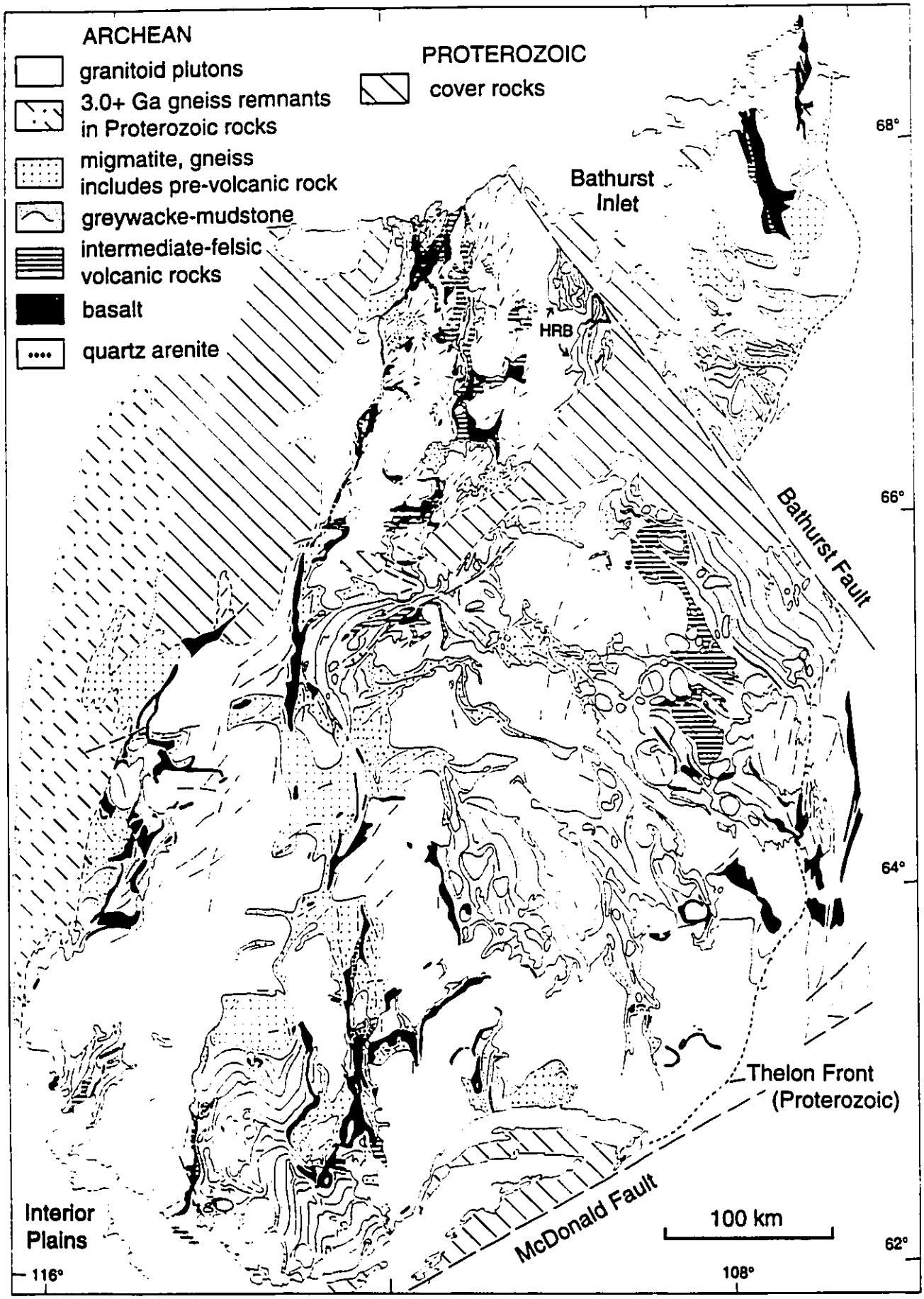
ARCHEAN
granitoid plutons
3.0+ Ga gneiss remnants in Proterozoic rocks
migmatite, gneiss includes pre-volcanic rock
greywacke-mudstone
intermediate-felsic volcanic rocks
basalt
quartz arenite
PROTEROZOIC
cover rocks
Bathurst Inlet
HRB
Bathurst Fault
Thelon Front (Proterozoic)
McDonald Fault
Interior Plains
100 km
68°
66°
64°
62°
116°
108°

snow by mid to late June.

Lichen, grasses and mosses are the principal ground cover on the open tundra, while sheltered valleys such as the Turner Lake valley contain dwarf birch and arctic willows. Turner Lake lies along a major migratory path for caribou. They pass through the area in early June. Muskoxen, sik-siks (arctic ground squirrels), and lemmings are indigenous species. Grizzly bears, arctic fox and wolves are present in small numbers. Gulls, ravens, ptarmigans, swans, loons, sparrows, buntings and other small varieties of birds are common. Mosquitoes and blackflies can be a nuisance from late July to August but winds are usually strong enough to provide relief.

1.3 Topography and outcrop

Local topographical relief attains 120 m and is greatest where Proterozoic diabase dykes form large resistant cliffs east of Turner Lake (260 m a.s.l. and more than 100 m above the floor of the Turner Lake valley). Beyond the valley the landscape is hilly with elevations ranging from 200 m to 325 m a.s.l. Rocks outcrop over approximately 80 % of the area with exposure decreasing north toward the James River, and especially south toward Pistol Lake, where metasedimentary rocks are weathered more readily than plutonic and metavolcanic rocks.

Prominent erratics rest on glacially smoothed bedrock surfaces, and glacial drift partially fills valleys. Continuous permafrost is evident in the form of patterned ground in the Turner Lake valley. Mud boils and sorted to non-sorted circles are common in glacial

debris. A small stream drains Turner Lake into the James River to the north.

1.4 Previous work

Until recently, published geological information on the Turner Lake area was limited to a regional 1 inch to 8 mile map of the Bathurst Inlet area based on a helicopter reconnaissance survey by the Geological Survey of Canada (Fraser, 1963a).

A gold prospect at Turner Lake, referred to hereafter as the "main showing", was discovered in the winter of 1963-64 by Noel Avadluk and George Turner who both worked as prospectors for Roberts Mining Company. During 1964 and 1965 visible gold was noted but assay results indicated the gold distribution was erratic (Thorpe, 1966). Generally less than 0.25 oz/ton were reported in what was referred to as "narrow lenses of a discontinuous band of micaceous quartzite within a massive amphibole-chlorite-biotite mica schist" (Carlson and Knutson, 1965). Schiller (1965) reported that the gold was not confined to a particular host but to a band tens of feet wide of arenaceous and amphibolitic rocks of the Yellowknife Supergroup in which there was disseminated arsenopyrite, in part gold-bearing, and sporadically distributed free gold. The band lay on the limb of a fold characterized by a westerly striking axial plane and steeply plunging axis.

In 1981 mineral occurrences in the area were visited as part of the assessment of the mineral potential of the proposed Bathurst Inlet National Park by Dr. S. Roscoe of the Geological Survey of Canada. A 1:250 000 compilation map based largely on a previous report (Fraser, 1963a) and accompanying map (Fraser, 1963b) including the Turner Lake

prospect was published (Roscoe, 1984).

In preparation for extensive exploration work at the showing carried out in the 1984-85 season, an airborne geophysical survey with line spacings of 125 m was conducted for Silver Hart Mining. This was part of a larger program, under the direction of C. Staargaard, that included 1:20 000 scale aerial photography, 1:10 000 scale regional mapping, and 1:1 000 detailed maps and trench samples with ground geophysics at the Turner Lake prospect. Christian Clode completed the first detailed study of the "main showing" and surrounding area as part of a Master's thesis at Queen's University (1987) in collaboration with Silver Hart operations. He examined the mineralized zone at the main showing, considered metamorphic conditions, and completed a 1:10 000 scale geological map of the Turner Lake area extending south from $67^0$15' for about 9 km and east of $109^0$00' for approximately 5.2 km. He concluded that the gold is hosted in a deformed felsic intrusive rock and mineralization is directly associated with quartz veins. The current study builds on the 1:10 000 lithologic map completed by Clode and S. Bishop (Staargaard, 1987) as part of Clode's thesis work.

In an independent report, C. Staargaard described the gold as "...native metal with arsenopyrite and pyrrhotite associated with stockwork quartz veining..." hosted by "...soda-rich albitite dykes cutting amphibolitized pyroxene gabbro where these rocks have been folded on a scale of about 500 metres." (Staargaard, 1987, p. 1)

Based on reconnaissance work at Turner Lake in the summer of 1988, J. S. Getzinger (1988, p. 24) confirmed that the gold was not confined to a single rock type but to a "mineralized metagreywacke and/or hornblende gneiss" of sedimentary origin. She related

compositional gradations to original interbedding of sedimentary and/or volcaniclastic rocks. The work of Getzinger agrees most closely with the present study in terms of stratigraphy, unit descriptions and interpretations.

In 1989 mapping and a drilling program was concentrated at the "main showing" and a 1:500 scale detailed map and report were produced (Fumerton, 1989). Fumerton (1989) described the host as a mineralized arenite with average gold assay values of 4.3 g/t. The gold-rich rock unit was seen as a channel-fill deposit in at least four lenses in "...a stacked sequence of arenaceous siltstones and fine sandstones" (Fumerton, 1989, p. I). The deposit was characterized as having a paleoplacer origin, with arenite beds marking the change from lower epiclastic amphibolite of basaltic komatiitic composition to an upper epiclastic amphibolite with an ultramafic komatiitic composition.

Concurrent with this thesis study, Geological Survey of Canada workers mapped the Hood River Belt at 1:50 000 scale (Henderson et al., 1991; Figure 1-3). This allows the Turner Lake area to be considered in a regional context. Detailed studies by Geological Survey of Canada workers along the James River and in the Fish-hook Lake area where outcrops are lichen free aided in deciphering details on stratigraphic relationships of rock units (Jefferson et al., 1990, 1992). Johnstone (1988, 1989, 1990a, b) has mapped the northern extension of the Hood River belt into the Torp Lake domain (Figure 1-2). In conjunction with Johnstone (1990c), Katherine Venance is currently completing an M.Sc. study at Carleton University on the constraints of metamorphism in the pelitic rocks within the Torp Lake domain (Venance, in prep.).

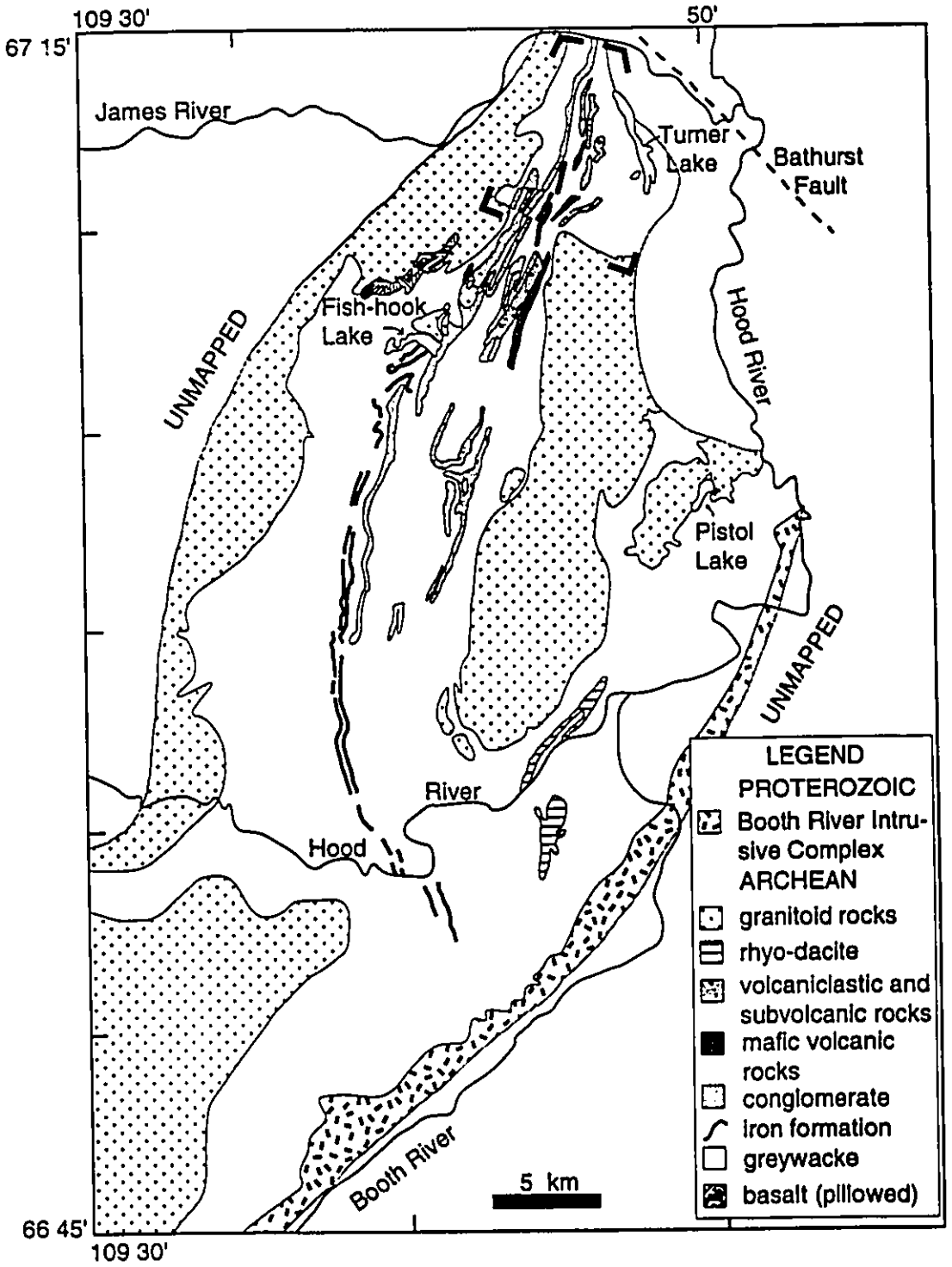

Figure 1-3. Geology of the Turner Lake - Pistol Lake area of the Hood River Supracrustal Belt (after Henderson et al., 1991). The Turner Lake map area is outlined. Diabase dykes have been omitted for clarity.

1.5 Mapping project: Description and methodology

Growing interest in the economic potential, notably gold deposits, and the tectonic setting of the Turner Lake - Pistol Lake area during the late 1980's prompted an alliance between government, university and industry investigators. Mapping carried out during the course of this study is part of a larger Government of the Northwest Territories, Geological Survey of Canada and Chevron Minerals Ltd. joint venture for mapping the Hood River supracrustal belt. Turner Lake lies within map area 10 with extensions into area 11 and 12 of 13 subdivisions of the Turner Lake - Pistol Lake area (Figure 1-4). R. Wyllie (University of New Brunswick) is presently completing an M.Sc. project in the Pistol Lake area (area 1). Personnel from the Geological Survey of Canada have covered the remaining subdivisions (see Henderson et al., 1991). I first visited the Turner Lake area during the 1988 field season, while working with Rob Johnstone (Government of the Northwest Territories) in the Torp Lake domain, northern Hood River belt (see Johnstone, 1988, 1989, 1990). A three month field season in 1989 (June to August) resulted in a 1:20 000 scale map of the thesis area. During a month-long field season in 1990 mapping at a scale of 1:10 000 was concentrated near Chevron's abandoned 1989 campsite for gold exploration.

Most of the mapping was completed by traversing and following geological contacts on foot. Chevron provided the use of a Bell 206 helicopter for access to the southern and western perimeters of the map area in 1989. During 1990 access from Turner Lake was entirely on foot.

SPOT and SAR images provided by A. Fabbri of (Canada Center for Remote Sensing)

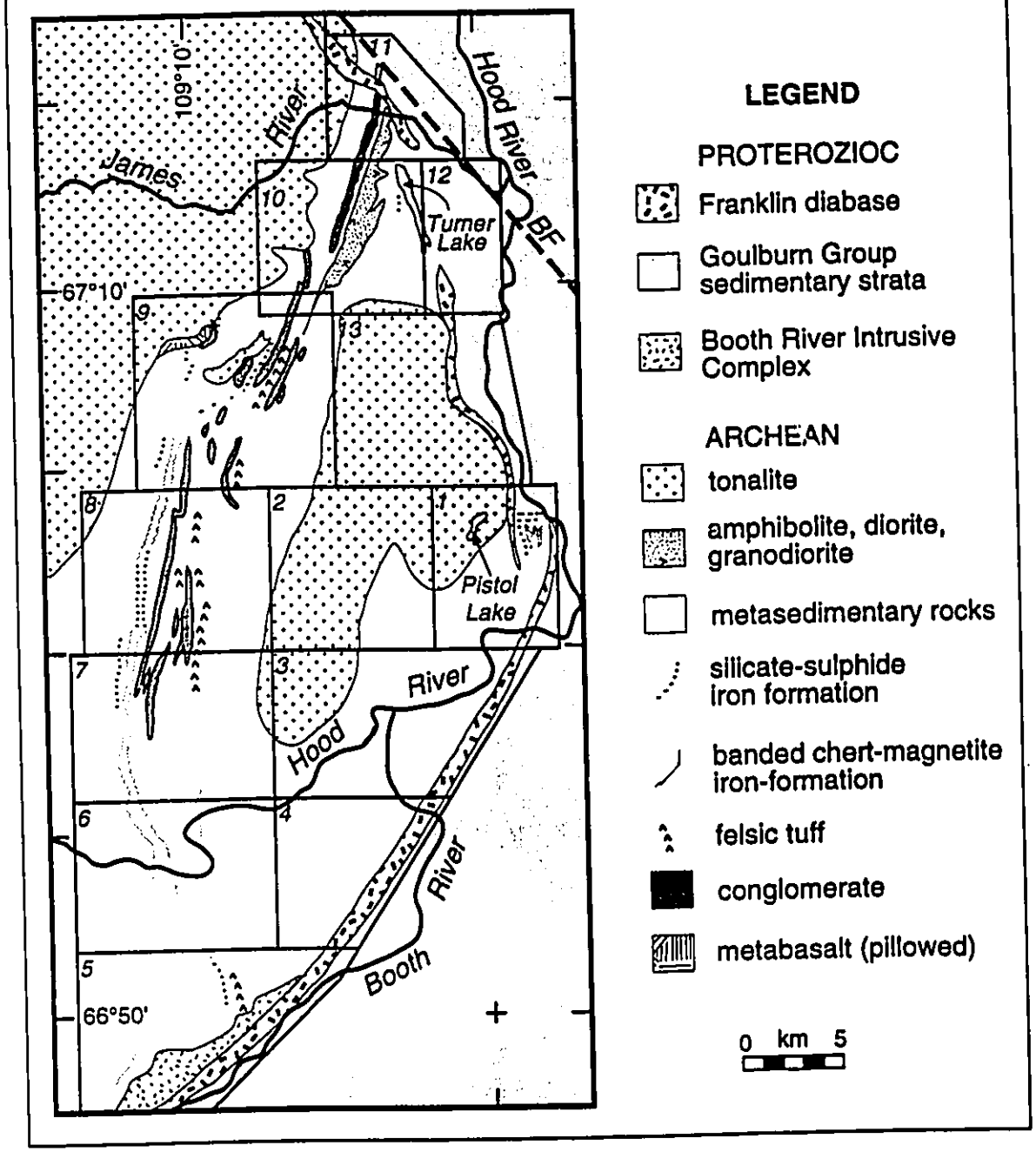

Figure 1-4. Geological sketch map of the Turner Lake - Pistol Lake area based on mapping prior to 1988 from a proposal for mapping of the Hood River Belt (modified from C. Jefferson, Geological Survey of Canada, Sept. 16, 1988). Proposed map areas are indicated. Map areas for this project include area 10 with extensions into area 11 and 12. Diabase dykes (Mackenzie Swarm) have been omitted for clarity. BF=Bathurst Fault.

to C.W. Jefferson were used as distortion-free basemaps. Lake positions were traced to mylar. 1:10 000 scale colour air photograph enlargements provided by Silver Hart mines and purchased by the Geological Survey of Canada were used to map the main showing and immediate Turner Lake area. 1:20 000 colour air photographs were used in the remaining areas with observations transferred to 1:10 000 photomosaics and plotted on the base map.

1.6 Objectives

The principal objectives of this study are:

1) to map the Turner Lake area of the Hood River belt;

2) to provide a detailed lithologic and stratigraphic analysis of rock units;

3) to document the structure and relative timing of deformational events;

4) to describe metamorphic mineral assemblages and infer pressure and temperature conditions; and,

5) to interrelate metamorphism and deformation.

1.7 Acknowledgements

Dr. W.K. Fyson is thanked for his support of my research. He provided many suggestions on improvement of the text and was very patient and understanding during its final stages. Co-advisor Dr. André Lalonde served as advisor during Dr. Fyson's sabbatical leave of 1990-91. Co-advisor Dr. C.W. Jefferson (Geological Survey of Canada) answered the call for "help" many times with guidance in field and laboratory methods. He arranged

for geochemical analyses, the preparation of many thin sections, and for me to take part in geochronology work under the patient guidance of Dr. O. van Breemen. 1:20 000 colour air photographs of the entire Turner Lake area were made available to Dr. Jefferson by Silver Hart Mines Ltd. and he provided 1:10 000 enlargements for, and contributed much of the detailed mapping around the main gold showing at Turner Lake. R. Johnstone (Mineral Initiatives Office, Yellowknife) provided my first employment and field experience in the region in 1988 and was involved in the inception of this study. Dr. W.A. Padgham, the Department of Indian and Northern Affairs, supported the project financially during 1989 and 1990. Chevron Minerals Ltd. provided logistic support for 1989 including the use of a Bell 206 helicopter. Dr. J.R. Henderson (Geological Survey of Canada) completed several traverses with me and both he and M. Henderson (Geological Survey of Canada) continued their interest in this project. A Northern Scientific Training Program grant through the University of Ottawa provided funds to transport an assistant to Yellowknife in 1990. Sari Penny and Anne Séguin are thanked for their assistance in mapping during 1989 and 1990 respectively. Val Jackson employed me in 1990 and provided invaluable guidance in field operations. Robin Wyllie is thanked for his thought provoking discussions and correspondence as well as the construction of a drafting table during the 1989 field season.

My colleagues at the Ottawa-Carleton Geoscience Centre have played an important role in the completion of this study. Discussions with Katherine Venance at Carleton University have been helpful for interpreting the metamorphic history of the Turner Lake samples. Kevin Telmer provided painless introduction to new and useful IBM compatible

computer software. Both he and Mark Mihalasky saved my diskettes from imminent destruction thanks to their skills as computer virus exterminators. I will be forever grateful to my friends especially those who were there when I needed them, namely Ann, Katherine and Natalie. Last but not least a warm hug goes to my late great canine assistant, Max, who was a great motivator for early morning traverses and proved to be a muskox marauder extraordinaire.

Chapter 2
General Geology of the Slave Province

2.1 Introduction

The Slave Structural Province, an area of about 213,000 km^2 in northern Canada (Figure 1-1), is mainly underlain by Archean rocks (Figure 1-2). The last period of extensive deformation and plutonism to affect the entire region is known as the Kenoran orogeny (Stockwell et al., 1970). The eastern tectonic boundary, the Thelon Front, represents a transition from relatively low grade metamorphic rocks on the Slave side to granulite grade rocks in the Churchill Province (Fraser, 1978), which includes the 2.02 to 1.91 Ga old Thelon Orogen (Hoffman, 1989). The Slave Province is bordered in the west by the Bear Structural Province, specifically the Wopmay Orogen (1.94 to 1.86 Ga; Hoffman, 1989). In the southwest it is overlain by Paleozoic cover of the Interior Plains. In the southeast and northwest, Archean rocks are unconformably overlain by lower Proterozoic strata. The Bathurst subprovince in the northeast contains moderately folded rocks of the lower Proterozoic Goulburn Group, which unconformably overlie Archean rocks and extend over much of Bathurst Inlet (adjacent to the thesis area; Figure 1-2).

2.2 Rock types

2.2.1 Introduction

Supracrustal rocks ranging in age from 2.71 to 2.65 Ga (Mortensen et al., 1988; Isachsen et al., 1991a) underlie approximately one third of the Slave Province. Of this, about

27% are mafic to felsic volcanic sequences (Padgham, 1985). The remaining 73% constitute mainly greywacke-mudstone units interpreted as turbidites, and their high grade metamorphic equivalents (Easton, 1985). These proportions contrast with those of most other Archean supracrustal terranes such as in the Superior Province, where volcanic rocks generally predominate. The remaining two-thirds of the province is underlain by granitoid intrusive rocks. One third to one half of these are mixed gneisses, migmatites and granite gneisses. Granitoid plutons of varying composition intrude the supracrustal rocks (Figure 1-2). All supracrustal rocks are metamorphosed to various degrees in the low pressure facies series.

2.2.2 Early gneiss (>2.8 Ga)

Heterogenous gneisses that predate the volcanic and sedimentary rocks outcrop locally in the southwest and west-central parts of the Slave Province (Figure 1-2). Contacts with the supracrustal rocks are generally obscured by deformation or intrusive rocks. The granitoid "basement" ranges in composition from tonalitic to trondhjemitic, locally granodioritic and granitic gneiss and migmatite (Hoffman, 1989). Included are the oldest intact crustal rocks yet identified, the 3.96 Ga Acasta gneiss (1, Figure 2-1; Bowring et al., 1989; Isachsen et al., 1991d). This foliated tonalite to granodiorite with potassic-granite in sheets, veins and small to outcrop scale masses lies on the western margin of the province. Amphibolite dykes cutting gneissic rocks are suspected to be feeders to the adjacent volcanic piles (Frith et al., 1977; Henderson, 1981; Easton et al., 1982). No examples of the early gneiss have been identified in the eastern part of the province and none are expected in light of the Pb-isotope results of Thorpe et al. (1982).

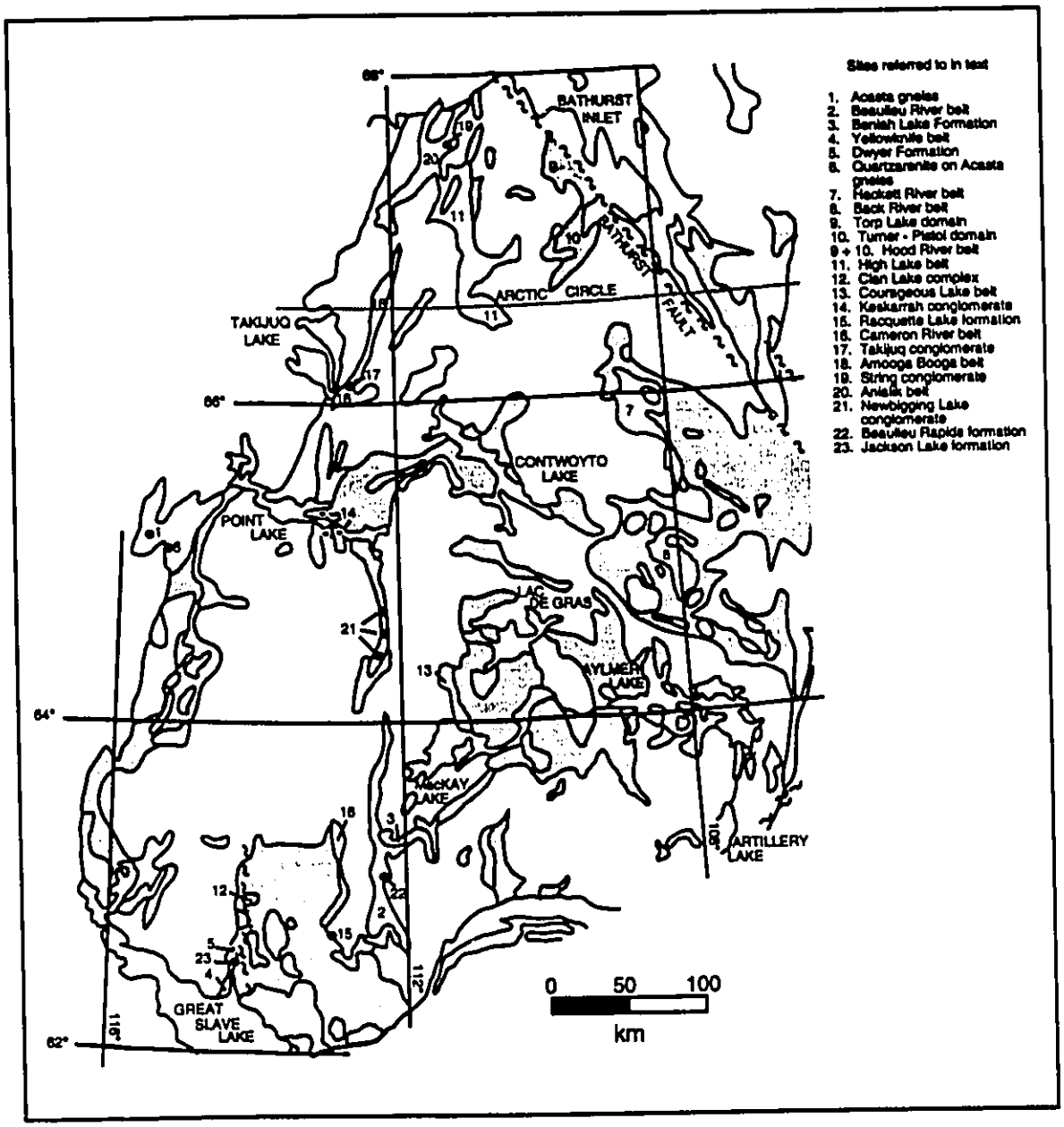

Figure 2-1. Index map for location of sites mentioned in text. Volcanic belts are outlined and turbiditic metasedimentary rocks are stippled (modified from Padgham and Fyson, 1992). Refer to Figure 1-2 for detailed geology.

2.2.3 Supracrustal rocks - The Yellowknife Supergroup

Henderson (1970) introduced the term Yellowknife Supergroup to include all Archean supracrustal rocks of the Slave Structural Province. Recent work has resulted in these supracrustal rocks being divided into at least three broad distinct stratigraphic sequences (Padgham and Fyson, 1992) including quartzarenites, volcanic and greywacke-mudstone successions (including conglomerate) and fluvial sediments that post date the intrusion of granitic rocks.

Predominant, widespread volcanic, greywacke-mudstone (turbidite) sequences have been described in detail by Henderson (1970, 1975a, 1985) and outcrop as patchy, ameboid-shaped, equant domains (McGlynn, 1977). Included are over 20 narrow linear volcanic belts, generally less than 5 km across. Many, but not all, are along contacts between intrusive granitoid rocks and the much more extensive greywacke-mudstones, generally in gradational and conformable contact, or are included within metasedimentary domains. Several greywacke-mudstone domains south of latitude 66^0 are greater than 50 km across (Figure 2-1). In places this volcano-sedimentary sequence is underlain by quartzarenite and overlain by fluvial sediments which are younger than most, if not all of the granitoid intrusions.

2.2.3.1 Basal quartzarenites

Quartzarenite successions have been recognized beneath the volcanic rocks and above granitoid basement of the Beaulieu River belt (2, Figure 2-1) near Beniah Lake (3, Figure 2-1) (Beniah Formation; Roscoe et al., 1989; Covello et al., 1988), beneath volcanic rocks at the north end of the Yellowknife belt (4, Figure 2-1) (Dwyer Formation; Isachsen et al.,

1991c) (5, Figure 2-1) and overlying the Acasta gneiss (6, Figure 2-1) (Padgham and Fyson, 1992). These basal quartzarenites are locally overlain by felsic pyroclastic rocks and chert-magnetite iron formations, and are commonly intruded by ultramafic sills and dykes. The quartzarenites have been interpreted as derived from pre-existing sialic crust and as deposited on a stable marine shelf that was subsequently covered by ensialic volcanic rocks (Roscoe et al., 1989). Quartzarenites imply a period of relative tectonic quiescence during the evolution of the Slave craton.

2.2.3.2 Metavolcanic rocks

Metavolcanic rocks range in composition from basalt to rhyolite and are nearly 45% intermediate to felsic (Padgham and Fyson, 1992). Isotopic dating (mainly of zircons) from the felsic volcanic rocks indicates an age range of about 2.7 to 2.65 Ga (Mortensen et al., 1988). Narrow basalt-dominated belts (Yellowknife-type of Padgham, 1985) extend along the margins of, and could thin into the sedimentary domains which have been interpreted as depositional basins (Henderson and Easton, 1977); however, the evidence is not clear-cut (Fyson and Helmstaedt, 1988).

Separate intermediate to dominantly felsic volcanic dominated belts or complexes with minor basalt (Hackett River type) are less common than the basaltic dominated belts. They predominate in a northwest trending zone southwest of the Bathurst Fault. The largest complexes are at Back River (8, Figure 2-1), where they form relatively equidimensional outcrop patterns and Hackett River, immediately to the north (7, Figure 2-1), which like the basaltic belts, is at the border between a more extensive metasedimentary domain to the east,

and a granitoid-migmatite-gneiss domain to the west.

Further north in the Hood River belt (9 and 10, Figure 2-1), both mafic and felsic volcanic rocks form minor components within metasedimentary rocks (Figure 1-3). The High Lake supracrustal belt in the northwestern part of the Slave province (11, Figure 2-1) comprises intermediate to felsic volcanic rocks intercalated with almost equal proportions of mafic volcanic and metasedimentary rocks (Figure 1-3).

2.2.3.3 Greywacke-mudstone succession

The metasedimentary rocks are dominantly greywacke-mudstone turbidites, less commonly conglomerate, carbonates and iron-formation (including gold-bearing units; Padgham, 1986) and are grouped with the metavolcanic succession as the second distinct sequence of supracrustal rocks in the province. Locally the turbidites contain abundant felsic rock fragments, with rare mafic clasts and quartz-plagioclase rock fragments (Henderson, 1981). These clasts are indicative of a mixed source terrane that included felsic volcanic material with lesser contributions by mafic volcanic and plutonic rocks (Jenner et al., 1981).

Minor carbonate sediments include rare limestone and more abundant stromatolitic dolostones, lying between the volcanic rocks and greywackes (Henderson, 1975b, 1981; Lambert et al., 1990). Iron formations within the turbidites are common in a broad zone extending northeastward across the province (Padgham and Fyson, 1992) and include oxide, carbonate, silicate and sulphide facies deposits.

2.2.3.4 Conglomerates

Included in the above volcanic and greywacke-mudstone succession are volcaniclastic

conglomerates such as those occurring within the Clan Lake Complex (12, Figure 2-1) (Hurdle, 1985), within the Courageous MacKay Lake belt (13, Figure 2-1) (Dillon-Leitch, 1981), and at Back River (8, Figure 2-1) (Lambert, 1988). These contain clasts which may have been shed from felsic centres or from basalt and andesite submarine flows (Lambert, 1978, 1988; Padgham, 1990; Lambert et al., 1992). Coarse granitoid boulder conglomerate interbedded with volcanic and volcaniclastic sequences occur at Point Lake (Keskarrah conglomerate; Stockwell, 1933; Henderson and Easton, 1977; Henderson, 1988) (14, Figure 2-1), within the Cameron River belt (16, Figure 2-1) (Racquette Formation; Henderson 1985) (15, Figure 2-1), within the Amooga Booga belt (18, Figure 2-1) (Takijuq conglomerate; Padgham, 1985) (17, Figure 2-1), within the Anialik belt (20, Figure 2-1) (String conglomerate; Padgham, 1985) (19, Figure 2-1), and at Newbigging Lake (Rice et al., 1990) (21, Figure 2-1).

2.2.3.5 Post-granitic sedimentary rocks

The third sedimentary sequence comprises the youngest supracrustal rocks in the province. These polymict conglomerates and quartz-rich arenites and rudites interpreted as fluvial sandstones are minor in extent and they may have been deposited along fault scarps in the older supracrustal rocks (Padgham and Fyson, 1992). Examples include the Beaulieu Rapids Formation (22, Figure 2-1) in the Beaulieu River Belt (2, Figure 2-1) (Roscoe et al., 1989), the Jackson Lake Formation (23, Figure 2-1) of the Yellowknife Belt (4, Figure 2-1) (Henderson, 1985) and some of the conglomerates in this study (van Breemen, pers. comm., 1993). Clasts include locally derived volcanic and granitoid boulders (2.605 Ga, Isachsen et

al., 1991b) with lesser greywacke, shale, quartzite and chert cobbles (Rice et al., 1990; Isachsen et al, 1991d; McGlynn and Henderson, 1972).

2.2.4 Granitic intrusive rocks

Metasedimentary and volcanic rocks grade into migmatites and mixed gneisses which have been interpreted as mainly metamorphosed and granitized equivalents. Some gneiss and migmatite have been isotopically dated as pre-volcanic and yet are indistinguishable petrographically from younger gneiss.

Granitoid plutons occur as discrete bodies within the supracrustal rocks or as larger masses between the supracrustal domains and underlie approximately 50% of the Slave Province. Dioritic, tonalitic and granodioritic plutons have an age range of about 2.6-2.7 Ga (Easton, 1985; King et al., 1990) that overlap in age and are younger than the volcanic rocks. Later syn- to late-deformational granodiorite and two mica granites dated as young as 2.58 Ga were derived from sedimentary rocks (Thompson, 1989a, b). Pegmatites are associated with these younger plutons.

Foliated granitoid cobbles within conglomerate such as the Keskarrah conglomerate at Point Lake (Henderson, 1988), the Takijuq conglomerate (Padgham, 1985), and the conglomerate near Newbigging Lake south of Point Lake (Rice et al., 1990) (Figure 2-1) may indicate unroofing and erosion of synvolcanic granitoid rocks (Padgham and Fyson, 1992).

2.2.6 Other intrusive rocks

Rare ultramafic intrusive rocks include sills and dykes associated with shelf-type quartzarenites (Roscoe et al., 1989; Templeton, 1988) and large lenses in the Acasta gneiss

(Padgham and Fyson, 1992). Bostock (1980) described ultramafic serpentinites and tremolite-chlorite schists in close proximity to a mylonitic zone on the west side of the Point Lake volcanic belt and similar remnants of ultramafic rock are present at the base of the Cameron River volcanic belt, also in association with mylonites (Kusky, 1988, 1990).

Subvolcanic gabbros include multiple, locally sheeted dykes and similar rocks in the Cameron and Beaulieu River belts (Lambert, 1988; Lambert and van Breemen, 1991). Gabbro dykes representing several phases of intrusion occur in the lower part of the Yellowknife belt (Henderson and Brown, 1966) and appear to have acted as feeder systems to contemporaneous and younger phases of volcanism (Falck, 1990).

Igneous intrusives younger than the Archean rocks include Proterozoic diabase dykes and Aphebian (Bear Province) alkaline intrusions. These make up less than 5% of the rocks of the Slave Province (Padgham, 1985).

In the Contwoyto Lake - Bathurst Inlet area two stages of diabase or gabbro sheets and possible related dykes have been recognized. An older suite cuts Archean rocks and Goulburn Group strata and are dated at 1 215 and 1 555 My (Fahrig et al., 1971). These are cut by north to north-northwesterly trending dykes of the Mackenzie swarm. The Mackenzie igneous event was dated using badellyite U-Pb at 1270 Ma (Lecheminant and Heaman, 1989). Younger Franklin diabase dykes, stage two, cut Goulburn strata and Archean rocks. These are dated at 723 $\pm$ 3 Ma (Heaman et al., 1990).

West of Bathurst Inlet, an alkaline granitic body in the ultramafic-mafic-felsic Proterozoic Booth River intrusive suite has been dated as 2023 Ma (Roscoe et al., 1987).

3.2.3 Deformation and Metamorphism

2.3.1 Introduction

The last period of intensive deformation in the Slave province, the Kenoran orogeny, ended around 2.58 Ga and was accompanied by plutonism and metamorphism. Metamorphic conditions across the province were low pressure and high temperature and grades range from lower greenschist to upper amphibolite (Thompson, 1989a, b). Away from the Early Proterozoic Wopmay orogen on the western margin and the Thelon Front in the east, the Archean rocks have only been locally affected by Proterozoic, brittle deformation: mainly faulting or extensional fracturing during dyke emplacement.

2.3.2 Deformation

Folds range in scale from early large-scale isoclinal structures that may lack cleavage through intermediate structures with associated mineral fabrics, to more open, late folds with associated crenulation cleavages. Steep homoclines in volcanic rocks commonly face away from bordering plutonic complexes with minor reversals in facing direction. These homoclines form the limbs of some of the major folds, here termed $F_{1\text{-}X}$, which are equated with the F_1 folds described by Fyson (1975) and F_0 folds of Fyson and Helmstaedt (1988). Within the sedimentary terranes, these early folds have axial surface traces that vary from 5 to greater than 20 km in length, and lack associated deformational fabrics. Hinges are obscure and the axial traces are often detected by opposing facing directions of later F_1 folds (Fyson, 1982, 1990).

Folds that overprint and obscure the earlier, larger $F_{1\text{-}X}$ structures are commonly the

first locally recognizable generation, hence the designation F_1 (Fyson and Helmstaedt, 1988). The F_1 folds which are best displayed in the metasedimentary rocks, are intermediate in scale with axial surface traces of 100 m to greater than 1 km. In the domains of low to moderate metamorphic grade, F_1 folds are most commonly upright to steeply-inclined and tight to isoclinal. These show up clearly on air photos and determine most fold trends compiled on maps (Figure 5). Few F_1 folds in the sedimentary rocks have a well-defined S_1 axial planar foliation although in some areas, bedding-parallel foliation on limbs of isoclines may be S_1 (Fyson, 1990). In volcanic rocks an S_1 fabric is partly defined by flattened pillows and rock fragments that are commonly parallel to bedding (Fyson, 1990; Fyson and Frith, 1979). Within the metasedimentary rocks, S_1 is commonly obscured by S_2, a later cleavage or schistosity that crosses F_1 folds obliquely, and which is associated with mesoscopic and possibly larger folds. S_2 is preserved locally as segregations in greywacke beds, as quartz inclusion trails in biotite and cordierite porphyroblasts (Fyson and Helmstaedt, 1988; King and Helmstaedt, 1989), and as a prominent segregation type cleavage which is oriented transverse to F_1 folds in felsic volcanic rocks (Hurdle, 1985).

Later foliations are assigned to S_2 and S_3. S_3 in some areas includes two or more subsets. Locally penetrative, F_3, minor folds are displayed in quartz veins and thinly bedded units. S_3 varies in character from an open crenulation of S_1 or S_2 to a penetrative cleavage or schistosity or a segregation cleavage (Fyson, 1975, 1980, 1982).

Orientations of structures and degrees of development in different rock types vary from area to area across the province. Fold sets and foliations terminate abruptly and are

replaced with little or no overlap or interference by sets aligned in other directions. This arrangement is described as domainal (Fyson, 1982, 1990; Fyson and Jackson, 1991; Schaan and Fyson, 1991).

2.3.3 Metamorphism

Yellowknife Supergroup rocks range from lower greenschist to upper amphibolite facies of low pressure, medium temperature regional metamorphism with the majority being amphibolite grade (Thompson, 1978, 1989a, b). The lowest grade metasedimentary rocks are surrounded by lower to upper amphibolite grade rocks with the transition from greenschist to amphibolite facies most easily recognized where cordierite porphyroblasts are present in pelitic schists (cordierite amphibolite facies of regional metamorphism). There is a steady increase from low to highest grade metamorphism with the most deeply eroded rock occurring at the highest grade (Thompson, 1989b). Isograds are both discordant and concordant to structural trends and it has been inferred that peak metamorphism was concurrent with a main phase of fabric development (F_2 above) and, in places, even outlasted deformation (Thompson, 1989b).

Metasedimentary rocks of the greenschist facies typically contain chlorite, white mica and biotite with plagioclase and quartz. With increasing metamorphic grade biotite occurs as porphyroblasts or "knots" in spotted phyllites. The greenschist-lower amphibolite facies boundary is defined by the first appearances of cordierite and/or andalusite in the absence of chlorite. Staurolite (locally occurring), cordierite and biotite with plagioclase and quartz occur in lower amphibolite rocks and the lower to upper amphibolite facies rocks are contain

sillimanite and K-feldspar with sillimanite without muscovite. Garnet is present in some rocks, particularly the pelites associated with iron formations and within rocks of the upper amphibolite facies (sillimanite, K-feldspar migmatite zone). Gedrite in medium grade rocks and chloritoid in lower grade rocks also occur locally (Staargaard, 1987). Closer to granitoid plutons, and within zones of migmatite, metasedimentary rocks are associated with coarse grained gneiss containing sillimanite, K-feldspar, cordierite, relict biotite and muscovite (McGlynn and Henderson, 1972; King and Helmstaedt, 1989). Muscovite is locally replaced by coarse K-feldspar (King and Helmstaedt, 1989).

Greenschist facies mafic volcanic rocks contain chlorite, some carbonate, plagioclase, epidote and actinolite (McGlynn and Henderson, 1972). Rocks of the cordierite amphibolite facies commonly contain hornblende as the dominant amphibole with some garnet and oligoclase-andesine plagioclase. Felsic volcanic rock prograde minerals include cummingtonite, anorthite and clinopyroxene at higher grades.

Kyanite is present in garnet bearing migmatites in the eastern part of the province along the Proterozoic Thelon Front (Thompson, 1978, 1989b), probably reflecting high pressure conditions during early Proterozoic reactivation of the Archean rocks (Henderson, et al., 1990).

Chapter 3
Rock Units and Stratigraphic Relationships in the Turner Lake Area

3.1 Introduction

Four main stratigraphic groups of supracrustal rocks which are designated as units with subunits (Figure 3-1) constitute an extensive, steeply inclined northerly trending sequence that appears to young eastward in the Turner Lake area. The sequence is intruded concordantly by gabbroic to dioritic sheets and crossed by granitoid rocks and Proterozoic mafic dykes (Map 1).

Previous studies include that of the Roberts Mining Company (1964) which reported a mixed volcanic and sedimentary assemblage at Turner Lake. Clode (1987) maintained that volcanic rocks are absent. Getzinger (1988) and Henderson et al. (1991) documented the presence of mafic volcanic rocks in the area. No extrusive textures are preserved in the rocks examined at Turner Lake during this study; however, volcaniclastic rocks have been identified. The present study was concurrent with that of Henderson et al. (1991), but took a litho-stratigraphic rather than purely lithologic approach to designating rock units. The different ways of assigning rock unit names are discussed below. Appendix I provides a correlation of the stratigraphy used herein with that of Henderson et al. (1991) and of previous workers. Chemical analyses of each rock unit (see Chapter 6) supplement field observations in the identification of rock types.

STRATIGRAPHY OF THE TURNER LAKE AREA

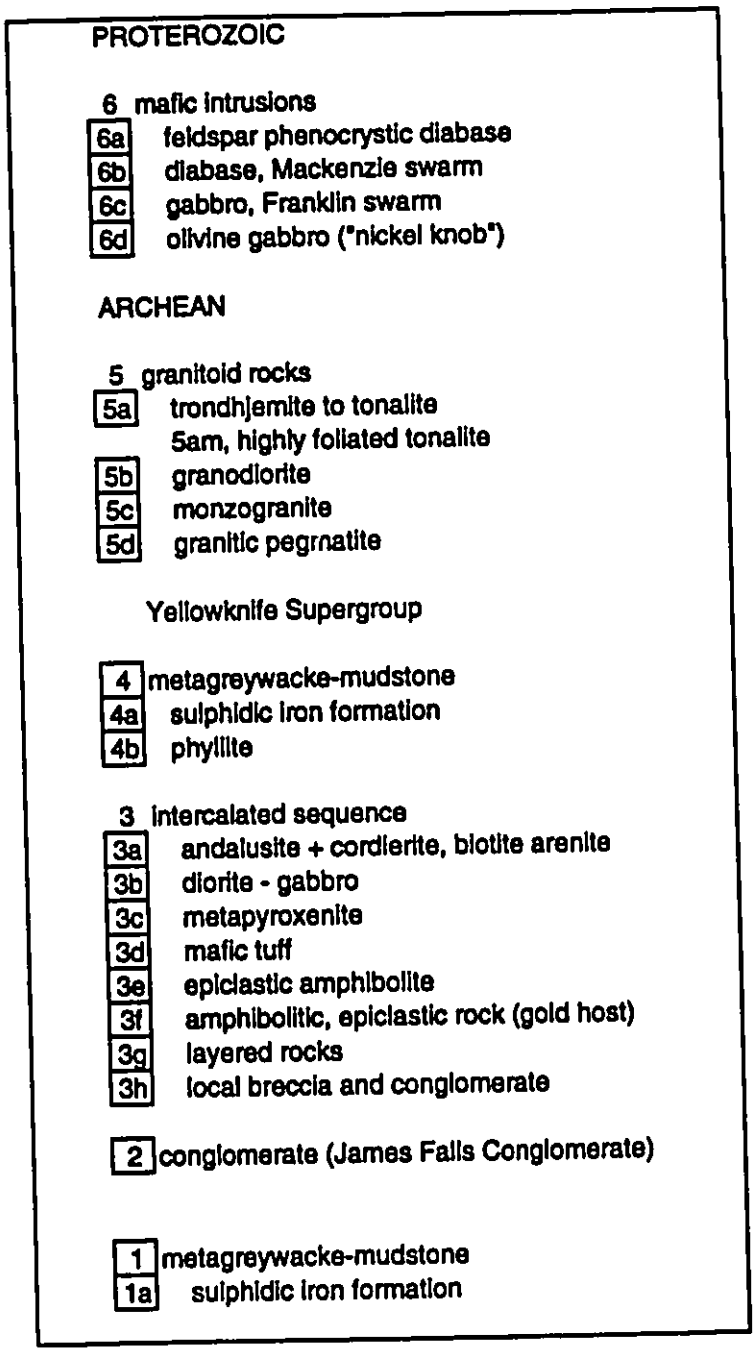

Figure 3-1. Stratigraphic column, Turner Lake area. Unit numbers correspond to those on Map 1 (in back pocket).

3.2 Unit Descriptions

The main mappable units of metamorphosed supracrustal rocks, listed in apparent stratigraphic order from west to east are: (Unit 1) greywacke-mudstones; (Unit 2) conglomerate (James Falls Conglomerate, Roscoe et al., 1988); (Unit 3) a complex of conglomerates, arenites, volcanic and volcaniclastic rocks that are intercalated with gabbroic to dioritic bodies; (Unit 4) greywacke-mudstones. The Turner High Strain Zone (Jefferson et al., 1990), referred to hereafter as the high strain zone, is characterized by intensely foliated, recessive rock and transects the map area and Unit 3 from north to south. It is coincident with a gently sinuous, drift-filled valley which forms a prominent, continuous lineament on air photos (Figure 3-2).

3.2.1 Metagreywacke-mudstone (Unit 1)

Andalusite ± fibrolite ± cordierite, biotite ± muscovite, quartz, feldspar schist, interpreted as representing metamorphosed greywacke-mudstone turbidites, underlies the western part of the study area. Sedimentary younging established from metamorphic reverse graded bedding (Figure 3-3) is both to the east and west, reflecting obscure folds, so that the stratigraphic relationship to adjacent conglomerate is not clear. However Henderson et al. (1991) have mapped an unconformity south of the study area where iron formation has been eroded and has provided clasts to the overlying conglomerate unit suggesting that the metagreywacke-mudstone unit is older than the conglomerate. Graded bedding from sandy metagreywacke to pelite ranges in thickness from 1 to 15 cm. Greywacke generally predominates, particularly toward the eastern contact with overlying conglomerate. The unit

has an apparent exposed thickness of 1.5 km. The true stratigraphic thickness is difficult to estimate because of deformation and intrusion by granitic plutons.

The mineral assemblage from nine samples examined in thin section (samples 89054, 89082, 90043, 90045, 90046, 90A14, 90A15, 90A17, and 90A35; Figure 3-4) includes 20-45% plagioclase feldspar, 20-40% quartz (quartz and feldspar vary in reverse proportions), 15-20% biotite, 5% muscovite and 2% tourmaline, with andalusite and/or cordierite porphyroblasts. Fibrolitic sillimanite is generally ubiquitous although near the Fish-hook Lake pluton in the northwest, sillimanite is prismatic (Figure 3-5). Layers of granitoid rock is common along the pluton margin. Locally the rocks have a gneissic appearance.

Unit 1a is thinly bedded (<20 cm) sulphidic iron formation containing coarse (up to 4 mm) garnets, which is confined to the southwestern margin of the area (sample 89147; Figure 3-4).

3.3.2 Conglomerate (Unit 2)

Polymict orthoconglomerate (Unit 2) is best exposed at the James Falls at the northern end of the map area where it apparently both conformably and unconformably overlies Unit 1 (Henderson et al., 1991). The conglomerate is exposed almost continuously 10 km southward across the area and continues about 21 km further south to where it appears to lense out (Henderson et al., 1991; Figure 1-3). At the falls on the James River the conglomerate has a minimum thickness of 170 m (Jefferson et al., 1990, Fig. 9). Approximately 2 km to the southwest its thickness increases to 400 m. Structural discontinuities including folds and late faults affect the unit in the southwestern part of the

map area.

Poorly sorted, moderately rounded granule to boulder-sized clasts include variable proportions of volcaniclastic, plutonic (diorite), and sedimentary (greywacke, iron formation) rocks (Figure 3-6). The clasts, identical in character to many of the nearby rock units, are evidently of local derivation. Rusty, sub-rounded, up to 6 cm sized clasts in the southwest part of the mapped area could have been eroded from nearby iron formation. The conglomerate matrix is sandstone, similar in composition to that in underlying Unit 1 and contains mm-sized euhedral poikiloblastic garnets. In many cases clasts of sedimentary rocks are only faintly distinguishable from the sandy matrix in thin section and are indistinguishable in outcrop (samples 89127b, 90089 and 90B6; Figure 3-4).

Minor lenses of cordierite-bearing metagreywacke occur within Unit 2. One such lens is wide enough to be distinguished in the northwest part of the map (Unit 1, Map 1).

3.3.3 Volcanic sequence (Unit 3)

Unit 3 is a heterogeneous sequence; volcanic and clastic rocks are intercalated with each other and with intrusive rocks. This sequence has an apparent thickness of up to 1.5 km but pinches out, both to the north (Johnstone, 1990) and about 15 km south of the map area (approximately 25 km southwest of the James Falls, Henderson et al., 1991). The following discussion and lettering of sub-units is not necessarily in stratigraphic order due to their intercalated nature. The units range in thickness from less than one metre to tens of metres.

Rusty weathering andalusite ± cordierite biotite feldspathic arenite (Unit 3a) lies east and stratigraphically above the conglomerate. Unit 3a is intercalated with diorite (Unit 3b),

tonalite (Unit 5a) and at the main gold showing epiclastic amphibolite (Unit 3e). Lenses of conglomerate a few metres wide and up to 800 m long which are similar to the James Falls conglomerate (labelled as Unit 2 on Map 1) are dispersed within the arenite (sample 90077; Figure 3-4). Conversely, as indicated above, narrow (<10 m) lenses of the arenite occur within the conglomerate. The arenites are cross bedded and fine planar laminated and contain no mica-rich pelitic units (Figure 3-7) although biotite is present. From eight samples examined in thin section (samples 89084, 89118, 89126, 89139, 90078, 90087, 90092 and 90A9; Figure 3-4) the rock averages approximately 50% quartz (45 to 60% range), 15 to 20% biotite, less than 10% muscovite, less than 15%, less than 10% feldspar with andalusite ± cordierite porphyroblasts.

Extensive dioritic to gabbroic units (Unit 3b) are subparallel to bedding and outcrop as discrete lenses (Map 1). The largest is 1.5 km long and about 275 m wide and is bordered by trondhjemite to tonalite (Unit 5a) and a mixture of arenite (Unit 3a) and trondhjemite to tonalite (Unit 5a) on the eastern and western sides respectively. Other lenses have been mapped within the arenite (Unit 3a), mafic tuff (Unit 3d) and epiclastic amphibolite (Unit 3e). Much of the dioritic to gabbroic rock is engulfed by tonalite (Unit 5a), therefore its original extent is unknown. Sills less than 20 m wide are too small to be mapped as distinct units (Figure 3-8). Larger lenses or sheets are finer grained and foliated at the margins (central parts are coarser grained) where the rocks are commonly often indistinguishable both texturally and mineralogically from the mafic tuff (Unit 3d) both in outcrop and in thin section. Finely crystalline chill margins are well exposed on the James River where the

diorite (or gabbro) intrudes arenite (Unit 3a). The exact stratigraphic position of these sheets is uncertain; geochronology may provide better constraints.

Thirteen samples (samples 89015, 89022, 89026, 89034, 89041, 89049, 89059, 89094, 89096, 90059, 90062, 90074, and 90088; Figure 3-4) examined in thin section are composed of up to 55% plagioclase (average of 36%), up to 55% subhedral, poikiloblastic hornblende (average 37%) and from 5-20% quartz (average 12%). Some samples include up to 15% cummingtonite intergrown with biotite and hornblende and up to 5% opaque minerals including ilmenite, chalcopyrite, pyrite and pyrrhotite. Penny (1990) noted that the sulphide minerals include fine-grained and finely disseminated arsenopyrite and ilmenite with minor chalcopyrite and sphalerite away from the high strain zone, whereas within the high strain zone the sulphide minerals chalcopyrite, pyrrhotite, pyrite and ilmenite with minor sphalerite and pentlandite (exsolved from pyrrhotite) are massive and coarse grained. Traces of titanite and minor chlorite (up to 2%) have been noted in this study. Coarser grained dioritic rocks in the middle of larger lenses contain feathery amphiboles. Bulk compositions range from that of diorite in finer grained examples to gabbro in coarser grained examples. Anorthite contents determined by the Michel Levy method range from An_{38} (sample 89094) to An_{50} (sample 89015; Figure 3-9) all of which typify diorites (An<50; see Hyndman, 1985). The mafic content varies from 25% in the finest grained samples (cf. diorites <40%; Hyndman, 1985) to 65% in the coarser grained samples (cf. gabbros >40%; Hyndman, 1985). The high proportions of mafic minerals are not sufficient to designate the rocks as a gabbro. Anorthite content of plagioclase feldspar is crucial.

Discontinuous bodies, a few tens of metres wide, of a mafic to ultramafic amphibole-rich rock (Unit 3c) are mainly restricted to the high strain zone within the Unit 3 complex. Here it is spatially associated with mafic tuff (Unit 3d) and contacts are not clearly visible but appear to be gradational. In the southern part of the area, several bodies less than 50 m wide of the amphibole rock lie within Unit 4 metagreywacke. Contacts are conformable to bedding. In the southwest, the amphibole rock (Unit 3c) intrudes arenite (Unit 3a).

Unit 3c amphibole rock is typified by rounded outcrops with a pitted, hackly weathered surface and characteristic dark green mm-sized knobs, which in thin section, are pyroxene-shaped phenocrysts pseudomorphed to amphibole (tremolite-actinolite) in a fibrous, amphibole-rich groundmass altered to talc (samples 89071, 89079, 89145, tr11-3, tr11-6, 90004, and 90100; Figure 3-4). These rocks could be ultramafic flows or sills but no diagnostic textures or structures have survived metamorphism and deformation (Figure 3-10). They are conspicuously lacking in plagioclase. The whole rock geochemical signature of this unit was used to identify the pyroxenite protolith (see Chapter 6).

Banded biotite-amphibole-rich rocks (Unit 3d), are mostly restricted to the eastern side of the high strain zone with a few sporadic outcrops in the southwestern part of the map area, and is spatially associated with 3c amphibole rock. The biotite-amphibole-rich rock grades into and is interbedded with epiclastic amphibolite (Unit 3e). The unit is distinguished from Unit 3c in the field by the lack of conspicuous dark green amphibole phenocrysts and by a banded appearance (bedding) although where exposure is poor this is often obscure. Graded bedding is defined by the coarseness of amphiboles (reverse metamorphic grading; Figure

3-11). These rocks are virtually monomineralic in thin section (samples 89013, 89069, 89038, and 89125; Figure 3-4) and are composed of fine to medium-grained, randomly oriented tremolite-actinolite amphibole which is frequently altered to biotite (Figure 3-11). Unit 3d is interpreted as a mafic tuff.

Epiclastic amphibolite (Unit 3e) is intercalated with and grades into the mafic tuff (Unit 3d) on the eastern side of the high strain zone (samples 89076, 89120, 90096, 90097, 90098, 90099, and 90A46; Figure 3-4). Rocks are typically medium to dark greyish green in colour and characterized in outcrop by mm- to cm-scale laminations (Figure 3-12a), that are considered as depositional features. In thin section the laminations comprise varying proportions of quartz and feldspar with amphibole and biotite (Figure 3-12b). Rocks of 3e are distinguished mineralogically from 3d by the significant component of quartz and feldspar and a greater abundance of biotite. They are interpreted to be the reworked equivalent of 3d mixed with some clastic material.

A sulphidic (ilmenite, chalcopyrite, asenopyrite), amphibolitic, fine-grained clastic rock (Unit 3f) is interbedded on a metre-scale with the epiclastic amphibolite (Unit 3e), pyroxenite (Unit 3c) and mafic tuff (Unit 3d) (Appendix II, Figure a). It is best exposed at the main showing where it is the host for visible gold associated with quartz veins with some disseminated gold noted in the matrix (G. Walton, pers. comm., 1989). A more complete description of this unit is presented in Appendix II.

A well layered rock (Unit 3g) is characterized by alternating dark and light coloured bands up to a few cm wide (samples 90009B, 89116; Figure 3-4). Well exposed outcrops

are restricted to a few locations along the high strain zone although lichen cover may obscure the sub-unit elsewhere along strike (Figure 3-13a). Compositions of bands are highly variable, however in general, darker bands contain hornblende with minor amounts of clinopyroxene; lighter-coloured bands contain clinopyroxene and/or epidote (Figure 3-13b). The layering is interpreted as primary, representing epiclastic sedimentation or tuff deposition. On the other hand, the formation of epidote is favoured by shear stress (Deer et al., 1966) and thus the layering could have resulted from segregation during deformation. The geochemical signature of this unit (see Chapter 6) is similar to that for highly deformed tonalites found elsewhere within the map area (Unit $5a_m$) however the high proportion of mafic minerals in this rock is atypical of the tonalitic rocks.

Thin (less than 2 m) conglomerates and breccias (Unit 3h) derived from volcanic rocks or hypabyssal intrusions are exposed along the eastern margin of the Unit 3 sequence and intercalated within the arenite. A monomict conglomerate of felsic volcanic clasts in an amphibole-rich matrix marks the contact between the upper part of the epiclastic amphibolite (Unit 3e) and the overlying metagreywacke (Unit 4) in the central part of the map area. Crude graded bedding is suggested by the coarsest of the felsic clasts being located preferentially on one side of beds in some outcrops (e.g. Figure 3-14a). Elsewhere along this contact, also included in 3h, is a less than 25 cm layer of pebble breccia with an amphibole-rich matrix (Figure 3-15b).

At the main showing monomict volcanogenic conglomerate of well rounded pebble to boulder sized clasts is present at the contact between diorite (Unit 3b) and an intercalated

sequence of mafic tuff (Unit 3d) and epiclastic tuff (Unit 3e; sample 90037; Figure 3-4). Light-coloured clasts, possibly derived from the amphibole rock (Unit 3c) contain amphibole phenocrysts. The matrix is fine-grained and mineralogically similar composition to the epiclastic amphibolite (Unit 3e; Figure 3-15). The middle stratigraphic position of this conglomerate differs from those described above. Drill core logged by Chevron geologists and C.W. Jefferson reveals graded bedding in Units 3d and e that indicates the conglomerate underlies the diorite.

Tonalite clasts in a conglomerate (see Chapter 6) at the contact of metagreywacke-mudstones (Unit 4) and metapyroxenite (Unit 3c) distinguish this conglomerate from the James Falls variety which lacks granitoid clasts. Contact relationships are obscure, however this sub-unit has a minimum thickness of 100 m; atypical of the other conglomerates described at this stratigraphic position. These sub-units are all considered under the sub-unit 3h due to their stratigraphic position that distinguishes them from the unique James Falls conglomerate.

3.3.4 Metagreywacke-mudstone (Unit 4)

Quartz-biotite-muscovite pelitic schist and psammite (metagreywacke-mudstone) with dispersed cordierite and andalusite porphyroblasts and fibrolitic sillimanite occupy the eastern portion of the map area. Further south the volcanogenic and conglomerate sequences (Units 2 and 3) die out and there is no clear lithologic distinction between western (Unit 1) and eastern (Unit 4) metagreywacke-mudstones (Figure 1-3). Further north, outside the map area, Unit 4 is truncated by the Bathurst Fault. Sedimentary younging varies from eastward to

westward indicating tight folding as in Unit 1. From the arrangement further south where tops are more commonly eastward than westward (Henderson et al., 1991) it is assumed that the unit 4 metagreywackes lie stratigraphically above the volcanogenic rocks of Unit 3. Evidence from the thesis area is however, not unequivocal. The unit is typified by massive sandy beds and laminated pelitic beds, often followed by quartz stringers with thicknesses ranging from 2 to 25 cm (Figure 3-17). The rocks are composed of 35-55% quartz, up to 30% feldspar (10-30% range), 10-20% biotite, 5-10% muscovite, 5% fibrolitic sillimanite and trace amounts of tourmaline with cordierite and/or andalusite porphyroblasts (samples 89005, 89006, 89011, 89019, 89023, 89039, 89072, 89089, 89093, 89153, 90001B, 90005, 90015, 90017, 90035, 90048, 90049, 90053, and 90064; Figure 3-4). Unit 4 is mineralogically and sedimentologically similar to Unit 1 with the main difference being an increased content of quartz in Unit 4.

Thin (less than 50 cm) beds of sulphidic iron formation (Unit 4a) are present in the metagreywacke-mudstones about 900 m west of the south end of Turner Lake and 200 m east of central Turner Lake. The iron formation is dark grey to black and contains coarse, mm-sized garnets and chiastolite (samples 89010, 89078B, 89156, 90067, 90069A, and 90069C; Figure 3-4).

Quartz, biotite ± cordierite phyllite, interpreted as representing metasiltstone (Unit 4b) is located in the southern part of the map area immediately east of the high strain zone (sample 89087; Figure 3-4). It is interbedded with and grades into Unit 4.

3.3.5 Granitoid intrusions (Unit 5)

Tonalitic sills found primarily within the volcanic sequence (Unit $5a_m$) are characterized in thin section by fractured feldspar porphyroclasts with patchy extinction surrounded by a finer grained recrystallized groundmass of quartz and feldspar (samples 89012, 89020, 89035, 89046, 89068, 89115, 89119, 89129, 89136, 89152, 90001, 90028, 90030, 90061, 90072, and 90095; Figure 3-17). This unit can be misidentified as an intermediate volcanic rock in the field, however in thin section, well formed feldspar phenocrysts are indicative of a hypabyssal or plutonic protolith. This rock type is significantly younger (2.6 Ga; van Breemen, et al., 1992) than volcanic rocks found elsewhere in the Slave Province which are between 2.71 and 2.65 Ga (Mortensen et al., 1988) (see Chapter 7). Its geochemical signature (see Chapter 6) reaffirms that this unit is indeed a strained plutonic rock. Clots of biotite ± amphibole (hornblende ± tremolite-actinolite) are diagnostic features in outcrop (Figure 3-18a) and thin section (Figure 3-18b). Muscovite present as microlites in plagioclase feldspar porphyroclasts is indicative of hydration and can be present as flakes (up to 30% noted). Epidote is often present (up to 5%) and minor amounts of calcite (up to 5%) have been noted in samples taken closest to the high strain zone. Along the high strain zone, interfingering of rock types and strong foliations make determination of protolithology highly speculative. The amount of calcite increases as does alteration (epidotization). Some samples that are structurally continuous with less deformed rock of the same unit are indistinguishable in thin section (sample 90072) due to alteration. Trace amounts of titanite were noted in most thin sections.

Less deformed equivalents are found outside the high strain zone area and away from

the margins of the intrusions. Because the transition from highly to moderately deformed rock is gradational in this unit, they are given the same unit number, 5a. These porphyritic trondhjemitic sills are more equigranular than their more highly strained equivalents but have the same overall mineralogy (Figure 3-19). They are characterized by a weak to very weak foliation defined by biotite ± amphibole (samples 89122, 89028, 90055, 90073, 90060, 90044, 89154; Figure 3-17).

Two granitoid plutons intrude the supracrustal rocks: the very weakly foliated, Fish-hook Lake biotite, muscovite monzogranite or granite (Unit 5c) and the variably foliated Pistol Lake biotite granodiorite (Unit 5b).

The Pistol Lake biotite granodiorite (sample 89100; Figure 3-17) in the southern part of the map area extends south to Pistol Lake (Figure 1-3). Although the contact with Unit 4 rocks is sharp, with no intervening gneiss zone, it does not show up well on air photographs. Two pointed indentations of Unit 4 which extend into the pluton have been mapped along the northern contact. Two thin sills, and one larger apophyse of the pluton extend into Unit 4.

The Fish-hook Lake monzogranite defines the western margin of the supracrustal belt (Henderson et al., 1991) and the map area. Where the pluton intrudes Unit 1 in the northern half of the map area a migmatitic zone of mixed metasedimentary rock and granitoid injection extends about 500 m from the mapped contact into Unit 1. In the southern half of the map area the contact is much sharper; there is no mixing zone. Grain size in the Fish-hook Lake pluton averages 1 mm and contains up to 3 mm long plagioclase feldspar phenocrysts. Clode

(1987) noted hornblende in this pluton but it has not been noted in petrographic examination in this study (samples 89033, 89036, 89037, 89055, and 89112; Figure 3-17).

Related apatite-, tourmaline- and muscovite-bearing lithium-enriched pegmatite bodies (Unit 5d) are most abundant near the contact of the Fish-hook Lake monzogranite and decrease in abundance toward the east (sample 89051; Figure 3-17).

3.3.6 Mafic intrusions (Unit 6)

The above Archean rocks are intruded by four mafic dyke swarms. Unit 6a comprises thin diabase dykes which are located near and parallel to the north-south high strain zone. One of these is shown on Figure 8 of Jefferson et al. (1990). These dykes appear to have been deformed. Relatively thin (less than 2 m), dark green diabase dykes (Unit 6a) trend east-west and contain plagioclase megacrysts. Outcrop relationships suggest these are younger than the pegmatites and so the mafic dykes must postdate plutonism, however contact relationships with other mafic dykes have not been established.

Unit 6b consists of N-NW trending Proterozoic Mackenzie diabase dykes. Mackenzie dykes dated in the northern Slave Province have a badelleyite U-Pb age of 1267 ± 2 Ma (Lecheminant and Heaman, 1989).

The youngest intrusion is a sill-like segment, probably of a Franklin gabbro dyke (Unit 6c), striking north-northwesterly immediately east of Turner Lake where it forms large resistant cliffs. Badelleyite from a similar body on Quadyuk Island in Bathurst Inlet was dated as part of the Franklin event (723 ± 3 Ma) by Heaman et al. (1990). These rocks are composed of 45% plagioclase and 25% olivine in ophitic intergrowth and 20% ilmenite

exsolution in magnetite (pale pink lamellae within white host). This unit is relatively fresh compared to the Archean rocks (Figure 3-20).

An unusual dark green, massive amphibolitized olivine gabbro plug (Unit 6d) 50 m wide and 160 m long, west of Turner Lake, informally named "nickel knob" (Staargaard, 1987), intrudes Unit 4. No plagioclase has been recognized in thin section (sample 89018; Figure 3-18). Alteration obscures original textures and grain sizes. Relict olivine is now largely altered to tremolite-actinolite and chlorite. A few larger grains, up to 2.5 mm, of amphibole completely replacing olivine have been identified. Tremolite-actinolite amphibole has a ragged bladed to acicular habit with grains up to 1 mm long. Large Mg-chlorite flakes up to 1 mm in size contain opaque minerals along cleavage planes. Finer aggregates of 0.1 mm chlorite flakes form the groundmass along with fine grained tremolite-actinolite (Figure 3-21). Staargaard (1987) noted fine-grained quartz with variable amounts of feldspar in this unit which he named metamorphosed actinolite-plagioclase-chlorite rock. Further thin sectioning would be required to confirm either the presence or absense of feldspar in this rock. Grab samples taken by Staargaard (1987) reported 2.56% Cu, 1.24% Ni, 039% Co and 0.020 oz/t Au from chalcopyrite, pyrrhotite and pentlandite within unit 4 at the margin of this plug. This plug may also be related to the Franklin event.

3.3 Discussion

Detailed correlation of units of this study to those of Henderson et al. (1991) is difficult. Correlations in Appendix I are based on description and distribution of rock types.

The main difference between these two studies arises as a result of scale of mapping and the lithologic-structural emphasis of Henderson et al. compared to the stratigraphic-lithological emphasis of this study. Unit subdivisions of Henderson et al. (1991) are not as detailed as for this study because of mapping at a 1:50 000 scale rather than at 1:10 000. For example, Henderson et al. (1991) do not recognize the deformed tonalite sheets (Units 5a and $5a_m$ of this study). The tonalitic sheets are mostly included within their Unit t (Henderson et al., 1991), a mixture of volcaniclastic and subvolcanic rocks. Additionally, Unit 3a (arenite) of this study is only locally distinguished by Henderson et al. (1991) from the overlying and underlying metagreywacke-mudstones. The arenite is labelled by Henderson et al. (1991) as unit y (greywacke), which here is equated to Units 1, 3a and 4. Despite differences in mineralogy, specifically less biotite in Unit 3a than in the metagreywacke-mudstones of Units 1 and 4, Unit 3a is only distinguished by Henderson et al. where it is intercalated with conglomerate and there it is labelled as y' (cross-bedded arenite). Unit s (mafic metavolcanic rocks) of Henderson et al. (1991) is equated to Unit 3b (diorite/gabbro) of this study.

Figure 3-2. Photograph of Turner Lake high strain zone taken approximately 2 km south of the main showing, characterized by a lack of outcrop and intensely foliated rock. Note its road-like appearance. View along the zone toward the north ($67^0$11'50" $108^0$57'13").

Figure 3-3. Nature of bedding in Unit 1 cordierite schist. Sedimentary younging to the east from graded bedding in metagreywacke-mudstone. Photograph taken in northwestern part of map area ($67^0$13'20" $108^0$58'23").

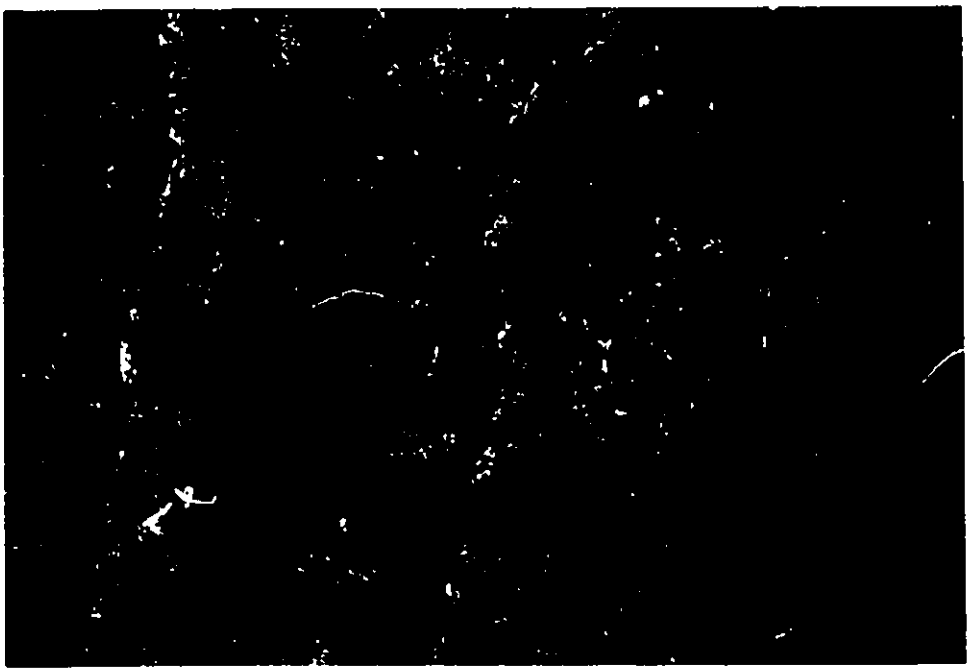

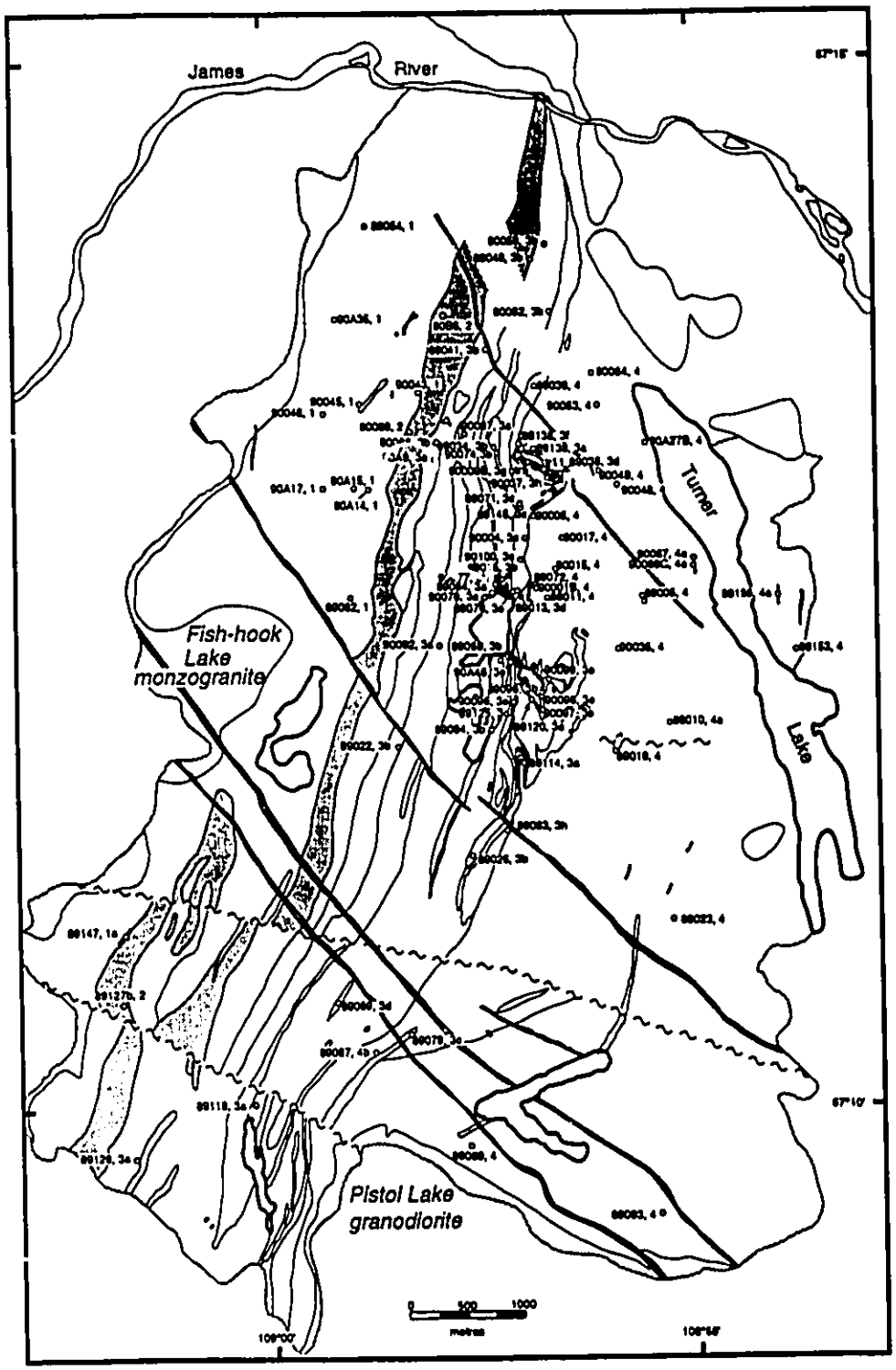

Figure 3-4. Sample location sketch map for supracrustal rock samples of the Turner Lake area. Sample number is given followed by unit number (see large scale maps 2a and 2b in back pocket). Diabase dykes are dark speckled units. Unit 2 conglomerate indicated with pale grey.

Figure 3-5. Prismatic sillimanite in Unit 1 in northwestern part of map area (67°12'40" 108°59'57").

Figure 3-6. Poorly sorted, moderately rounded clasts in James Falls conglomerate (67°13'24" 108°58'4").


5 5 5
CENTIMETRE
CANADA-NWT MINERAL
DEVELOPMENT AGREEMENT
INCH
5

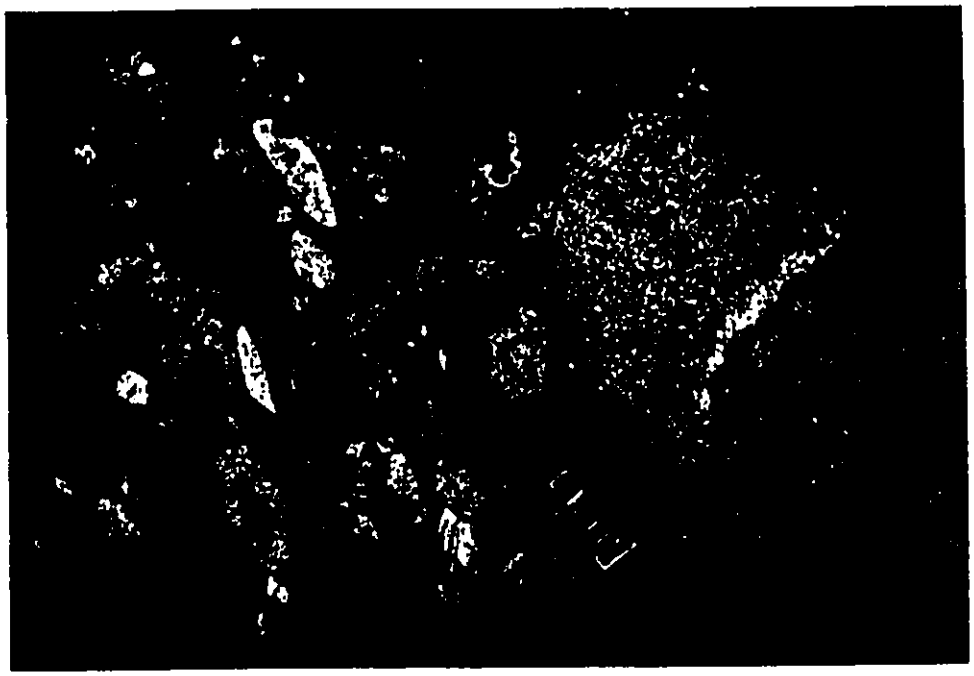

Figure 3-7. Cross-bedded and fine planar laminations in Unit 3a, arenite facing east. Photograph taken in central part of map area (67°12'50" 108°57'24").

Figure 3-8. Gabbro/diorite sills (Unit 3b) hosted in the west by unit 3a and in the east by a mixture of Unit 3a and Unit 3d (67°12'29" 108°57'11").

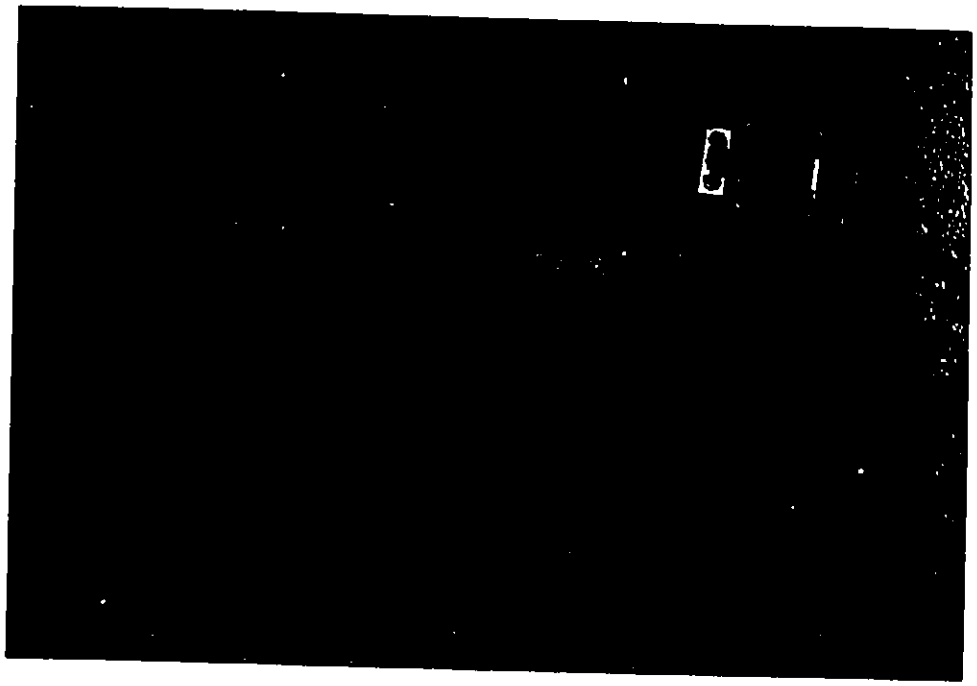

Figure 3-9. Photomicrographs of Unit 3b. (a) Coarse grained rock with gabbroic composition (sample 89094). Crossed polars. Field of view is 2.5 mm; (b) Fine grained diorite (sample 89015). Crossed polars. Field of view is 5 mm.


Pl
Hbl

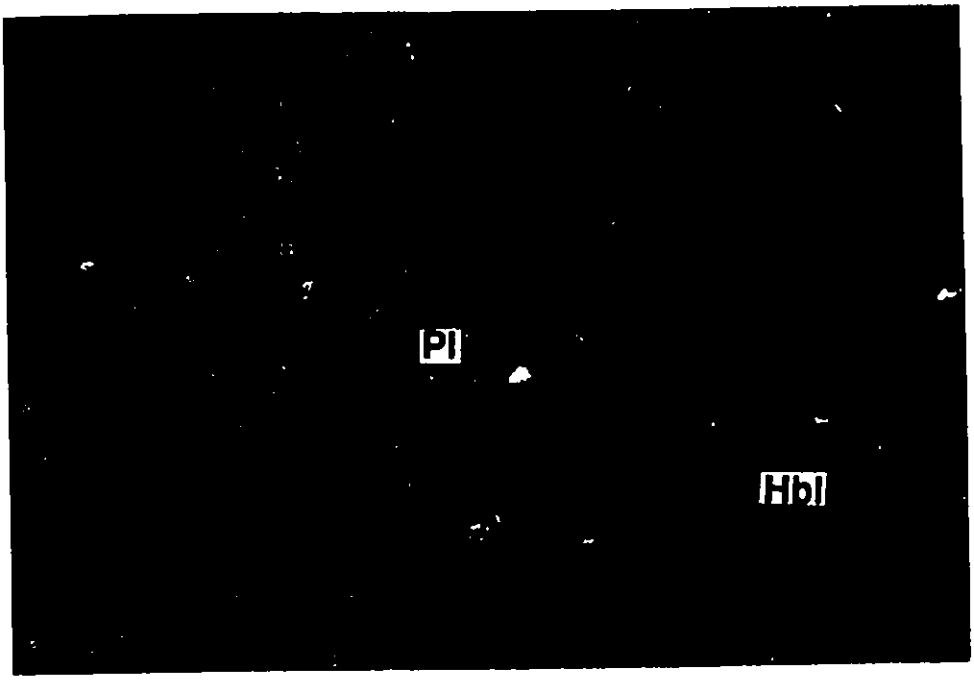
Pl
Hbl

Figure 3-10. Metapyroxenite with characteristic dark green pyroxene phenocrysts (Unit 3c).

Figure 3-11. Banded appearance of Unit 3d (mafic tuff). Banding caused by metamorphic reverse graded bedding ($67^0$12'55" $108^0$56'56").

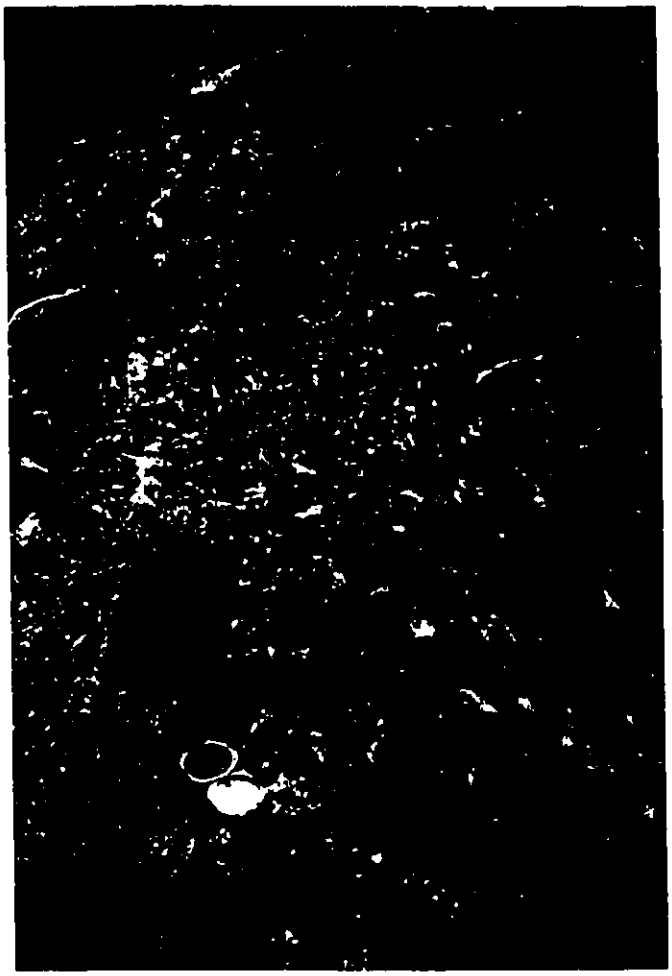

Figure 3-12. Unit 3e, epiclastic amphibolite. (a) Characteristic planar cross-laminations (67°11'47" 108°56'33"); (b) Photomicrograph showing laminations resulting from varying proportions of quartz and feldspar with amphibole and biotite (sample 90098). Plane polarized light. Field of view is 15 mm.

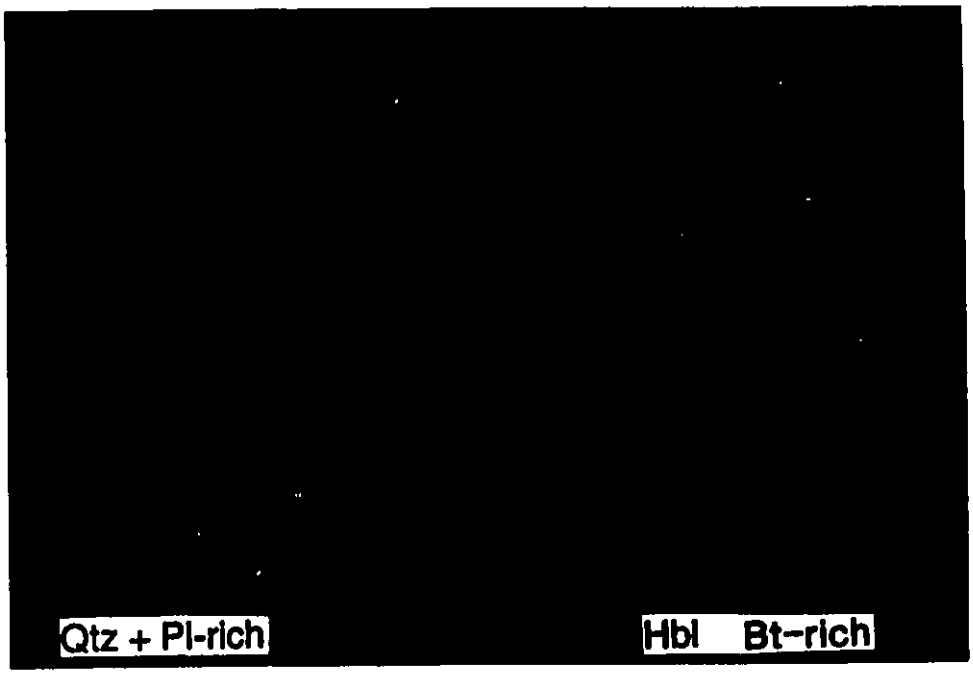
Qtz + Pl-rich
Hbl Bt-rich

Figure 3-13a. Layered Unit 3g characterized by alternating mafic and felsic bands ($67^0$13'2" $108^0$57'6"). (b) Photomicrograph of layered unit. Dark layers are rich in hornblende. Lighter layers are rich in clinopyroxene (sample 90009B). Plane polarized light. Field of view is 14.5 mm.

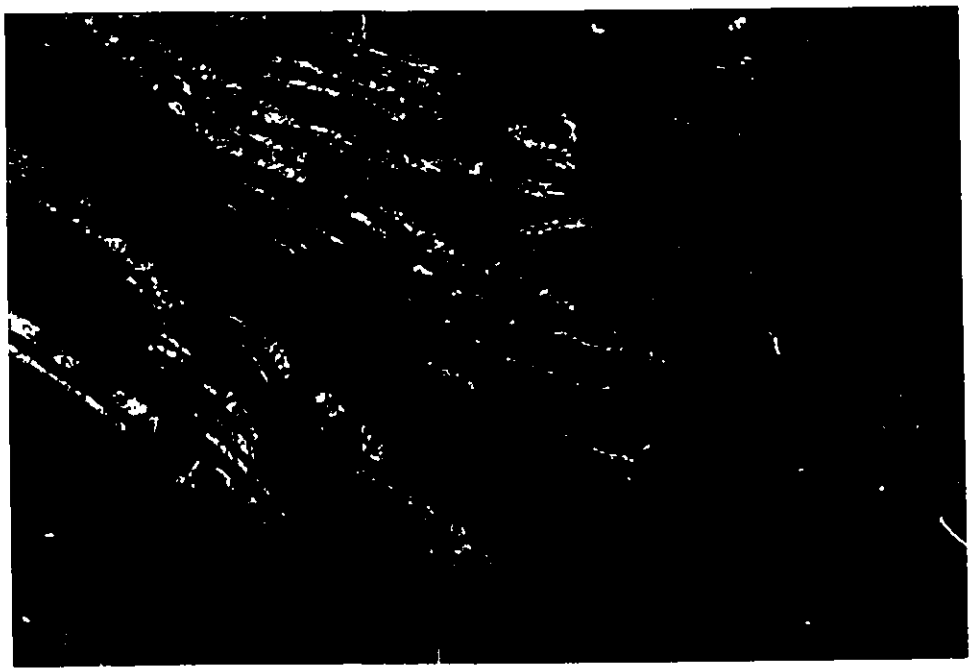


Hbl-rich
CPX-rich

Figure 3-14. Local conglomerate and breccia (Unit 3h). (a) felsic clasts in amphibole-rich matrix with graded bedding at contact of Unit 3e and Unit 4 (67°11'35" 108°56'49"); (b) Pebble breccia at contact of Unit 3e and 4 (67°11'53" 108°56'17").

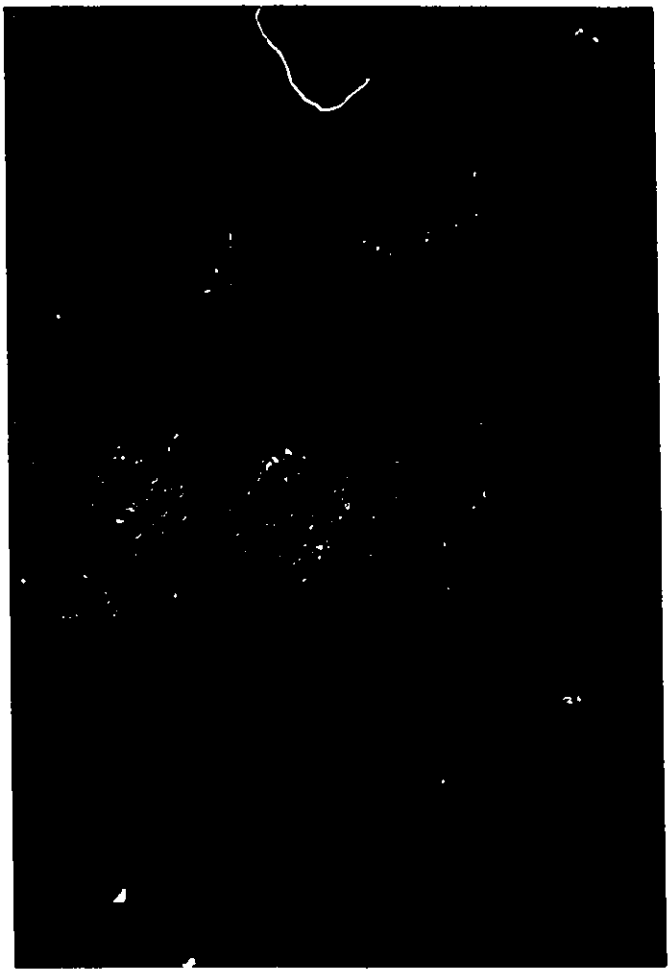

Figure 3-15. Conglomerate (Unit 3h) at main showing developed at contact between Unit 3b and a sequence of Units 3d and 3e ($67^0$13'1" $108^0$56'39").

Figure 3-16. Bedding in cordierite schist (Unit 4). Grading from metagreywacke to mudstone. Photograph taken in southeastern part of map area ($67^0$10'11" $108^0$56'3").

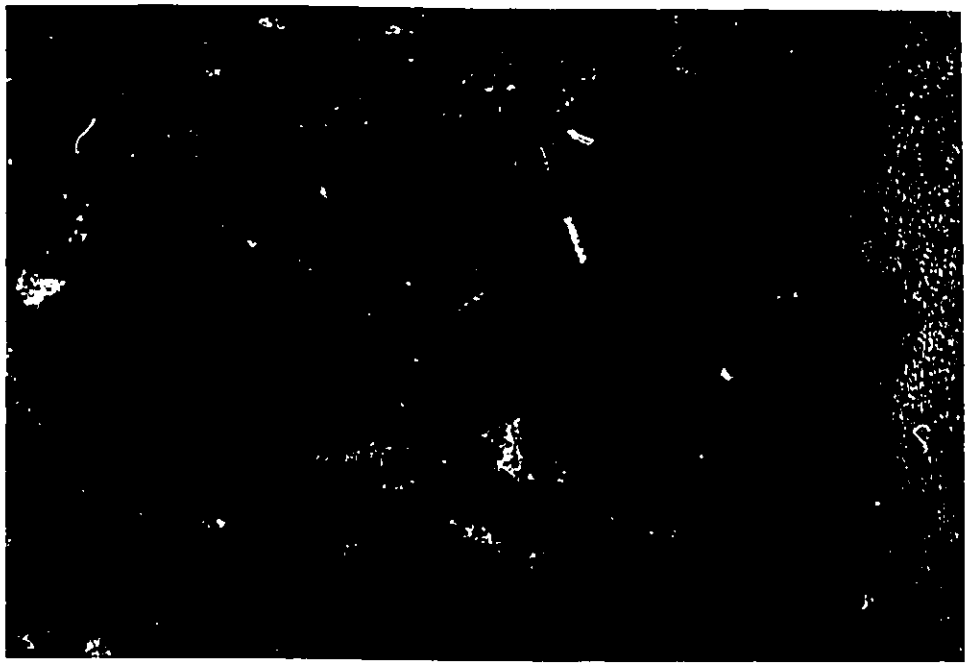

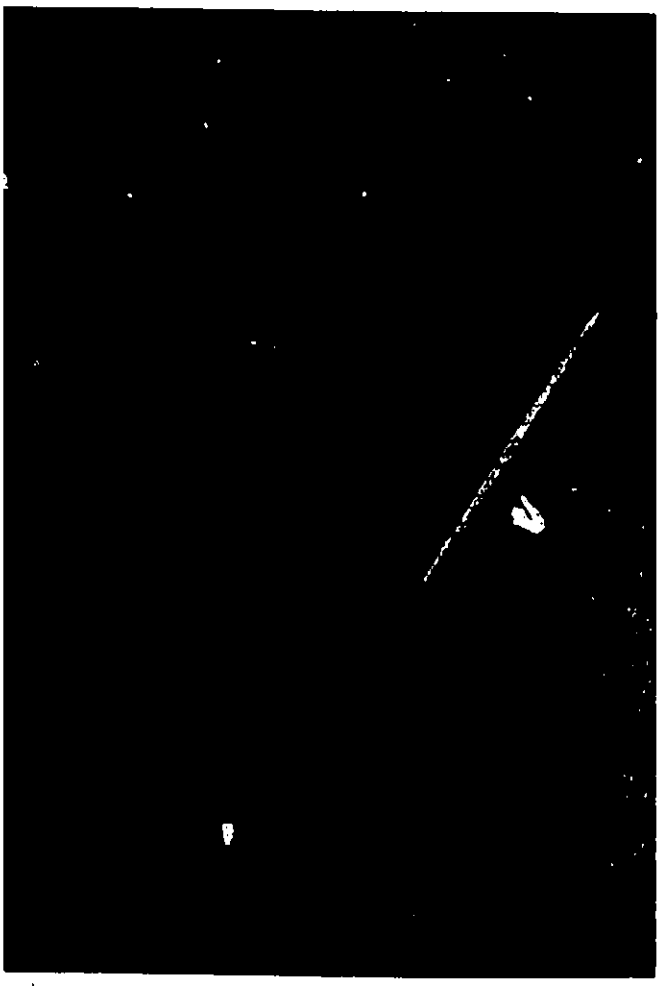

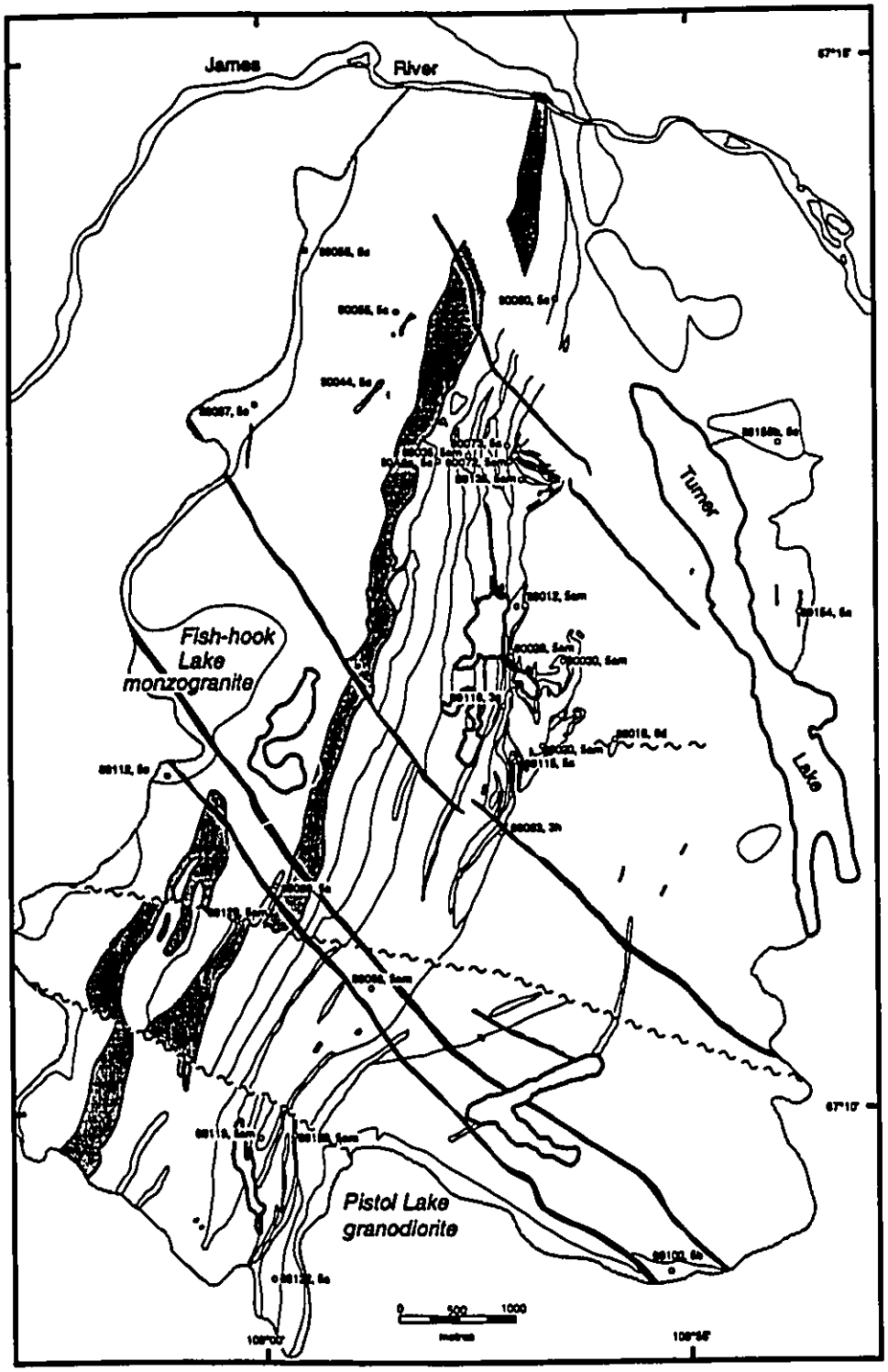

Figure 3-17. Sample location sketch map for plutonic rock samples of the Turner Lake area. Sample number is given followed by unit number (see large scale maps 2a and 2b (in pocket). Diabase dykes are dark speckled units. Unit 2 conglomerate indicated with pale grey.

Figure 3-18. Highly strained tonalite (Unit $5a_m$). (a) typical weathered surface appearance in outcrop ($67^0$13'48" $108^0$56'25"); (b) photomicrograph of deformed tonalite showing characteristic clots of biotite and hornblende with relict feldspar phenocrysts (sample 89119). Crossed polars. Field of view is 7 mm.

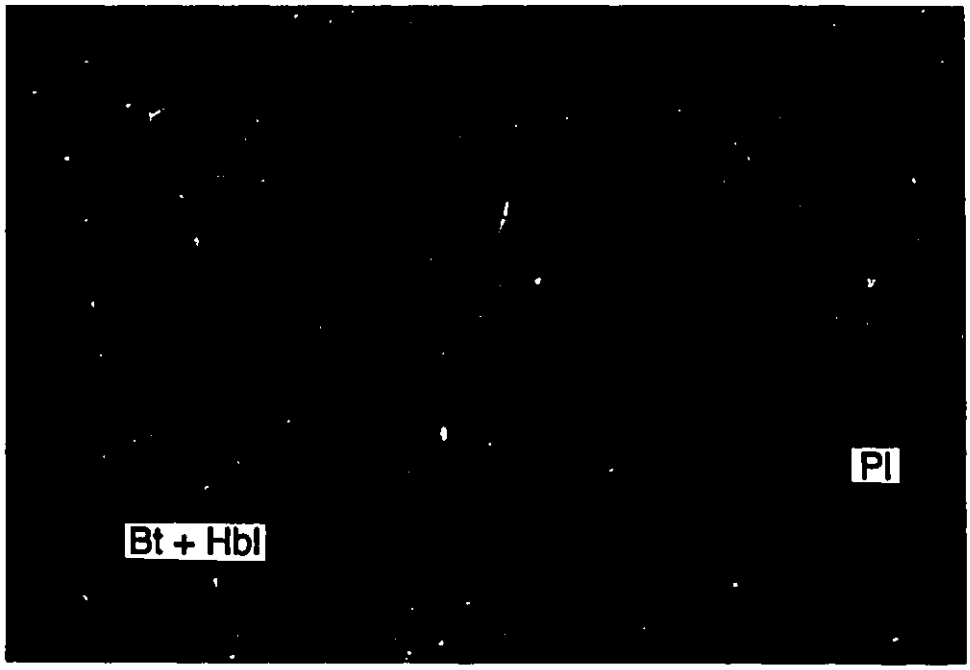
Pl
Bt + Hbl

Figure 3-19. Less deformed tonalite to trondhjemite (Unit 5a). (a) typical appearance in outcrop with characteristic feldspar phenocrysts; (b) Photomicrograph of trondhjemite. Note that this rock is less deformed than Unit $5a_m$ (sample 90055). Crossed polars. Field of view is 7.5 mm.

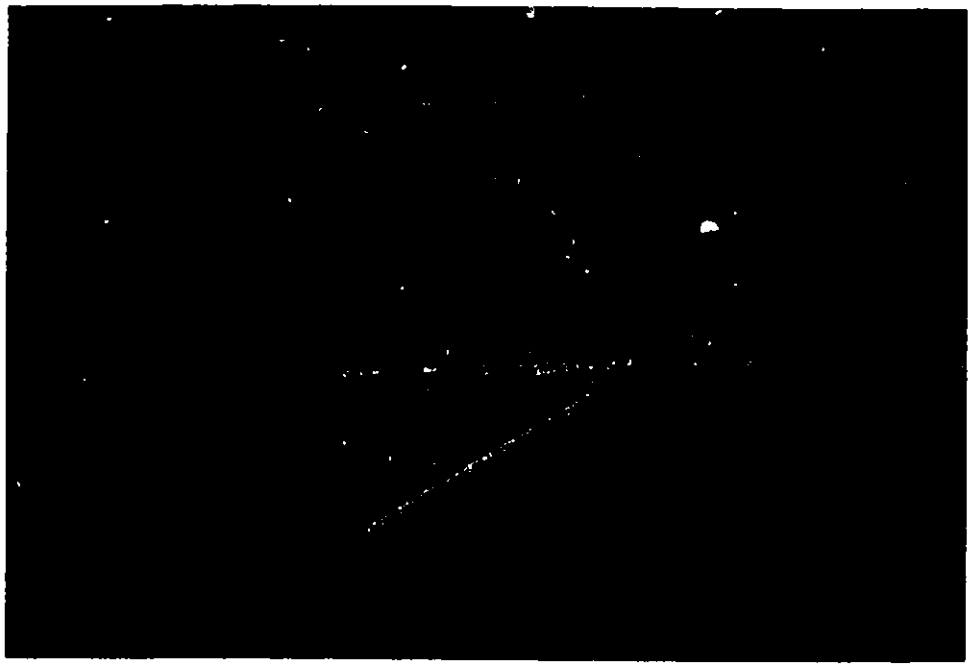


Pl

Figure 3-20. Photomicrograph of Franklin gabbro (sample 89155, Unit 6c). Crossed polars. Field of view is 19.5 mm.

Figure 3-22. Photomicrograph of "Nickel Knob" amphibolitized olivine gabbro (sample 89018, Unit 6d). Crossed polars. Field of view is 19.5 mm.


Ol

Chapter 4
Structural Geology

4.1 Introduction

In addition to the primary depositional features described in Chapter 3, most supracrustal rocks display deformational fabrics that record a complex structural history (Map 1). A prominent high strain zone and faults are conspicuous map-scale features. Several generations of structures were identified during field work, augmented by examination and interpretation of oriented thin sections. The arrangement of these structures, with additional data from Henderson et al. (1991) is shown on a page-sized form-line map (Figure 4-1).

North of the Turner Lake area within the Torp Lake domain most of the supracrustal sequence appears to be stratigraphically below the James Falls conglomerate. The rocks range from greenschist facies (below the biotite in isograd) to upper amphibolite facies (Venance, 1991; Johnstone, 1990a, b) with the high-grade rocks similar to the Turner Lake assemblage. The lower grade rocks preserve fabrics not evident in higher grade examples. Consequently, in order to interpret the structural history, a scheme is adopted that incorporates these fabrics even though they have not been clearly identified at Turner Lake (Table 4-1). A map covering the areas between the Booth and James Rivers (Henderson et al., 1991) provides a regional context (Figure 4-2).

Folds and cleavages reflect four main phases of progressive deformation (D_1, D_2, D_3 and D_4), a relative chronological sequence that does not imply four discrete deformational events. The metamorphic history of the Turner Lake area is closely tied to the deformational

Figure 4-1. Form line map of structural elements from the Turner Lake area including additional data from Henderson et al. (1991). For simplicity only the plutonic rocks (Units 5a, b and 5am) and conglomerate (Unit 2) are distinguished. Stereonets show orientations of structures.

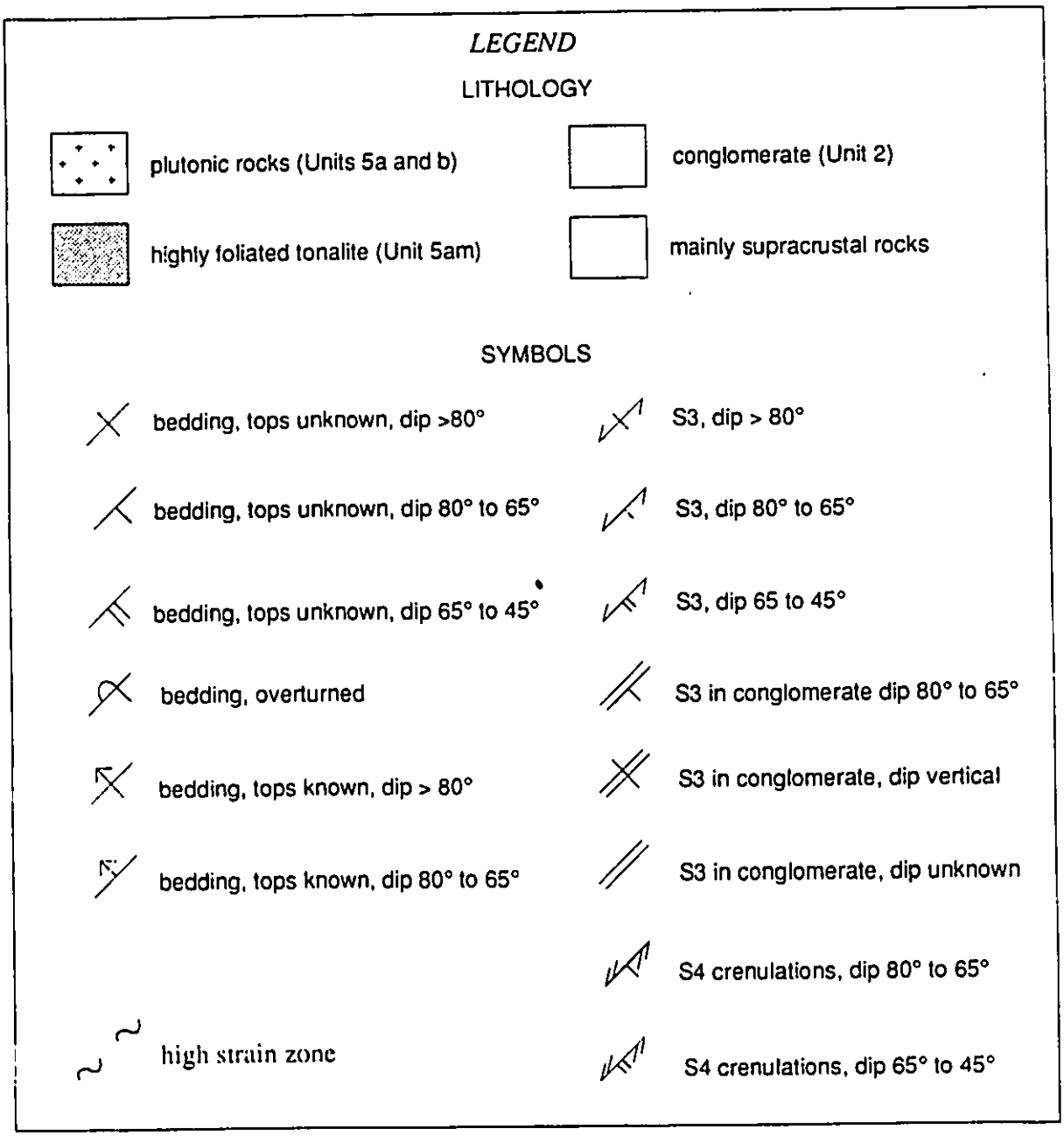

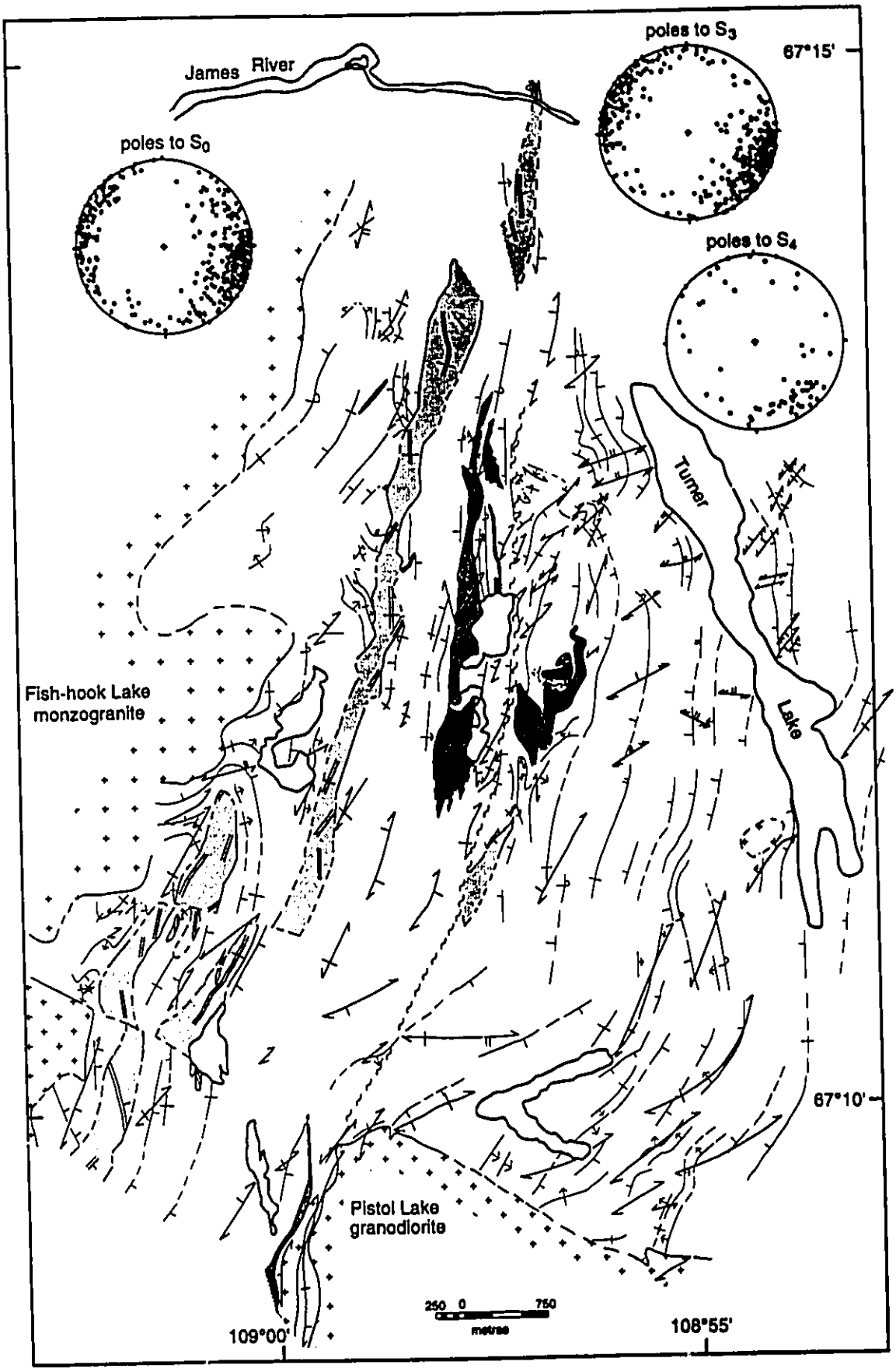
poles to S_3
67°15'
James River
poles to S_0
poles to S_4
Turner
Lake
Fish-hook Lake
monzogranite
67°10'
Pistol Lake
granodiorite
250 0 750
metres
109°00'
108°55'

Figure 4-2. Regional geology of the Hood River belt south of the James River including structural form lines (modified from Henderson et al., 1991). Area mapped for this thesis is roughly blocked out by brackets. The S3 fabric within the conglomerate Unit 2) is labelled using the same S3 symbol as for the other map units in the area.

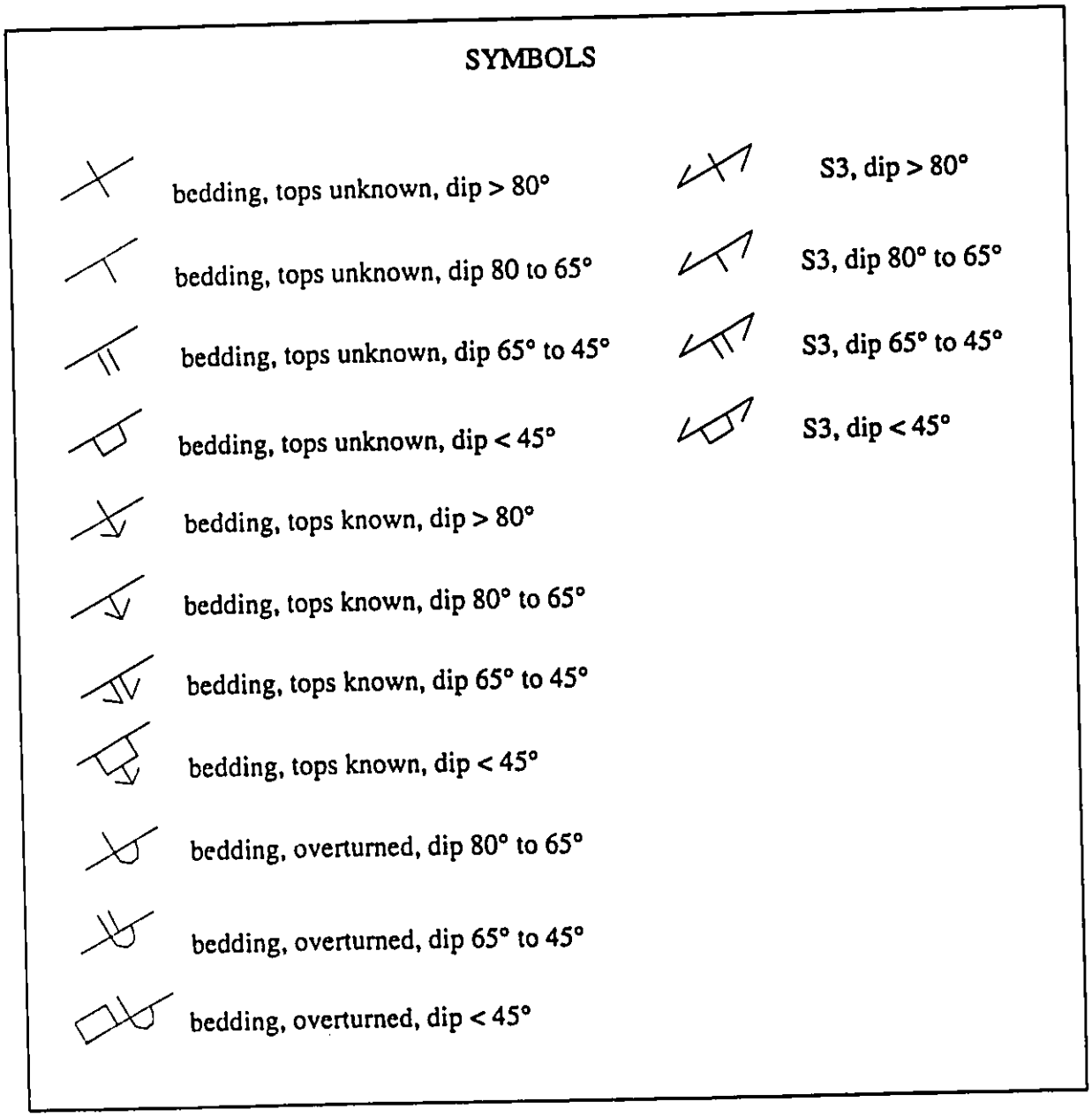

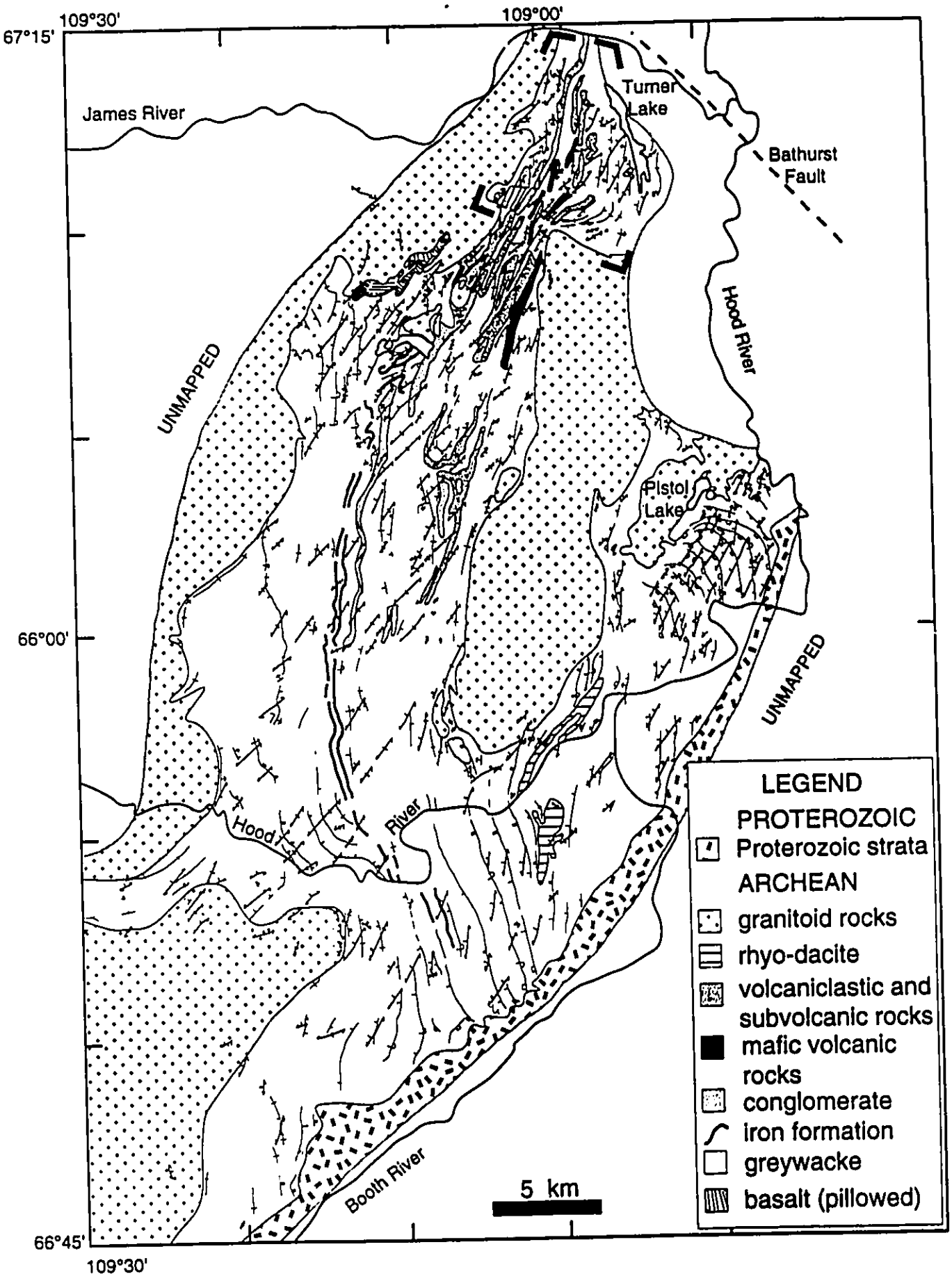
109°30'
109°00'
67°15'
66°00'
66°45'
109°30'
James River
Turner Lake
Bathurst Fault
Hood River
UNMAPPED
Pistol Lake
UNMAPPED
Hood River
Booth River
5 km
LEGEND
PROTEROZOIC
Proterozoic strata
ARCHEAN
granitoid rocks
rhyo-dacite
volcaniclastic and subvolcanic rocks
mafic volcanic rocks
conglomerate
iron formation
greywacke
basalt (pillowed)

Table 4.1 Synthesis and correlation of structural elements in the Hood River domain. Items in bold italic are present within the Turner Lake area; Others are from references cited from elsewhere (Torp Lake, Pistol Lake).

EVENT	FABRIC	STRUCTURE
	S0	***Bedding defined by compositional variation, emphasized by quartz stringers (S1 - S2?) parallel to bedding.*** S0: bedding parallel foliation folded by F1 isoclinal folds (Johnstone, 1990b) S0: moderate to steeply dipping, north to northwest strike (Johnstone, 1990a). S1-x: fine laths of white mica parallel to S0 in low grade pelitic rocks below biotite formation; not as distinct in psammites (Venance, 1991).
D1-D2	***F1 - F2***	***Upright, isoclinal folds defined by reversals in sedimentary tops within metasedimentary rock units; fold closures obscure.*** F1: major tight to isoclinal folds (wavelength 2 to 12 km) with subvertical to east-dipping axial planes and shallow to moderate plunge south; a transition to northerly plunge is recognized along some hinge lines (Johnstone, 1990a). F1: folds S1-x (Venance, 1991).
	S1 - S2	***Si: locally preserved bedding-parallel? foliation as quartz inclusion trails in sub-equant (blocky) biotite.*** S1: fracture cleavage, composite quartz veins (Johnstone, 1990b). S1: composite quartz veins and northwest biotite foliation in southern tonalites and diorites, Torp Lake domain (Venance, 1991). Si: internal fabric preserved in porphyroblasts consisting mainly of bedding laminations but some represent a local fabric (Henderson et al.,1991). S1: weak bedding parallel fabric preseved as elliptical quartz inclusions in younger porphyroblasts (J.R. Henderson, pers. comm., 1993). S2: inclusion trails of quartz and mica in cordierite porphyroblasts (Johnstone, 1990a). S2: locally within the Torp Lake area is a steeply dipping northwest trending foliation; sub-parallel to bedding and axial planar to tight folds in quartz veins (Johnstone, 1990b).
D3	F3	F3: steeply dipping northeast trending open folds; amplitude 1 cm to 1 m typical but can range up to 50 to 150 m (Johnstone, 1990b). F3: Open S-folds with vertical hinges (Henderson and Wright, 1993).
	S3	***Two directional sets: S3A and S3B; relative timing ambiguous.*** ***First well-defined tectonic fabric in Turner Lake area; defined by muscovite and biotite in metasedimentary rocks, amphibole + biotite in other lithologies. Most flattened clasts in conglomerate lie parallel to S3. Porphyroblasts lie with long axes in plane of S3 but are randomly oriented. S3 deflects around cordierite and is preserved in andalusite when both porphyroblasts occur in the same sample.*** S3: axial planar to F3 folds; steeply dipping, northeast strike (Johnstone, 1990b). S3: greenschist grade = slaty cleavage; higher grade = schistosity or crenulation cleavage (Johnstone, 1990a, b). andalusite, sillimanite undeformed but tend to be elongate parallel to S3 (Johnstone, 1990b). S3: at greenschist and lower amphibolite grade = slaty cleavage; at mid amphibolite grade, S3 external = biotite or biotite + fibrolite foliation. Deforms cordierite and andalusite porphroblasts and wraps around andalusite. relict andalusite and cordierite porphyroblasts preserve inclusion trails of S3 defined by quartz and biotite (Venance, 1991). S1: post-dates porphyroblastesis, penetrative, vertical, no associated folds (Henderson et al., 1991). S3: flattening of sedimentary and igneous rock clasts and flattening of porphyroblasts; defined by muscovite in metagreywacke, amphibole and biotite in other lithologies; regionally clockwise to bedding; refraction from pelite to psammite (J.R. Henderson, pers. comm., 1993).
D4	***F4***	***Mesoscopic, disharmonic open to tight folds; steep to vertical fold axes.***
	S4	***S4: local crenulation of bedding-parallel S3, moderately dipping, deforms late porphyroblasts.*** S4: sub-horizontal crenulation cleavage in greenschist and lower amphibolite facies pelites (Johnstone, 1990a). S4: spaced, sub-horizontal crenulation cleavage concentrates white mica and squeezes out quartz to either side of cleavage (Venance, 1991). S2: local crenulation cleavage axial planar to south plunging F2 folds (Henderson et al., 1991).
	S5	overprints S4 in greenschist facies pelites; steeply dipping northwest striking crenulation cleavage in Torp Lake area (Johnstone, 1990a).

history. Structures of different generations are distinguished based on overprinting relationships and their relationship to metamorphic mineral assemblages. Metamorphic minerals are particularly useful to distinguish fabrics where overprinting is not evident. Locations of examples figured at the end of this chapter are shown in Figure 4-3.

4.2 Structural Elements

4.2.1 Primary Structures

Bedding, S_0, is defined by compositional variation visible in both outcrop and in thin section. Lithologic characteristics are described in Chapter 3.

4.2.2 Early Structures (pre-F_1 folding)

Within the Torp Lake domain, fine laths of white mica parallel to S_0 form a S_{1-x} foliation in sub biotite grade pelites (Johnstone, 1990a; Venance, 1991). A foliation defined by similar low-grade minerals is not recognized in the Turner Lake area due to the higher metamorphic grade and obliteration by pervasive later foliations.

4.2.3 D_1-D_2 Structures

4.2.3.1 F_1-F_2 folds

Although fold closures are obscure, large-scale upright isoclinal folding of units 1 and 4 metagreywacke-mudstone is inferred from reversals in the direction of sedimentary tops in beds that are dominantly steep to slightly overturned. Hingelines of these folds must be sharp and in the Torp Lake domain fold axes are subhorizontal, plunging shallowly to moderately south with a transition to a northerly plunge along some hingelines (Johnstone 1990a, c).

Both Johnstone (1990a) and Venance (1991) indicate that the isoclinal folds, designated as F_1, affect an earlier fabric (S_{1-x}). The earlier fabric could also be considered as S_1 so that the isoclines are F_2 structures. At Turner Lake where hinges are obscure, the isoclines could include both F_1 and F_2 folds. F_1 or F_2 folding of the conglomerate (Unit 2) may account for repetitions of this unit in the southwestern part of the map area.

Traces of F_1 axial surfaces at Turner Lake appear to extend on a northerly trend over a minimum distance of 3 km based on facing directions of bedding. The long limbs face consistently eastward over a minimum of 500 m. One west-facing panel of rocks interpreted as a short limb can be traced out to a minimum distance of 300 m in the central part of the map area. In the Torp Lake domain, axial surface traces appear to extend at least 1 km, however it is difficult to extrapolate further due to variations in top directions.

South of Turner Lake toward the Hood River, beds predominantly young eastward which has suggested (Henderson et al., 1991) an east-facing homoclinal succession. However, the facing reversals at Turner Lake, and similar but more abundant reversals further north within the Torp Lake domain (Johnstone, 1990c) and also south at Pistol Lake are not in agreement with a simple homocline.

At Turner Lake and throughout most of the Hood River - Torp Lake domain, the F_1 or F_2 isoclines are steeply inclined. At Pistol Lake on the easternmost extremity, many folds are overturned eastward, some with axial-surfaces dipping less than 45^0 (Henderson et al., 1991), whereas in the north near the western extremity of the Torp Lake domain, folds are overturned westward. The steeply inclined folds at Turner Lake are locally overturned

eastward, as are folds further south that lie east of a poorly defined axial zone of fold divergence. The zone, marked by upright folds, trends northward across the Torp Lake portion of the supracrustal succession.

4.2.3.2 S_1-S_2 Foliation

Bedding is enhanced locally by parallel quartz stringers most commonly in laminated metasiltstone-mudstone in the eastern part of the map area (Figure 4-4). The stringers, which can be up to a few millimeters wide, may have formed as a result of metamorphic differentiation either during F_1 or F_2 folding.

The presence of elliptical quartz inclusion trails (S_1-S_2 or S_i) locally preserved in, sub-equant (blocky) biotite porphyroblasts from metagreywacke-mudstones is evidence for an early deformation event in the Turner Lake area. One sample taken east of Turner Lake clearly exhibits this fabric. The straight quartz trails are parallel to S_0 (Figure 4-5) and may have formed as an axial planar foliation to either F_1 or F_2 folds. These internal trails have been examined in detail from various locations both north and south of Turner Lake in biotite, cordierite and andalusite porphyroblasts. The quartz and mica inclusion trails within cordierite are assumed to have developed parallel to S_0 (Johnstone, 1990a; Henderson et al., 1991). The angular relationship of S_i to bedding varies from samples of metagreywacke-mudstone taken from various locations in the Hood River Belt (J. R. Henderson, pers. comm., 1993). The biotite porphyroblasts do not have pressure shadows which could be used as evidence for rotation or non rotation with respect to the external fabric.

4.2.4 D_3 Structures

4.2.4.1 F_3 Folds

At Torp Lake steeply inclined, F_3 open folds trend northeastward with typical amplitudes of 1 cm to 1 m, in the metagreywacke-mudstones but range up to 50 m to 150 m; they are accompanied by an axial planar S_3 cleavage (Johnstone, 1990a, b). Rare, open S-folds with vertical hinges are present along the Hood River southwest of Pistol Lake (Henderson et al., 1991). At Turner Lake, F_3 folds were not observed.

4.2.4.2 S_3 Foliation

The earliest recognizable fabric in outcrop which affects most rock types is a regional mineral foliation, S_3. S_3 developed as part of a multi-stage metamorphic culmination and is intimately linked to the growth of cordierite and andalusite porphyroblasts. S_3 formation varied locally from pre to post peak metamorphism. Two directional sets of the S_3 foliation have been identified, however they do not occur together and relative timing is ambiguous. The nomenclature S_3A (north northwest to northwest striking) and S_3B (northeast striking) is used to differentiate between these two orientations. S_3A and S_3B are best preserved as a bedding-oblique to locally bedding-parallel mineral foliation in the supracrustal rocks, including the metagreywacke-mudstones of Units 1 and 4, arenite (Unit 3a) and amphibolitic rocks (unit 3d and e). In the conglomerate (Unit 2), S_3A and S_3B are defined by flattened clasts. The two directional orientations are most obvious in this unit. The ambiguity in relative age is not unique to Turner Lake; for example similar ambiguous relationships are described in the Contwoyto Lake area where these are domainally developed, post thermal

peak cleavages in northwest and northeast-striking sets (Relf, 1990, 1992). For the purpose of discussion of fabric characteristics S_3 includes S_3A and S_3B. Both north and south of Turner Lake, the S_3 cleavage dominantly strikes northeast, clockwise to more northerly striking beds (Figure 4-6). Where beds curve to other directions, S_3 is anticlockwise (Figure 4-7).

Within the metagreywacke-mudstones (Units 1 and 4), S_3 is defined by aligned quartz, muscovite and or biotite crystals. Local refraction of S_3 in metagreywacke-mudstones of Units 1 and 4 from pelite to psammite does not show on the scale of mapping for this thesis but it may explain some small variations in strike. In many cases refraction results in a lower angle to bedding in psammites and a higher angle to bedding in pelites, the opposite of what would normally be expected. In pelitic beds where cordierite porphyroblasts are densely packed, their higher abundance could impart a greater relative viscosity (competency) than the psammitic beds which contain fewer porphyroblasts (Figure 4-8). There is no preferred orientation to the crystals. Normal refraction whereby S_3 is at a greater angle to S_0 in psammitic beds than in pelitic beds occurs in beds containing fewer or no porphyroblasts. The blocky biotite porphyroblasts which preserve S_1-S_2 are flattened along and are overgrown by S_3 (Figure 4-5).

Cordierite and andalusite porphyroblasts indicative of metamorphic peak conditions lie within the S_3 plane. Short axes of the cordierite porphyroblasts are perpendicular to the cleavage with a random orientation of the long axes in the cleavage plane (Figure 4-9). The mica foliation wraps around the porphyroblasts. Apparently cordierite growth was

preferentially in this flattening plane perhaps due to the anisotropy created during the early stages of its development. Cordierite growth began early in the development history prior to extensive growth of biotite and muscovite. As S_3 developed it was deflected around the porphyroblasts.

Johnstone (1990a) noted that porphyroblasts at Torp Lake preserve bedding-parallel S_2 (his assigned fabric) and an incipient northeast-trending crenulation cleavage (S_3). At Turner Lake, S_3 can be preserved in cordierite porphyroblasts as inclusion trails of biotite, quartz and opaque minerals. The trails within the cordierite are straight and continuous with an external fabric that is deformed by S_4 crenulations (Figure 4-10). The cordierite crystals therefore grew after S_3 had formed but before S_4. Andalusite rims to cordierite, with no aligned inclusions, also overgrow S_3 (Figure 4-11).

Thus two stages in the development of the S_3 foliation with respect to the peak of metamorphism can be outlined. Early-S_3 cordierite and andalusite porphyroblasts are inclusion-free and the foliation warps around them and post dates them. Development of porphyroblasts was preferentially in the S_3 flattening plane. In some cases where beds were "choked" with cordierite there is no preferred growth orientation. Late or post-S_3 cordierite includes S_3. Where conditions permitted the growth of both porphyroblasts, cordierite was apparently early (no aligned inclusions) whereas andalusite rims the cordierite and includes S_3.

Tonalitic to trondhjemitic sheets or tabular intrusions (Unit 5a) that approximately follow bedding are massive to moderately foliated parallel to S_3 in the adjacent

metasedimentary rocks and partly discordant to the margins. The foliation, assumed to be S_3, is usually defined by biotite ± hornblende. In coarser-grained examples, feldspar porphyroclasts are weakly aligned parallel to the mica foliation (Figure 4-12). The biotite ± hornblende foliation warps around relict pods of unrecrystallized feldspar and quartz (Figure 4-13) or relict feldspar phenocrysts (Figure 4-14) in recrystallized tonalite-trondhjemite intrusions along the main high strain zone.

Form lines of both bedding and the oblique S_3 cleavage gently curve in proximity to the northwestern margin of the Pistol Lake granodiorite (Unit 5b) where they are truncated by weakly or unfoliated granodiorite. The foliations within the pluton appear to be restricted to near the margins (Henderson et al., 1991). S_3 curves into parallelism with the pluton margin with curvature more pronounced than bedding (see Discussion for significance).

4.2.4.3 L_3 Lineation

Clasts in the conglomerate (Unit 2 and some in Unit 3h) are generally flattened in the S_3 plane. However, some are elongated (triaxial ellipsoid) and plunge northerly (Figure 4-15).

Dioritic to gabbroic sheet-like intrusions (Unit 3b) lie parallel to the bedding and are variably deformed. Along the high-strain zone there is a well developed lineation of hornblende (Figure 4-16) and based on fourteen measurements (Clode, 1987) the plunge varies from 40-60^0 north-northwest to north-northeast.

4.2.5 D_4 Structures

4.2.5.1 F_4 folds

Non penetrative, domainally developed F_4 folds vary from crenulations of the S_3

foliation to cm-scale warping of bedding to mesoscale open to isoclinal folds of bedding and bedding-parallel S_3. F_4 folds are preserved almost exclusively in the supracrustal rocks east of the high strain zone, most commonly in biotite-rich rocks including the epiclastic amphibolite (Unit 3e), mafic tuffs (Unit 3d) and metagreywacke-mudstones (Unit 4). A fold at the main showing bending S_0 has limbs extending approximately 400 m and may be an F_4 fold. Moderate to steeply dipping axial surface traces of F_4 folds range from a northeast to east-west orientation (Figure 4-1).

Metre-scale disharmonic folds of bedding and bedding-parallel S_3, with steep to vertical fold hinges are not uncommon. Some fold styles noted include tight to open folds (Figure 4-17; Figure 4-18; Figure 4-19) tight to isoclinal (Figure 4-20) and open folds (Figure 4-21).

4.2.5.2 S_4 Crenulation

The variability of style and orientation of D_4 structures is evident even on the scale of a thin section (Figure 4-10). In some areas, S_4 crenulations are tight with dark seams along the axial surface traces, presumably due to pressure solution whereas within a few millimetres in the same thin section the crenulations are open. Orientation of the axial surface trace varies from northeast to more easterly.

Centimetre- to millimetre-scale S_4 crenulations of S_3 are most strongly developed in pelitic beds where S_3 is sub-parallel to bedding (Figure 4-4 and 4-22). The relationship between S_3 and S_4 is illustrated in Figure 4-22a with details shown in Figures 4-22b and c. In psammitic beds where S_3 is at a higher angle to S_0, S_4 crenulations are not developed.

Commonly, the S_3 and S_4 cleavages are parallel and are not readily distinguishable in the field. Axial planes of microscopic S_4 crenulations of S_3 in one outcrop form a cleavage resembling parallel S_3 foliation displayed in an adjacent outcrop. Possible confusion over the generation (S_3 or S_4) of the parallel fabrics can be resolved by thin section examination where the crenulation of S_3 is apparent (Figure 4-22a-c). S_3 lying at a high angle to bedding in psammitic units curves into a similar mineral foliation within pelites, where it subparallels the layering and is crenulated. Axial planes of the crenulations forming S_4 in the pelite are nearly parallel to S_3 in the psammite. There is no conspicuous mineral alignment parallel to the axial surface trace of the crenulations, confirming that they formed later than the sub-parallel mineral fabric in adjacent, uncrenulated psammitic beds is S_3. Porphyroblasts of cordierite in some beds are mildly deformed at their edges by S_4 (Figure 4-11); evidently the crenulation is post peak metamorphism.

As shown in Figure 4-22, S_3 in pelitic beds is at less of an angle to bedding than in the psammites. The change in angle is extreme (up to 90^0) and cannot be explained by simple refraction. Possibly flattening across S_0 occurred, perhaps enhanced by slip along bedding surfaces. In the finer-grained more micaceous pelitic units, the S_3 foliation would rotate toward bedding. The S_3 foliation in the more quartz-rich psammitic beds would not be affected. Thus the angle between S_3 and S_0 in the pelite would be decreased making it susceptible to S_4 crenulation.

Similar relationships exist in the biotite and amphibole-rich amphibolitic units where S_3 appears to parallel S_0 and is crenulated by S_4 (Figure 4-23).

4.3 Discussion

4.3.1 Deformation and Metamorphism

The fabric elements present at Turner Lake considered with fabrics documented by other researchers in the Hood River belt, suggest a four-fold history of deformation which is considered in terms of the timing of porphyroblast growth. D_1 or D_2 deformation with isoclinal folding may have been accompanied by the development of an axial planar fabric (S_1 or S_2) at low metamorphic grades whereas D_3 was accompanied by peak regional metamorphism. Early, blocky biotite preserves S_1-S_2 as S_i. Early D_3 cordierite porphyroblasts grew preferentially in pelitic beds imparting to them a higher competency during later deformation than the less congested psammitic beds. Regional S_3 cleavage developed during early to mid-D_3 deformation. In the early stages of S_3 formation, porphyroblasts of cordierite or andalusite grew along the plane of anisotropy which was the site of biotite and muscovite growth. During continued mineral growth, andalusite developed as rims around cordierite and included the S_3 fabric. Following the peak of metamorphism, there was local F_4 folding and crenulations of S_3 where sub-parallel to bedding in pelitic units. S_3 in psammitic beds, where subparallel to S_4, was unaffected.

4.3.2 Structures and pluton emplacement

Although both S_0 and S_3 curve in the southeastern part of the map area approaching the Pistol Lake granodiorite, these curvatures do not mimic each other. The curves are envisaged to have developed under progressive compressive deformation and changing stress conditions. The Pistol Lake pluton was emplaced to present levels late in the D_3 event.

During early ascent it warped bedding and later may have modified the stress field influencing the orientation of S_3. It is suggested that the cleavage warped around the pluton as the S_3 foliation tended to develop in a flattening plane parallel to the margin, thereby reflecting variations in strain during regional deformation (cf. Fyson and Frith, 1979; Fyson and Jackson, 1991). A high fluid pressure aureole associated with the intrusion could be responsible. The pluton reached its present stratigraphic level following the development of the S_3 fabric hence the truncation of this fabric along the northern margin.

4.4 Late Structures

4.4.1 High strain zone

A north to north-northeast trending high strain zone transects the eastern side of the Unit 3 sequence and is offset by the Turner Lake faults. It is characterized by recessive weathering, carbonate and epidote altered rocks with a steeply dipping, strongly developed foliation in its immediate vicinity. The spatial association of highly foliated tonalite (Unit $5a_m$), amphibolitic rocks (Units 3d and e; mafic tuffs and epiclastic amphibolite respectively) and recrystallized layered volcanic rocks (Unit 3g) is also characteristic (Figure 4-24a). It is difficult to determine the protolith of some of the recrystallized rocks along this zone (Figure 4-24b). The zone lies oblique (trends about 10 to 30^0 counterclockwise) to the regional S_3 foliation.

The ultramafic pyroxenite rock (Unit 3c) occurs almost exclusively east of and along the high strain zone. It is possible that it was tectonically emplaced along the zone or that

the zone was the site of later movement along a pre-existing break which was the site of ultramafic volcanism.

4.4.2 Proterozoic Faults

Proterozoic faults are shown by topographic features and offset of lithological units (Figure 4-25). The Turner Lake valley appears to follow two north-northwest striking faults partly marked by steep rock faces along the lake. Northwest of Turner Lake, a minimum offset of approximately 280 m is suggested by offset of the conglomerate (Unit 2).

Offsets of variable sense are shown by two west northwest to east-southeast trending faults in the southern part of the area (Figure 4-25).

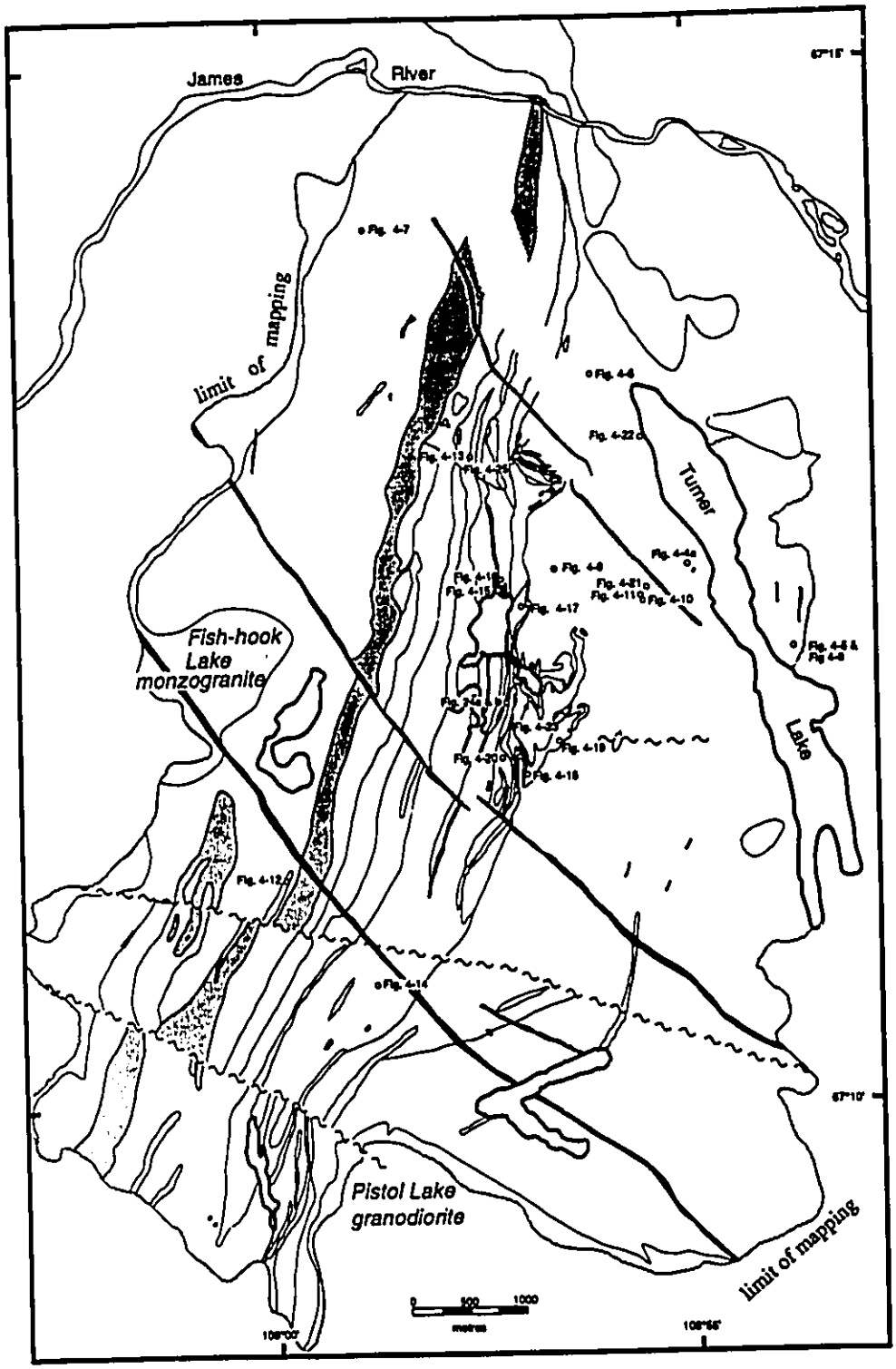

Figure 4-3. Location of examples figured (photographs and photomicrographs) in chapter 4. Diabase dykes trend northwest across area. Unit 2 conglomerate indicated with pale grey.

Figure 4-4a. Metagreywacke-mudstone (Unit 4) west shore of Turner Lake. Note bedding-parallel quartz stringers (S_1-S_2). Weakly crenulated bedding-parallel laminations are evident in the psammitic bed (left side of photograph) however S_3 is poorly developed. S_3 is slightly oblique to S_0 and is crenulated in the pelitic bed. The crenulations augment the appearance that S_3 is parallel to S_0. Brunton compass points north. Pen magnet is parallel to S_4. Refer to Figure 4-22 for details on S_3 and S_4 relationships.

Figure 4-4b. Sketch emphasizing details from a.

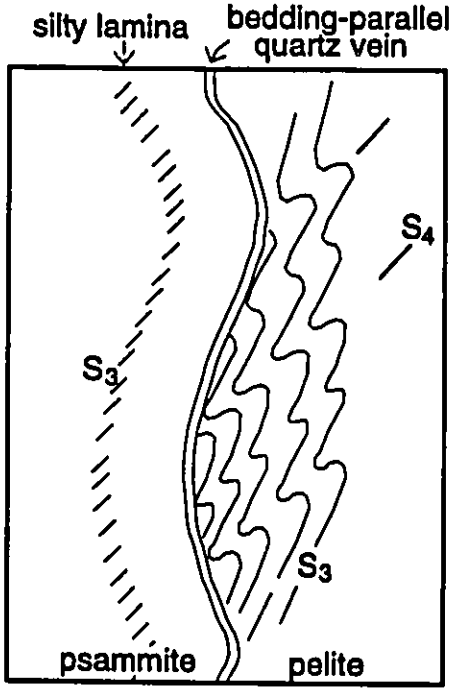

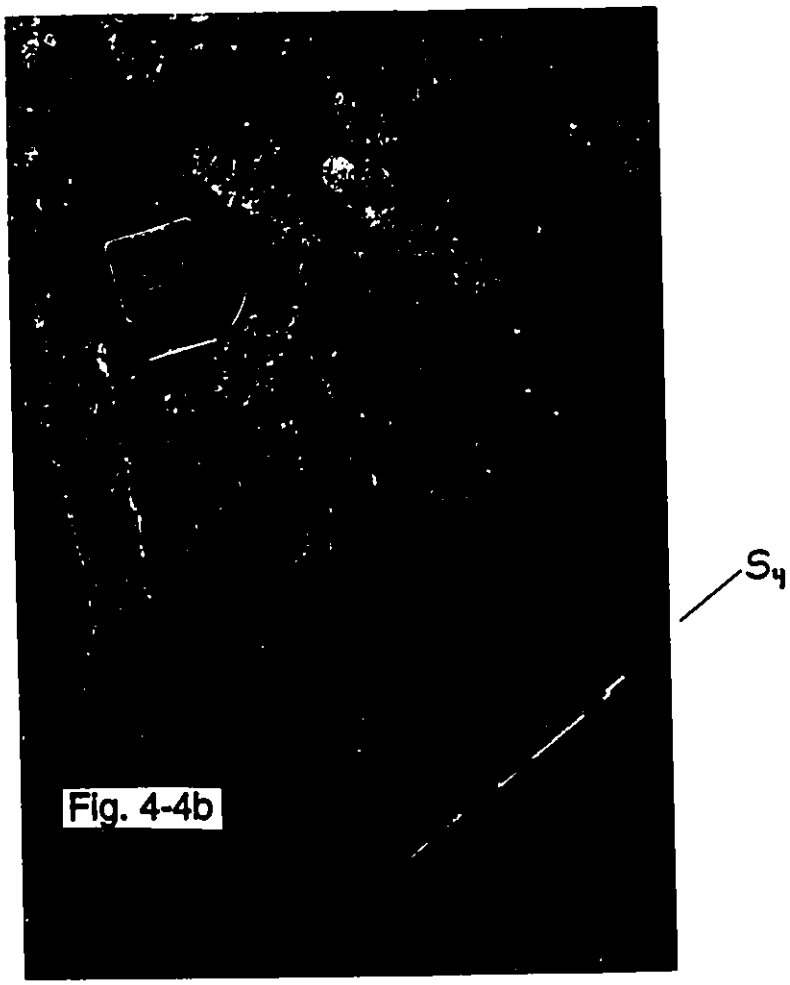

Fig. 4-4b

Figure 4-5. Straight quartz inclusion trails (S_1-S_2 or S_i) in sub-equant biotite porphyroblasts in metagreywacke-mudstone (Unit 4, sample 89153) from east of Turner Lake. The enveloping surface of northerly-striking bedding undulates and is indicated by the dashed line. Crossed polars in upper frame. Plane polarized light in lower frame. Field of view is 9.5 mm. Refer to Figure 4-8 for wider field of view.

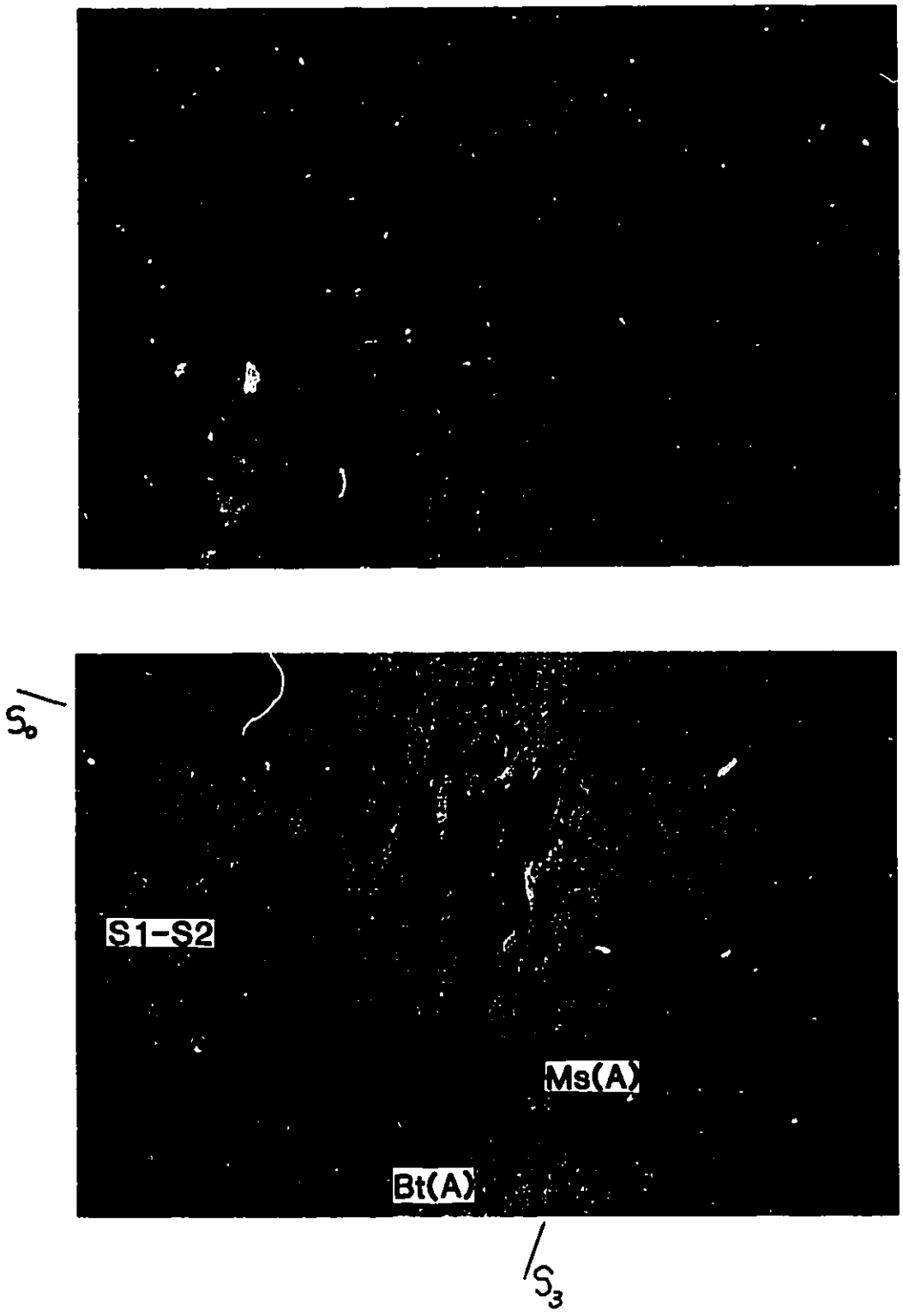
S1-S2
Ms(A)
Bt(A)
S3

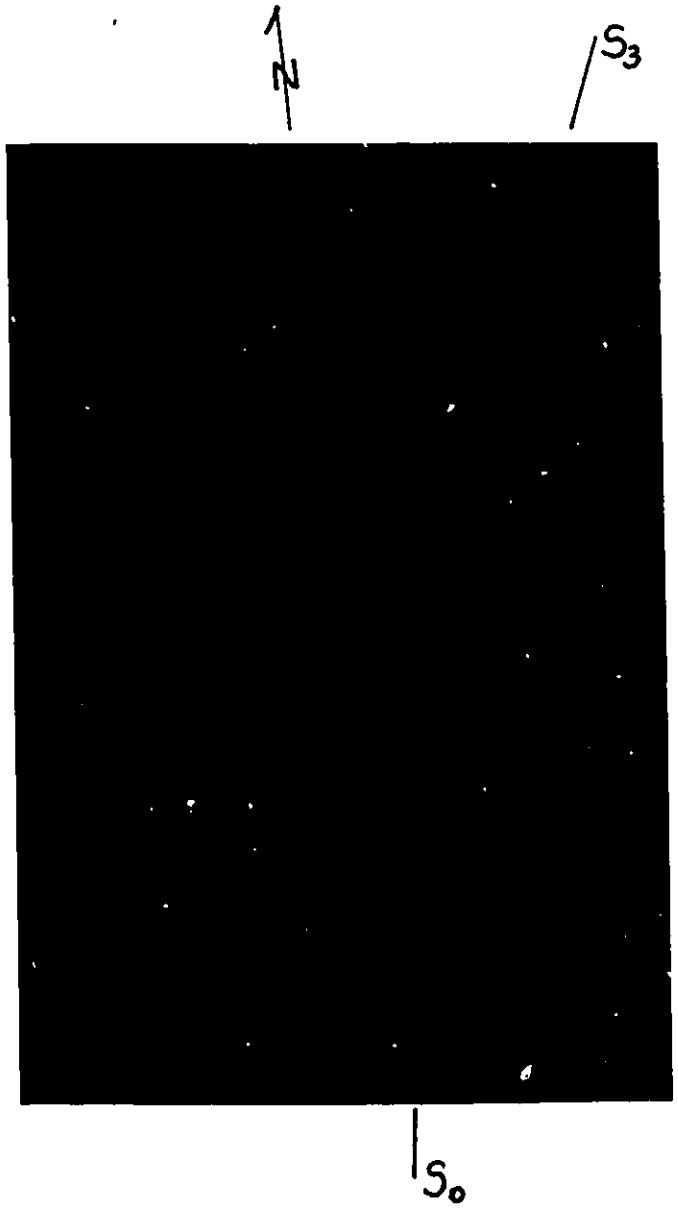

Figure 4-6. Photomicrograph of metagreywacke approximately 650 m northwest of Turner Lake from Unit 4 (sample 90064) with S_3, muscovite and biotite foliation striking northeast (202/81) clockwise from north-south, vertical bedding. Plane polarized light. Field of view is 8 mm.

Figure 4-7. Photomicrograph of metagreywacke (Unit 1, sample 89054) from approximately 1.5 km south of the James River with a weakly developed anticlockwise to S_0, northerly-striking biotite + muscovite foliation (S_3). Thin section cut perpendicular to northeasterly-striking bedding. Crossed polars in upper frame. Plane polarized light in lower frame. Field of view is 8 mm.

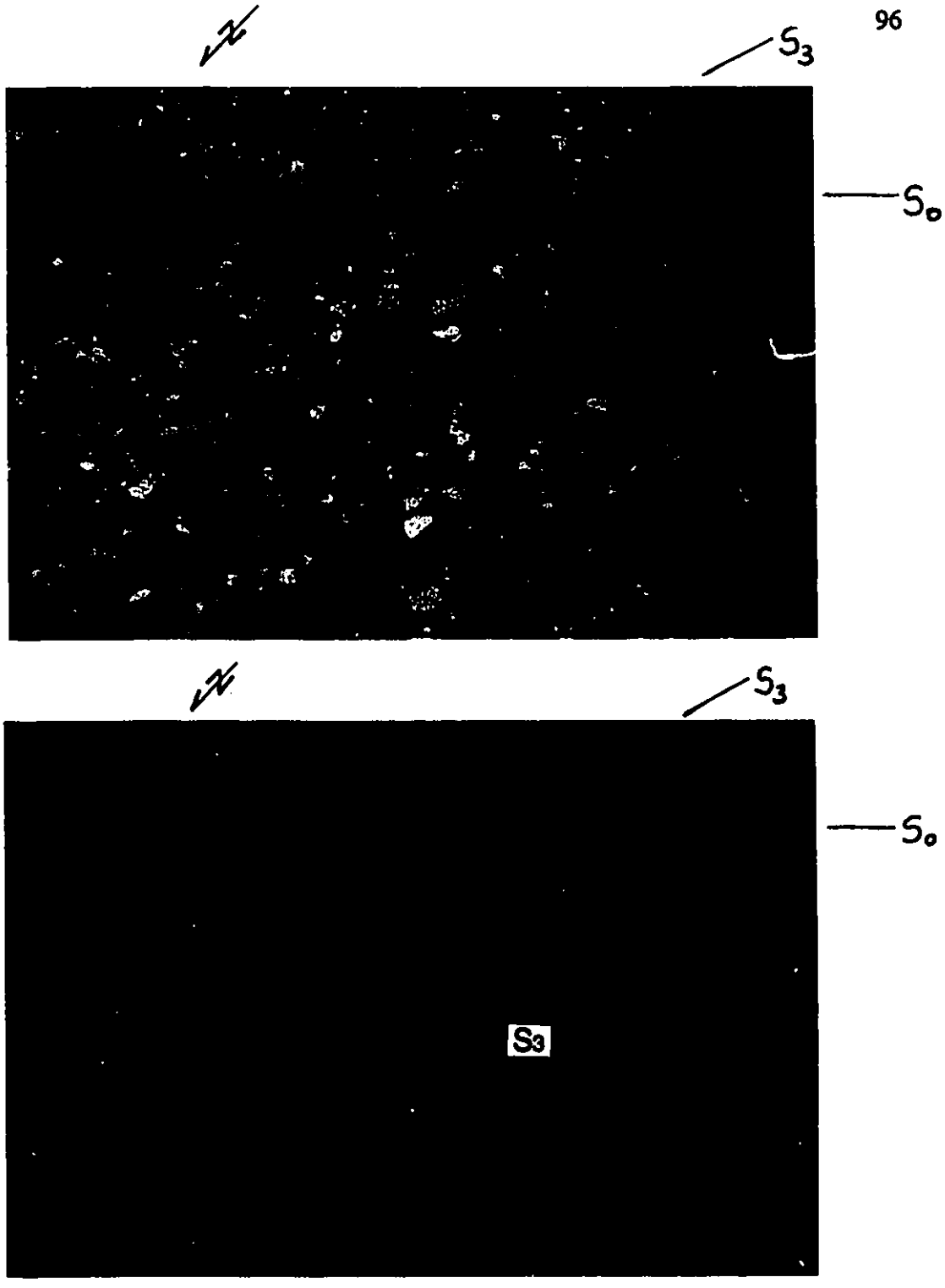
N
S3
So
N
S3
So
S3

Figure 4-8a. Anomalous refraction of S_3 cleavage in metagreywacke-mudstone (Unit 4, sample 89153) east of Turner Lake. S_3 is at a lower angle to bedding in the psammitic bed and a higher angle to bedding in the cordierite-rich pelitic bed. The cordierite porphyroblasts are densely packed and are more abundant in the pelitic bed imparting to it a higher competency than the psammitic bed, which contains fewer porphyroblasts. Location of Figure 4-5 is in bottom right hand corner. Field of view is 30 mm.

b. Idealized sketch of bedding/cleavage relationships based on thin section description above.

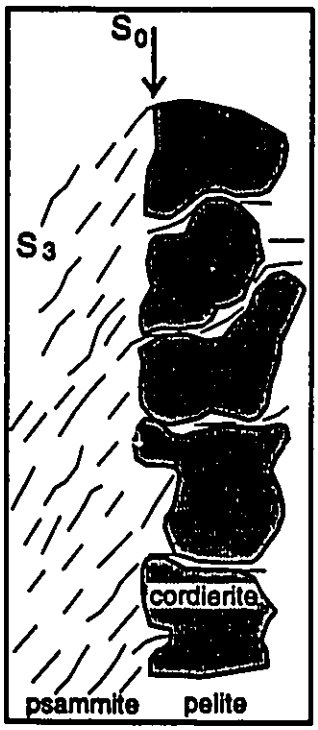

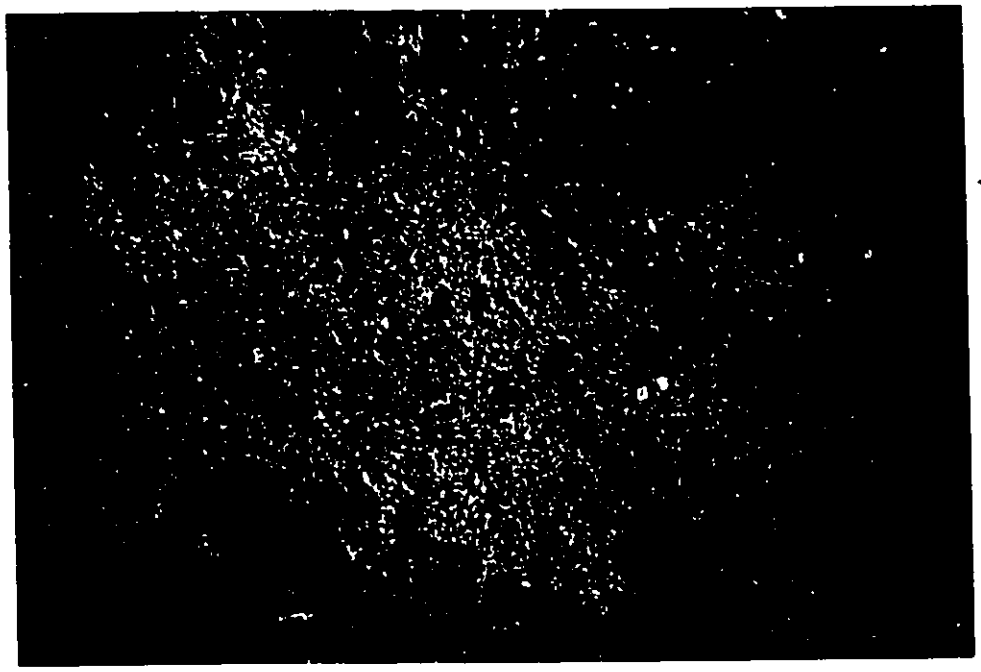
S_o

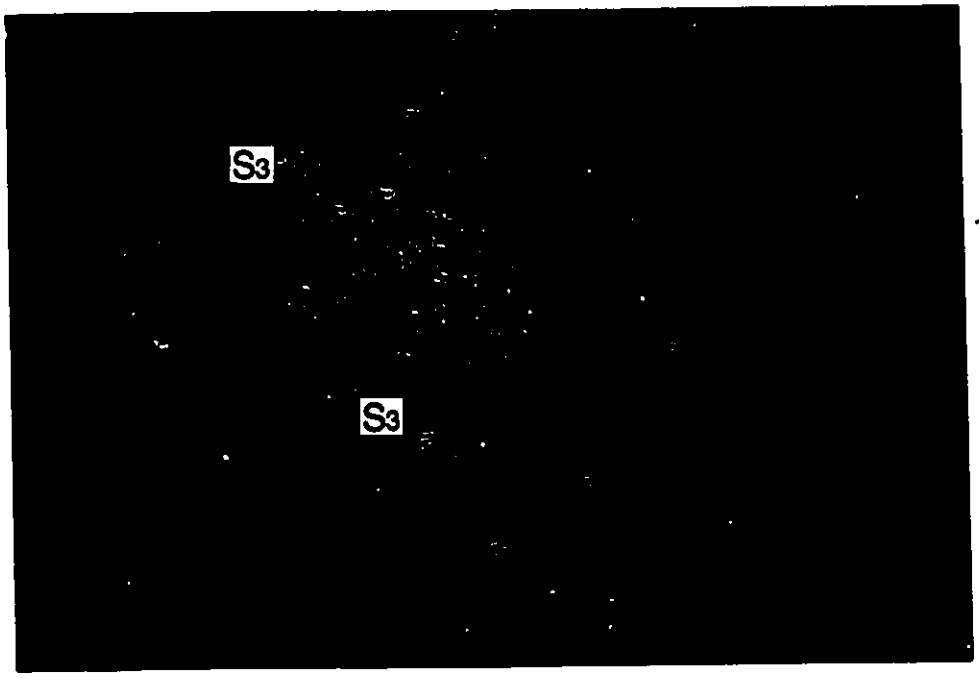
S_3
S_3
S_o

Figure 4-9. Photomicrograph of metamudstone from Unit 4 west of Turner Lake (sample 90015) with altered porphyroblasts (probably cordierite) developed along the anisotropy created by the S_3 flattening plane. The biotite + muscovite S_3 foliation warps around the porphyroblasts. Crossed polars in upper frame. Plane polarized light in lower frame. Field of view is 13.5 mm.

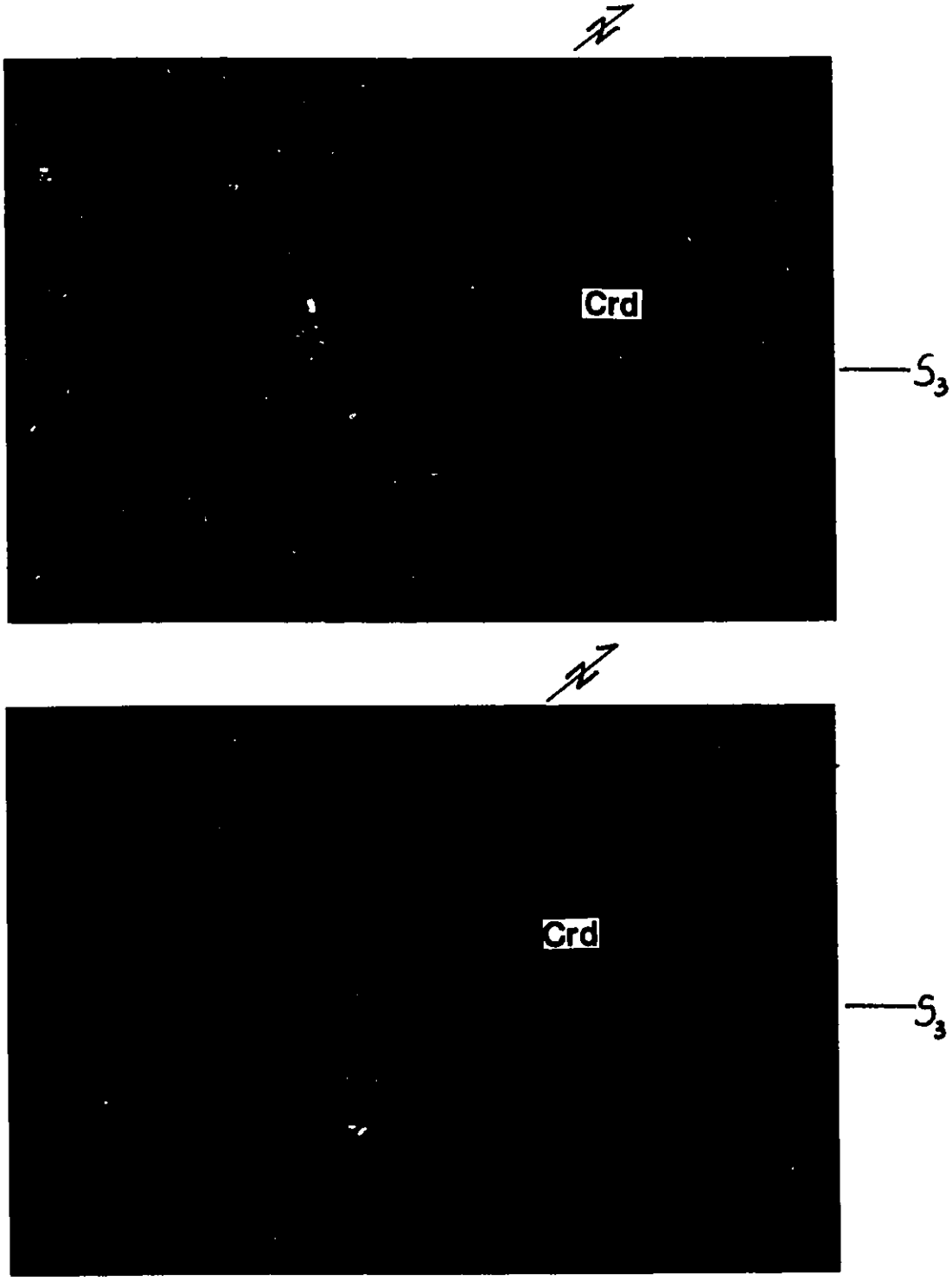
100
Crd
S_3
Crd
S_3

Figure 4-10. Photomicrographs of crenulated cordierite, muscovite, biotite schist (Unit 4, sample 89006) illustrating the effect of rock anisotropy on fold style and orientation. Cordierite porphyroblasts preserve a straight S_3 fabric internally defined by biotite, quartz and opaque minerals. The internal fabric is continuous with an external, S_3 biotite + muscovite foliation crenulated by S_4. The margins of the porphyroblasts are mildly deformed where the S_3 fabric is affected by S_4. Crenulations vary from open undulations near porphyroblasts to tight to isoclinal folds where more distant. Axial surfaces of open folds adjacent to porphyroblasts in the southwest quadrant strike easterly at high angles to straight internal foliations whereas where folds tighten, axial surfaces curve northeastward. The overgrowth indicates that porphyroblast growth was post S_3 development but pre S_4 crenulation. Thin section cut perpendicular to S_3 foliation. Crossed polars upper frame. Plane polarized light in lower frame. Field of view is 13 mm.

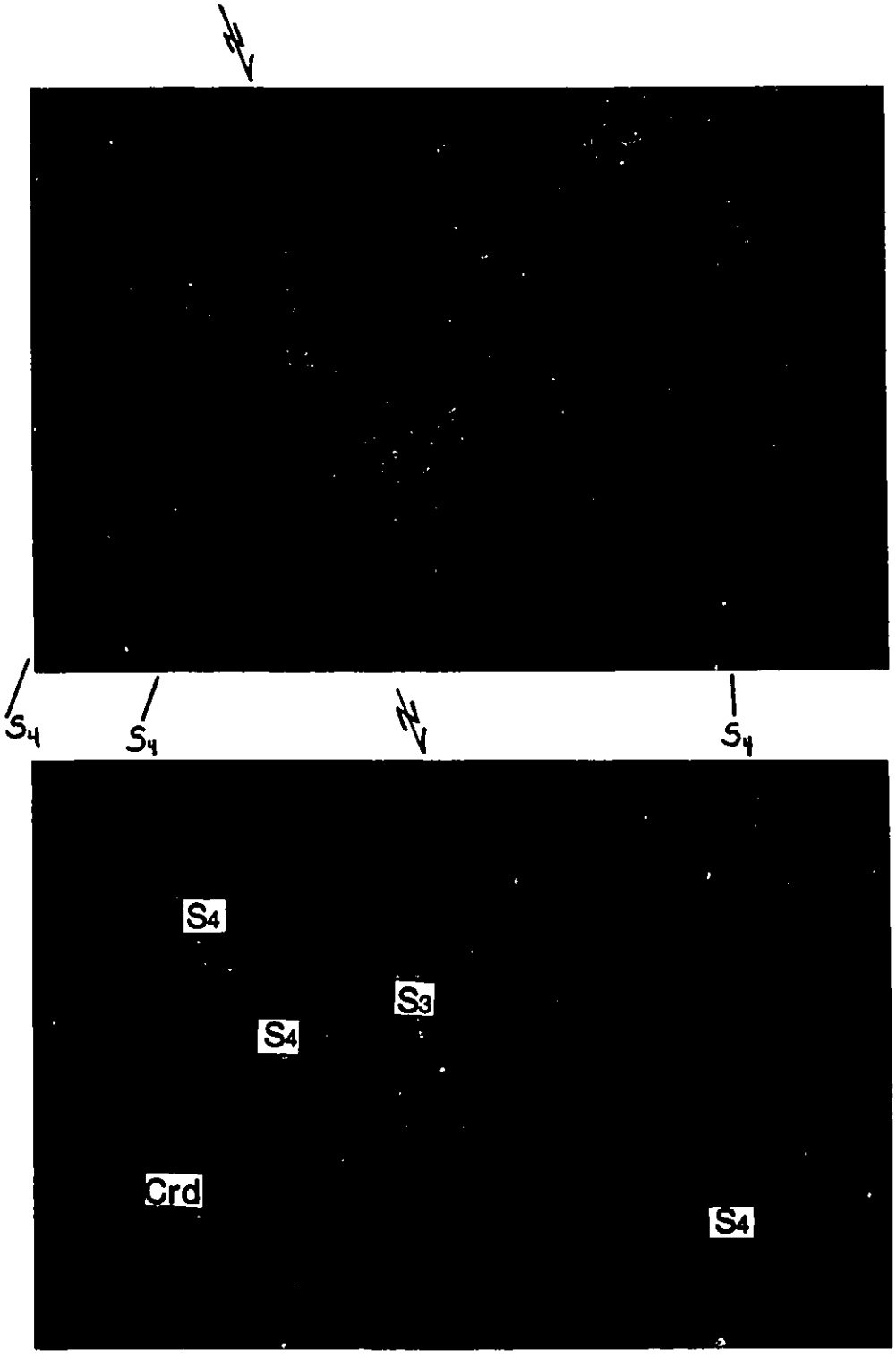
S4
S4
S4
S4
S3
S4
Crd
S4

Figure 4-11. Andalusite in a pelitic schist in metagreywacke-mudstone unit (left side of photomicrograph) preserves a straight S_3 foliation defined by biotite, quartz and ilmenite (Unit 4, sample 89005). The external S_3 biotite + muscovite foliation is crenulated. Note that the bedding-parallel quartz vein subgrains are parallel to the axial surface trace of the crenulations. Crossed polars in upper frame. Plane polarized light in lower frame. Field of view is 10.5 mm.

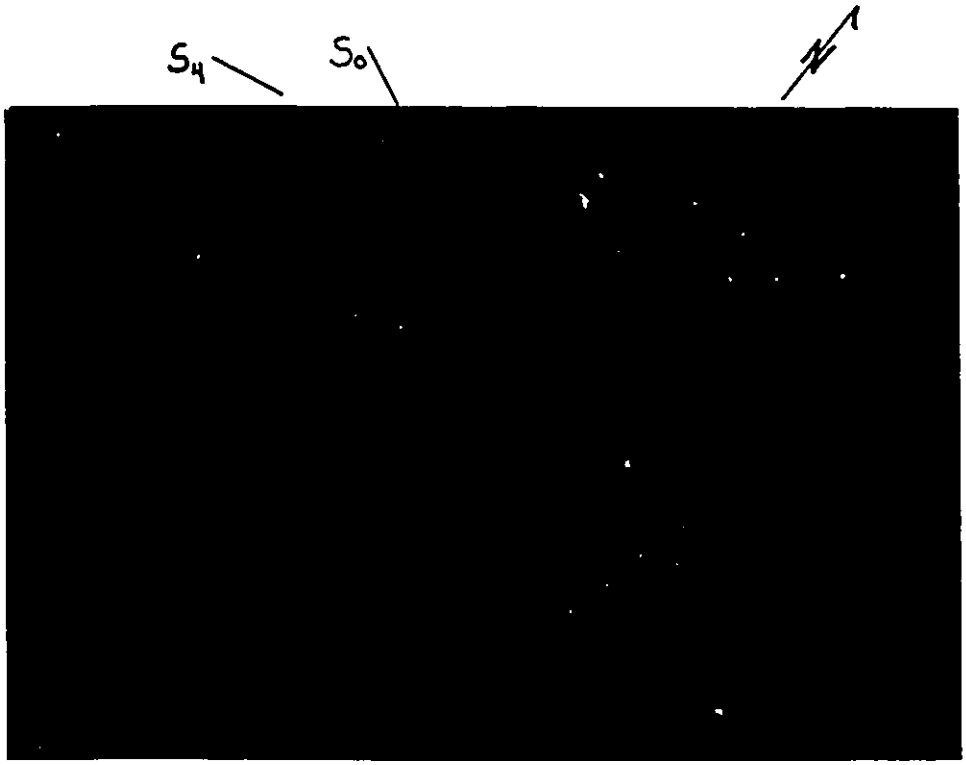
S_4
S_0
N

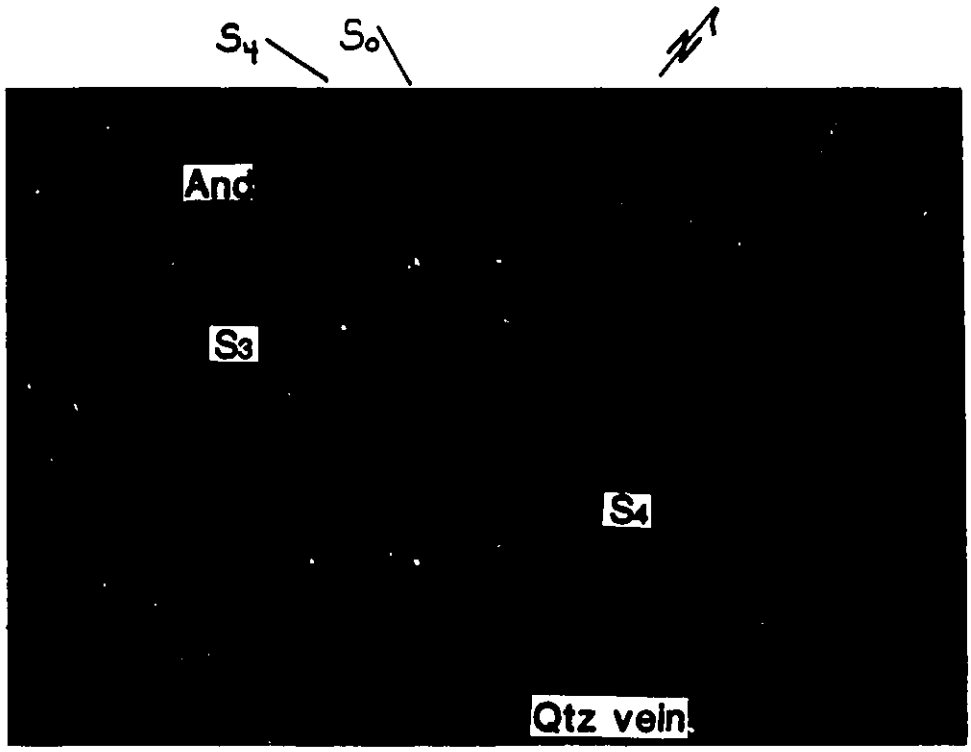
S_4
S_0
N
And
S_3
S_4
Qtz vein

Figure 4-12. Photomicrograph of trondhjemite (Unit 5a, sample 89028) from the southwestern part of the map area. A weak S_3 foliation is defined by biotite and the alignment of feldspar porphyroclasts. Crossed polars in upper frame. Plane polarized light in lower frame. Field of view is 20 mm.

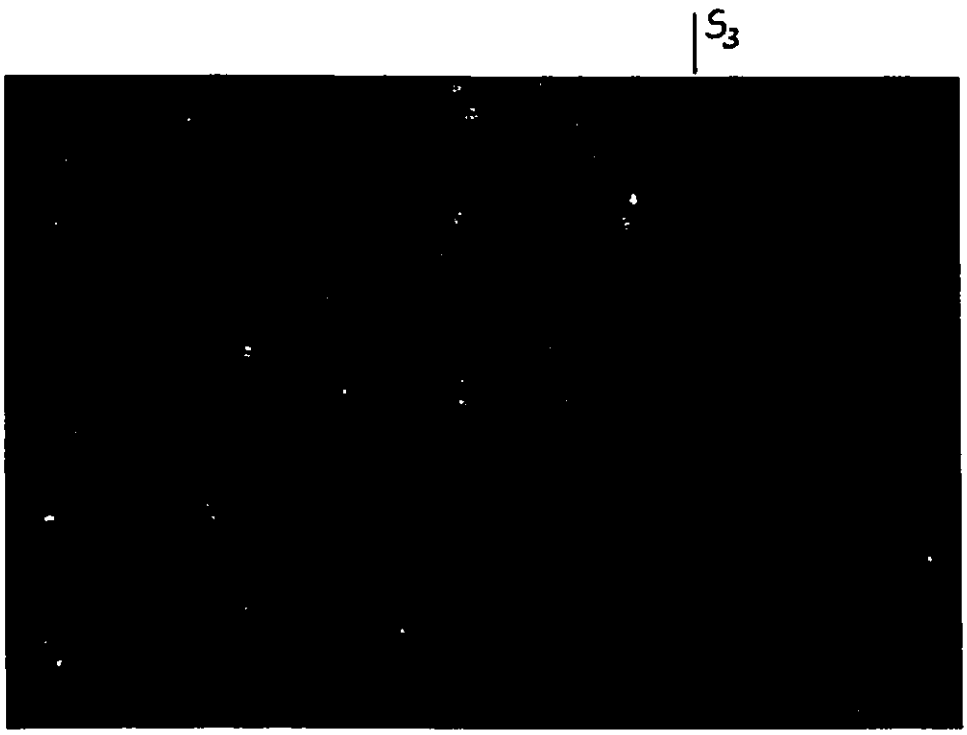
S3

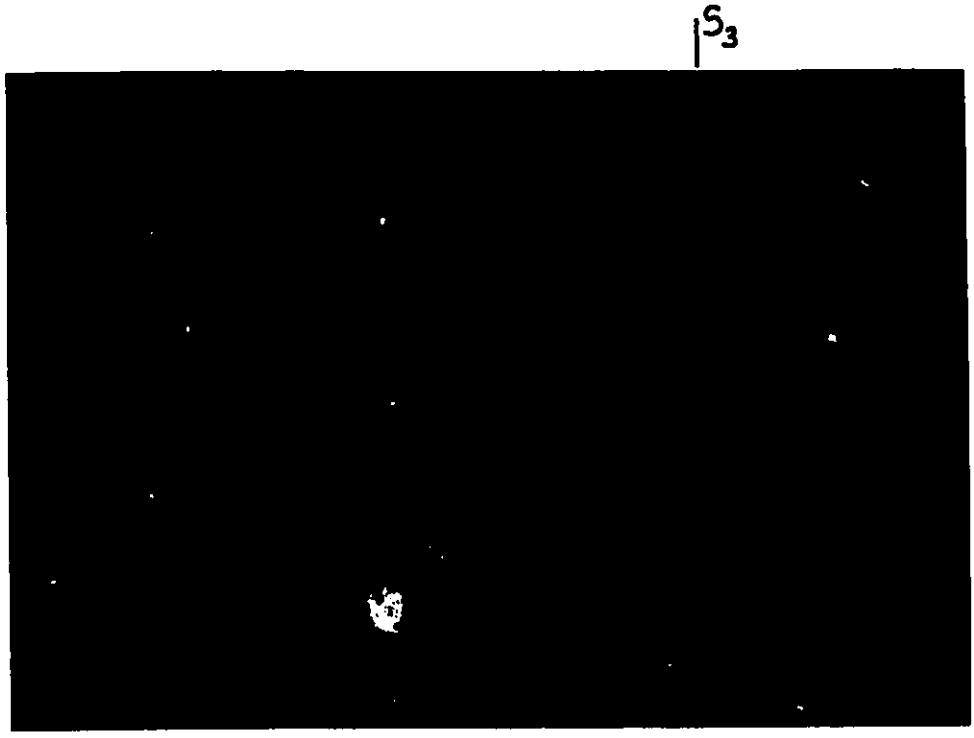
S3

Figure 4-13. Photomicrographs of foliated tonalite with relict coarse-grained pods of feldspar (Unit $5a_m$, sample 89035). The S_3 foliation defined by biotite ± hornblende warps around the unrecrystallized pods. Crossed polars in upper frame. Plane polarized light in lower frame. Field of view is 6.5 mm.

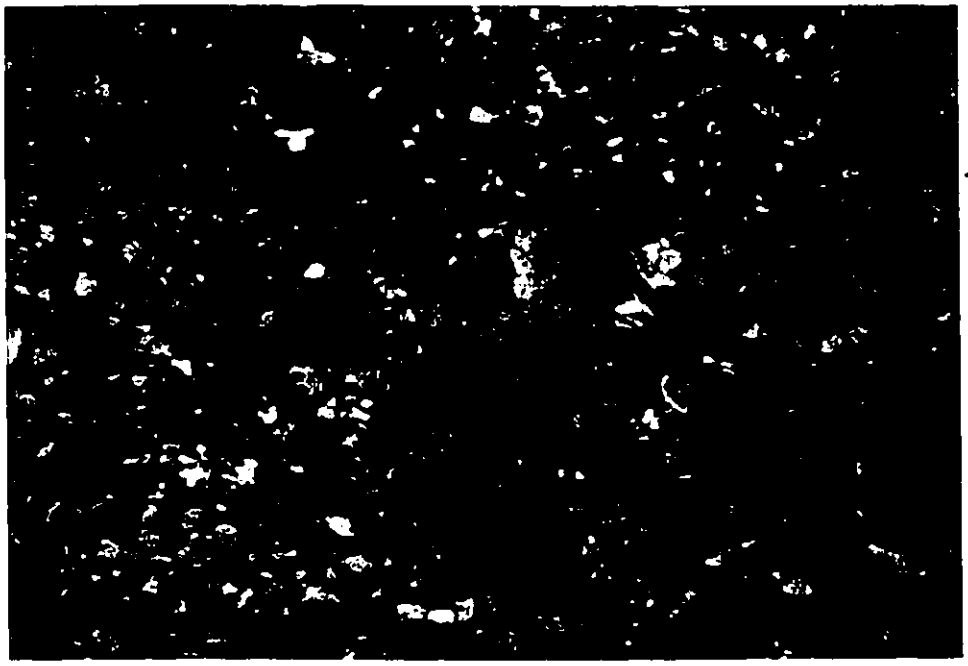
S_3


S_3

Figure 4-14. Photomicrograph of highly foliated tonalite (Unit 5am, sample 89068) with relict feldspar porphyroclasts. S_3 biotite foliation curves around the phenocrysts. Crossed polars in upper frame. Plane polarized light in lower frame. Field of view is 3 mm.


S_3


S_3

Figure 4-15. Triaxial ellipsoidal-shaped cobble in Unit 3h conglomerate from the central part of the map area. The long axis plunges 045 N. Brunton compass points north.

Figure 4-16. Photomicrographs of lineated diorite from west of the high strain zone (Unit 3b, sample 89015).
a. Thin section cut perpendicular to lineation defined by hornblende. Plane polarized light. Field of view is 9.5 mm.
b. Thin section cut parallel to lineation. Plane polarized light. Field of view is 10 mm.

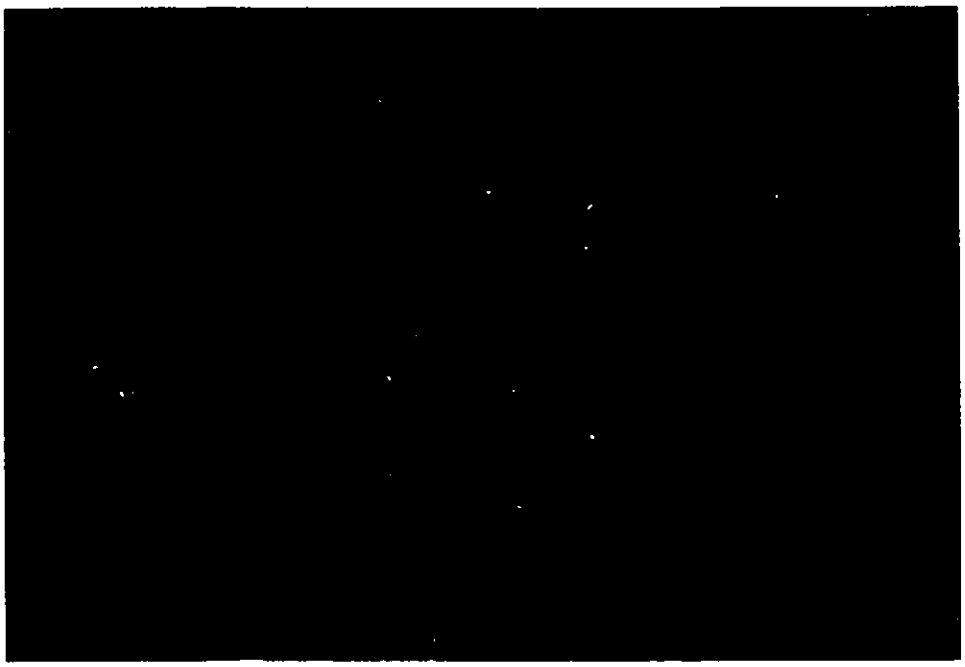

Figure 4-17. Tight to open mesoscopic F_4 fold in epiclastic amphibolite (Unit 3e) east of the high strain zone in the central part of the map area. Pencil points north. Fold to east of pencil appears to die out rapidly southwestward.

Figure 4-18. Open to closed mesoscopic F_4 folds in foliated mafic tuff (Unit 3d) east of the high strain zone in the central part of the map area south of Figure 4-19. Pencil points north.

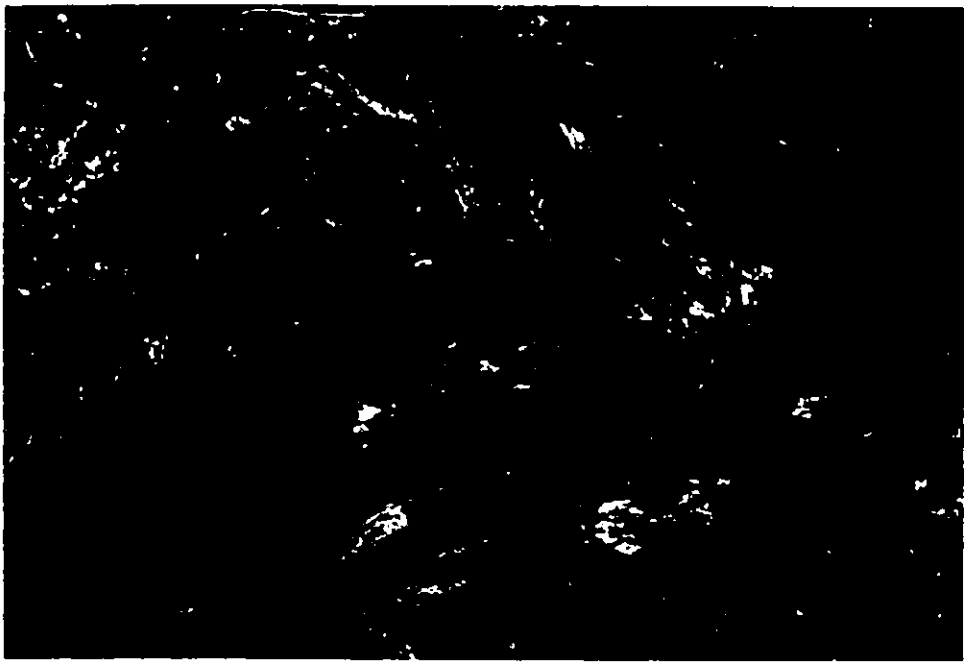

Figure 4-19. Tight to open F_4 crenulations of S_3 in epiclastic amphibolite (Unit 3e) east of the high strain zone in the central part of the map area near the contact with Unit 4 metagreywacke-mudstones. The steep S_4 axial surface trace varies in orientation but on average is 080. Brunton compass points north.

Figure 4-20. Disharmonic tight to isoclinal F_4 fold in epiclastic amphibolite (Unit 3e) just east of the high strain zone in the central part of the map area.

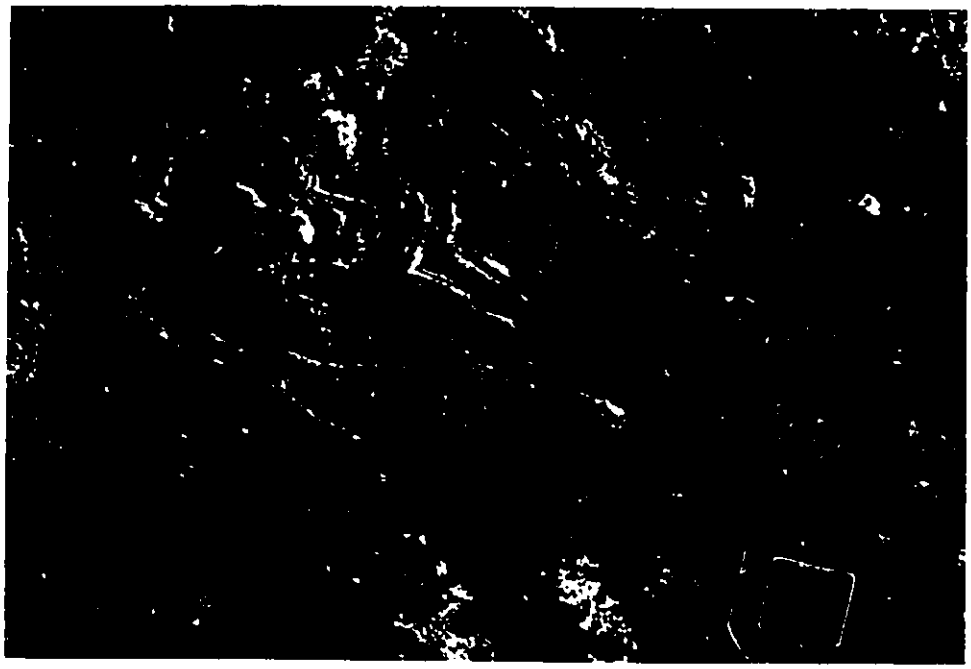

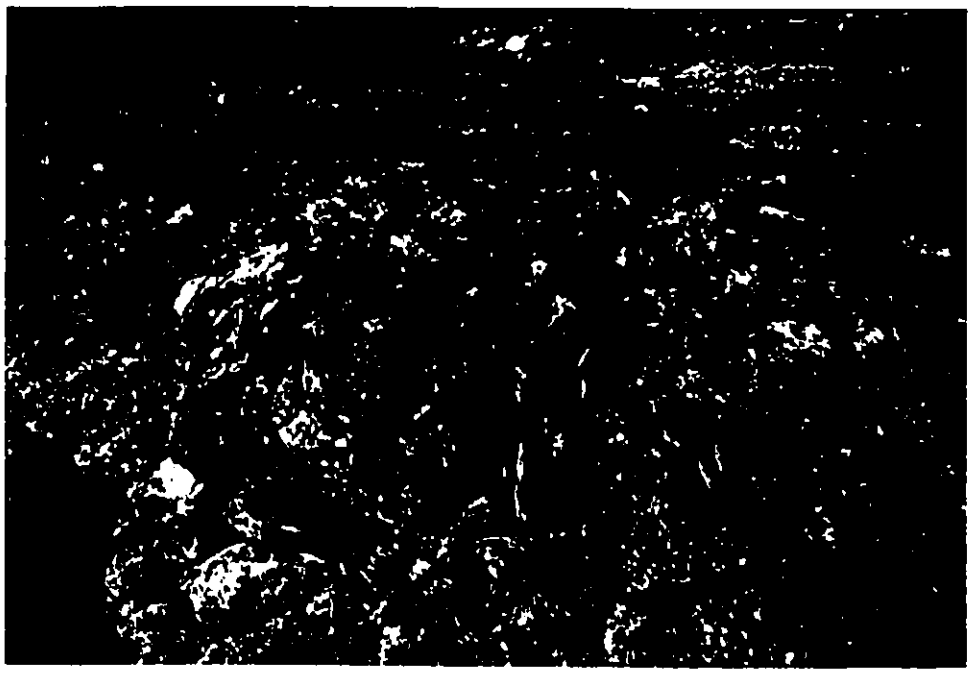

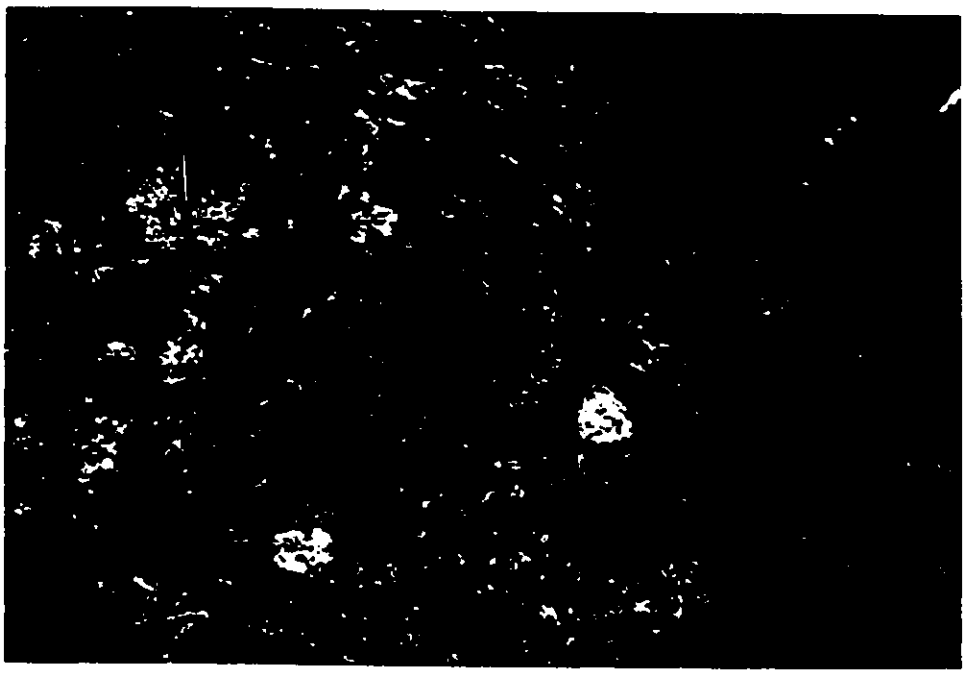

Figure 4-21. Outcrop scale F_4 open fold of bedding and bedding-parallel S_3 foliation in metagreywacke-mudstones of Unit 4. Axial surface trace = 053.

Figure 4-22a. Generalized sketch of thin section from metagreywacke-mudstone (sample A27B, Unit 4). The S_3 biotite + muscovite foliation is at a high angle to bedding surfaces in quartz-rich layers and curves into a near bedding-parallel orientation in mica-rich layers where it is crenulated. Note the effect of the cordierite porphyroblast on the foliation. The S_3 foliation is at a higher angle to bedding where it interacts with the porphyroblast than in the more quartz-rich bed. The andalusite porphyroblast preserves the pre-crenulated S_3 fabric as quartz and ilmenite inclusion trails. Locations of Figures 22b and c are outlined. Scale bar is 1 cm.

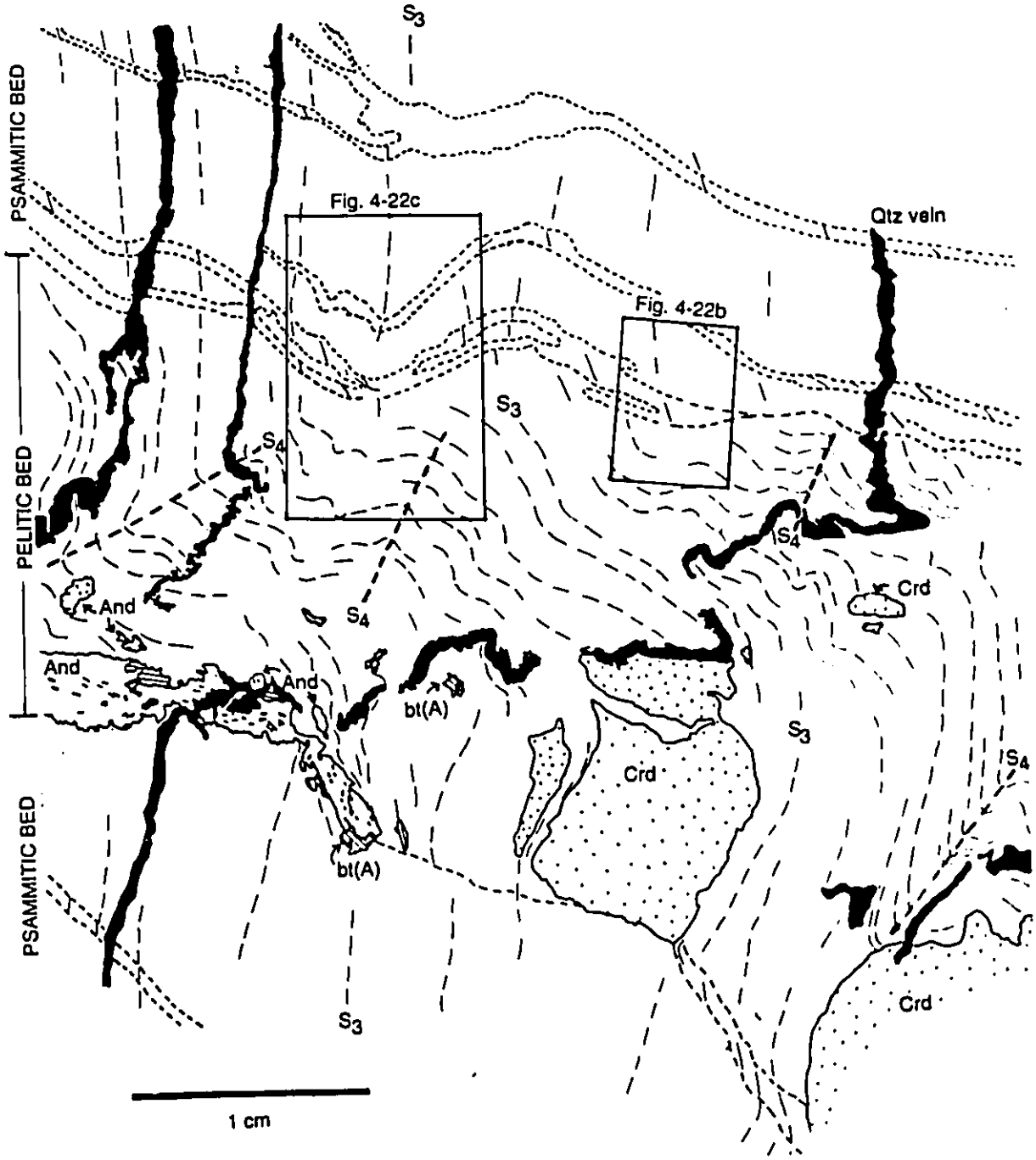
S3
PSAMMITIC BED
Fig. 4-22c
Qtz veln
Fig. 4-22b
S3
S4
PELITIC BED
S4
Crd
And
S4
And
And
bt(A)
S3
Crd
S4
PSAMMITIC BED
bt(A)
Crd
S3
1 cm

Figure 4-22b. Refraction of S_3 biotite + muscovite cleavage in metagreywacke-mudstone (Unit 4, sample A27B) from northwest of Turner Lake. See also Figure 4-24. Curve of S_3 micas from alignment at a high angle to S_0 in quartz-rich, psammitic layers (left side of photomicrograph) to sub-parallel where more mica-rich and where crenulated about S_4 (right side of photomicrograph). Micas are bent by S_4 crenulations. Note that only one mica fabric is present in both the quartz-rich and mica-rich portions. Therefore, although virtually parallel to S_4 crenulation axial traces, the aligned mica in the quartz-rich layers is not due to transposition or new growth along S_4. Horizontal thin section across steep bedding and foliations. Plane polarized light. Field of view is 7 mm.

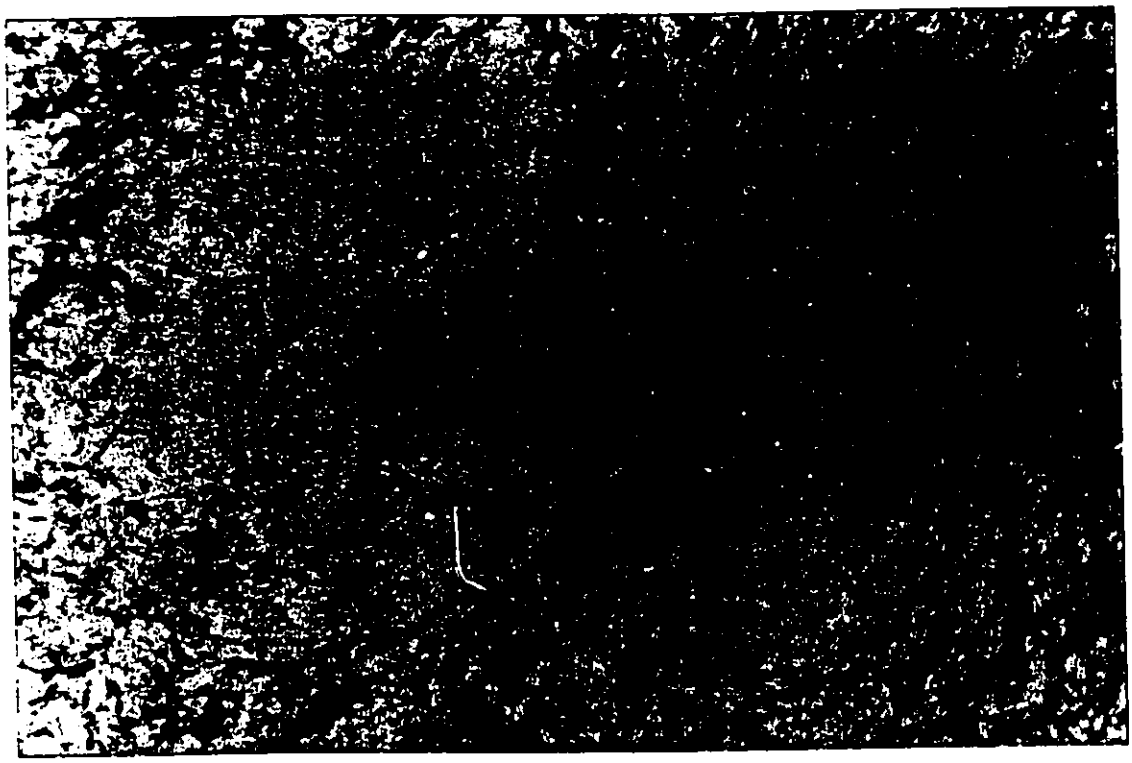

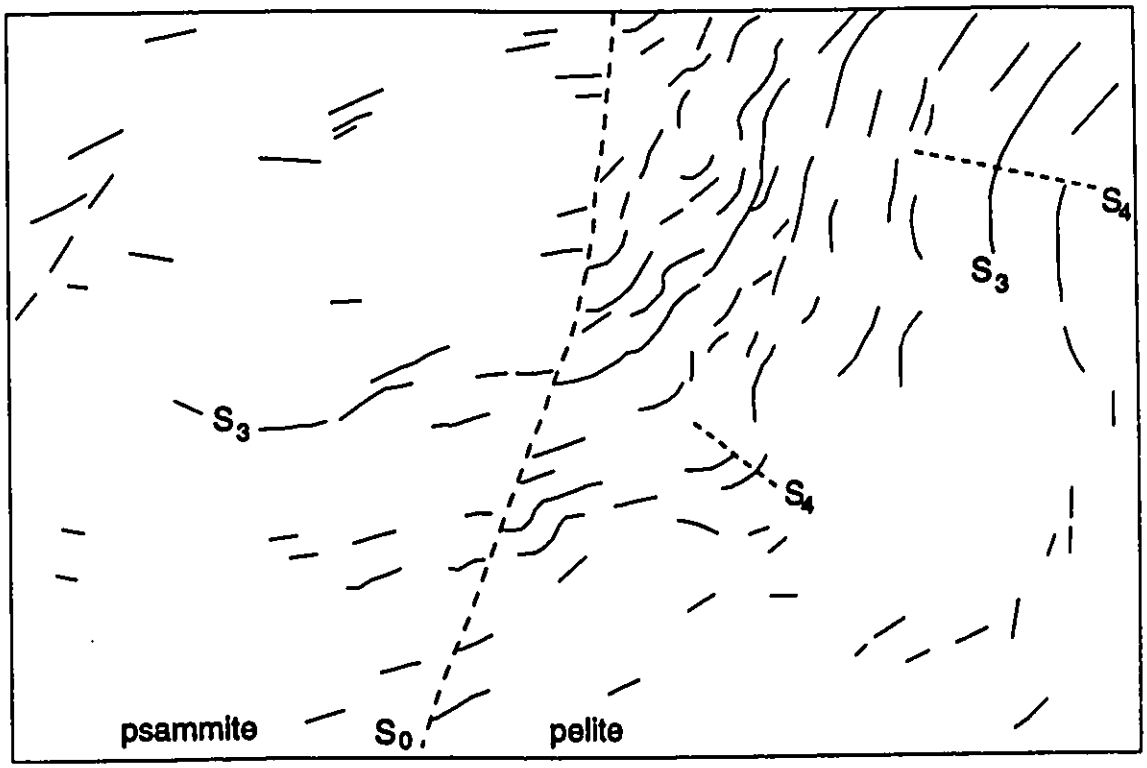
S4
S3
S3
S4
psammite
S0
pelite

Figure 4-22c. Laminated psammitic and pelitic schist showing variations in orientation of S_3 and F_4 crenulations. S_3 biotite + muscovite foliation at a high angle to bedding surfaces in quartz-rich layers curves into a near bedding-parallel orientation in mica-rich layers where it is crenulated and forms an S_4 cleavage (Unit 4, sample A27B). S_3 in quartz-rich layers (right side of photomicrograph) is nearly parallel to the S_4 axial surface trace of the crenulations in the mica-rich layers (left side of photomicrograph). No micas are aligned along the S_4 traces. Refer to Figure 4-6 for appearance in outcrop and Figure 4-8 for details. Horizontal thin section across steep bedding and foliations. Crossed polars in upper frame. Plane polarized light in lower frame. Field of view is 13 mm.

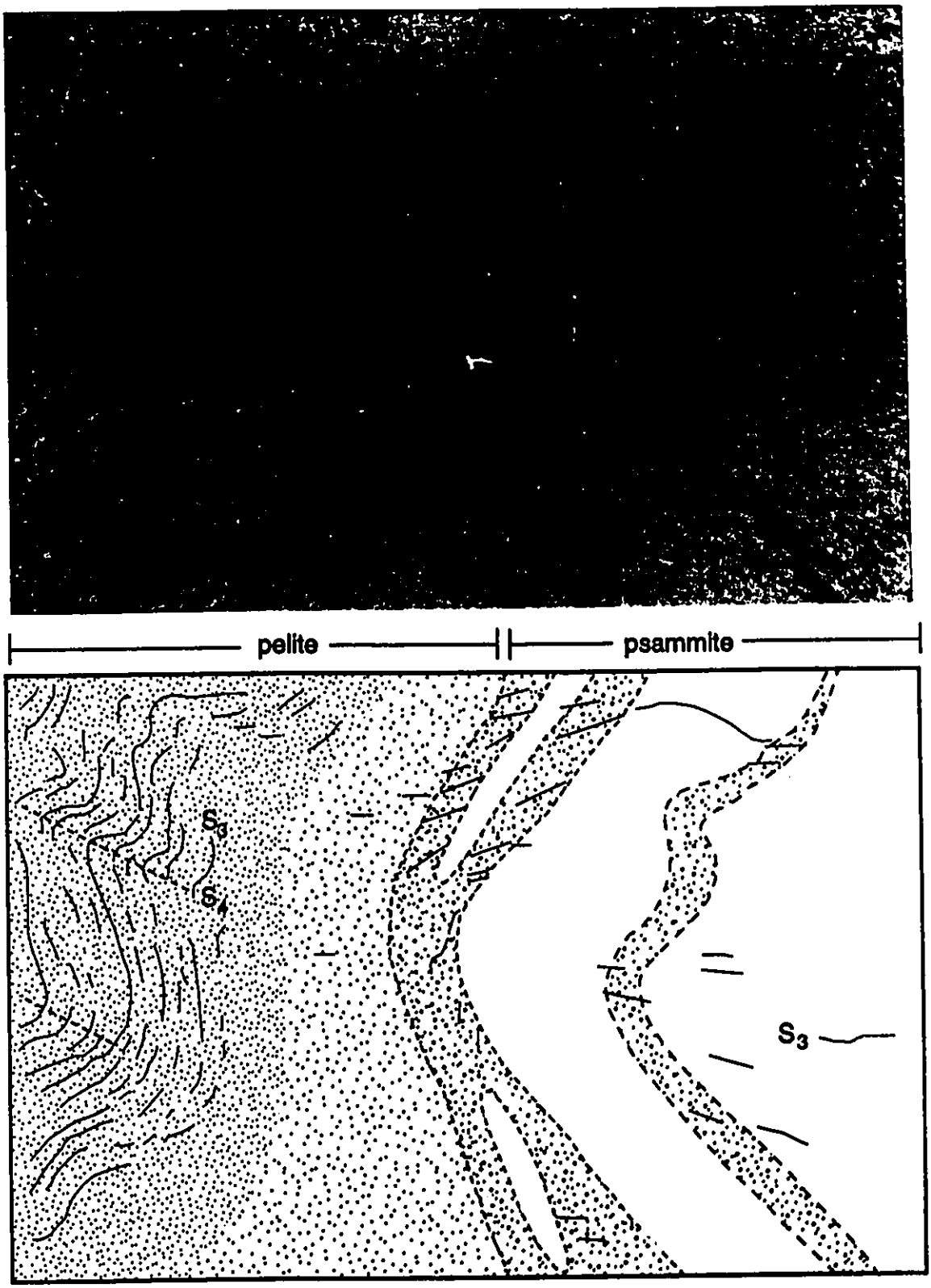
pelite
psammite
S_3
S_4
S_3

Figure 4-23. Photomicrograph of S_4 crenulations in epiclastic amphibolite (Unit 3e) east of the high strain zone in the central part of the map area. S_3 appears to be parallel to S_0 and is crenulated by S_4. Axial surface trace of crenulations is 107/60. Crossed polars in upper frame. Plane polarized light in lower frame. Field of view is 28 mm.

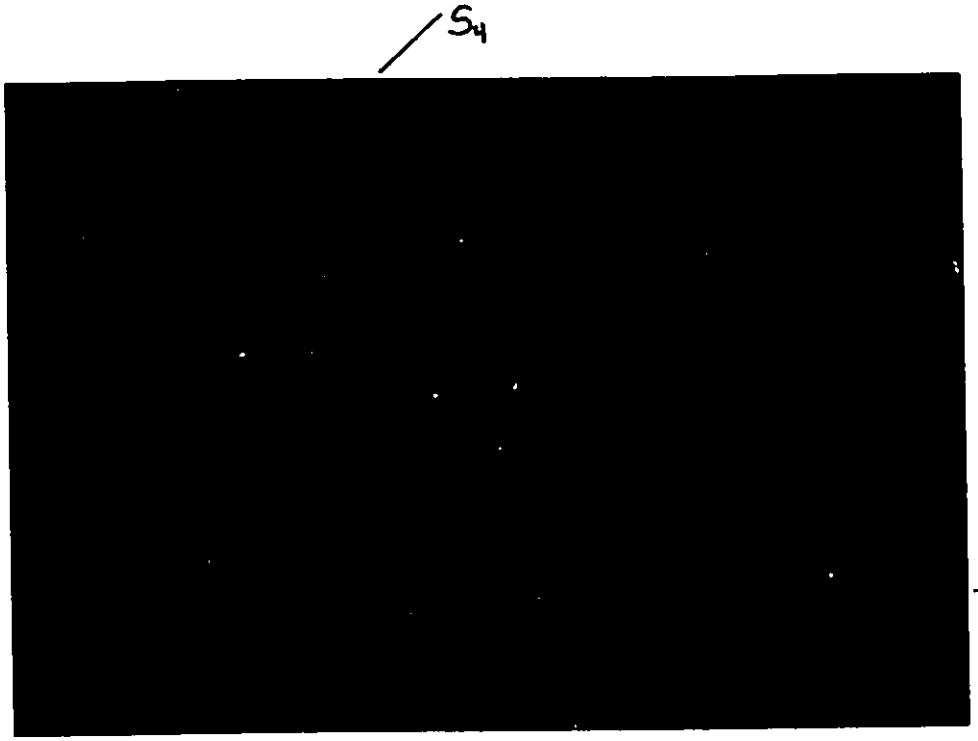
S_4
S_0+S_3

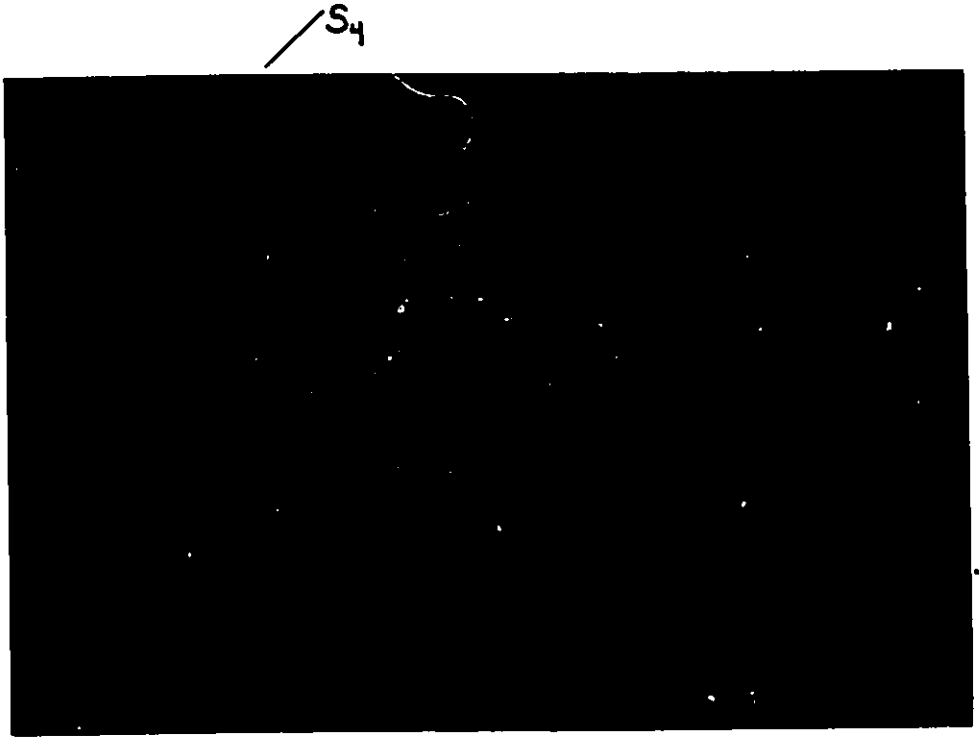
S_4
S_0+S_3

Figure 4-24a. Highly recrystallized, epidotized, layered volcanic rock along the main high strain zone (Unit 3g; sample 89116). Sample located in central part of map area.

Figure 4-24b. Photomicrograph of recrystallized layered volcanic rock along main high strain zone (Unit 3g, sample 89116). Layers are defined by being either epidote-rich or hornblende-rich. Plane polarized light. Field of view is 5 mm.

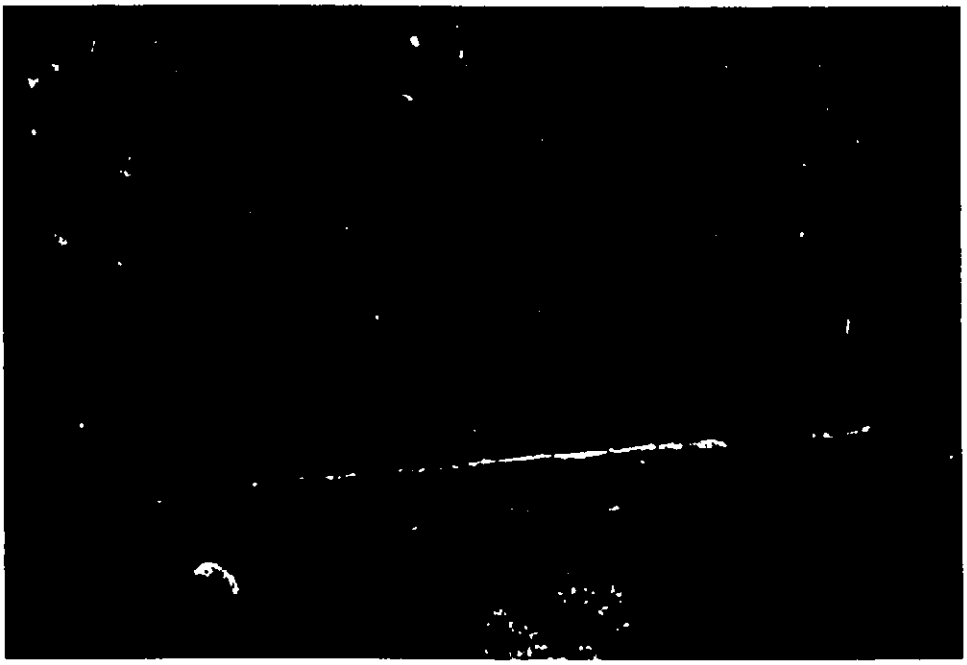

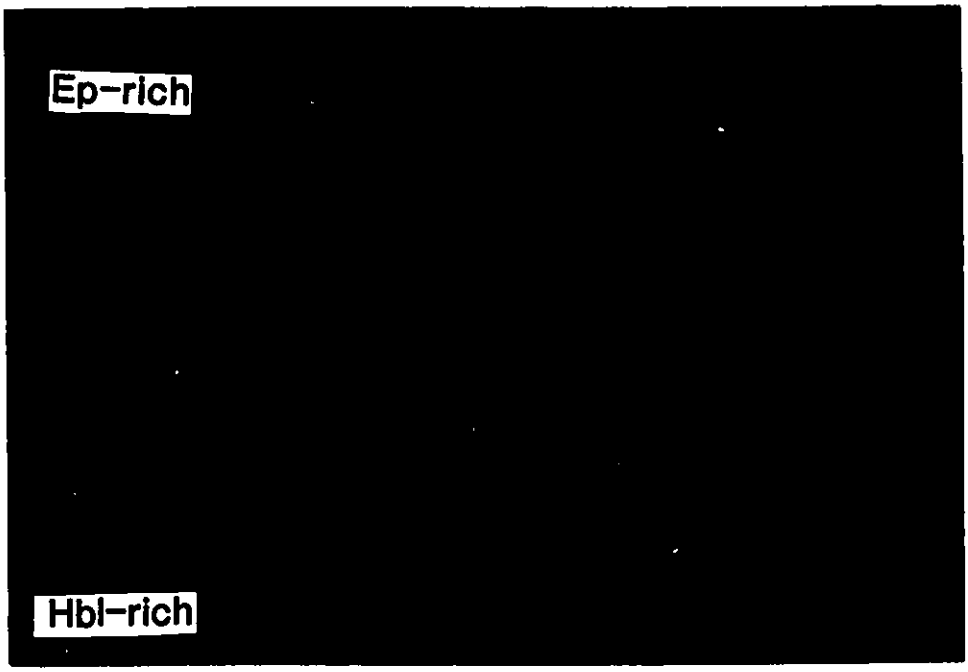
Ep-rich
Hbl-rich

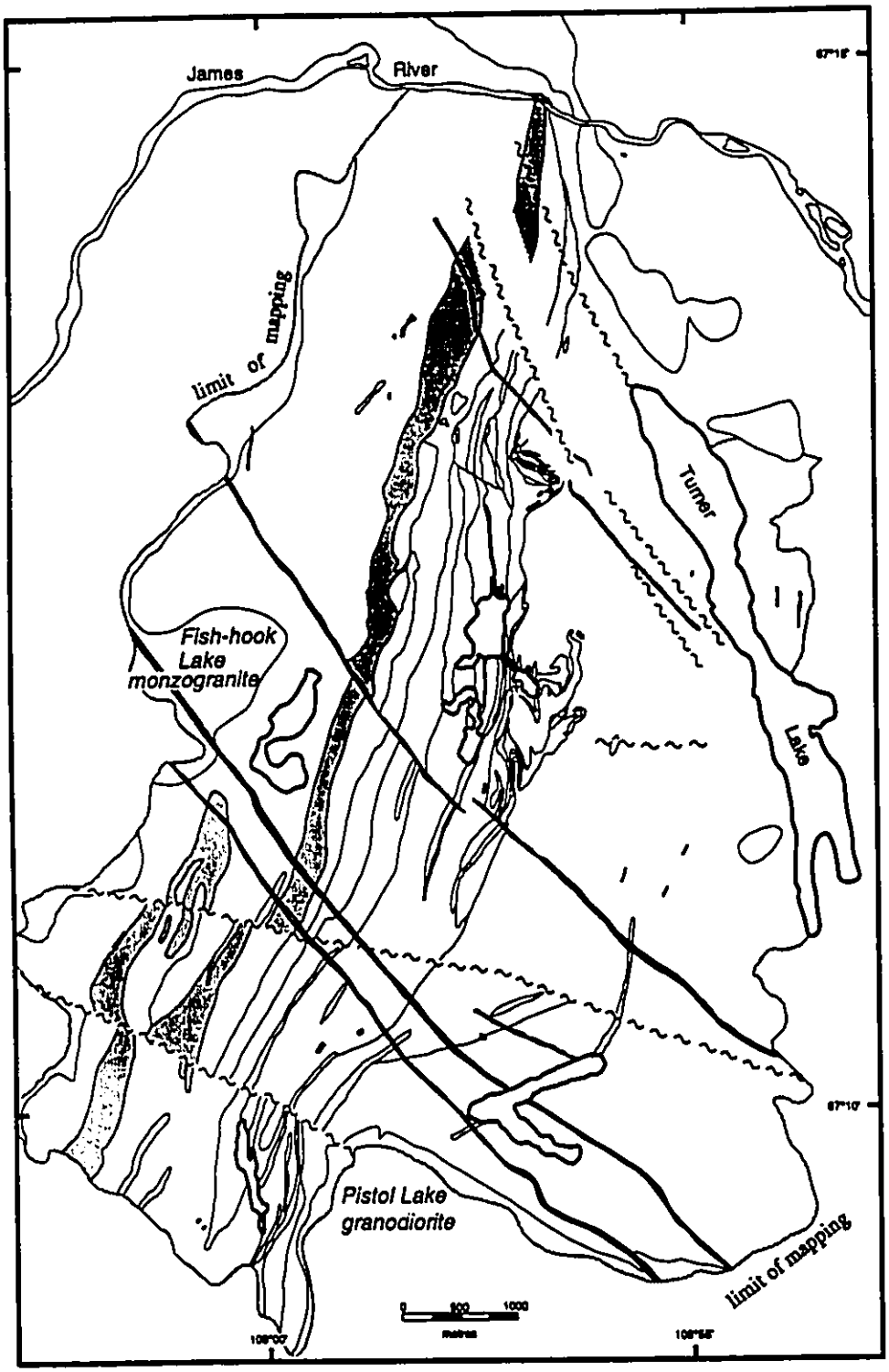

Figure 4-26. Location map of faults in the Turner Lake area. Diabase dykes trend northwest across map. Unit 2 conglomerate indicated with pale grey.

Chapter 5
Metamorphism

5.1 Introduction

Metamorphic mineral assemblages documented throughout the Slave Province are indicative of a range of temperatures at relatively low pressures which developed following the main phases of folding at about 2.6 Ga (Thompson, 1978). The supracrustal rocks in the Turner Lake area have been regionally metamorphosed to amphibolite facies. The metasedimentary rocks in the map area, primarily Units 1 and 4 metagreywacke-mudstones, exhibit diagnostic mineral assemblages of prograde metamorphism. They mostly occur away from the main high strain zone and as a result have not undergone the epidotization and carbonate alteration associated with this zone which overprints thermal peak mineral assemblages.

Isograds must have a shallow dip since grade is uniform across at least 5 km of nearly vertical beds. The assemblage cordierite ± andalusite ± sillimanite (fibrolite) in the metasedimentary rocks is diagnostic. Grade apparently increases in the northwest area of the map approaching the Fish-hook Lake pluton.

In this chapter the metamorphic mineral assemblages of metasedimentary rocks are described based on field and thin section observations. Data from low grade rocks north of the study area (Torp Lake domain) are incorporated into this discussion. Textural criteria used to determine the timing of mineral growth with respect to deformation, including observations from Chapter 4, are summarized (Table 5-1). Emphasis is on metasedimentary

Table 5-1. Mineral assemblages from metamorphic rocks of the Turner Lake area. Number in column refers to the number of thin sections in which the assemblages were observed. Mineral abbreviations used in this table and in the text are from Kretz (1983).

Pelitic Assemblages	Unit 1 (west)	Unit 4 (east)
Qtz-Pl-Bt in all assemblages		
Ms		1
Ms-Crd		7
Ms-And		1
Ms-Sil*	1	
Ms-Sil*-And	2	1
Ms-Crd-And-Sil*		2
Ms-Sil-And	1	
Grt	1	

Arenites	Unit 3a
Qtz-Pl-Bt-Ms in all assemblages	
And	1
And-Sil*	5
Grt	1

*sillimanite as fibrolite

Table 5-2. Textural criteria used for establishing timing of mineral growth in the Turner Lake area.

MINERAL	TEXTURE	FIGURE	TIMING OF GROWTH
CHLORITE	a) in Torp Lake area (Venance, 1991) b) interleaved with and replacing biotite c) alteration of cordierite	Fig. 5-2 Fig. 5-3	a) prograde; sub cordierite grade b) retrograde c) retrograde
MUSCOVITE	a) Muscovite(A): as aligned plates parallel to S3 b) Muscovite(B);: as corroded, random crystals overprinting S3 near the Fish-hook Lake monzogranite	Fig. 5-6, 5-8, 5-7, 5-8 Fig. 5-5	a) prograde growth, D3 b) late thermal effect of pluton, D3?
BIOTITE	a) Biotite(A): blocky porphyroblasts containing straight quartz inclusion trails (S1-2) overgrown by cordierite. b) Biotite(B): aligned plates parallel to S3	Fig. 5-4 Fig. 5-5, 5-6, 5-7, 5-8	a) post D1-2, pre S3 cleavage b) prograde growth, D3
CORDIERITE	a) porphyroblasts containing straight S3 inclusion trails (opaques, qz, bi, ap) continuous with crenulated S3 foliation (S4). b) porphyroblasts with no aligned internal foliation with S3 warped around and long axis of porphyroblasts in the S3 plane.	Fig. 4-11  Fig. 4-10 	late D3 early D3
ANDALUSITE	a) S3 foliation warps around b) porphyroblasts containing straight S3 inclusion trails (opaques, qz, bi, ap) continuous with S3 foliation +/- rimming oriented inclusion-free cordierite. S3 may or may not be crenulated.	Fig. 5-7  Fig. 5-6 	a) most early D3, pre S3 b) late D3
SILLIMANITE	a) fibrolite: as mats with biotite ± muscovite along S3 nucleating on andalusite porphyroblasts b) prismatic sillimanite with muscovite	Fig. 5-8, 5-11, 5-12 Fig. 5-9, 5-19, 5-12 Fig. 5-13	a) D3 b) late D3

rocks, however metamorphic mineral assemblages of amphibole-rich rocks are presented for completeness. Possible metamorphic reactions deduced from relevant metamorphic mineral assemblages from metasedimentary units will be discussed. Metamorphic conditions at Turner Lake will be interpolated from a petrogenetic grid.

5.2 Metamorphic mineral assemblages of prograde metamorphism: Metasedimentary rocks

5.2.1 Introduction

The metamorphic mineral assemblages from the metasedimentary rocks of the Turner Lake area have been used to estimate metamorphic conditions. Equilibrium assemblages and applicable mineral reactions were considered. Major prograde minerals (greater than 5% overall abundance) observed in thin section from the map area are listed in Table 5-2. Accessory phases (less than 5% of modal analysis) are not listed with the major minerals but are discussed. Some minerals are present only as retrograde products of prograde minerals.

5.2.2 Chlorite

In the northeastern part of the Torp Lake domain prograde chlorite is present in lower greenschist facies rocks and below the cordierite isograd coexisting with fine-grained laths of white mica (K.E. Venance, pers. comm., 1993). In the Turner Lake area chlorite has only been observed in thin section as a retrograde mineral interleaved with or totally replacing biotite (Figure 5-1) or as an alteration of cordierite (Figure 5-2).

5.2.3 Biotite

Biotite is readily observed in hand specimen. Examination of thin section indicates

two morphological types of biotite which developed during two different stages in the metamorphic history. Early, sub-equant (blocky) porphyroblasts, hereafter referred to as biotite(A), randomly overgrew and included a planar quartz fabric (S_1-S_2) described in the preceding chapter and illustrated in Figure 4-5. These porphyroblasts are most common in psammitic beds. The biotite producing reaction is not clear from the Turner Lake samples, however further north in the Torp Lake domain, mineral assemblages from upper-greenschist facies rocks provide clues. Euhedral biotite porphyroblasts occur in a matrix of chlorite, white mica, quartz, feldspar, detrital zircons and apatite. A reaction involving biotite formation at the expense of chlorite and white mica has been suggested (Venance, in prep.).

The alignment of thin, 0.25 to 0.5 mm long biotite ± muscovite plates (S_3) imparts a schistosity to the rocks. The biotite here is referred to as biotite(B). S_3 overgrows the earlier biotite porphyroblasts with the muscovite overgrowth most obvious due to differences in pleochroism between biotite and muscovite (Figure 5-3).

Thus there were two stages in the growth of biotite. Sub-equant crystals that grew pre-D_3 overgrowing S_1-S_2 and aligned plates that grew during D_3 to form the S_3 foliation with muscovite.

5.2.4 Muscovite

Muscovite was less easy to identify in hand specimen than biotite due to its paler colour but it imparts a cleavage to the rocks and, in more muscovite-rich samples the cleavage surfaces have a diagnostic, silvery sheen to them.

Two different morphological types and growth stages of muscovite have been

identified. Aligned 0.25 to 0.5 mm long muscovite and biotite plates define the S_3 foliation. These are referred to as muscovite(A).

Randomly oriented flakes of muscovite, hereafter referred to as muscovite(B) average .5 mm in size and cross S_3 in proximity to the Fish-hook Lake pluton. These flakes typically have a corroded appearance (Figure 5-4). They are considered to be a late metamorphic mineral since the crystals overgrow the earlier S_3 fabric; however the relationship to S_4 is unknown.

In summary, muscovite(A) crystallized mainly during D_3 and is aligned parallel to S_3 with some minor, late or post deformational random crystallization of muscovite(B) in the northwestern part of the map area.

5.2.5 Cordierite

Whitish, ovoid to irregular porphyroblasts of cordierite are readily recognized in outcrop. The size of cordierite is dependant on lithology. Development is more prominent in pelitic beds as opposed to more psammitic beds. The result is a reversed grading effect. As the amount of mudstone increases toward the top of a bed the porphyroblasts tend to increase in size and abundance (Figure 3-3). It does appear that quartz is important to the formation of cordierite. Although growth is preferred in pelitic beds quartz is necessary and so some beds extremely rich in biotite and muscovite contain no porphyroblasts whereas in the same bed where the quartz content increases in abundance porphyroblasts have developed.

Poikiloblasts are partially or completely altered to pinite and/or sericite (both are fine grained micas) with minor amounts of chlorite (Figure 5-2). Abundant inclusions in less

altered porphyroblasts include quartz, biotite, ilmenite, apatite and zircons which are aligned parallel to the external S_3 foliation. The zircons impart yellowish pleochroic haloes to the cordierite. This is a useful diagnostic tool.

Relationships between the internal foliation and the external matrix foliation vary. Two growth stages of cordierite are apparent. Cordierite developed during the early stages of S_3 grew and included the earlier biotite(A) porphyroblasts (Figure 5-3). In these porphyroblast-choked pelitic beds it is difficult to tell if the porphyroblasts preserve an internal foliation. The external S_3 biotite + muscovite foliation is deflected around the cordierite. The increased competency effect of porphyroblast congestion in pelitic beds and abnormal refraction (discussed in the previous chapter) constrains growth in these cases to the early stages of S_3 development. Most commonly in less congested beds, poikiloblasts have no internal foliation and developed along the S_3 plane. The cordierite could have formed during early D_3 and developed in the direction of least stress, namely the foliation, perhaps due to the anisotropy created during the early stages of its development. Finally, in a few cases, some relatively unaltered porphyroblasts preserve an internal S_3 foliation which is continuous with the external S_3 foliation. The crenulation of the external foliation and rare deformation of cordierite porphyroblasts indicates that porphyroblast growth was post S_3 cleavage development but pre D_4 (Figure 4-10).

The internal foliation contains no muscovite suggesting that cordierite crystallized at the expense of muscovite. In addition the matrix contains no chlorite. Cordierite may have originated via a reaction whereby chlorite and muscovite reacted until one was completely

consumed. The assemblage:

chlorite + white mica + biotite + quartz + plagioclase

exists below the cordierite isograd in the Torp Lake domain (Venance, 1991). It is assumed that chlorite and muscovite reacted until one (presumably in this case chlorite) was consumed at relatively low pressures via the reaction:

muscovite + chlorite + quartz = cordierite + biotite + H_2O

(Ramsay, 1974).

In terms of deformation, most cordierite growth occurred during the early stages of S_3 cleavage development. Some later growth includes the S_3 foliation. No cordierite crystals overgrow the S_4 crenulations however weakly deformed crystals exhibit undulose extinction at their edges.

5.2.6 Andalusite

Andalusite is most commonly found in the arenites (Unit 3a) and to a lesser extent in the greywacke-mudstones of Units 1 and 4. Euhedral to subhedral crystals are pale pink in outcrop.

A growth sequence similar to that of cordierite existed for andalusite. Inclusion-free andalusite developed during the earliest stages of S_3 cleavage formation, has the external S_3 biotite + muscovite foliation wraped around it. In many cases andalusite contains straight inclusion trails of biotite and opaque minerals. The inclusions are aligned parallel to the external S_3 foliation. The external foliation may or may not be crenulated. In any case, andalusite poikiloblasts including S_3 are late D_3 but pre S_4 crenulations. Where cordierite and

andalusite occur together in the same rock the former is often highly altered and contains no aligned inclusions. S_3 deforms around the altered cordierite poikiloblasts but is preserved in the andalusite (Figure 5-5). This relationship has been noted in a metamorphic study of pelitic rocks across the Slave Province where "andalusite has overgrown a micaceous foliation that wraps around cordierite poikiloblasts" (Thompson, 1989b, p. 250). This indicates that in these cases, cordierite grew early during the development of S_3 defined by biotite + muscovite and andalusite growth was late-S_3 development where conditions permitted the growth of both porphyroblasts.

The andalusite variety chiastolite has been identified in the iron formations (Units 1a and 4a). Euhedral to subhedral crystals range up to 1 cm in cross-section. Most crystals are fractured with sericite alteration along these fractures. Unaltered areas of the crystals appear to be inclusion-free. Lines of included carbonaceous matter which impart the diagnostic "cross" to chiastolite are altered to sericite. The external S_3 muscovite + biotite foliation warps around the andalusite (Figure 5-6).

5.2.7 Sillimanite

Sillimanite is ubiquitous in the metagreywacke-mudstones of Units 1 and 4 and the arenite (Unit 3a). Sillimanite first appears as fine-grained microscopic needles of fibrolite. Fibrolite is difficult to identify in hand sample however the biotite in these rocks has a diagnostic reddish-brown colour. Most of the rocks at Turner Lake containing andalusite also contain sillimanite but the sillimanite does not usually grow directly from the andalusite. The occurrence of both andalusite and sillimanite together, their textural association and the

fibrolitic nature of sillimanite suggests that the physical conditions were close to the andalusite/sillimanite phase boundary.

In the greywacke-mudstones of Units 1 and 4 fibrolite needles usually grow in clusters with biotite and muscovite along the S_3 foliation (Figure 5-7). The fibres are aligned in the S_3 foliation plane. Fibrolite also occurs as rims around andalusite poikiloblasts intergrown with biotite (Figure 5-8) and as minute fibres associated with or nucleating on andalusite (Figures 5-9 and 5-10).

A similar growth relationship exists in the arenite unit (3a) where the spatial association with andalusite is more notable. Fibrolite growth is at the edges of or near andalusite along the S_3 mica foliation with biotite often as a coexisting phase (Figure 5-11).

The two distinct associations of sillimanite with biotite and muscovite or with andalusite, suggests two sillimanite growth mechanisms. The first appears to be the product of a reaction involving biotite and/or muscovite. Sillimanite needles rimming and growing out of andalusite implies the inversion of andalusite to sillimanite. The association with biotite complicates the interpretation. The growth of sillimanite can be considered to be the result of metasomatic cation exchange reactions. There is a gradual consumption of reactants which is balanced by the appearance of products. Under these conditions it is possible for sillimanite to grow at the expense of andalusite without being in physical contact with the andalusite (Carmichael, 1969). The reactions are considered as part of a progressive sequence.

Similar metamorphic mineral associations and textures to those at Turner Lake have

been described in kyanite-bearing rocks (Carmichael, 1969). The sillimanite at Turner Lake may have developed via a similar complex reaction mechanism with andalusite as a reactant instead of kyanite in a system involving three reactions and the exchange of ions among local systems. Aluminum is considered to be immobile and the inversion of andalusite to sillimanite involves the following reactions:

$$3 \text{ andalusite} + 3 \text{ quartz} + 2K^{+} + 3\ H_2O = 2 \text{ muscovite} + 2\ H^{+}$$

$$\text{biotite} + Na^{+} + 6\ H^{+} = \text{albite} + K^{+} + 3\ (Mg, Fe)^{++} + 4\ H_2O$$

$$2 \text{ muscovite} + \text{albite} + 3\ (Mg, Fe)^{++} + H_2O =$$

$$\text{biotite} + 3 \text{ sillimanite} + 3 \text{ quartz} + K^{+} + Na^{+} + 4\ H^{+}$$

(Carmichael, 1969). The third reaction produces an intergrowth of biotite, sillimanite and quartz, a texture recognized in the rocks at Turner Lake. The net reaction in the rock is:

$$3 \text{ andalusite} = 3 \text{ sillimanite}$$

The Al, Si and O ions from which the sillimanite formed are not the same ions that were formerly contained in andalusite (Carmichael, 1969). Thus even though sillimanite can be remote from andalusite in these rocks and intergrown with biotite, nevertheless the simple net reaction andalusite = sillimanite may have been the relevant process.

Coarse, prismatic sillimanite was observed in one thin section (Figure 5-12) and several outcrops (Figure 3-7) in the northwestern part of the map area near the contact with the Fish-hook Lake monzogranite. It is possible that grade may increase slightly here. In thin section, sillimanite crystals are intergrown with one another and with muscovite (Figure 5-12). The lack of prismatic sillimanite along the southern contact of the Fish-hook Lake

monzogranite with the metasedimentary rocks of Unit 1 suggests that this is not a contact metamorphic aureole. Johnstore (1990c) mapped a sillimanite isograd which is cut by the northern extension of this pluton north of the James River, further evidence that this is a regional isograd. This also constrains pluton emplacement to its present level to post sillimanite growth or post peak metamorphism.

In summary, sillimanite growth occurred in two stages which are considered to be the result of an increase in metamorphic grade. Fibrolite developed along and parallel to the S_3 foliation grew as part of a series of cation exchange reactions under progressive metamorphism. The resultant reaction is andalusite = sillimanite. Prismatic sillimanite in the northwestern part of the map area could be an equilibrium intergrowth of sillimanite and andalusite or it may be a pseudomorphic replacement of earlier andalusite with an increase in metamorphic grade.

5.2.8 Minor minerals

Pink to reddish euhedral to subhedral garnet is present mainly within the pelitic iron formation units and the matrix of the conglomerate (Unit 2). Crystal sizes range from 1 to 3 mm. The garnet is generally inclusion-free except for some minor, randomly oriented opaque minerals. In the conglomerate matrix poikiloblastic garnets range from 1-3 mm. It is often difficult to distinguish between clasts and matrix in this unit so observations are tenuous. It appears that the S_3 foliation is slightly deflected around the garnets (Figure 5-13).

Tourmaline occurs in trace amounts in the Unit 1 and 4 metagreywacke-mudstones. Euhedral to subhedral green crystals are developed preferentially in biotite-rich layers and

average .2 mm in cross section. Trace amounts also occur in the matrix of the Unit 2 conglomerate. The crystals are randomly oriented with respect to S_3 and S_4 placing growth at post D_4.

Prisms of euhedral to subhedral yellowy brown tourmaline are developed in the mafic tuff unit (Figure 5-17). Cross sections are up to .5 cm across and crystal length can range up to a few centimetres. The growth of tourmaline is probably related to a nearby pegmatite intrusion and some related boron metasomatism.

5.3 Metamorphic mineral assemblages of prograde metamorphism: Mafic volcanic rocks (amphibolite schists)

5.3.1 Amphiboles

Hornblende is a common metamorphic mineral in the mafic rocks at Turner Lake. In some gabbroic/dioritic bodies, hornblende crystals are zoned from a bluish-green core to a colourless rim (Figure 5-14). Hornblende is commonly altered to biotite.

Cummingtonite-grunerite has been identified in the gold host (Unit 3f). Moving up in the stratigraphy, the composition of the amphibole changes from cummingtonite (Mg-rich member) to grunerite (Fe-rich member) and increases in abundance from 10% to 20%. Diffusion of Mg from the underlying ultramafic rock unit may have a metasomatic effect on surrounding units. Getzinger (1988) suggested a metasomatic reaction involving the movement of magnesium from the ultramafic unit into the host and movement of potassium from the host rock into the ultramafic rock (metapyroxenite) leading to a zonation in the

abundance of cummingtonite.

Millimetre-sized, euhedral to subhedral, dark green to black amphibole porphyroblasts are visible in outcrop and are diagnostic of the pyroxenite rock (Unit 3c). In thin section, pyroxene phenocrysts are pseudomorphed to tremolite-actinolite in a talc-rich matrix. In foliated samples the S_3 foliation warps around the phenocrysts (Figure 5-15).

The "nickel knob" gabbro contains olivine which has been replaced by serpentine and tremolite-actinolite (Figure 5-16).

5.3.2 Clinopyroxene

Clinopyroxene although rarely preserved, has been identified in less altered samples of the layered rocks (Unit 3g; Figure 3-13b). The presence of clinopyroxene is consistent with conditions of amphibolite grade metamorphism.

5.3.3 Discussion

The metamorphic minerals cummingtonite-grunerite, tremolite-actinolite and hornblende are all amphiboles common in amphibolite facies volcanic rocks. Hornblende is one of the most common constituents of regionally metamorphosed rocks and has a wide field of stability from greenschist to lower granulite facies (Deer et al., 1983). These minerals alone are not sufficient to constrain the conditions of metamorphism at Turner Lake but are compatible with the metasedimentary assemblages and have been presented for the purpose of a complete record of the metamorphic mineral assemblages present in the Turner Lake area.

5.4 Petrogenetic Grid

5.4.1 Cordierite

Cordierite is an abundant metamorphic mineral in the metasedimentary rocks at Turner Lake and as such is a useful mineral to use to help constrain metamorphic conditions.

Siefert (1970) considered cordierite in an iron-free, pure system. His experiments used phlogopite as opposed to biotite in reactions thus excluding iron from all phases. This simplifies the system which otherwise creates too many components for consideration as well as producing great variability of chemical phases involved in the reaction. He examined the reaction:

$$\text{muscovite} + \text{chlorite} + \text{quartz} = \text{cordierite} + \text{phlogopite} + H_2O$$

The rocks at Turner Lake do contain biotite and it would be negligent to exclude it from petrogenetic considerations. Ramsay (1974) examined the composition of mineral assemblages of metasedimentary rocks near Yellowknife and applied the work of Siefert (1970) to natural rocks. He considered the reaction:

$$\text{chlorite} + \text{muscovite} + \text{biotite} + \text{quartz} [+ \text{albite} + \text{ilmenite}] = \text{cordierite} + \text{biotite} + H_2O$$

Biotite becomes more abundant and changes composition during this reaction (Ramsay, 1974; Ramsay and Kamenini, 1977). The cordierite isograd approximates the 550°C isotherm (Ramsay, 1974). It is this reaction curve which has been used in this thesis (Figure 5-18).

5.4.2 Andalusite and Sillimanite

The experimental results for the three polymorphs of Al_2SiO_5 are variable. It is uncertain where the true phase boundaries and the triple point lie. This dilemma is discussed

at length by Winkler (1979). The coexistence of andalusite and sillimanite infers that conditions were close to the andalusite/sillimanite phase boundary. The absence of kyanite in the rocks at Turner Lake constrains pressure conditions to less than approximately 3.5 kb.

Most papers written on the Al_2SiO_5 polymorphs use either Holdaway (1971) or Richardson et al. (1969) with a few using Althaus (1967) or Brown and Fyfe (1971) for their boundary curves and triple points. The differences between the authors lies in the location of the triple point and slopes of the univariant reaction boundaries. Robie and Hemingway (1984) considered thermodynamic properties for kyanite, andalusite and sillimanite respectively in experiments. This work incorporates and accommodates the data of Holdaway (1971). These are the phase boundaries adopted in this thesis (Figure 5-18).

The upper limit of metamorphism is constrained by a lack of K-feldspar in the metasedimentary rocks. Chatterjee and Johannes (1974) have experimentally located the reaction curve for:

$$\text{muscovite} + \text{quartz} = \underset{\text{(K-feldspar)}}{\text{sanidine}} + \text{andalusite} + H_2O$$

5.5 Conclusions: An estimate of metamorphic conditions at Turner Lake

The co-existence of cordierite, andalusite and sillimanite has been used to estimate the metamorphic pressure and temperature conditions at Turner Lake. Pressure-temperature conditions inferred from the petrogenetic grid (Figure 5-19) indicate that rocks were subjected to temperatures between approximately 550 and 600^{0}C and pressures up to approximately 3.5

Kb. The exposed surface is a result of erosion across shallow dipping isograds.

Metamorphic conditions of regional amphibolite grade prevail in the Turner Lake area. Metamorphic grade is uniform across the map area with a possible increase in the northwestern corner indicated by the presence of prismatic sillimanite. Metamorphism was part of a multi-stage progressive episode during the D_3 phase of deformation involving sequential porphyroblast growth of biotite, cordierite, andalusite and finally sillimanite. Cordierite developed preferentially in mudstone beds and andalusite was preferentially developed in arenites. Andalusite became more abundant at the expense of cordierite in beds containing both. Cordierite without aligned inclusions preceded the development of S_3, which was followed by the overgrowth of andalusite. The growth of a biotite $\pm$ muscovite S_3 foliation in the metasedimentary rocks occurred during the D_3 deformation phase. Where S_3 inclusion trails exist in either cordierite or andalusite porphyroblast growth is interpreted to post date S_3. Sillimanite as fibrolite grew along the S_3 foliation as a breakdown product of biotite + muscovite and as an inversion product of andalusite. Prismatic sillimanite grew as a polymorphic inversion of andalusite. During D_4 crenulation there was no accompanying mineral growth. Metasomatic tourmaline grew in lithologic units close to pegmatite intrusions. Late random muscovite overgrowth may be the result of late granitoid intrusions.

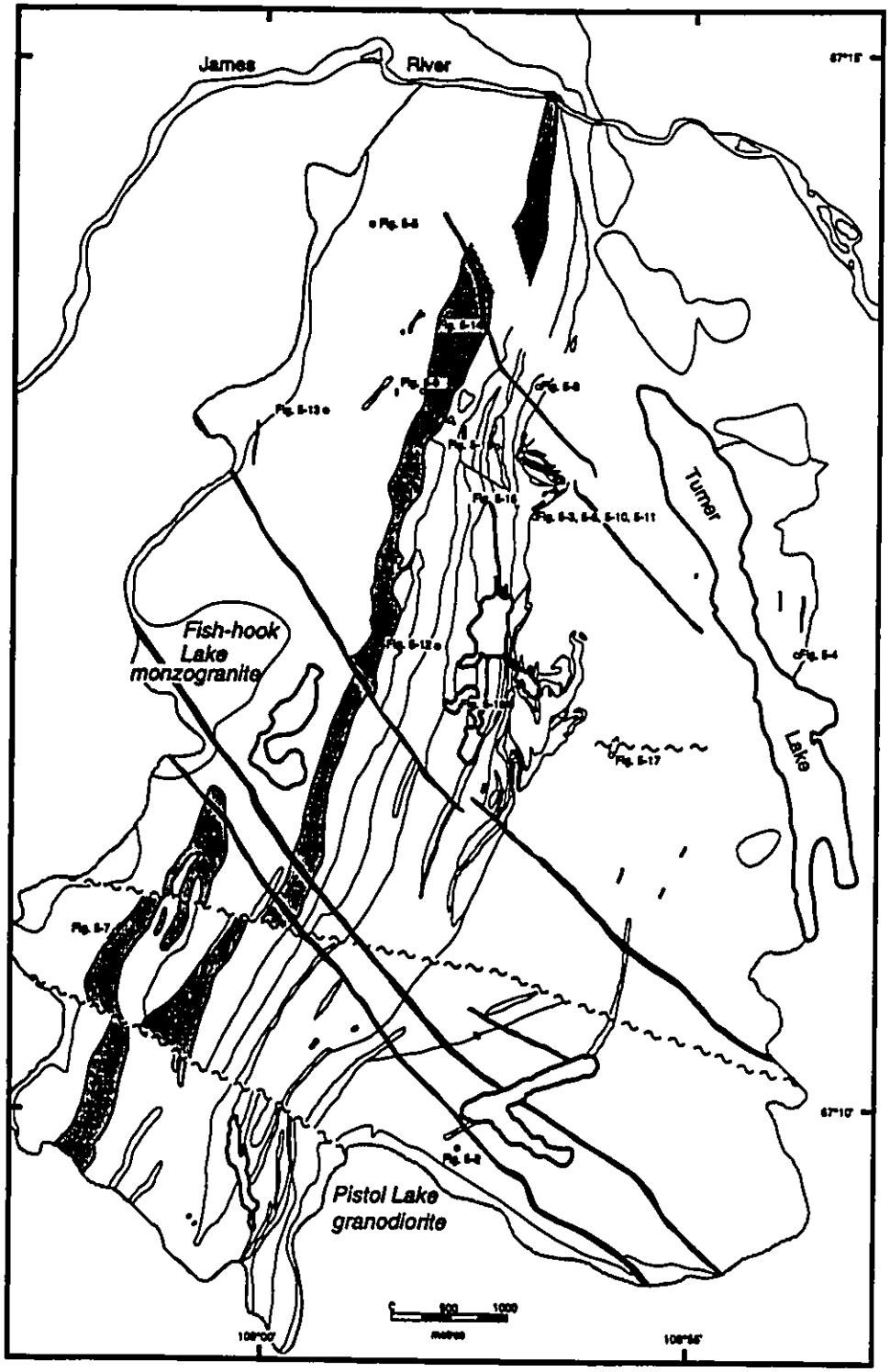

Figure 5-1. Location map of examples figured in chapter 5. Diabase dykes trend northwest across area. Unit 2 conglomerate indicated with pale grey.

Figure 5-2. Biotite(B) porphyroblasts defining S_3 foliation in metagreywacke (Unit 4, sample 89089) interleaved with and replaced by retrograde chlorite. Plane polarized light. Field of view is 2.5 mm.

Figure 5-3. Relict cordierite porphyroblast replaced by retrograde chlorite (Unit 4, sample 90005). Crossed polars. Field of view is 2.75 mm.

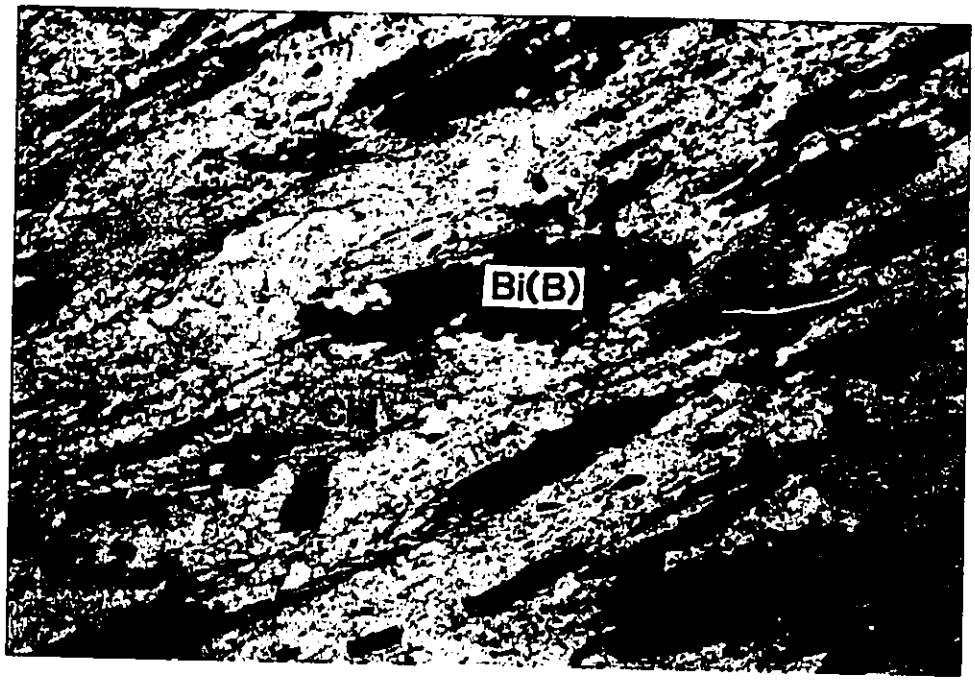
Bi(B)


Crd
Chl

Figure 5-4. Biotite(A) porphyroblast in metagreywacke-mudstone (Unit 4, sample 89153) overgrown by S_3 foliation defined by biotite(B) and muscovite. Muscovite overgrows biotite(A). Cordierite porphyroblasts overgrow and include the early biotite(A) porphyroblasts. Crossed polars in upper frame. Plane polarized light in lower frame. Field of view is 5.5 mm.

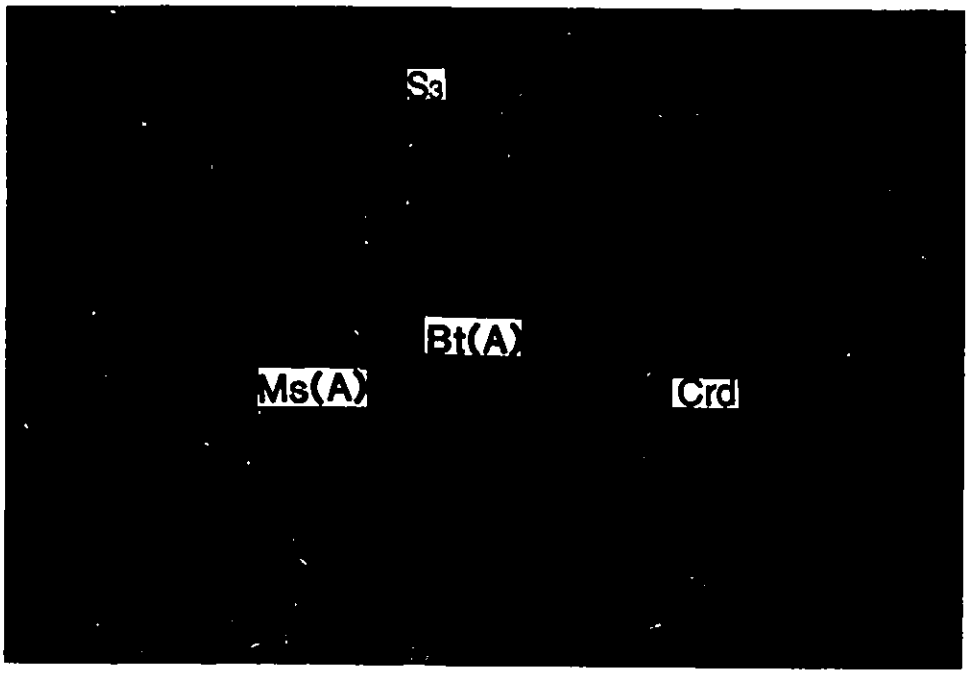
Sa
Bt(A)
Ms(A)
Crd

Figure 5-5. Late random muscovite(B) overgrows the S_3 foliation (Unit 1, sample 89054). Crossed polars in upper frame. Plane polarized light in lower frame. Field of view is 6.5 mm.

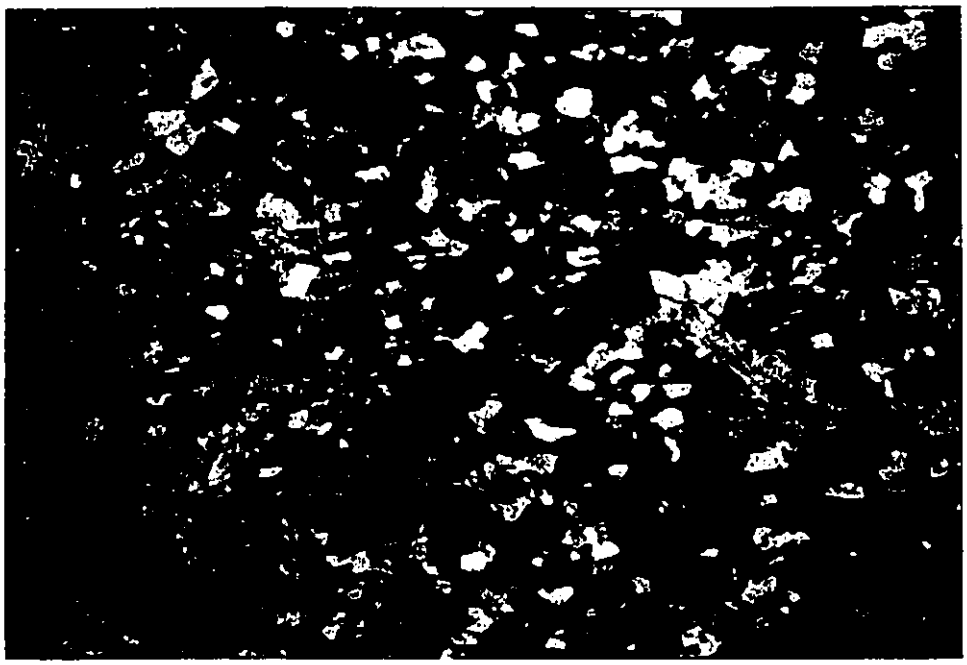

Figure 5-6. Biotite(B) + muscovite S_3 foliation warps around altered cordierite porphyroblasts (lacking aligned inclusions) but is preserved in andalusite (Unit 4, sample 90005). Crossed polars in upper frame. Plane polarized light in lower frame. Field of view is 15 mm.

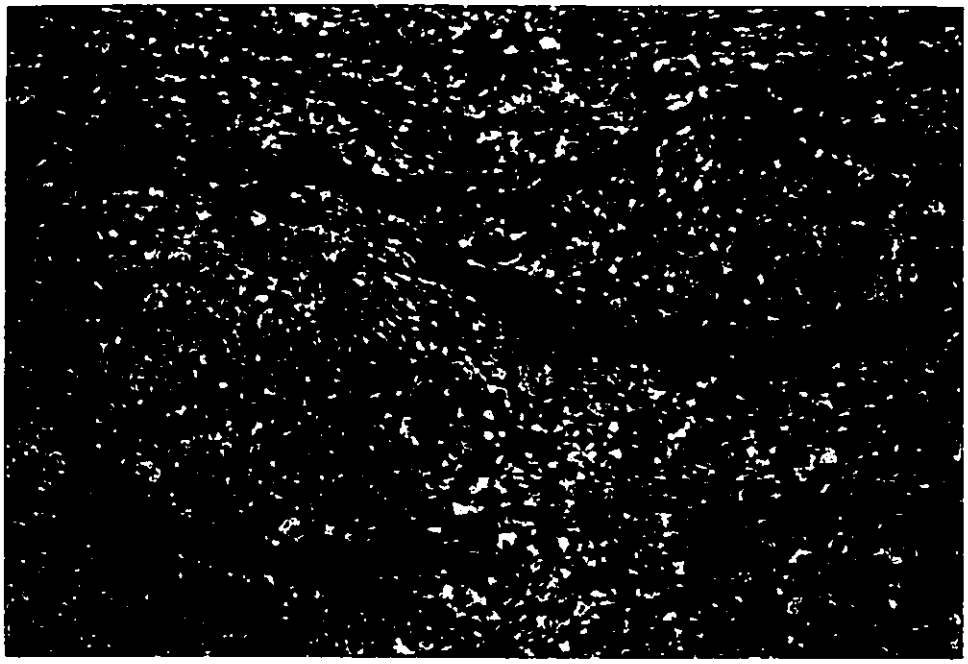

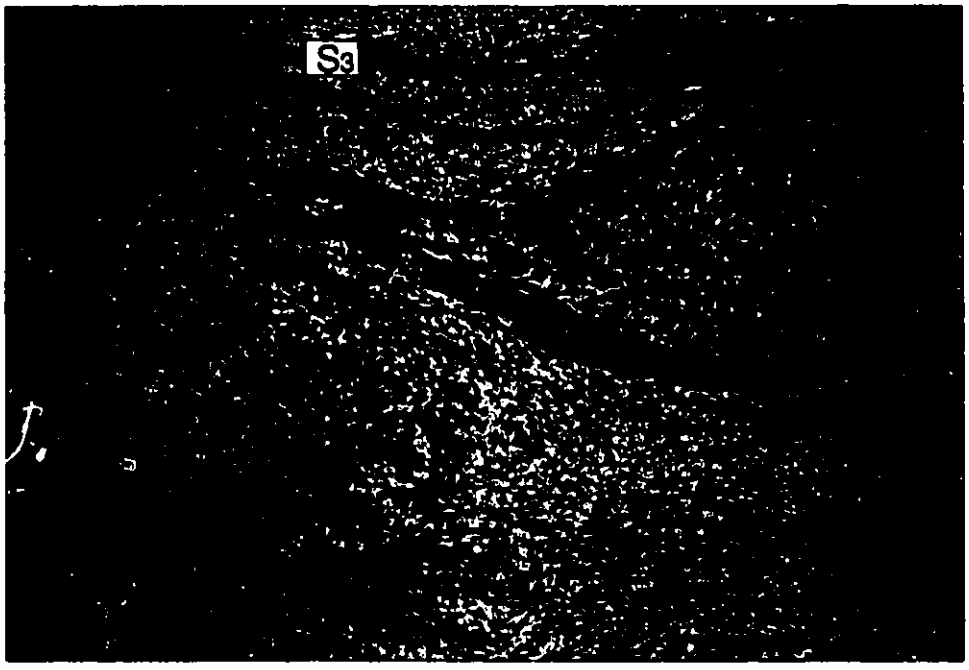
S3

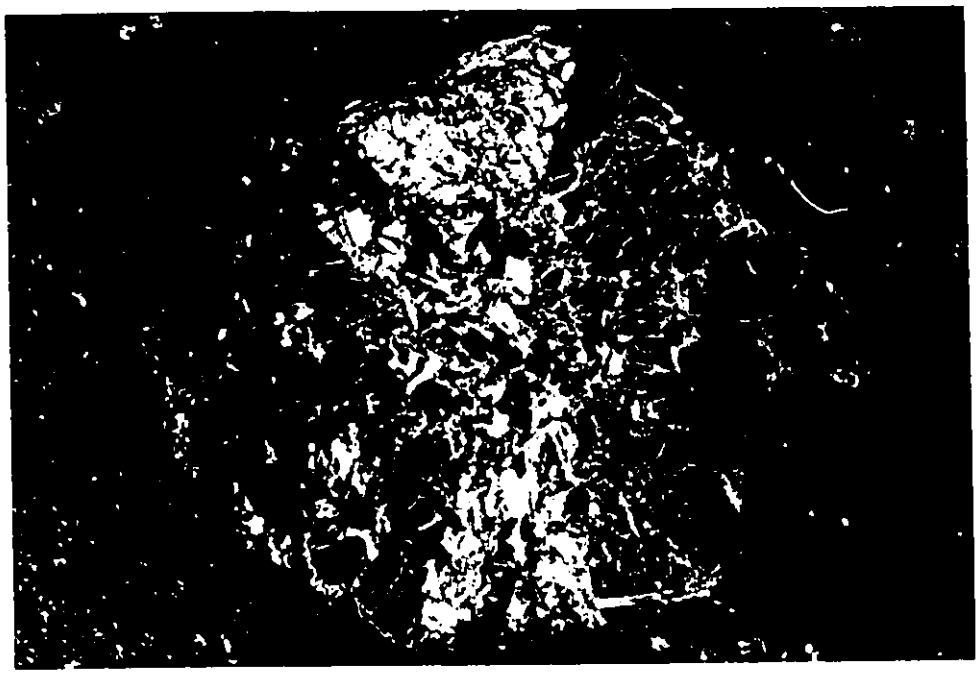

Figure 5-7. Andalusite, variety chiastolite, in iron formation (Unit 1a, sample 89147). Sericite alteration occurs along fractures and lines of included carbonaceous material. The external muscovite + biotite(B) S_3 foliation warps around the crystal. Crossed polars. Field of view is 14.5 mm.

Figure 5-8. Fibrolite aligned in the S_3 foliation plane grows in clusters with biotite(B) and muscovite(A) (Unit 4, sample 89039). Note the minor tourmaline in the upper left corner of the photograph. Crossed polars upper frame. Plane polarized light lower frame. Field of view is 3.5 mm.

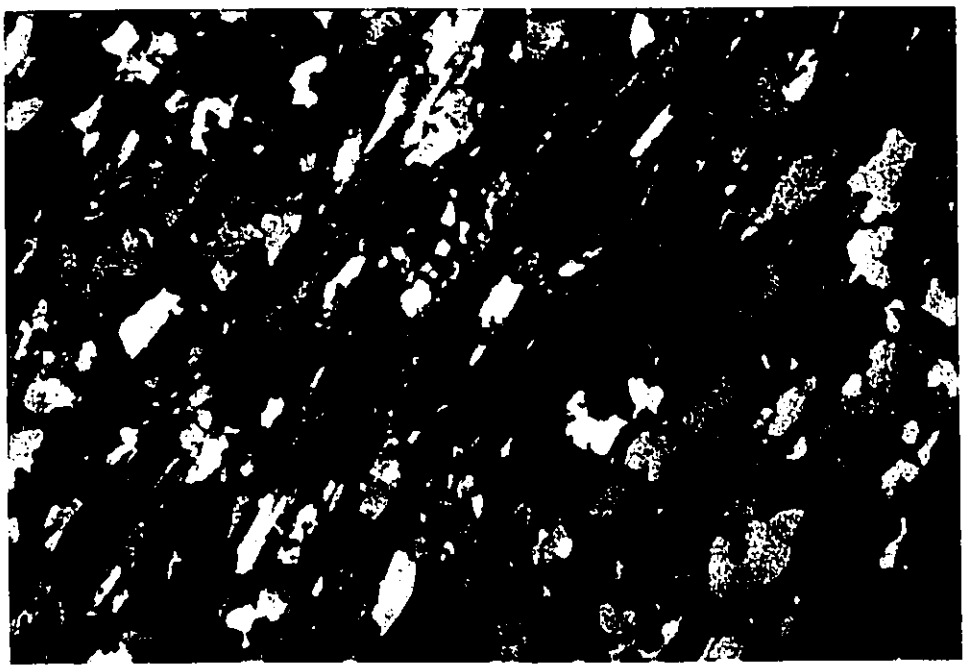

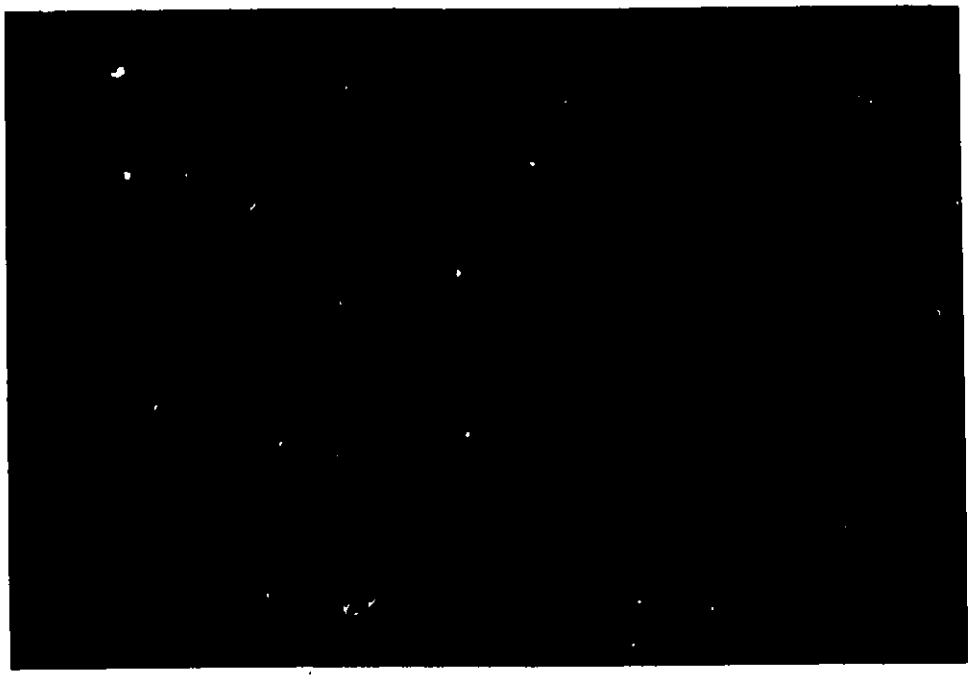

Figure 5-9. Fibrolite intergrown with biotite nucleating on relict poikiloblastic andalusite (Unit 1, sample 90043). Plane polarized light. Field of view is 8 mm.

Figure 5-10. Fibrolite growing as a pseudomorph of andalusite in metamudstone (Unit 4, sample 90005). Crossed polars upper frame. Plane polarized light in lower frame. Field of view is 1.25 mm.

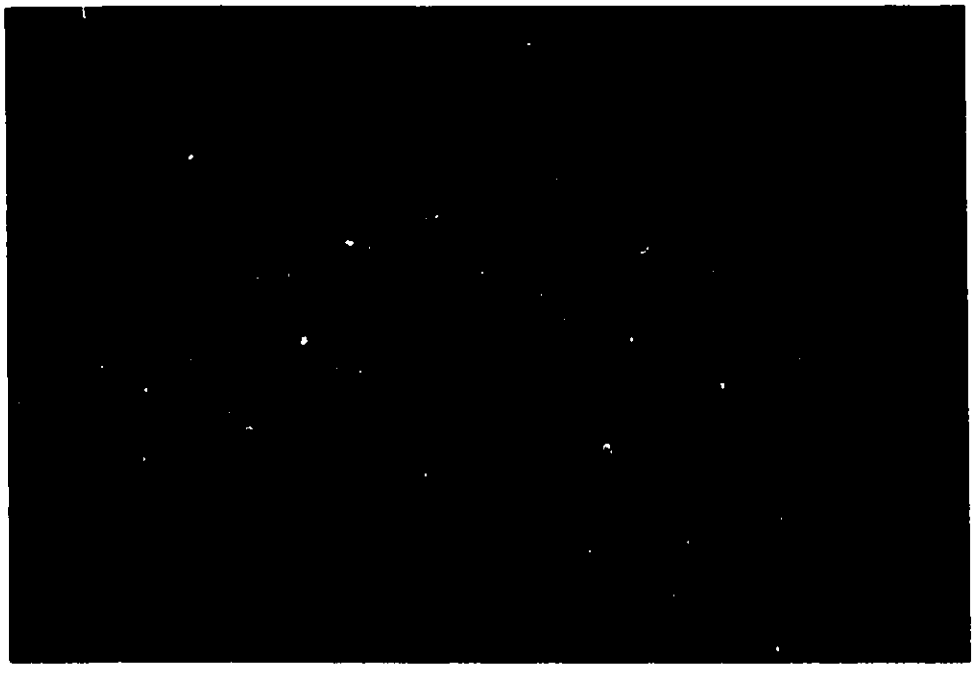

Figure 5-11. Fibrolite with andalusite growing in the S_3 foliation plane (Unit 4, sample 90005). Crossed polars upper frame. Plane polarized light in lower frame. Field of view is 3 mm.

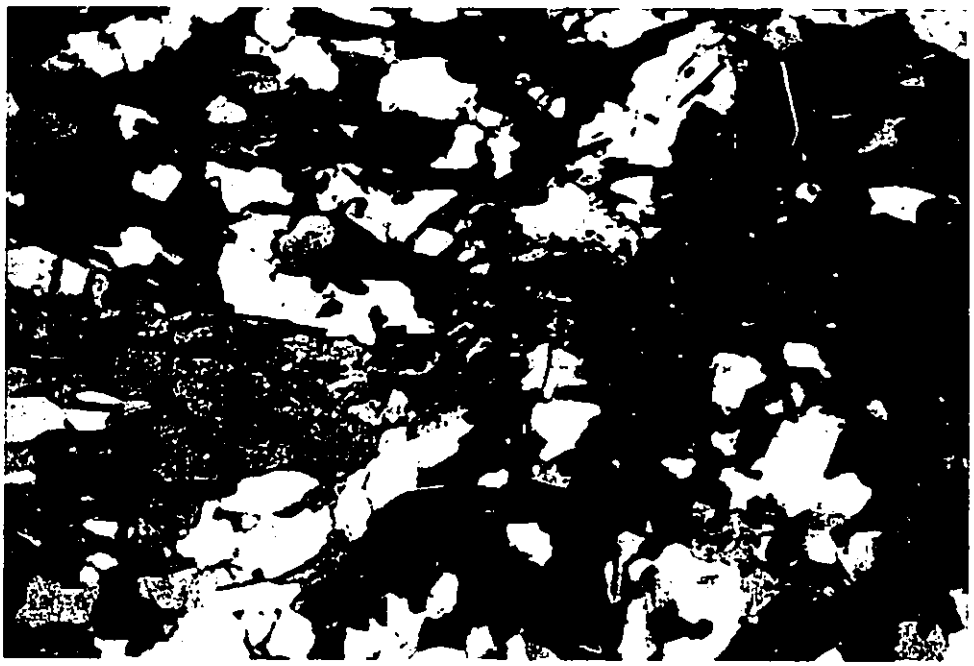


Sil

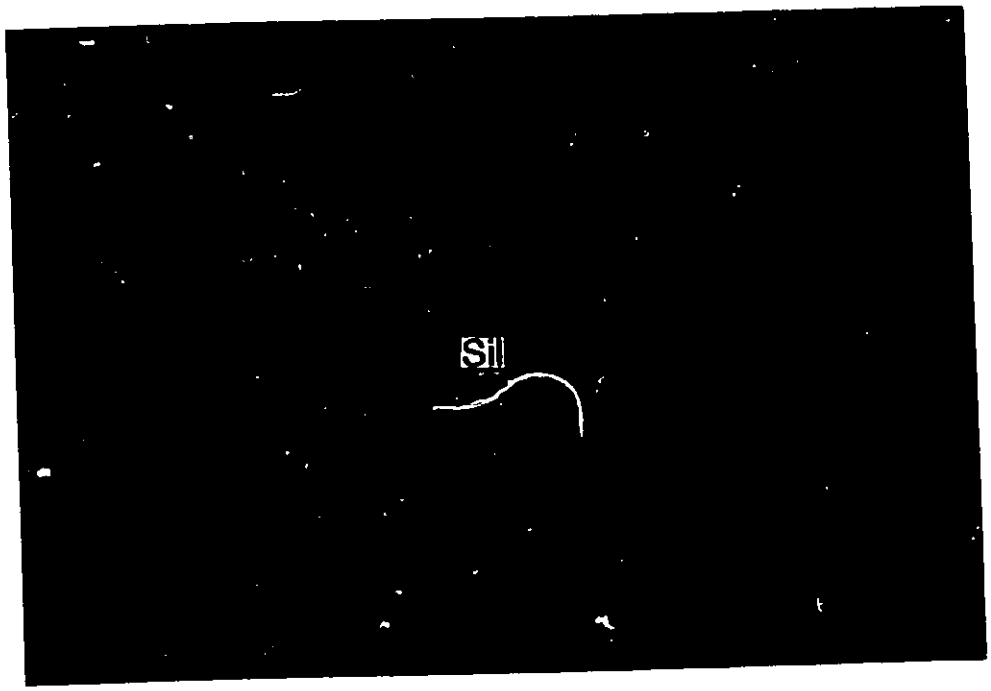

Figure 5-12. Fibrolite nucleating on and near relict andalusite poikiloblasts along the S_3 fo'iation with biotite as a coexisting phase (Unit 3a, sample 90092). Plane polarized light. Field of view is 4.5 mm.

Figure 5-13. Coarse, prismatic sillimanite intergrown with muscovite (Unit 1, sample 90046). Intergrain boundaries are well defined. Crossed polars upper frame. Plane polarized light in lower frame. Field of view is 8 mm.

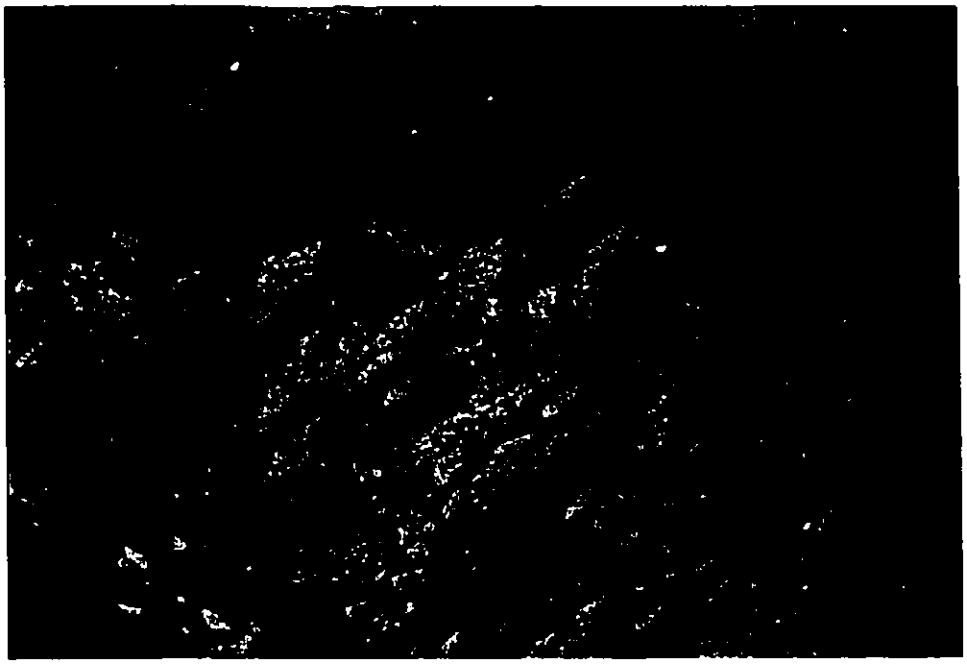

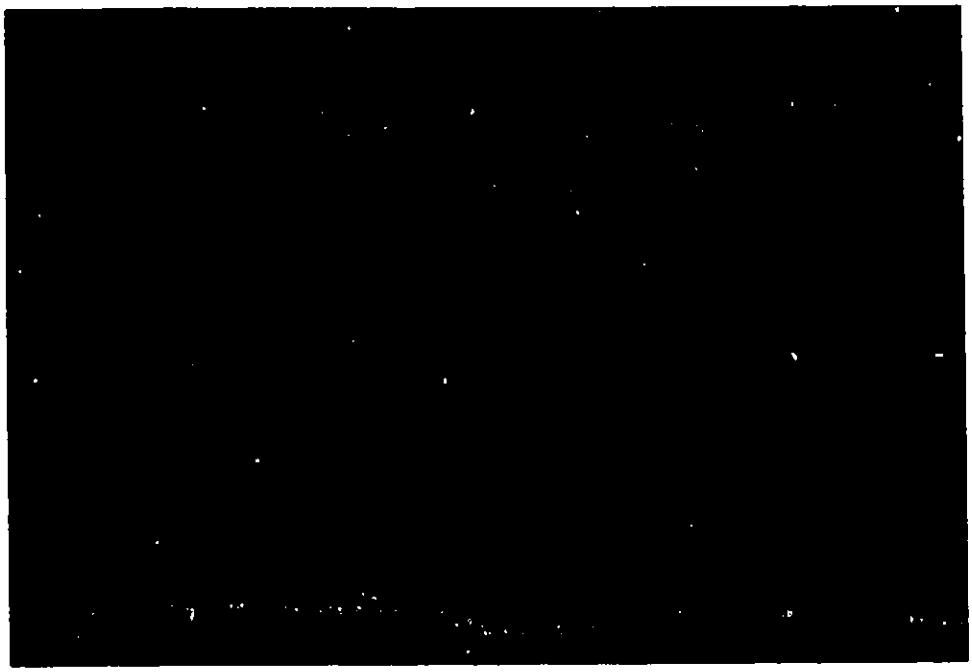

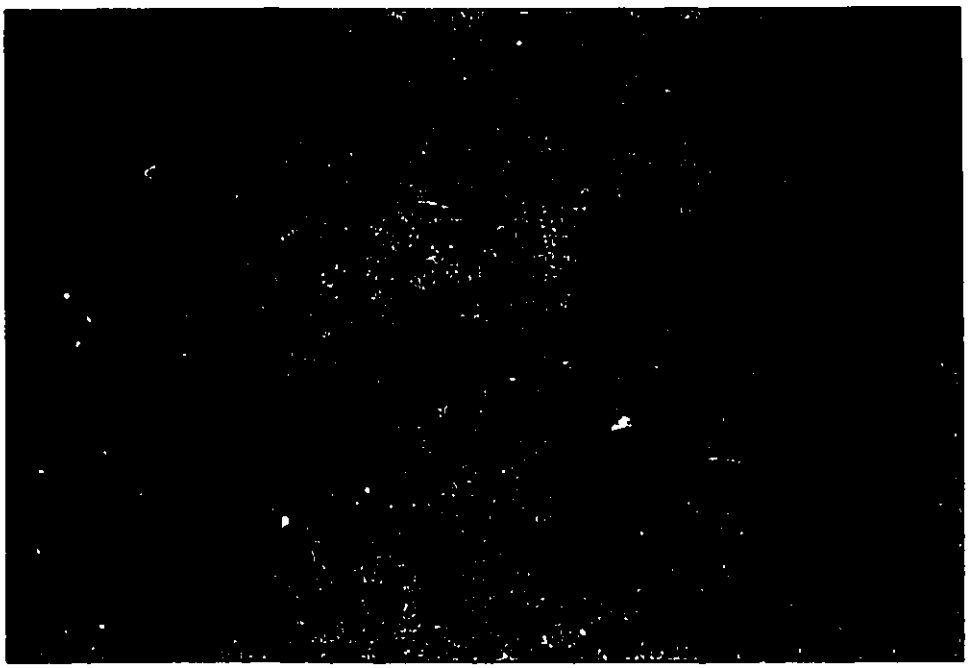

Figure 5-14. Euhedral to subhedral garnet crystals in matrix of James Falls Conglomerate (Unit 2, sample 90B6). The S_3 biotite(B) foliation is weak but appears to be slightly deflected around the garnets. Plane polarized light. Field of view is 6.5 mm.

Figure 5-15. Zoned hornblende crystals from a bluish-green core to a colourless rim (Unit 3b, sample 89034). Crossed polars in upper frame. Plane polarized light in lower frame. Field of view is 1.25 mm.

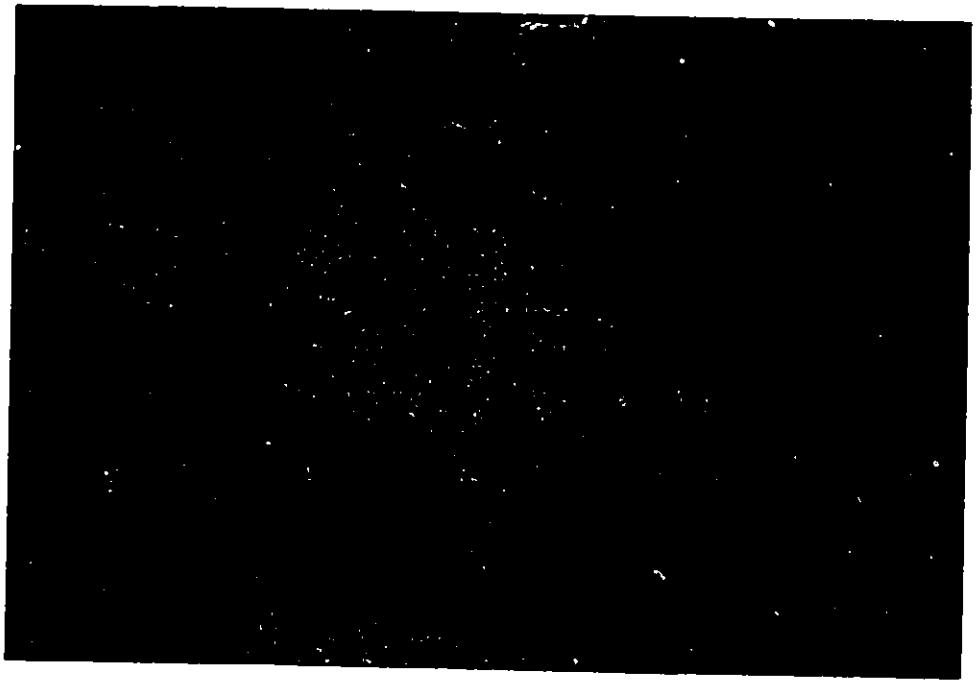

Figure 5-16. Foliated pyroxenite rock (Unit 3c, sample 89071) with S_3 foliation warped around tremolite-actinolite pseudomorphs after pyroxene. Crossed polars. Field of view is 2.5 mm.

Figure 5-17. Olivine in gabbro at Nickel Knob (Unit 6a, sample 89018) replaced by tremolite-actinolite and serpentine. Crossed polars in upper frame. Plane polarized light in lower frame. Field of view is 6.5 mm.

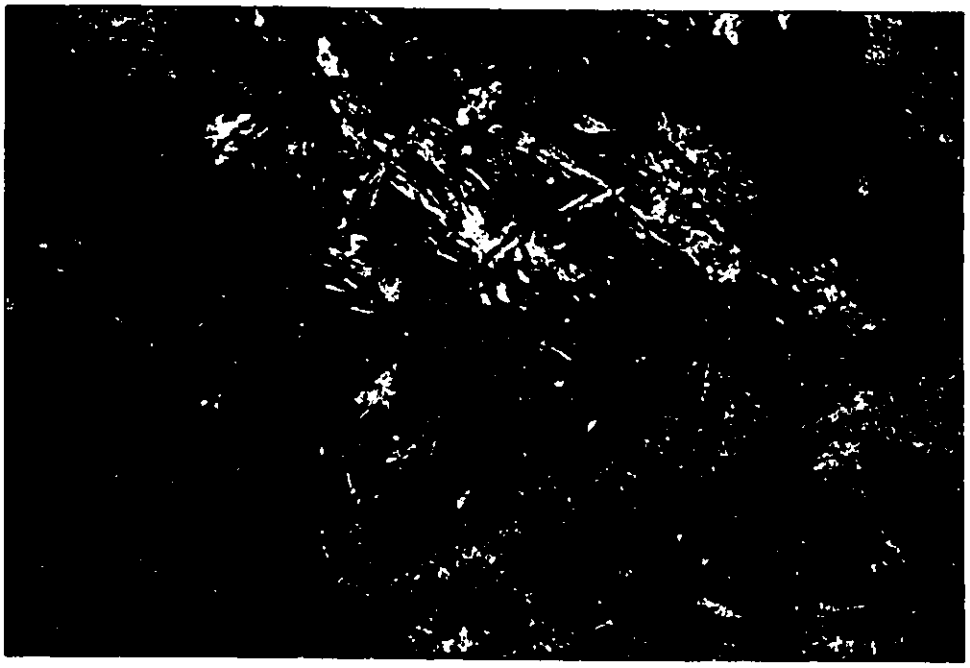

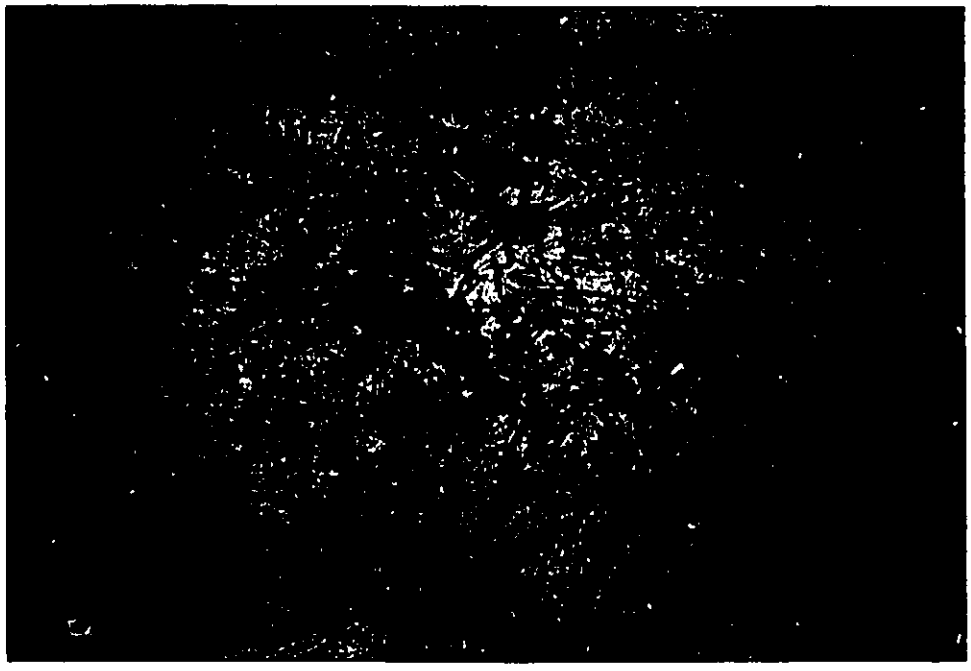

Figure 5-18. Euhedral to subhedral tourmaline crystals in mafic tuff (Unit 3d, sample 89125). Plane polarized light. Field of view is 10 mm.

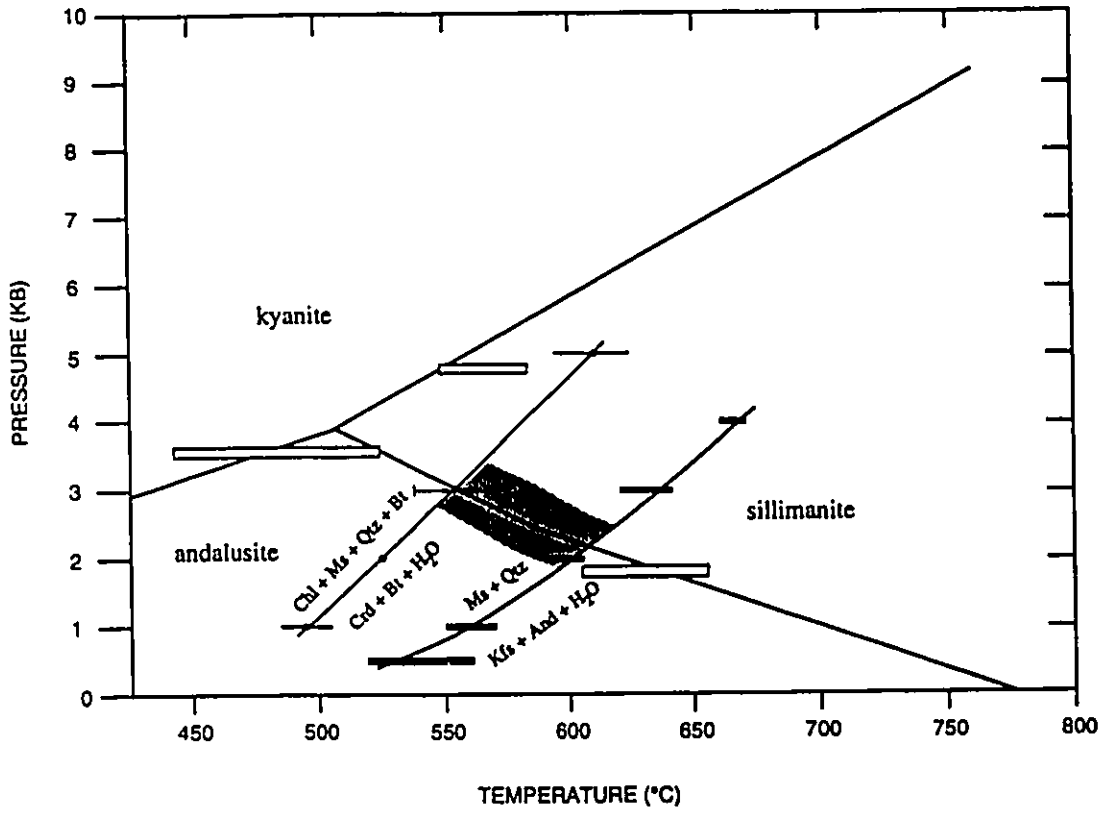

Figure 5-19. Pressure (kb) - temperature (°C) diagram showing a) stability fields for andalusite, sillimanite and kyanite from Robie and Hemingway (1984), white error bars; b) boundary for muscovite (Ms) + quartz (Qz) = K feldspar + Al silicate + H_2O as located by Chatterjee and Johannes (1974), black error bars; c) Boundary for Fe-free system: muscovite + chlorite + quartz = cordierite + phlogopite + H_2O as located by Siefert (1970) open bracket error bars and black circles; data for Fe-bearing system for the reaction: chlorite + muscovite + biotite + quartz [+ albite + ilmenite] = cordierite + biotite + H_2O as located by Ramsay (1974), closed bracket error bar and white circle. Approximate conditions at Turner Lake are indicated by shaded area. The co-existence of cordierite, andalusite and sillimanite in rocks at Turner Lake places conditions near the andalusite/sillimanite phase boundary. Rocks lacking fibrolite lie below the boundary curve.

Chapter 6
Geochemistry

6.1 Introduction

Representative samples from each Archean rock type within the map area were analyzed for major elements (Appendix III), numerous trace elements (Appendix IV) and some rare earth elements (Appendix V). Sample locations for each analyzed rock are shown in Figure 6-1.

Although AFM diagrams are commonly used for plotting the major element geochemistry of metamorphic rocks they use equal volumes of rock as opposed to equal weights and are susceptible to metamorphic effects. During metamorphism and deuteric processes both the alkalic (Na, K) and calcium contents of rocks can be affected and this will be reflected in the normative content and composition of plagioclase upon which many classifications are based. Irvine and Baragar's (1971) classification of volcanic rocks relies on colour and texture. The main criteria for a final recognition of rock type is by normative colour index and plagioclase composition. These traditional methods of data presentation are unreliable and subjective, and colour index is often deceiving especially in altered rocks.

Most of the supracrustal rocks at Turner Lake are thought to have been deposited subaqueously and to have undergone some degree of alteration and associated element mobility. With this in mind it is important to find a method to present geochemical analyses that will minimize the effects of alteration in the supracrustal rocks. The use of relatively immobile elements can help to achieve this. Jensen Cation Plots (Jensen, 1976) have been

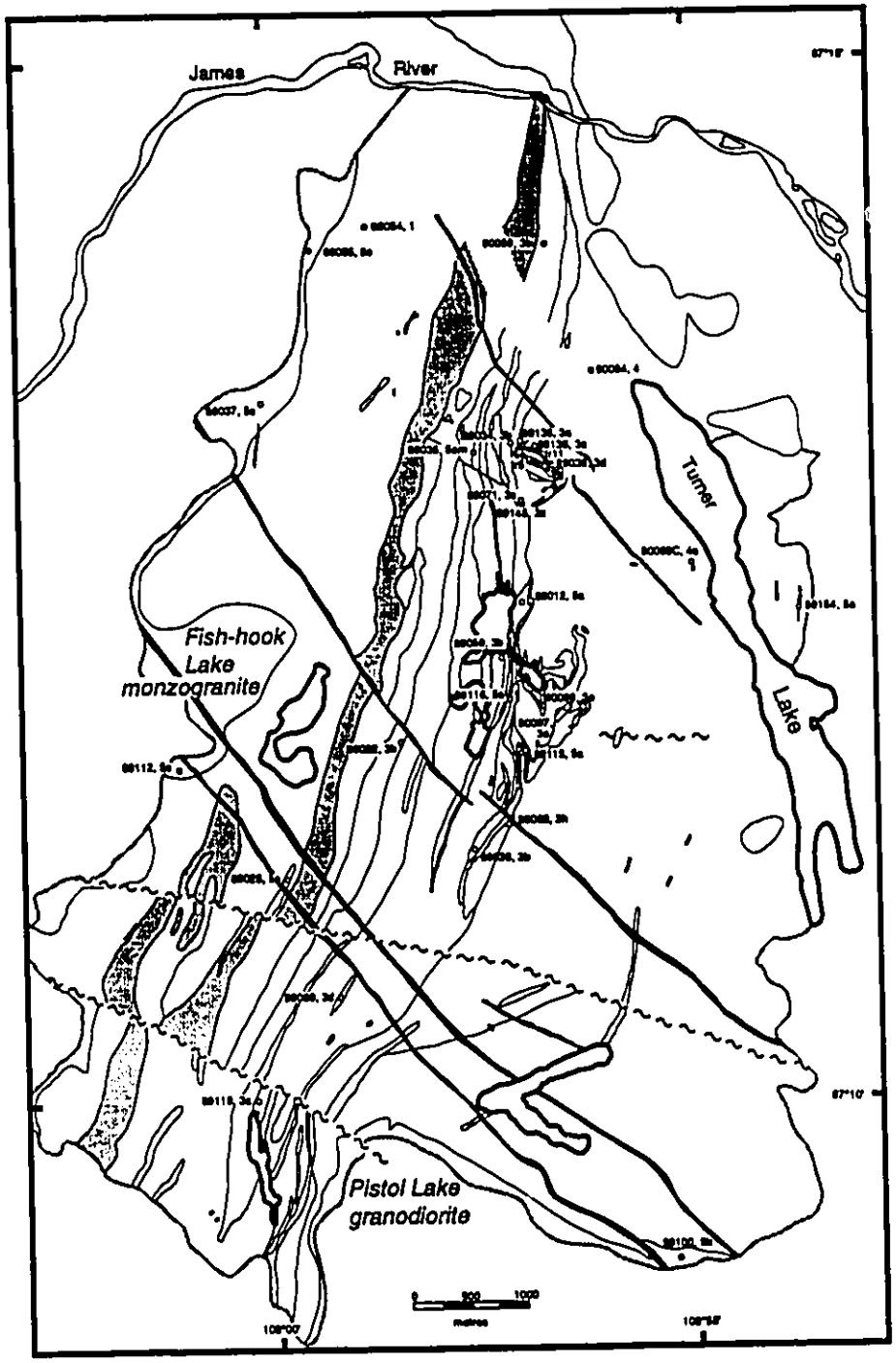

Figure 6-1. Sample location sketch map for geochemical analyses of the Turner Lake area. Sample number is given followed by unit number (see large scale maps 2 and 3 in back pocket). Diabase dykes are dark speckled units. Unit 2 conglomerate indicated with pale grey.

used in previous studies of the Archean rocks at Turner Lake (Fumerton, 1989; Clode, 1987; Staargaard, 1987) and are used here to compare the findings of Fumerton (1989) with this study for Units 3c, d, e and f. All volcanic-related rocks (Units 3b, c, d, e, and f) are plotted on a plot of SiO_2 vs. Zr/TiO_2 (after Winchester and Floyd, 1977) to classify them. Plutonic rocks (Unit 5) are classified according to the scheme by O'Connor (1965). Chondrite normalized rare earth element plots provide a geochemical signature of the Archean rock units in the map area.

6.2 Jensen Cation Plots and volcanic rocks

The cations used for Jensen plots, namely Al_2O_3, $FeO + Fe_2O_3 + TiO_2$ and MgO, are relatively stable and bear a relationship to rock colour. They vary in inverse proportion to one another and lend themselves to comparative plotting. Fe and Mg are less susceptible to chemical migration than K, Na, Ca and Si. Leaching or enrichment of small amounts of K_2O, Na_2O, CaO and SiO_2 within a rock has no great effect on the ratio derived from relative amounts of Al_2O_3, $FeO + Fe_2O_3$ and MgO. Jensen cation plots relate cation percentages of Al_2O_3, $FeO + Fe_2O_3 + TiO_2$ and MgO in a ternary plot (Figure 6-2a) and were designed to recognize and discriminate between differentiation trends of komatiitic, tholeiitic and calc alkalic suites of subalkalic volcanic rocks. They are not designed to name volcanic rocks but rather to show compositional trends within a volcanic sequence.

Jensen cation values for the average mean composition of Yellowknife volcanic rocks (Table 2 in Cunningham and Lambert, 1989) including those for dacite, andesite, basaltic

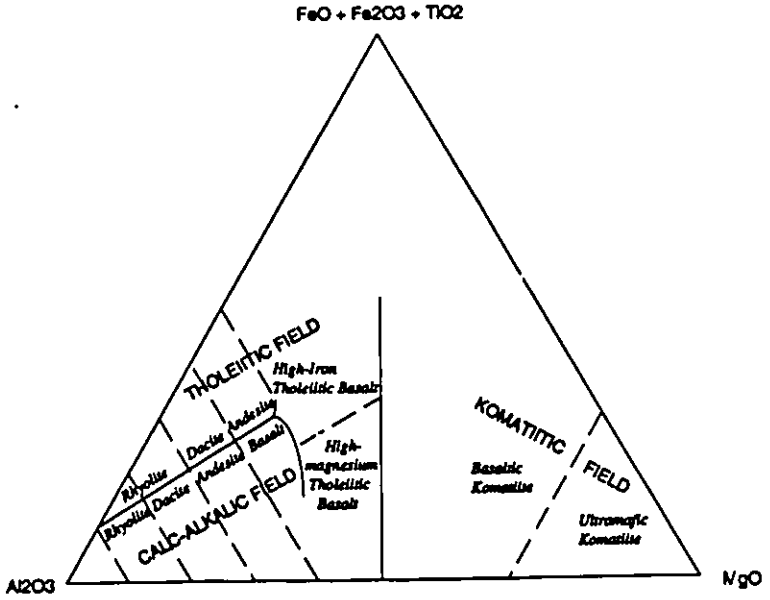

(a)

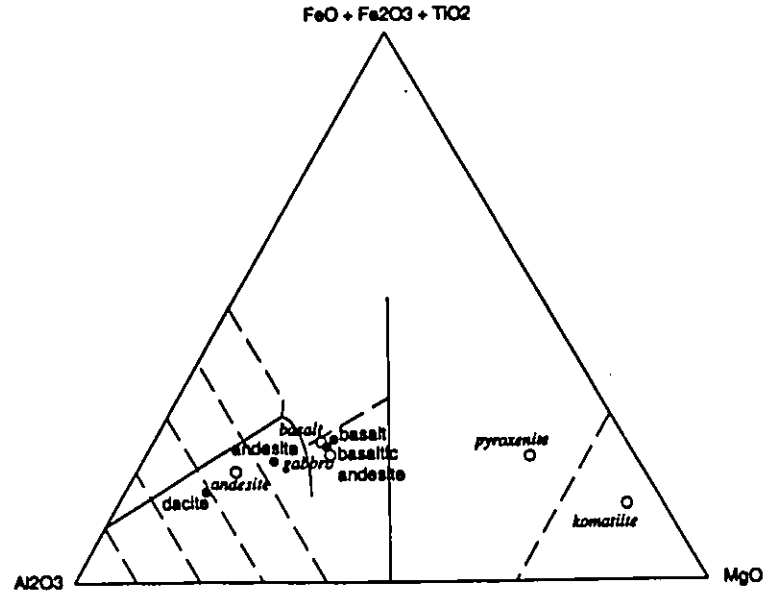

(b)

Figure 6-2. Jensen cation plots involving the percentages of Al2O3, FeO + Fe2O3 + TiO2, and MgO (after Jensen, 1976); (a) fields labelled in capital letters, rock types in italic; (b) average chemical analyses of common igneous rocks (open circles, italic type; from Table 3-7 of Hyndman, 1985). Average values of mean composition of rock type for Yellowknife volcanic rocks (solid circles, regular print; from Table 2 of Cunningham and Lambert, 1989).

andesite and basalt and of other common igneous rocks including basalt, gabbro, pyroxenite and komatiite (Table 3-7 in Hyndman, 1985, with data from LeMaitre, 1976) (Figure 6-2b) were calculated and plotted for comparison with the analyses of rock units in this study. Rock names do not necessarily plot in their corresponding fields emphasizing that the Jensen plot should be used with a suite of rocks to determine compositional trends rather than to give individual rock unit names.

Amphibole-rich rocks from Turner Lake have been the subject of much speculation by previous workers (Staargaard, 1987; Clode, 1987; Fumerton, 1989). They considered them as a single unit and did not differentiate between the subunits identified in this thesis as amphibole rock (Unit 3c), mafic tuff (Unit 3d), epiclastic amphibolite (Unit 3e) and the amphibolitic, epiclastic gold host rock (Unit 3f). Speculations as to protolithology of the amphibole rock (Unit 3c) include a high Mg-pyroxene-phyric gabbro or porphyritic pyroxenite (Staargaard, 1987) and metaperidotite (Clode, 1987) which plots within the komatiitic field of the Jensen cation plot. Fumerton (1989) considered the amphibole-rich units as a stacked series with upper and lower sequences however these divisions are poorly described. Rocks described by Fumerton as massive ultramafic flows could be equated to the amphibole rock (Unit 3c); However, Fumerton did not note the characteristic pyroxene-shaped pseudomorphs of 3c described above (Chapter 3). Unfortunately the analyses of Fumerton (1989) do not indicate assignment of his samples to a subunit of either the upper or lower amphibolite sequence. Therefore, Fumerton's sample numbers are not shown in Figure 6-3b. Fumerton used the Jensen plots to attribute basaltic and ultramafic komatiitic signatures to the lower and

upper sequences respectively but did not elaborate on a protolith beyond stating that they are komatiitic. For comparative purposes the analyses for Units 3c, d, and e (Figure 6-3a, b) plot within the field of basaltic komatiites on Jensen cation plots. However this does not imply that these rocks are indeed komatiites because no spinifex has been observed by the writer nor reported by Fumerton.

Many Archean komatiites occur within a thick sequence of intermediate to felsic volcanic rock units in association with the felsic volcanic rocks (Brooks and Hart, 1974). Brooks and Hart's observation contrasts strongly with the geology at Turner Lake which comprises only minor volcanic rocks. If the amphibole rock (Unit 3c) is indeed a komatiite then it is quite unusual in both its lithologic setting and in the lack of diagnostic textures (see Chapter 3). Brooks and Hart (1974) have characterized komatiites and listed analyses of 22 diverse rock types with basaltic komatiitic chemistry including olivine basalt, picrite, olivine gabbro, olivine dolerite, basalt, ankaramite, clinopyroxenite, andesite and basalt tuff. The whole rock analyses for samples from the amphibole rock (Unit 3c) listed in Appendix III are comparable to these, further indication that they need not be komatiites despite their komatiitic chemistry. The mineralogy of the rock is then an important consideration for determining a possible protolith. It is most likely that the amphibole rock (Unit 3c) is a metamorphosed pyroxenite. The inferred protolith pyroxenite is now altered to tremolite-actinolite and contains no feldspar or quartz. This agrees with the plot position for a typical pyroxenite composition on the Jensen plot (Figure 6-2b).

Unit 3d, mafic tuff has a similar chemical signature to the amphibole rock (Unit 3c)

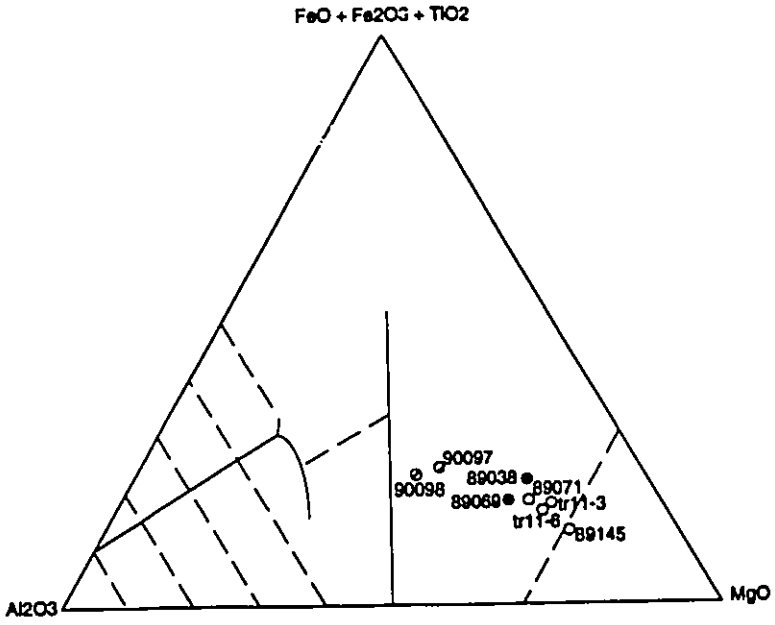

(a)

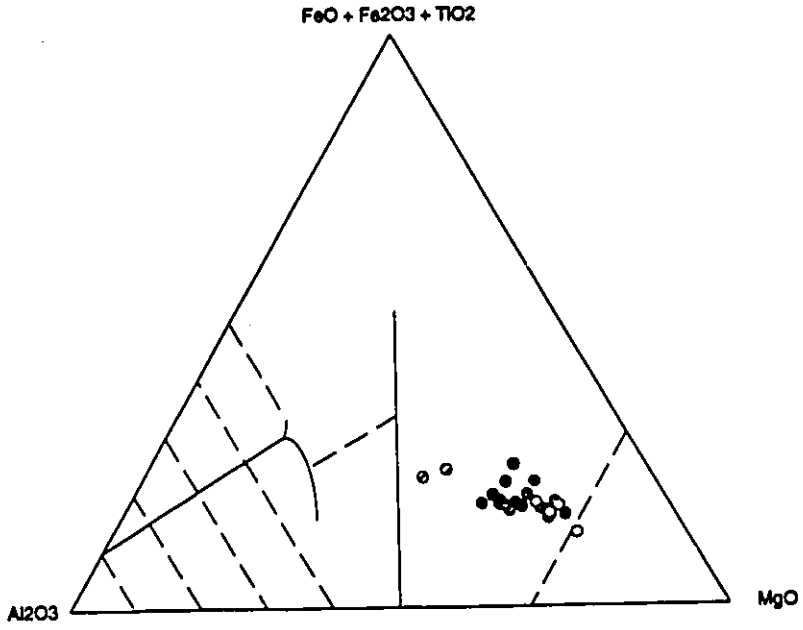

(b)

Figure 6-3. Jensen cation plot of amphibole-rich volcanic rocks from Turner Lake; (a) unit 3c (open circles), 3d (black circles) and e (diagonally striped circles). (b) samples from (a) compiled with upper and lower amphibolite analyses from Fumerton, 1989 (stippled circles).

(Figure 6-3a). This is considered to be indicative of consanguinity. Likewise the mafic tuff (Unit 3d) and epiclastic amphibolite (Unit 3e) have comparable chemical signatures with the epiclastic amphibolite (Unit 3e) plotting to the left. The epiclastic amphibolite (Unit 3e) is spatially associated with the mafic tuff (Unit 3d) which is associated with the amphibole rock (Unit 3c). The epiclastic amphibolite (Unit 3e) is a result of minor clastic input (contamination) of the mafic tuff (Unit 3d), hence the similarities in composition.

All of the samples of Unit 3f, the clastic, amphibolitic gold host, plot within the andesite field of tholeiitic volcanic rocks (Figure 6-4a). This does not mean that these rocks are andesites but is does support petrographic observations that this unit is a variation of the epiclastic amphibolite (Unit 3e). Greater clastic input may have caused the further shift to the left on the Jensen plot from the plot position of Unit 3e. This is in accordance with stratigraphic relationships whereby Unit 3f is part of a sequence of rocks including Units 3b, d and e (Appendix II). The analyses of Fumerton (1989) for "mineralized arenite" are equated to the clastic, sulphidic, amphibolitic rock (Unit 3f) of this study. Fumerton's samples plot mostly within the andesitic field of tholeiites (Figure 6-4b). It should be stressed here again that the Jensen plot is not meant to imply that the host unit is a tholeiitic andesite. It has merely been employed here as a means of comparison with the work of Fumerton (1989) to show an overall compositional similarity with the rocks of this study and those of Fumerton (Figure 6-4c).

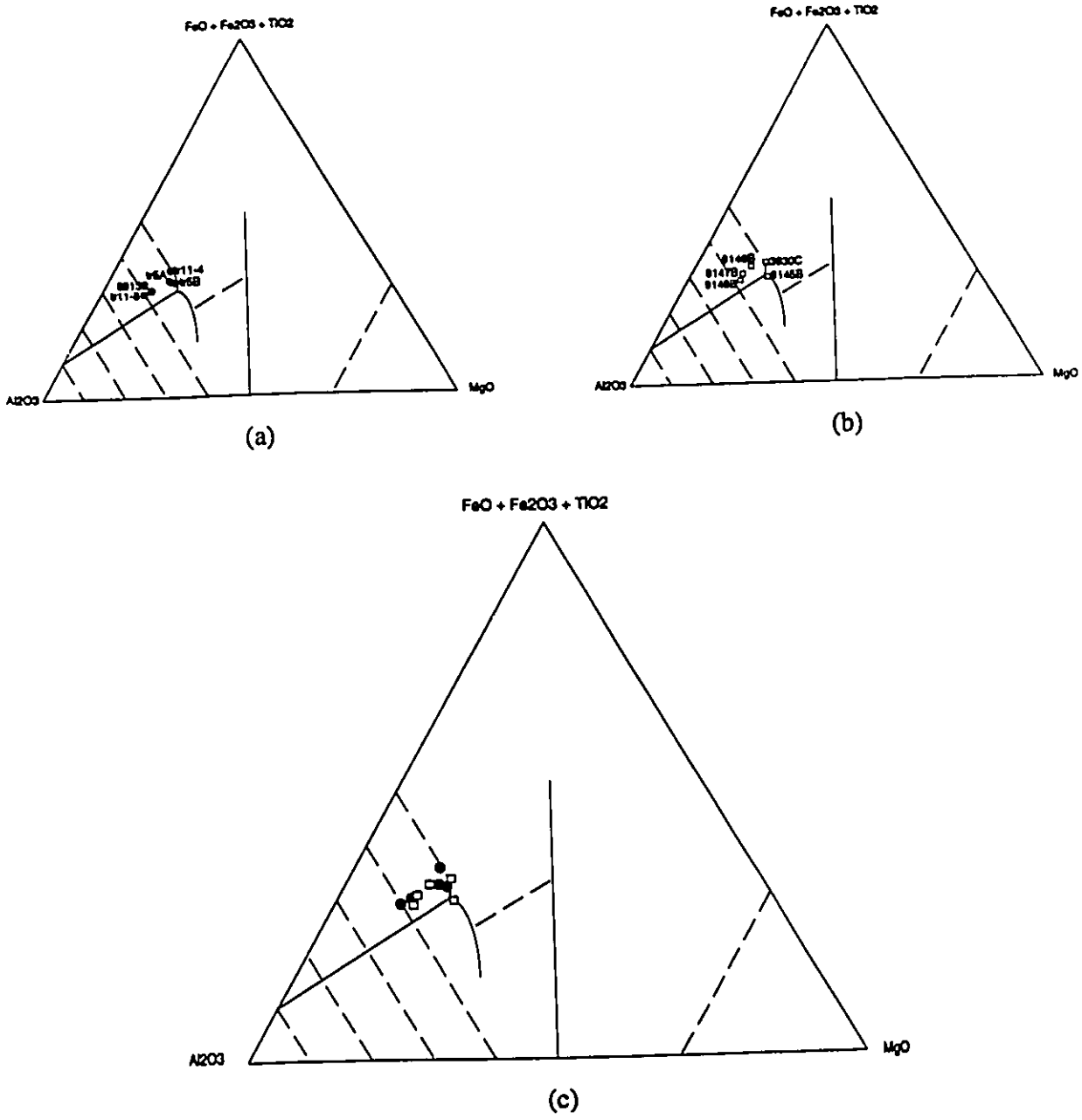

Figure 6-4. Jensen cation plot showing position of gold host unit (3f) fromTurner Lake; (a) analyses from this study with sample numbers indicated; (b) analyses from Fumerton, 1989 with sample numbers indicated; (c) combination of (a) and (b).

6.3 Trace Element Geochemistry

Chemical analyses of volcanic-related rocks including diorite/gabbro (3b), amphibole rock (3c), mafic tuff (3d) and epiclastic amphibolite (3e) were plotted on the SiO_2 vs Zr/TiO_2 diagram after Winchester and Floyd (1977) designed for naming volcanic rocks (Figure 6-5). Analyses of volcanic rocks from the Yellowknife Supergroup (Table 2 from Cunningham and Lambert, 1988) were included in this plot as a basis for comparison with the samples from Turner Lake. The andesite sample did not fall into the correct field in the Jensen plot (Figure 6-2b) but is in its corresponding field here. This further emphasizes the fact that the Jensen plot should not be used as the sole means by which volcanic rocks are named or their protolithologies identified.

Samples of the host rock (Unit 3f) have a wide distribution. This is probably a function of the amount of SiO_2 in the rocks. The gold at the Turner Lake main showing is associated with quartz veining and the amount of veining within a sample will dramatically alter its plot position. This is illustrated by the samples from trench 5. Sample 5A is predominantly of a gold-bearing quartz vein whereas sample 5B is of the matrix. 5A plots much higher on the graph than 5B (Figure 6-5). An andesitic composition is inferred for the host subunit which agrees with the Jensen plot. However, since this rock unit is considered to be epiclastic in origin a volcanic rock name is not completely appropriate.

The samples of epiclastic amphibolite (Unit 3e) all plot as subalkaline basalts (samples 90097, 90098; Figure 6-1). Samples of the mafic tuff (Unit 3d) (samples 89038 and 89069; Figure 6-1) and those of the amphibole rock (3c) (samples tr11-3, tr11-6, 89071 and 89145;

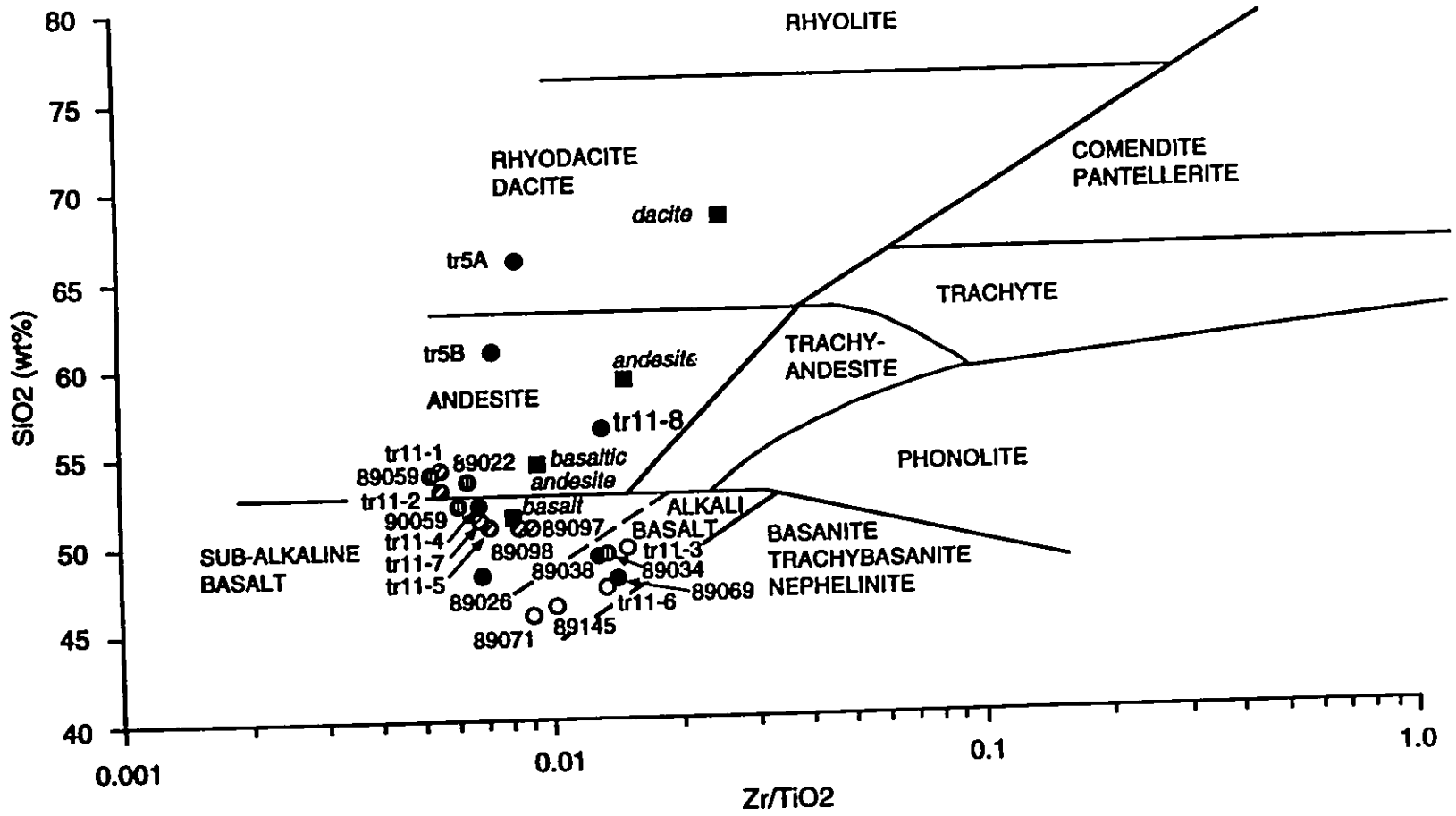

Figure 6-5. SiO2 - Zr/TiO2 diagram for naming volcanic rocks (after Winchester and Floyd, 1977). Field boundary locations approximate. Analyses from Table 2 of Cunningham and Lambert,1988 (squares); unit 3d, mafic tuff (black circles), unit 3e, epiclastic amphibolite (diagonally striped circles); unit 3c, (white circles); unit 3f, host (stippled circles); unit 3b, diorite (vertically striped circles). Sample numbers are given for each point.

Figure 6-1) plot as alkali basalt. This shift in composition is most likely the result of progressive contamination by a clastic source from the amphibole rock (Unit 3c) to the mafic tuff (3d) to the most contaminated epiclastic amphibolite (Unit 3e).

This plot does not take into account the amount of MgO in the analysis, a distinguishing characteristic of Units 3c, d and e. Perhaps the most important contribution by this diagram is its demonstration that the use of different parameters in the presentation of geochemical data will greatly affect the interpretation of a protolithology. In this case, outcrop relationships and mineralogy are the most important considerations in speculating on a protolith for these rocks.

Samples of diorite/gabbro (Unit 3b) show a varied distribution about a basaltic composition. This distribution is a function of the coarseness of the sample. From coarsest to finest they are samples: 89034, 90059, 89026 and 89022 (same grain size) and 89059. The intrusive equivalent of basalt is gabbro or diorite. This is in agreement with petrographic observations which identified this rock as dioritic to gabbroic.

6.4 Plutonic rock classification

The plutonic rocks in the study area are quartz-rich (they contain >10% quartz) and can be represented by points on a quartz-orthoclase-albite-anorthite (Qz-Or-Ab-An) tetrahedron. In rocks containing greater than 10% quartz, variation in quartz content becomes negligible when determining rock type. The parameters used in the O'Connor classification (1965) are Or, Ab and An. In contrast to modal compositions used in the IUGS classification

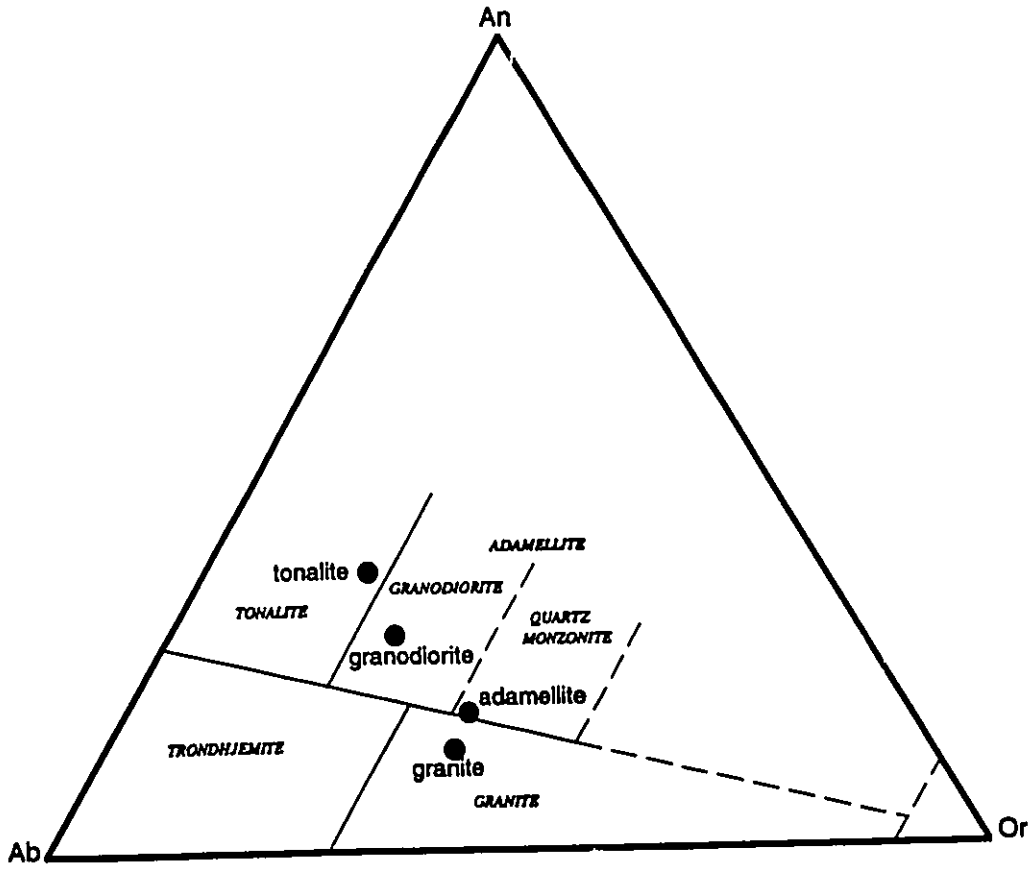

Figure 6-6. Plot of plutonic rocks after O'Connor (1965). Fields indicated by italics. Standard samples (black circles) from Table 3-7 (Hyndman, 1985) labelled with regular print.

scheme (Strekeisen, 1976), O'Connor's classification requires the use of normative feldspar composition expressed in molecular % (O'Connor, 1965). It was adopted for use in this thesis in preference to the IUGS classification scheme because it does not rely on the determination of modal mineralogy. Many of the plutonic rocks in the Turner Lake area are locally intensely deformed, recrystallized and fine-grained, especially along the main high strain zone ($5a_m$). As a result, many minerals are difficult to identify in thin section let alone point count. The O'Connor plot allows their composition to be compared with coarser grained, samples for which thin section identification was completed, such as the Pistol Lake granodiorite (Unit 5b) and the Fish-hook Lake monzogranite (Unit 5c).

The average chemical analyses of common granitoid varieties of igneous rocks (from Table 3-7 in Hyndman, 1985 with data from LeMaitre, 1976) have been compiled. Granitoid varieties which are listed in this table and are present in the study area were plotted on the O'Connor tetrahedron as standards for comparison with the samples from the study area (Figure 6-6).

Highly deformed plutonic rocks (Unit $5a_m$, samples 89035, 89012, 89115; Figure 6-1) plot as tonalites and granite (Figure 6-7a). Less deformed equivalents of this unit (Unit 5a, samples 89028, 89154; Figure 6-1) plot as trondhjemites (Figure 6-7a). In agreement with petrographic observations the Pistol Lake pluton (Unit 5b, sample 89100; Figure 6-1) plots as granodiorite and the Fish-hook Lake pluton (Unit 5c, samples 89055 and 89112; Figure 6-1) as granite (Figure 6-7b). Units $5a_m$ and 5b have similar compositions and may be related just as the Fish-hook Lake granite has associated pegmatites (not analyzed).

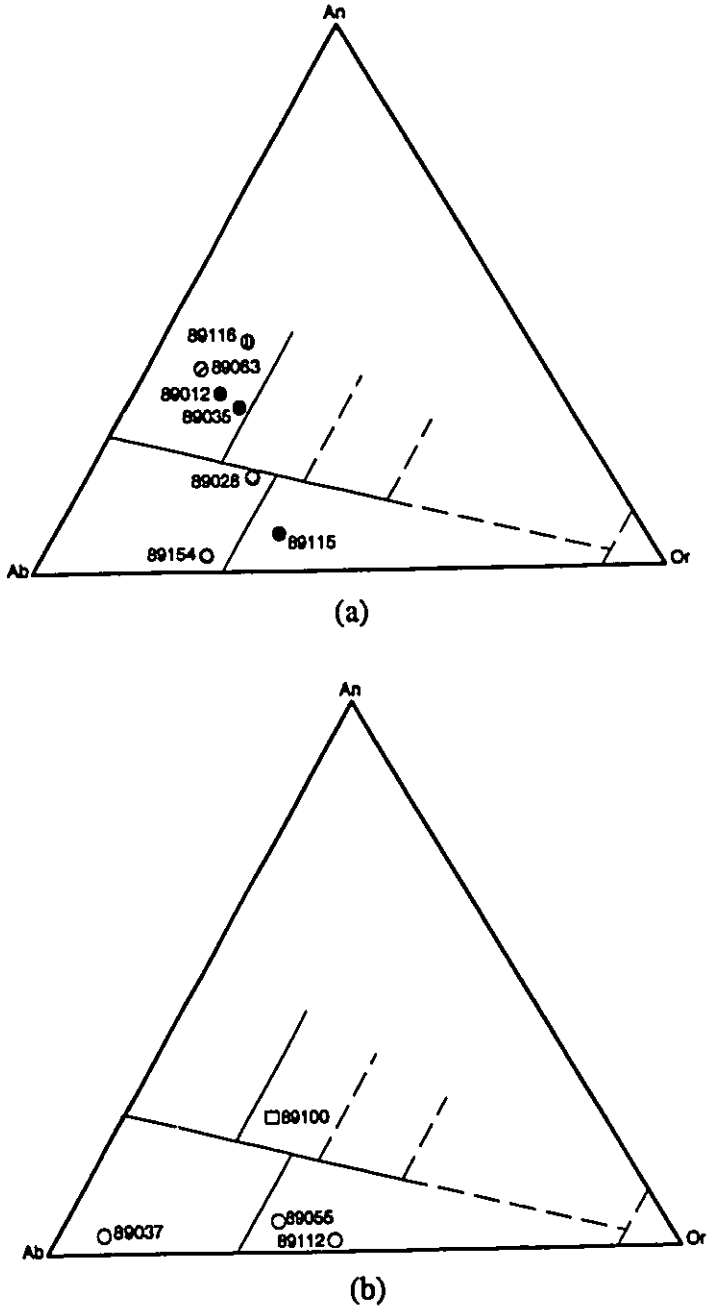

Figure 6-7. Plot of plutonic rock geochemistry from the Turner Lake area (after O'Connor, 1965). Field labels as in Figure 6-6. (a) Samples of unit 5am, strained tonalite (black circles) and less deformed equivalent, Unit 5a (stippled circles). Unit 3g; banded rock (vertically striped circle). Cobble from Unit 2 conglomerate (diagonally striped circle). (b) Pistol Lake granodiorite (square) and Fish-hook Lake granite (open circles). Numbers refer to samples.

A cobble from a conglomerate (Unit 2h) at the contact of metagreywacke-mudstones (Unit 4) and metapyroxenite (Unit 3c) plots as a tonalite. Apparently this conglomerate is not part of the James Falls conglomerate which lacks granitoid cobbles.

Petrographic examination of the banded/layered rock (Unit 3g) was inconclusive as to rock type. The chemical signature of this rock (sample 89116, Figure 6-1) is atypical of other volcanic rocks from the area. It has higher amounts of SiO_2 and lower amounts of both TiO_2 and Fe_2O_3 than the diorite/gabbro (Unit 3b) and amphibolitic (Units 3e and 3e) samples. The whole rock geochemical signature is reminiscent of the plutonic rather than the volcanic rocks and in fact this rock plots within the same area as the samples of unit $5a_m$ on the O'Connor diagram (Figure 6-7a).

6.5 Rare earth element geochemistry

Rare earth element analyses by XRAL, of representative samples of each rock unit are listed in Appendix IV. Rare earth elements undergo minor fractionation during sedimentary processes (McLennan and Taylor, 1984) and are only occasionally altered during metamorphism (Taylor and McLennan, 1980). Unless processes of metamorphism, hydrothermal alteration and weathering are obviously severe, they will not cause major changes in the patterns or abundances of the rare earth elements in the rocks (Hanson, 1980). Rare earth elements are useful in petrogenetic studies because they are geochemically very similar (Hanson, 1980). However they are subject to the Oddo-Harkins effect: the occurrence of a higher concentrations from elements with even atomic numbers compared to

concentrations of elements with odd atomic numbers. As a result it is necessary to normalize their abundances in chondrites by dividing the concentration of a given element in the rock by the concentration of the same element in a chondritic meteorite. Chondrites are used because they are primitive solar material and may have been the parental material of the earth. The rocks from the map area have been normalized with the Leedy 6 Chondrite (Masuda et al., 1973).

Rare earth element signatures of the metasedimentary units including arenite (Unit 3a) and metagreywacke (Units 1 and 4) are depleted in heavy rare earth elements (HREE) and have no negative Eu anomaly (Figure 6-8). The similarity between the signatures of Units 1 and 4 (western and eastern metagreywacke sequences respectively) suggests a geochemically similar, if not the same, source terrane. Their rare earth element signature also resembles that of the Burwash and Walsh formations (sedimentary rocks) of Yellowknife (Jenner et al., 1981) which lack significant negative Eu anomalies. The similarity between Units 1 and 4 does not have any strong bearing on their stratigraphic position or age. Notwithstanding, there are similarities in the rare earth element signature of the metagreywacke-mudstones of the study area with those in the obviously unrelated Yellowknife area.

It is possible to speculate on a source terrane for the sedimentary units in the Turner Lake area on the basis of their REE signatures. Any lithology with significant negative Eu anomalies could not be an important source rock. The granitic gneisses mapped in parts of the west and southwestern Slave Province are thought to be basement to the Yellowknife

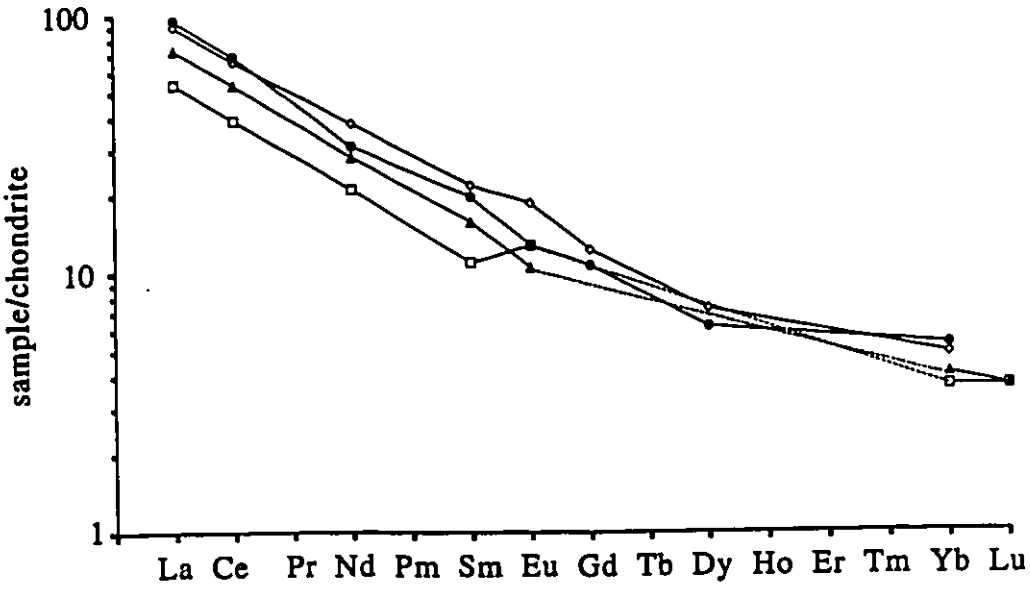

Figure 6-8. Chondrite normalized rare earth element plot of Unit 1 (white diamond, sample 89054), Unit 3a (white square, sample 89118 and black triangle, sample 89139) and Unit 4 (black circle, sample 90064). Grey line indicates interpolated path.

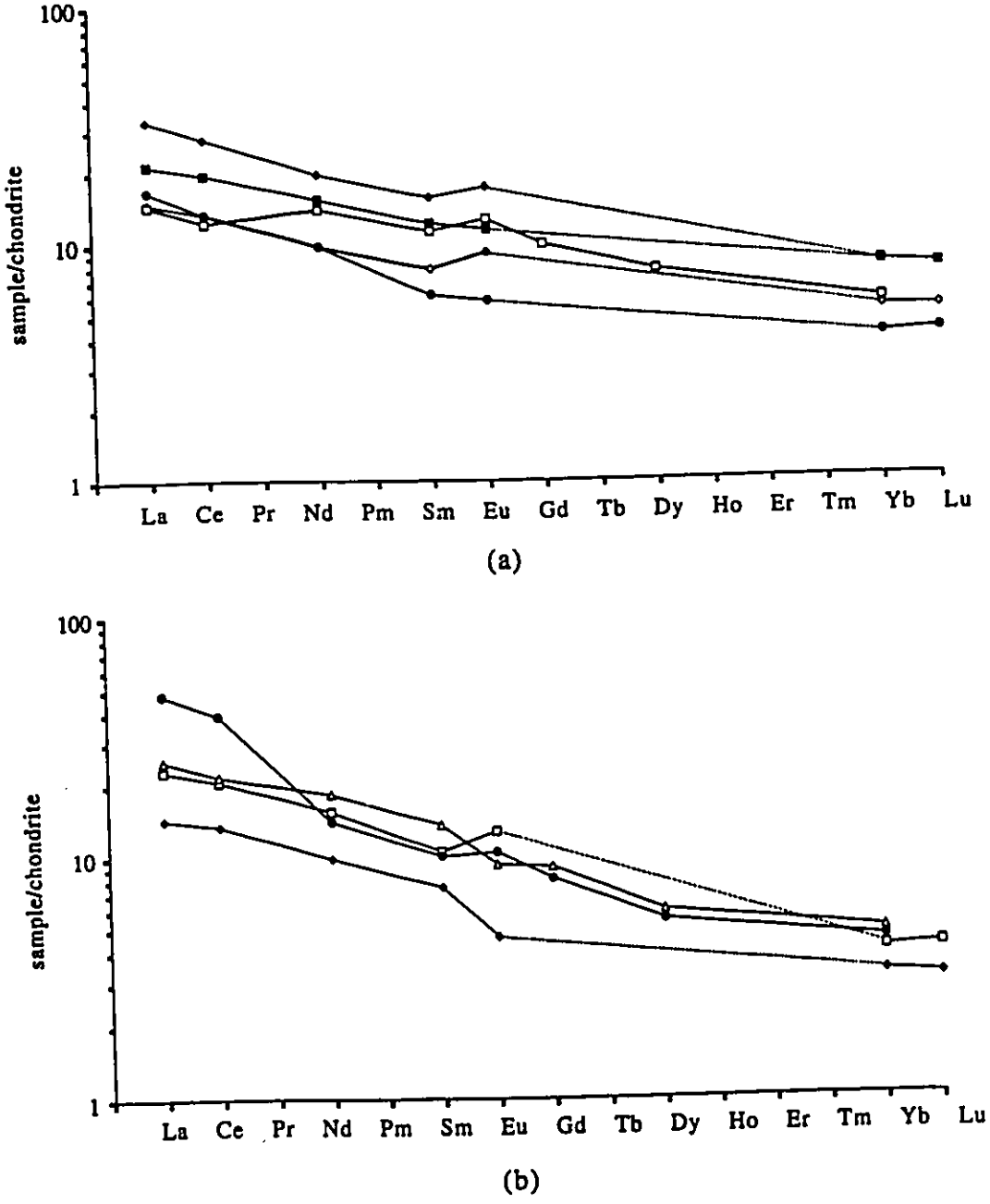

Figure 6-9. Chondrite normalized rare earth element plots. (a) Diorite samples (Unit 3b): sample 89022, black square; sample 89026, white diamond; sample 89034, black circle; sample 89059, white square; sample 90059, black diamond. (b) Pyroxenite (Unit 3c): sample 89071, white square; sample 89145, black diamond; sample tr11-3, black square; sample tr11-6, white triangle. Grey line indicates interpolated path.

Supergroup. REE signatures for these rocks have significant Eu anomalies (Jenner et al.,1981) and therefore they could not have been a significant source for the metasedimentary units 3a, 1 and 4 at Turner Lake.

Patterns for the diorite/gabbro (Unit 3b, samples 89022, 89026, 89034, 89059, 90059; Figure 6-1), pyroxenite (Unit 3c, samples 89071, 89145, tr11-3, tr11-6; Figure 6-1), mafic tuff (Unit 3d, samples 89038, 89069; Figure 6-1) and epiclastic amphibolite (Unit 3e, samples 90097, 90098; Figure 6-1) are similar (Figure 6-9a, b; Figure 6-10a). They are all fairly flat with a slight HREE depletion and no negative Eu anomaly.

Samples of the gold host unit (Unit 3f) have a fairly unique signature from other rocks in the area. The plot is similar to the epiclastic amphibolite (Unit 3e) but flatter (less HREE depletion) (Figure 6-10b).

The plutonic rock signatures (Unit 5) are also HREE depleted and lack significant Eu anomalies (Figures 6-11a, b, c). As K-rich granites are typified by Eu depletion (Taylor and McLennan, 1985) the REE signature is expected considering the monzogranitic and granodioritic composition. Their rare earth element signature is similar to that of the synkinematic granites (HREE depleted) from the Yellowknife area described by Jenner et al. (1981) but differs from that of the post-kinematic granites which are typified by negative Eu-anomalies (Jenner et al., 1981).

The REE signatures of the highly deformed plutonic rocks (Unit $5a_m$, samples 89115, 89035, 89012; Figure 6-1) are almost identical to one another, suggesting that they are all from the same source. In addition, the signature of Unit 3g (sample 89116, Figure 6-1) is

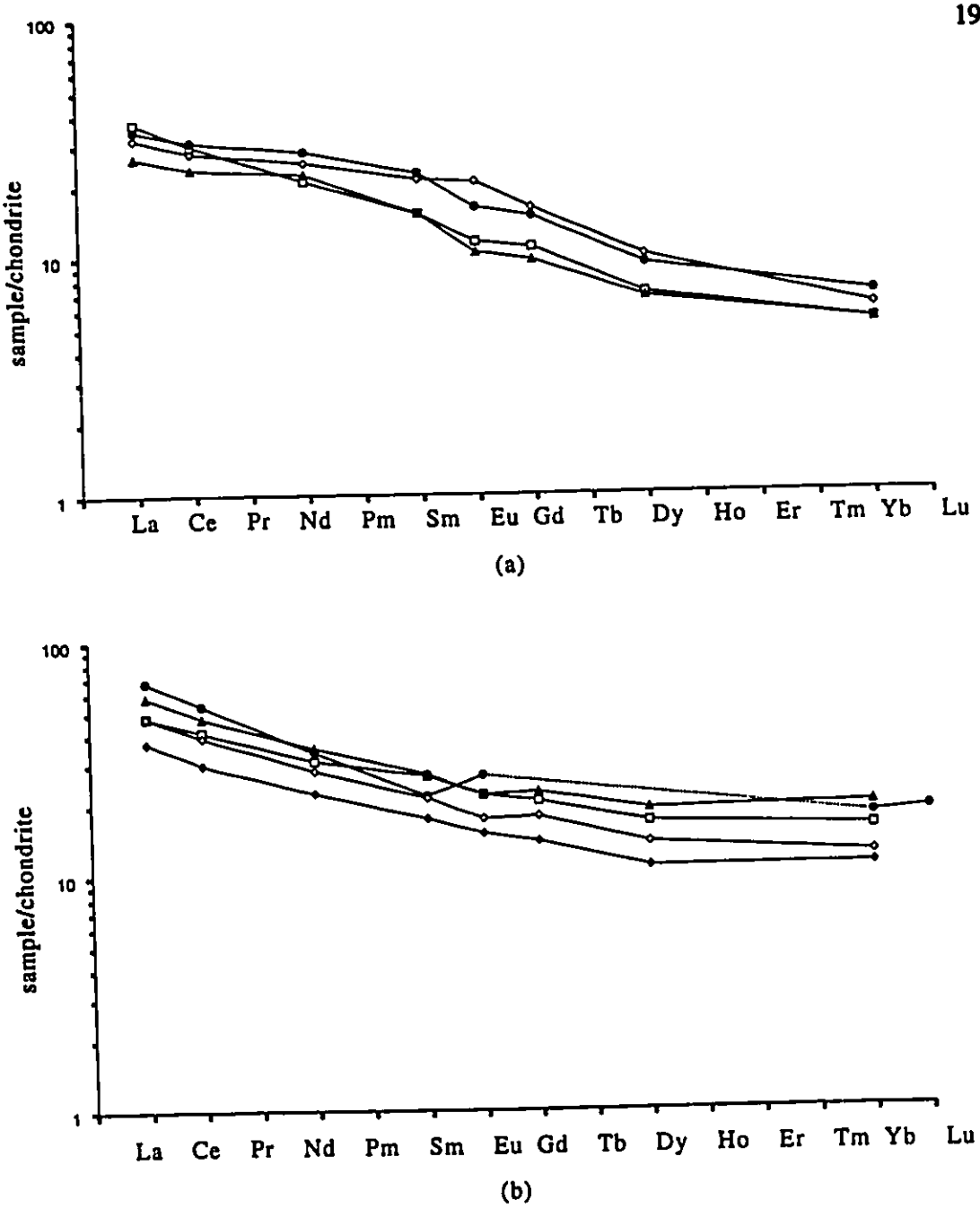

Figure 6-10. Chondrite normalized rare earth element plots of mafic tuff, epiclastic amphibolite and gold host: Units 3d, 3e and 3f respectively. (a) Unit 3d: sample 89038, white square; sample 89069, black triangle; Unit 3e: sample 90097, black circle; sample 90098, white diamond. (b) Gold host unit, amphibolitic epiclastic rock (Unit 3f): sample 89138, black circle; sample tr11-4, white square; sample tr11-8, black triangle; sample tr5A, black diamond; sample tr5B, white diamond. Grey line indicates interpolated path.

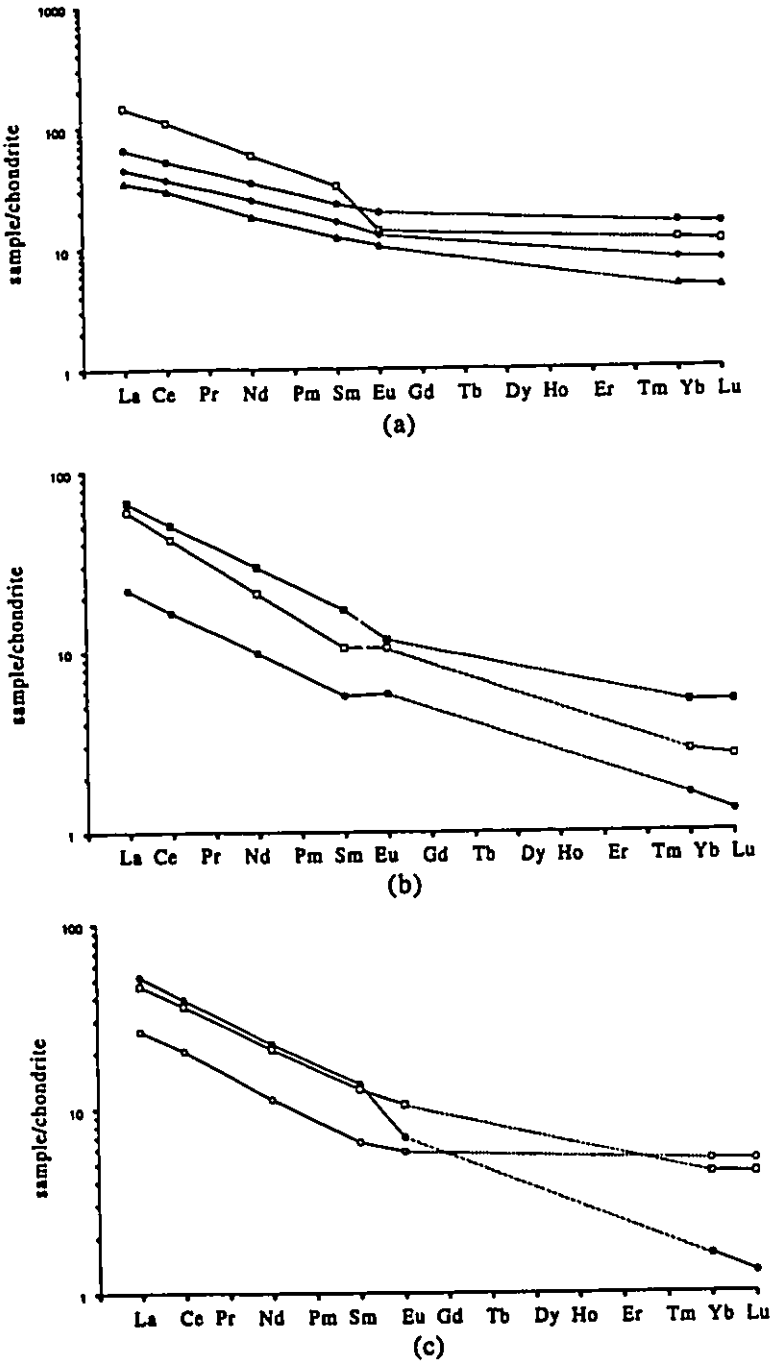

Figure 6-11. Chondrite normalized rare earth element plot of plutonic rocks. (a) Unit 5am, sheared tonalite: sample 89115, white square; sample 89035, white triangle; sample 89012, black diamond; Unit 3g, banded rock: sample 89116, black circle. (b) less deformed Unit 5a, trondhjemite. Sample 89154, black circle; sample 89028, black square; sample 89063, white square. (c) Pistol Lake granodiorite (Unit 5b): sample 89100, white square; Fish-hook Lake granite; sample 89055, black circle; sample 89112, white circle. Grey line indicates interpolated path.

almost identical. It therefore seems reasonable that the banding within this unit has resulted from tectonic intermixing along the high strain zone of a tonalitic plutonic rock and perhaps some volcanic (mafic-rich) material. The REE signatures of Unit 5a (samples 89154, 89028, 89063; Figure 6-1) have greater HREE depletion than $5a_m$. This may reflect a later stage of intrusion than $5a_m$. Both of these units have REE signatures that more closely resemble the signature of the Pistol Lake granodiorite (Unit 5b, sample 89100; Figure 6-1) than the Fish-hook Lake granite (Unit 5c, samples 89055 and 89112; Figure 6-1) with respect to the amount of HREE depletion and are most likely related (see Chapter 8 for further discussion).

6.6 Discussion

The Archean rocks studied at Turner Lake have been metamorphosed and altered to varying degrees. It is therefore difficult to apply traditional models of depositional environments based on geochemical data. Cenozoic models are abundant, however it is tenuous to attempt to apply these to Archean volcanic rock geochemistry because most are based on elements that would be mobile during metamorphism and alteration. Although several authors have attempted to make the comparison (Cunningham and Lambert, 1989) and to speculate on the depositional environment of rocks of the Yellowknife Supergroup, the general consensus is that without further refinement, Cenozoic models cannot be applied in the Archean (Pearce and Cann, 1973). Any attempt to do so is highly speculative.

Chapter 7
Geochronology

7.1 Introduction

The plutonic and volcanic rocks of the map area were dated using U-Pb zircon geochronology as part of an ongoing mapping project of the entire belt by the Geological Survey of Canada. The writer assisted in the production of two preliminary results: a highly foliated plutonic rock dated at 2607 ± 1.3 Ma and the Pistol Lake pluton dated at 2600 ± 2 Ma (van Breemen et al., 1992).

Until recently, geochronological information for the Slave Province was sparse, particularly for supracrustal rocks. It has been augmented in recent years with improved techniques for isotope analysis of rocks from greater areas of the province. U-Pb zircon dating of felsic volcanic rocks has been concentrated in the east, central and northern Slave province (Mortensen et al., 1988). The timing of volcanism in the western Slave is almost completely unknown and in the eastern Slave, no volcanic rocks are older than about 2.7 Ga (Mortensen et al., 1988). Mortensen et al. (1988) provides a good summary and documentation of ages of felsic volcanism in the Slave and Kusky and de Paor (1991) document and discuss ages of crystalline "basement" rocks (pre-Yellowknife Supergroup rocks).

Granitoid rocks in the Slave Province have been placed into three broad groups based on age and relationships to supracrustal successions. 4.0 - 2.8 Ga gneisses and granite predate 2.71 - 2.65 Ga volcanic and turbiditic rocks of the Yellowknife Supergroup (Van

Breemen et al., 1992). Synvolcanic plutonism spanned from 2695 to 2650 Ma. Most of the granitoid rocks in the Slave province are post-volcanic and syndeformational, crystallizing between 2625 and 2580 Ma. Late to post deformational granitoids range in age from 2605 to 2580 Ma (van Breemen et al., 1992).

Complications in obtaining precise dates of any rocks can be incurred in some cases due to the effects of minor inheritance owed mainly the incorporation of xenocrystic zircon (Mortensen et al., 1988). A recurring problem in dating rocks involves the determination of the protolith. High degrees of strain and moderately high grades of metamorphism are typical Slave province conditions which often can obscure a protolith lithology (Mortensen et al., 1988).

7.2 Sampling and analytical procedure

Samples were collected by Dr. O. van Breemen and Dr. C.W. Jefferson of the Geological Survey of Canada during the 1988 season and Dr. Jefferson during 1989. Attempts were made to avoid weathered faces and altered zones when sampling. Where this was not possible the weathered margins were sawed off prior to crushing. Results from two samples are presented in this chapter including a sample of the Pistol Lake granodiorite (sample 89JP177) and sample of a foliated tonalite sill within the Unit 3 sequence (sample 89JP178). Sample locations are shown on Figure 7-1.

Heavy mineral separates were prepared by technicians at the Geological Survey of Canada by crushing and grinding the sample to a fine sand size, then separating the material

by use of a Wilfley table and heavy liquid flotation. The heavy separates were magnetically separated using a Frantz™ LB-1 separator by the author. The least magnetic separates of sample 89JP178 were sieved to +149, -149+105, -74+62 micron size fractions, the latter of which was divided into best and poorer quality zircons. Zircons in sample 89JP177 were more magnetic than in 89JP178 and were separated into a least magnetic -74+62 micron size fraction and a weakly magnetic fraction of -62 microns and two weakly magnetic fractions of -149 microns.

Zircon crystals were selected for analysis by hand picking in ethyl alcohol by the author. The largest, clearest, most fracture-free grains were selected to minimize discordance. To further minimize the effects of peripheral lead loss all fractions were strongly air abraded in pyrite until terminations and other sharp faces were removed (Krogh, 1982). These polished grains were photographed under the microscope.

The remainder of the analyses were completed by technicians in the geochronology laboratory at the Geological Survey of Canada. The dissolution and cation exchange column procedures used to extract U and Pb isotopes from zircon is summarized in Parrish et al. (1987). Mass spectrometry, data reduction and error propagation techniques are outlined in Roddick et al. (1987). Linear regression analysis was used to deal with errors. Isotopic data is presented in Table 7-1 and plotted in Figure 7-2.

7.3 Results

The Pistol Lake pluton (sample 89JP177) ranges in composition from tonalite to

granodiorite and has an age of 2600 ± 2 Ma (Figure 7-2). The discordant nature of the data may be the result of cumulative lattice damage due to radiactive decay over time and later lead loss. The data for individual fractions is consistent and has a low intercept. The sample is unfoliated with subhedral feldspar phenocrysts up to 3 mm in size. The feldspars contain muscovite microlites. Minor epidote occurs with biotite and replacing feldspar. Some of the biotite is replaced by chlorite. Minor amounts of carbonate have also been identified in thin section (Figure 7-3).

The highly foliated tonalite sample (89JP178) dated at 2607 ± 1.3 Ma (Figure 7-2) contains sub to anhedral feldspar phenocrysts in a fine-grained matrix of feldspar, quartz and biotite (Figure 7-4). The phenocrysts contain muscovite microlites; carbonate is present in places in the matrix. Based on field observations, the intercalation of this unit with the succession of Unit 3, including the epiclastic amphibolites and mafic tuffs, suggested that the unit, mapped as a sheared granodiorite (Clode, 1987) was synvolcanic. However the rock is mineralogically similar to the sample of the Pistol Lake pluton, although texturally there is a greater contrast between the phenocrysts and the matrix due to deformation, and determination of protolith is difficult. This rock is most likely a deformed hypabyssal equivalent of the pluton. The similarity in age and similar geochemical signature to the Pistol Lake pluton (Chapter 6) suggests these two rocks are related and may have a similar post-volcanic origin.

Boulders from both the James Falls conglomerate and granitoid cobbles from the conglomerates within the intercalated sequence (Unit 3) are currently being dated. Future

dating of volcaniclastic and the dioritic/gabbroic rocks from within the intercalated sequence (Unit 3) and of detrital zircons from greywackes could prove useful for modelling the evolution of the Turner Lake area.

Table 7-1. U-Pb isotopic data, Turner Lake

Fraction	Weight (ug)	U (ppm)	Pb (ppm)	206Pb 204Pb	Pbc (pg)	208Pb (atomic %)	206Pb 238U	207Pb 235Pb	correlation coefficient	207Pb 206Pb	207/206 age Ma
89JP177											
A	8	213	112	1787	29	603	.4857 ± .10%	11.649 ± .11%	0.9409	.17395 ± .04%	2596.0 +1.3/ -1.3
B	12	201	104	3835	19	5.6	.4841 ± .09%	11.594 ± .10%	0.9588	.17370 ± .03%	2593.6 +1.0/ -1.0
C	3	216	114	2760	7	5.8	.4930 ± .10%	11.840 ± .11%	0.9561	.17418 ± .03%	2598.1 +1.1/ -1.1
D	5	238	122	2694	16	5.9	.4778 ± .10%	11.424 ± .11%	0.9631	.17342 ± .03%	2590.9 +1.0/ -1.0
89JP178											
A	20	124	73	4190	18	15.3	.4937 ± .09%	11.942 ± .10%	0.9489	.17543 ± .03%	2610.1 +1.1/ -1.1
B	13	98	58	2312	17	15.6	.4938 ± .09%	11.899 ± .11%	0.9520	.17477 ± .03%	2603.9 +1.1/ -1.1
C	7	149	81	1928	15	14.2	.4641 ± .11%	11.058 ± .12%	0.9657	.17279 ± .03%	2584.9 +1.1/ -1.1
D	2	94	55	2245	15	14.9	.4925 ± .10%	11.870 ± .11%	0.9397	.17479 ± .04%	2604.1 +1.3/ -1.3

Errors are 1 std. error of mean in % except 207/206 age errors which are 2 std. errors in Ma.

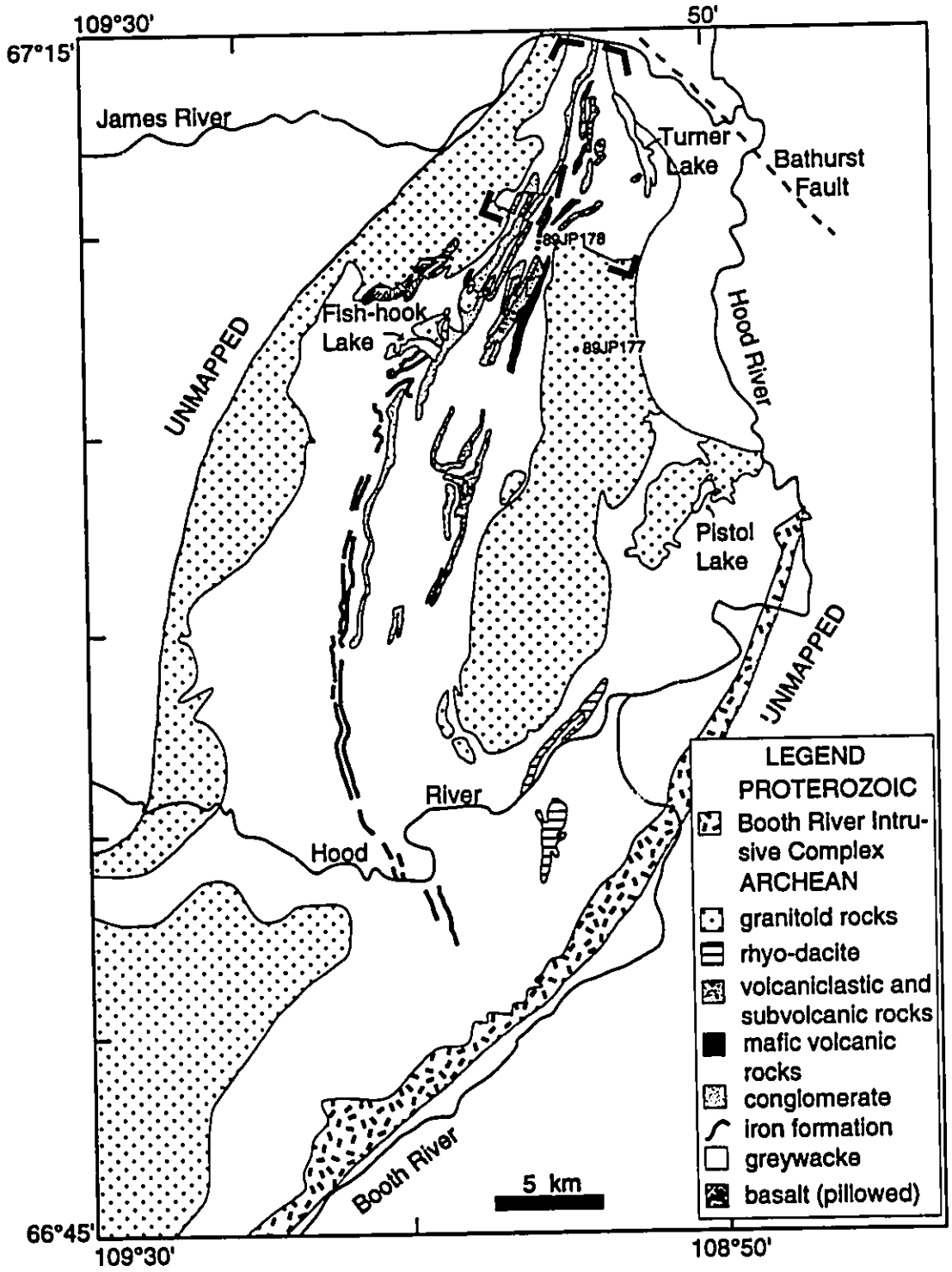

Figure 7-1. Geology of the Turner Lake - Pistol Lake area of the Hood River Supracrustal Belt (after Henderson et al., 1991) with locations of geochronology samples indicated. The Turner Lake map area is outlined. Diabase dykes have been omitted for clarity.

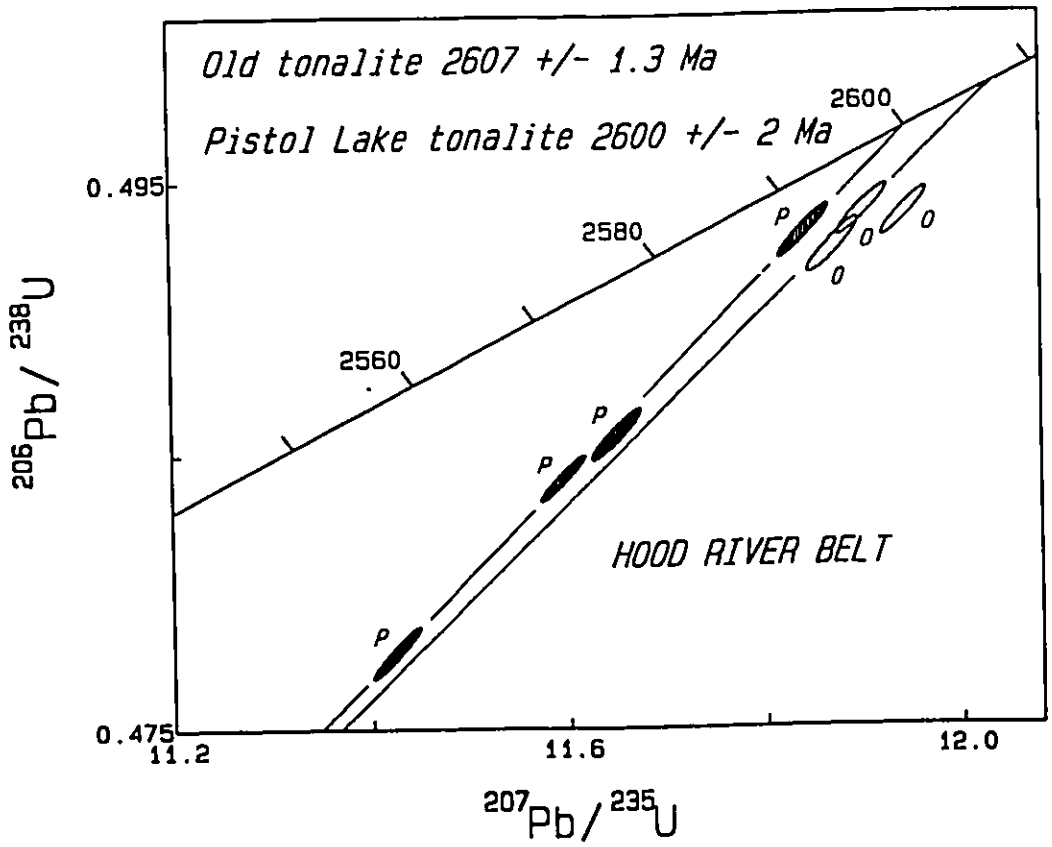

Figure 7-2. U-Pb concordia plot for zircons from the Pistol Lake pluton (sample 89JP177, shaded ellipses) and from a highly foliated tonalite (sample 89JP178, open ellipses).

Figure 7-3. Photomicrograph of unfoliated Pistol Lake granodiorite (sample 89JP177). Note the minor amount of carbonate. Crossed polars. Field of view is 12 mm.

Figure 7-4. Photomicrograph of sample from a highly foliated tonalite sill (sample 89JP178). Note the muscovite microlites in the relict feldspar phenocrysts. Carbonate is present in the matrix. Crossed polars. Field of view is 7.5 mm.

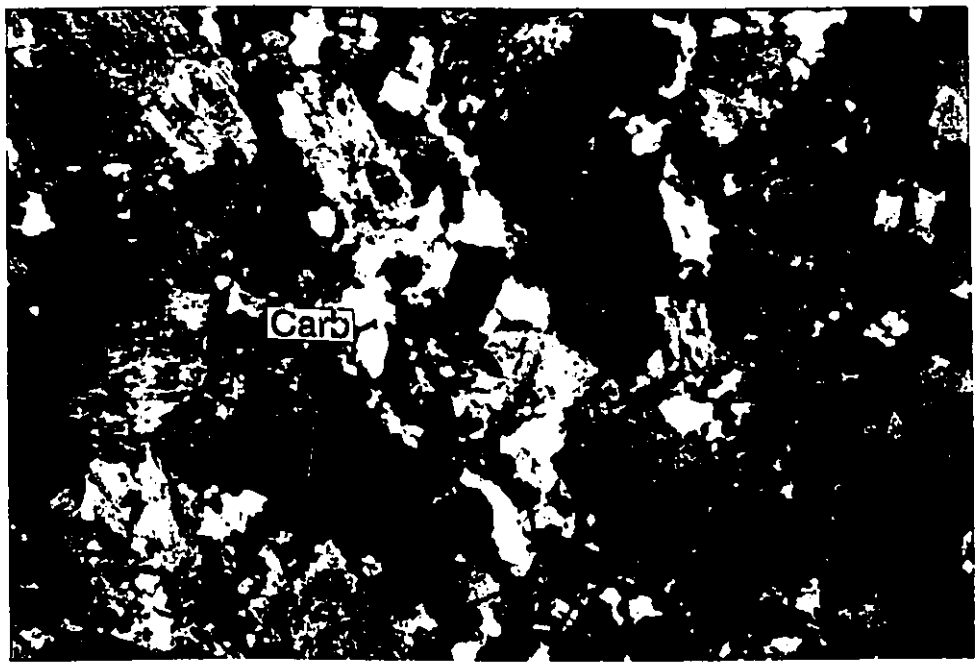
Carb

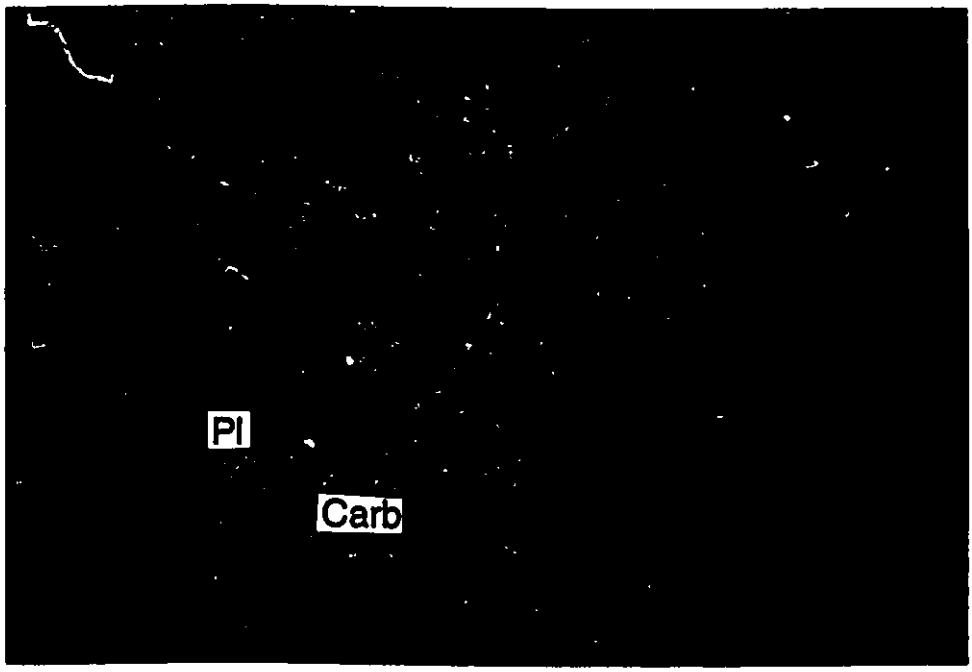
Pl
Carb

Chapter 8
Summary and Suggestions for Further Work

8.1 Summary

Archean metasedimentary and metavolcanic rocks in the Turner Lake area of the Archean Hood River domain, form a laterally extensive succession at least 5 km in apparent thickness. Isoclinal folds interpreted from numerous reversals in sedimentary tops prevents estimation of true stratigraphic thicknesses. The sequence includes volcaniclastic rocks and metapyroxenite (in Unit 3) which could have been deposited close to a volcanic edifice. Rare earth element signatures for both Units 1 and 4 metagreywacke-mudstones are typical of Yellowknife Supergroup turbidites.

Later deformation and metamorphism of the supracrustal rocks are intimately linked with emplacement of plutons; their inter-relationships are schematically illustrated in Figure 8-1. During early phases of deformation (D_1-D_2), marked by complex isoclinal folding, an axial planar quartz fabric (S_1 or S_2) may have formed at low metamorphic grades. As isotherms rose during regional metamorphism blocky biotite(A) porphyroblasts overgrew and preserved the early fabric. During later progressive deformation (D_3), peak amphibolite grade metamorphic conditions were attained. Early D_3 cordierite porphyroblasts grew randomly in pelitic beds, imparting to them a higher competency than the psammitic beds as shown by refraction of the S_3 schistosity. Continued growth of cordierite and andalusite porphyroblasts occurred preferentially along the S_3 plane of anisotropy. Biotite and muscovite flakes contained in S_3 warped around the earlier formed cordierite and andalusite porphyroblasts and

overgrew the biotite(A) porphyroblasts. Further growth of andalusite and cordierite included the S_3 foliation. Andalusite developed as rims on cordierite porphyroblasts. Fibrolite grew ubiquitously along S_3 as a polymorphic transition of andalusite and as prismatic sillimanite in the northwest.

As indicated by the deflection of S_3 around some porphyroblasts, the S_3 alignment of other porphyroblasts, and the inclusion within others, S_3 was forming at about the time of peak metamorphic conditions as opposed to post porphyroblastesis as proposed by Henderson et al. (1991). Pressure, constrained by a lack of kyanite, reached a maximum of approximately 3.5 kb during metamorphism. Temperatures, constrained by a lack of K-feldspar, reached a maximum between approximately 550 and 600^{0}C.

Two mutually exclusive directional sets of the S_3 foliation with ambiguous timing relationships have been identified. S_3A strikes northwesterly and is best preserved as a fabric of flattened pebbles aligned counterclockwise from bedding in the James Falls conglomerate (Unit 2). S_3B of similar morphology, strikes northeasterly, mainly clockwise from bedding, and is the dominant regional foliation. This variation in orientation could reflect changes in stress orientations through time.

The ascent of the 2600 $\pm$ 2 Ma Pistol Lake pluton warped bedding and modified the local stress field influencing the orientation of the developing S_3 foliation in the vicinity of the pluton. Late D_3 emplacement of the Pistol Lake pluton to its present level truncated S_3 along the northern pluton contact.

Following the metamorphic peak, D_4 deformation produced local F_4 folds in bedding

and crenulations of the S_3 foliation in pelitic layers, mainly where the foliation was at a low angle to S_0. No mineral growth is associated with the crenulations. The axial surface trace of F_4 crenulations in pelites lies at a high angle to bedding and partly parallels S_3 in psammites. Thus the parallelism of structures does not imply that they are the same generation.

Local deflection of the S_3 foliation in layers into parallelism with S_0 is possibly due to the confinement of pre-D_4 bedding-slip of pelitic units. S_3 in the coarser-grained and psammitic beds was unaffected.

8.2 Suggestions for further work

Continued studies in the Turner Lake area should include geochronology. It is necessary to determine more precisely the stratigraphic and temporal relationships of the intercalated volcaniclastic, intrusive and sedimentary rocks of Unit 3 to the bordering metagreywacke-mudstones of Units 1 and 4.

The upper and lower contacts of the James Falls conglomerate should be carefully examined. The unconformity mapped south of Turner Lake (Henderson et al., 1991) with the underlying metagreywacke-mudstones is evidence for local angular discordance, however further documentation is necessary in the Turner Lake area to test for a regional feature. The contact of the conglomerate with the overlying arenite should be further investigated to determine whether or not it is conformable. The contact of the volcanic succession (Unit 3) with the overlying metagreywacke-mudstones should also be mapped to see if local

conglomerates and breccias indicate an unconformity.

Plutonic clasts in the local conglomerates and breccias within the Unit 3 sequence should be analyzed to determine provenance and age.

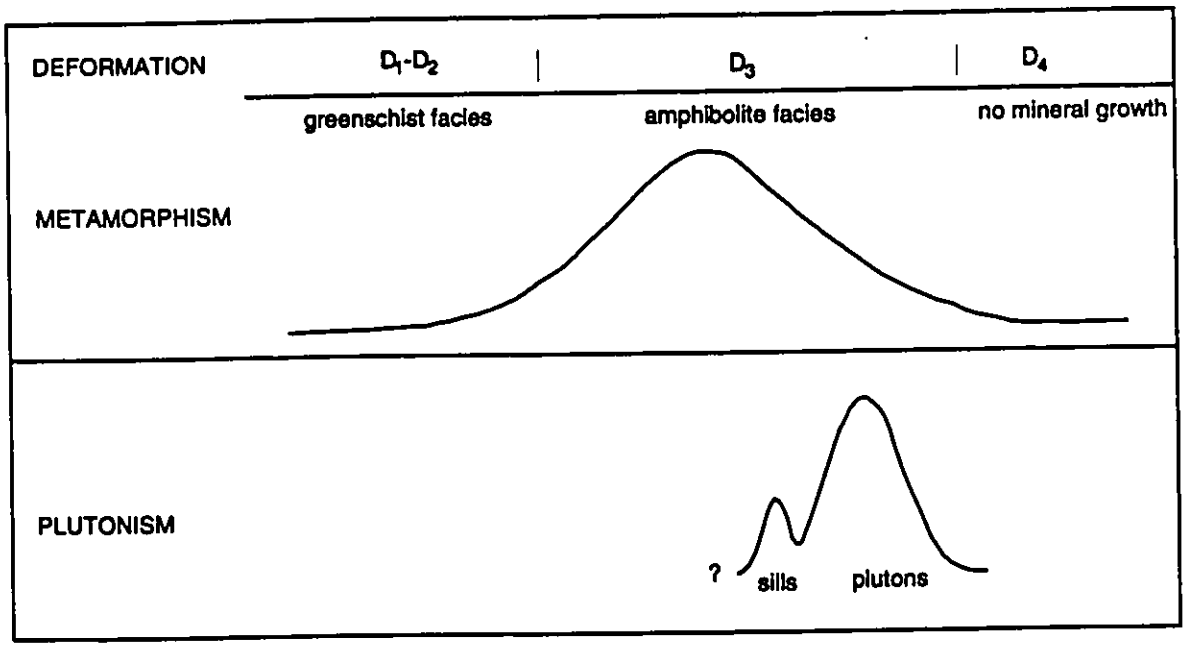

Figure 8-1. Schematic history of the Turner Lake area interrelating deformation, metamorphism and plutonism.

References

Althaus, E., 1967. The triple point andalusite-sillimanite-kyanite. An experimental and petrologic study. Contributions to Mineralogy and Petrology, v. 16, p. 29-44.

Bostock, H.H., 1980. Geology of the Itchen Lake area. Geological Survey of Canada, Memoir 391, 101 pp.

Bowring, S.A., I.S. Williams and W. Compston, 1989. 3.96 Ga gneisses from the Slave Province Northwest Territories, Canada. Geology, v. 17, p. 971-975.

Brooks, C. and S.R. Hart, 1974. On the significance of komatiite. Geology, v. 2, p. 107-110.

Brown, G.C. and W.S. Fyfe, 1971. Kyanite-andalusite equilibrium. Contributions to Mineralogy and Petrology, v. 33, p. 227-231.

Carlson, C.I. and H.A. Knutson, 1965. Roberts Mining Company, geology of the CC1 claims and the surrounding area; Turner Lake, Bathurst Inlet: District of Mackenzie, NWT. Donald H. Hase and Jack V. Everett eds. 51 pp.

Carmichael, D.M., 1969. On the mechanism of prograde metamorphic reactions in quartz-bearing pelitic rocks. Contributions to Mineralogy and Petrology, v. 20, p. 244-267.

Chatterjee, N.D. and W. Johannes, 1974. Thermal stability and standard thermodynamic properties of synthetic M_1-muscovite, $KAl_2[AlSi_3O_{10}(OH)_2]$. Contributions to Mineralogy and Petrology, v. 48, p. 89-114.

Clode, C., 1987. The Geology of the Turner Lake Gold Prospect, Bathurst Inlet, Northwest Territories. Unpublished M.Sc. thesis, Queen's University, Kingston, Ontario, 50 pp.

Covello, L., S.M. Roscoe, J.A. Donaldson, D. Roach, W.K. Fyson, 1988. Archean quartz arenite and ultramafic rocks at Beniah Lake, NWT. Current Research, Part C. Geological Survey of Canada, Paper 88-1C, p. 223-232.

Cunningham, M.P. and R. St. J. Lambert, 1989. Petrochemistry of the Yellowknife volcanic suite at Yellowknife, N.W.T. Canadian Journal of Earth Sciences, v. 26, p. 1630-1646.

Deer, W.A., R.A. Howie and J. Zussman, 1966. An Introduction to the Rock Forming Minerals. Longman, 528 pp.

Dillon-Leitch, H.C.H., 1981. Volcanic stratigraphy structure and metamorphism in the Courageous-Mackay Lake greenstone belt, Slave Province, Northwest Territories. Unpublished M.Sc. thesis, University of Ottawa, 169 pp.

Easton, R.M., 1985. The nature and significance of pre - Yellowknife Supergroup rocks in the Point Lake area, Slave Structural Province, Canada. In Evolution of Archean Supracrustal Sequences, L.D. Ayres, P.C. Thurston, K.D. Card and W. Weber, eds. Geological Association of Canada Special Paper 28, p. 153-167.

Easton, R.M., Boodle, R.L. and L. Zalusky, 1982. Evidence for gneissic basement to the Archean Yellowknife Supergroup in the Point Lake area, Slave Structural Province, District of Mackenzie. Current Research, Part B. Geological Survey of Canada, Paper 82-1B, p. 33-41.

Fahrig, W.F., E. Irving and G.D. Jackson, 1971. Paleomagnetism of the Franklin diabases. Canadian Journal of Earth Sciences, v. 8. p. 455-467.

Falck, H., 1990. A glimpse of an Archean volcano: A description of volcanic and sedimentary rocks in the Yellowknife greenstone belt, Giant Section, N.W.T. M.Sc. thesis, Carleton University, Ottawa, Ontario, 184 pp.

Fraser, J.A., 1978. Metamorphism in the Churchill Province, District of Mackenzie. In Fraser, J.A. and W.W. Heywood eds. Metamorphism in the Canadian Shield. Geological Survey of Canada, Paper 78-10. p. 195-202.

Fraser, J.A., 1963a. Geological notes of Northeastern District of Mackenzie, Northwest Territories. Geological Survey of Canada, Paper 63-40, 20 pp.

Fraser, J.A., 1963b. Geological Survey of Canada Map 45-1963.

Frith, R., R.A. Frith, and R. Doig, 1977. The geochronology of the granitic rocks along the Bear - Slave Structural Province boundary, northwestern Canadian Shield. Canadian Journal of Earth Sciences, v. 14, p. 1356-1373.

Fumerton, S., 1989. Report on trenching, sampling and geological mapping carried out in 1989 on the Turner Lake gold occurrence, project M711. Unpublished report for Chevron Minerals Ltd., 40 pp.

Fyson, W.K., 1990. Structural development of angular volcanic belts in the Archean Slave Province. Canadian Journal of Earth Sciences, v. 27, p. 403-413.

Fyson, W.K., 1982. Complex evolution of folds and cleavage in Archean rocks, Yellowknife, Northwest Territories. Canadian Journal of Earth Sciences, v. 19, p. 878-893.

Fyson, W.K., 1980. Fold fabrics and emplacement of an Archean granitoid pluton, Cleft Lake, Northwest Territories. Canadian Journal of Earth Sciences, v. 17. p. 325-332.

Fyson, W.K., 1975. Fabrics and deformation of Archean metasedimentary rocks, Ross Lake-Gordon Lake area, Slave Province, Northwest Territories. Canadian Journal of Earth Sciences, v. 12, p. 765-776.

Fyson, W.K. and V. Jackson, 1991. Reorientation of structures plutons and orthogonal lineaments, Russell Lake supracrustal domain, Southwestern Slave Province. Canadian Journal of Earth Sciences, v. 28, p. 126-135.

Fyson, W.K. and H. Helmstaedt, 1988. Structural patterns and tectonic evolution of supracrustal domains in the Archean Slave Province, Canada. Canadian Journal of Earth Sciences, v. 25, p. 301-315.

Fyson, W.K. and R.A. Frith, 1979. Regional deformations and emplacement of granitoid plutons in the Hackett River greenstone belt, Slave Province, Northwest Territories. Canadian Journal of Earth Sciences, v. 16, p. 1187-1195.

Getzinger, J.S., 1988. Geology of the Turner property, Mackenzie mining district, N.W.T. Unpublished report for Chevron Minerals Ltd., 67pp.

Hanson, 1980. Rare earth elements in petrogenetic studies of igneous systems. Annual Reviews in Earth and Planetary Sciences, v. 8, p. 371-406.

Heaman, L.M., A.N. LeCheminant and R.H. Rainbird, 1990. A U-Pb Badelleyite study of Franklin igneous events, Canada. Vancouver 90, Geological Association of Canada/Mineralogical Association of Canada annual meeting program with abstracts. v. 15, p. 55.

Henderson, J.B., 1988. Keskarrah Bay area, District of Mackenzie, N.W.T. Geological Survey of Canada, Map 1679A.

Henderson, J.B., 1985. Geology of the Yellowknife - Hearne Lake area, District of Mackenzie: a segment across an Archean basin. Geological Survey of Canada, Memoir 414, 135 pp.

Henderson, J.B., 1981. Archaean basin evolution in the Slave Province, Canada.

Precambrian Plate Tectonics, A. Kroner ed. Elsevier, Amsterdam, p. 213-236.

Henderson, J.B., 1975a. Sedimentology of the Archean Yellowknife Supergroup at Yellowknife, District of Mackenzie. Geological Survey of Canada, Bulletin 246, 62 pp.

Henderson, J.B., 1975b. Archean stromatolites in the northern Slave Province, N.W.T., Canada. Canadian Journal of Earth Sciences, v. 9, p. 1619-1630.

Henderson, J.B., 1970. Stratigraphy of the Archean Yellowknife Supergroup, Yellowknife Bay-Prosperous Lake area, District of Mackenzie. Geological Survey of Canada, Paper 70-26, p. 12.

Henderson, J.B. and R.M. Easton, 1977. Archean supracrustal-basement rock relationships in the Keskarrah Bay map area, Slave Structural Province, District of Mackenzie. Report of Activities, Part A, Geological Survey of Canada, Paper 77-1A, p. 217-221.

Henderson, J.B., P.H. McGrath, R.J. Theriault and O. van Breemen, 1990. Intracratonic indentation of the Archean Slave Province into the early Proterozoic Thelon tectonic zone of the Churchill Province, northwestern Canadian Shield. Canadian Journal of Earth Sciences, v. 27, p. 1699-1713.

Henderson, J.F. and Brown, 1966. Geology and structure of the Yellowknife greenstone belt, District of Mackenzie. Geological Survey of Canada, Bulletin 141, 87 pp.

Henderson, M.N., J.R. Henderson, C.W. Jefferson, T.O. Wright, R. Wyllie and S. Schaan, 1991. Preliminary geological map of the Hood River belt (NTS 76 K/N). Geological Survey of Canada, Open File 2413.

Hoffman, P.F., 1989. Precambrian geology and tectonic history of North America. The Geology of North America - An overview, A.W. Bally and A. R. Palmer eds. Geological Society of America, The Geology of North America, v. A, p. 447-512.

Holdaway, M.J., 1971. Stability of andalusite and the aluminum silicate phase diagram. American Journal of Science, v. 271, p. 97-131.

Hurdle, E., 1985. Stratigraphy, Structure, and Metamorphism of Archean rocks, Clan Lake, Northwest Territories. Unpublished M.Sc. Thesis, University of Ottawa, Ottawa, Ontario, 146 pp.

Hyndman, D.W., 1985. Petrology of Igneous and Metamorphic Rocks. McGraw-Hill, Inc.,

786 pp.

Irvine, T.N. and W.R.A. Baragar, 1971. A guide to the chemical classification of common volcanic rocks. Canadian Journal of Earth Sciences, v. 8, p. 523-548.

Isachsen, C.E., S.A. Bowring and W.A. Padgham, 1991a. Geochronolgy of the Yellowknife volcanic belt, N.W.T., Canada: New constraints on the timing and duration of greenstone belt magmatism. Journal of Geology, v. 99, p. 55-67.

Isachsen, C.E., S.A. Bowring and W.A. Padgham, 1991b. U-Pb Geochronolgy of the Yellowknife Supergroup at Yellowknife, N.W.T.: Constraints On Its Evolution. Geological Association of Canada, Program with Abstracts, v. 16, p. A59.

Isachsen, C.E., S.A. Bowring and W.A. Padgham, 1991c. Geology and U-Pb geochronolgy of the Dwyer Formation and underlying gneisses in the southern Slave Province: A basement-cover sequence beneath the Yellowknife Greenstone Belt. Geological Association of Canada, Program with Abstracts, v. 16, p. A59.

Isachsen, C.E., S.A. Bowring and W.A. Padgham, 1991d. U-Pb zircon geochronology of the Yellowknife volcanic belt, N.W.T., Canada: New constraints on timing and duration of greenstone belt magmatism. Journal of Geology, v. 99. p. 55-68.

Jefferson, C.W., M.N. Henderson, J.R. Henderson, T.O. Wright, R. Wyllie and S. Schaan, 1992. Geology of the Archean Hood River Belt, northeastern Slave Structural Province, District of Mackenzie (NTS 76K, N), N.W.T. In MDA Summary Volume, NWT. D.G. Richardson and M. Irving, eds. Geological Survey of Canada Open File 2484, p. 193-197.

Jefferson, C.W., M.N. Henderson, J.R. Henderson and S.E. Schaan, 1990. Geological setting of stratabound gold occurrences in the Fish-hook - Turner lakes belt, Bathurst Inlet area, District of Mackenzie, N.W.T. Current Research, Part C, Geological Survey of Canada, Paper 90-1C, p. 349-361.

Jenner, G.A., B.J. Fryer and S.M. McLennan, 1981. Geochemistry of the Archean Yellowknife Supergroup. Geochimica et Cosmochimica Acta, v. 45, p. 1111-1129.

Jensen, L.S., 1976. A new cation plot for classifying subalkaline volcanic rocks. Ontario Division of Mines, Miscellaneous Paper 66, 22pp.

Johnstone, R.M., 1990a. Geology of the Torp Lake metasedimentary belt and report on new gold/base metal showings (76 N/3, 5, 6 & 11). Exploration Overview 1990. p. 30-32.

Johnstone, R.M., 1990b. The lower Hood/James River project. Canada-Northwest Territories Mineral Development Agreement. GNWT-DIAND Geoscience Projects 1989 Annual Report p. 13-19.

Johnstone, R.M., 1990c. Geology of the Torp Lake metasedimentary belt, parts of NTS 76N/3, 5, 6, 7, 11, 12, NWT (EGS 1990-21). NWT Geology division, Indian and Northern Affairs Canada.

Johnstone, R.M., 1989. Preliminary geology of the Torp Lake area NTS 76N/5, 6. Torp Lake metasedimentary belt, NWT (EGS 1989-7). NWT Geology Division, Indian and Northern Affairs Canada.

Johnstone, R.M., 1988. Geology of the Torp Lake area, western Bathurst Inlet (76N/5,6). Exploration overview 1988, Northwest Territories, NWT Geology Division - Northern Affairs Program, Indian and Northern Affairs Canada, p. 41-43.

King, J.E., W. J. Davis, C. Relf and T. Van Nostrand, 1990. Geology of the Contwoyto - Nose Lakes map area, central Slave Province, District of Mackenzie, N.W.T. Current Research, Part C, Geological Survey of Canada, Paper 90-1C, p. 177-187.

King, J.E. and H. Helmstaedt, 1989. Deformational history of an Archean fold belt, eastern Point Lake area, Slave structural Province, N.W.T. Canadian Journal of Earth Sciences, v. 26, p. 106-113.

Kretz, R, 1983. Symbols for rock-forming minerals. American Mineralogist, v. 68, p. 277-279.

Krogh, T.E., 1982. Improved accuracy of U-Pb ages by the creation of more concordant systems using an air abrasion technique. Geochimica et Cosmochimica Acta, v. 46, p. 637-649.

Kusky, T.M. and D.G. dePaor, 1991. Deformed sedimentary fabrics in metamorphic rocks: Evidence from the Point Lake area, Slave Province, Northwest Territories, Geological Society of America Bulletin, v. 103, p. 486-503.

Kusky, T.M., 1990. Evidence for Archean ocean opening and closing in the Slave structural Province. Tectonics, v. 9. p. 1533-1563.

Kusky, T.M., 1988. Thrusting between the Cameron River greenstone belt and the Sleepy Dragon metamorphic complex, Slave Province, District of Mackenzie. Contributions to the geology of the Northwest Territories, v. 3. N.W.T. Geology Division, Indian

and Northern Affairs Canada, p. 97-102.

Lambert, M.B., C. Beaumont-Smith and D. Paul, 1992. Structure and stratigraphic succession of an Archean stratovolcano, Slave Province, Northwest Territories. Current Research, Part C. Geological Survey of Canada, Paper 92-1C, p. 189-200.

Lambert, M.B., G. Burbidge, C.W. Jefferson, C. Beaumont-Smith and R. Lustwerk, 1990. Stratigraphy, facies and structure in volcanic and sedimentary rocks of the Archean Back River volcanic complex, N.W.T. Current Research, Part C. Geological Survey of Canada, Paper 90-1C, p. 151-165.

Lambert, M.B., 1988. Cameron River and Beaulieu River volcanic belts of the Archean Yellowknife Supergroup, District of Mackenzie, N.W.T. Geological Survey of Canada, Bulletin 382, 145 pp.

Lambert, M.B., 1978. The Back River volcanic complex - a cauldron subsidence structure of Archean age. Current Research, Part A. Geological Survey of Canada, Paper 78-1A, p. 153-157.

Lambert, M.B. and O. van Breemen, 1991. U-Pb zircon ages from the Sleepy Dragon complex and a new occurrence of basement rock within the Meander Lake plutonic suite, Slave Province, N.W.T. Radiogenic Age and Isotopes Report 4, Geological Survey of Canada, Paper 90-2, p. 79-84.

LeCheminant, A.N. and L.M. Heaman, 1989. Mackenzie igneous event, Canada: Middle Proterozoic hotspot magmatism associated with ocean opening. Earth and Planetary Science Letters, v. 96. p. 38-48.

LeMaitre, R.W., 1976. The chemical variability of some common igneous rocks. Journal of Petrology, v. 17, p. 589-637.

Masuda, A., N. Nakamura and T. Tanaka, 1973. Fine structures of mutually normalized rare-earth patterns of chondrites. Geochimica et Cosmochimica Acta, v. 37, p. 239-248.

McGlynn, J.C., 1977. Geology of the Bear-Slave Structural Provinces, District of Mackenzie. Geological Survey of Canada, Open File 445.

McGlynn, J.C. and J.B. Henderson, 1972. The Slave Province. In Variations in tectonic styles in Canada. Geological Association of Canada, Special Paper 11, R.A. Price and R.J.W. Douglas eds. p. 506-526.

McLellan, S.M. and S.R. Taylor, 1984. Archean sedimentary rocks and their relation to the composition of the Archean continental crust. Archean Geochemistry: The Origin and Evolution of the Archean Continental Crust. A. Kroner, G.N. Hanson and A.M. Goodwin eds., p. 47-72.

Mortensen, J.K., R.I. Thorpe, W.A. Padgham, J.E. King and W.J. Davis, 1988. U-Pb zircon ages for felsic volcanism in Slave Province, N.W.T. Radiogenic and Isotopic Studies: Report 2, Geological Survey of Canada, Paper 88-2, p. 85-95.

O'Connor, J.T., 1965. A classification for quartz-rich igneous rocks based on feldspar ratios. United States Geological Survey, Professional Paper 525-3. p. 879-884.

Padgham, W.A. and W.K. Fyson, 1992. The Slave Province: a distinct Archean craton. Canadian Journal of Earth Sciences, v. 29, p. 2072-2086.

Padgham, W.A., 1990. The Slave Province, an overview. In Mineral deposits of Slave Province, Northwest Territories, Field Trip Guidebook, 8th IAGOD Symposium. W.A. Padgham and D. Atkinson eds. Geological Survey of Canada Open File 2168, p. 1-40.

Padgham, W.A., 1986. Turbidite-hosted gold-quartz veins in the Slave Structural Province, N.W.T. In Turbidite-hosted gold deposits. Geological Association of Canada Special Paper 32. Keppie, J.D., R.W. Boyle and S.J. Haynes eds., p. 119-134.

Padgham, W.A., 1985. Observations and Speculations on Supracrustal successions in the Slave Structural Province. In Evolution of Archean Supracrustal Sequences, L.D. Ayres, P.C. Thurston, K.D. Card and W. Weber, eds., Geological Association of Canada, Special Paper 28, p. 133-151.

Parrish, R.R., J.C. Roddick, W.D. Loveridge and R.W. Sullivan, 1987. Uranium-lead analytical techniques at the geochronology laboratory, Geological Survey of Canada. Radiogenic Age and Isotopic Studies: Report 1, Geological Survey of Canada, Paper 87-2, p. 3-7.

Pearce, J.A. and J.R. Cann, 1973. Tectonic setting of basic volcanic rocks determined using trace element analyses. Earth and Planetary Science Letters, v. 19, p. 290-300.

Penny, S, 1990. The Geology and Geochemistry of Metasedimentary, Metavolcanic and Plutonic Rocks near Turner Lake, Bathurst Inlet Area, District of Mackenzie, N.W.T. unpublished B.Sc. thesis, University of Ottawa, Ottawa, Ontario, 30 pp.

Ramsay, C.R., 1974. The cordierite isograd in Archaean meta-sediments near Yellowknife,

N.W.T., Canada - Variations on en experimentally established reaction. Contributions to Mineralogy and Petrology, v. 47, p. 27-39.

Ramsay, C.R. and D.C. Kamenini, 1977. Petrology and Evolution of an Archaean Metamorphic Aureole in the Slave Craton, Canada. Journal of Petrology, v. 18, p. 460-486.

Relf, C.D., 1992. Two distinct shortening events during late Archean orogeny in the west-central Slave Province, Northwest Territoires, Canada. Canadian Journal of Earth Sciences, v. 29, p. 2104-2117.

Relf, C.D., 1990. Archean deformation and metamorphism of metasedimentary rocks in the Contwoyto - Nose Lakes area, Central Slave Province, N.W.T. Current Research, Part C, Geological Survey of Canada, Paper 90-1C, p. 97-106.

Rice, R.J., D.G.F. Long, W.K. Fyson and S.M. Roscoe, 1990. Sedimentological evaluation of three Archean metaquartzite and conglomerate-bearing sequences in the Slave Province, N.W.T. Current Research, Part C, Geological Survey of Canada, Paper 90-1C, p. 305-322.

Richardson, S.W., M.C. Gilbert, and P. Bell, 1969. Experimental determination of kyanite-andalusite and andalusite-sillimanite equilibria; the aluminuim silicate triple point. American Journal of Science, v. 267-272.

Robie, R.A. and B.S. Hemingway, 1984. Entropies of kyanite, andalusite, and sillimanite: additional constraints on the pressure and temperature of the Al_2SiO_5 triple point. American Mineralogist, v. 69, p. 298-306.

Roddick, J.C., W.D. Loveridge and R.R. Parrish, 1987. Precise U/Pb dating of zircon at the sub-nanogram Pb level, Isotope Geoscience, v. 66, p. 111-121.

Roscoe, S.M., M. Stubley and D. Roach, 1989. Archean quartz arenites and pyritic paleoplacers in the Beaulieu River supracrustal belt, Slave Structural Province, N.W.T. Current Research, Part C, Geological Survey of Canada, Paper 89-1C, p. 199-214.

Roscoe, S.M., M.N. Henderson, P.A. Hunt and O. van Breemen, 1987. U-Pb zircon age of an alkaline granite body in the Booth River Intrusive Suite, N.W.T. Radiogenic Age and Isotopic Studies, Report 1. Geological Survey of Canada, Paper 87-2, p. 95-100.

Roscoe, S.M., 1984. Assessment of mineral resource potential in the Bathurst Inlet area, NTS 76J, K, N, O including the proposed Bathurst Inlet national park. Geological Survey

of Canada, Open File 788, 75 pp.

Roscoe, S.M., C.F. Staargaard and S. Fraser, 1988. Stratigraphic setting of gold concentration in Archean supracrustal rocks near the west side of Bathurst Inlet, N.W.T. Current Research, Part C, Geological Survey of Canada, Paper 88-1C, p. 367-372.

Schiller, E.A., 1965. Mineral Industry of the NWT. Geological Survey of Canada Paper 65-11, p. 8, 9.

Schaan, S.E., and W.K. Fyson, 1991. Geology of the Fat Lake Map Sheet: Preliminary Results (75 M/5 and part of 75 M/4) in Exploration Overview 1991 Northwest Territories. Mining, exploration and geological investigations. NWT Geology Division - NAP. p. 35-36.

Siefert, F., 1970. Low-temperature compatibility relations of cordierite in haplopelites of the system K_2O-MgO-Al_2O_3-SiO_2-H_2O. Journal of Petrology, v. 11, p. 73-99.

Staargaard, C.F., 1987. Report on a 1986 program of geological mapping, sampling, and magmatic-VLF surveying on the Turner Lake property, Bathurst Inlet area, district of Mackenzie, N.W.T. unpublished report for Silver Hart Mines Ltd., 30 p.

Stockwell, C.H., 1970. Geology and Economic Minerals of Canada. R.J.W. Douglas ed. Geological Survey of Canada, Economic Geology Report No. 1, p. 44-54.

Stockwell, C.H., 1933. Great Slave Lake - Coppermine River area, Northwest Territories. Geological Survey of Canada, Summary Report 1932, Part C, p. 37-63.

Stockwell, C.H., J.C. McGlynn, R.F. Emslie, B.V. Sanford, A.W. Norris, J.A. Donaldson, W.F. Fahrig and K.L. Currie, 1970. Geology of the Canadian Shield. In Geology and Economic Minerals of Canada; R.J.W. Douglas ed. Geological Survey of Canada, Economic Geology Report #1, p. 43-150.

Streckeisen, A., 1976. To each plutonic rock its proper name. Earth Science Reviews, v. 12 p. 1-33.

Taylor, S.R. and S.M. McLennan, 1985. The Continental Crust: its Compsosition and Evolution. An Examination of the Geochemical Record Preserved in Sedimentary Rocks. Blackwell Scientific Publications, 312 pp.

Templeton, S., 1988. A Petrographic Study of Metadunite in the Beniah Lake Region, N.W.T. B.Sc. thesis. University of Ottawa, Ottawa, Ontario, 70 pp.

Thompson, P.H., 1989a. Moderate overthickening of thinned sialic crust and the origin of granitic magmatism and regional metamorphism in low-P-high-T terranes. Geology, v. 17, p. 520-523.

Thompson, P.H., 1989b. An empirical model for metamorphic evolution of the Archaean Slave Province and adjacent Thelon tectonic zone, north-western Canadian Shield. in Daly, J.S.; Evolution of Metamorphic Belts. F.A. Cliff and B.W.D. Yardley eds. Geological Society Special Publication 43, p. 245-263.

Thompson, P.H., 1978. Archean regional metamorphism in the Slave Structural Province - A new perspective on some old rocks. in J.A. Fraser and W.W. Heywood eds. Metamorphism in the Canadian Shield. Geological Survey of Canada, Paper 78-10, p. 85-102.

Thorpe, R.I., 1982. Lead isotope evidence regarding Archean and Proterozoic metallogeny in Canada; Revista Brasilieira de Geociencias, v. 12, p. 510-521.

Thorpe, R.I., 1966. Mineral Industry of the NWT. Geological Survey of Canada, Paper 66-52, 44 pp.

van Breemen, O., W.J. Davis and J.E. King, 1992. Temporal distribution of granitoid plutonic rocks in the Archean Slave Province, northwest Canadian Shield. Canadian Journal of Earth Sciences, v. 29, p.2186-2199.

Venance, K. 1991. Constraints on metamorphism in the Torp Lake area, Northern Slave Structural Province (NTS 76N/3, 4, 5, 6, 11) in Exploration Overview 1991, p. 38-39.

Venance, K. in prep. Petrography, Microstructures and Regional Metamorphism of the Torp Lake Area, Northern Hood River Belt, Slave Structural Province. unpublished M.Sc. thesis, Carleton University, Ottawa, Ontario.

Winchester, J.A. and P.A. Floyd, 1977. Geochemical discrimination of different magma series and their differentiation products using immobile elements. Chemical Geology, v. 20, p. 325-343.

Winkler, H.G.F., 1979. Petrogenesis of Metamorphic Rocks fifth Edition. Springer-Verlag, 348 pp.

APPENDICES

APPENDIX I: CORRELATION OF GEOLOGICAL MAP UNITS, TURNER LAKE AREA (1964 TO 1993)

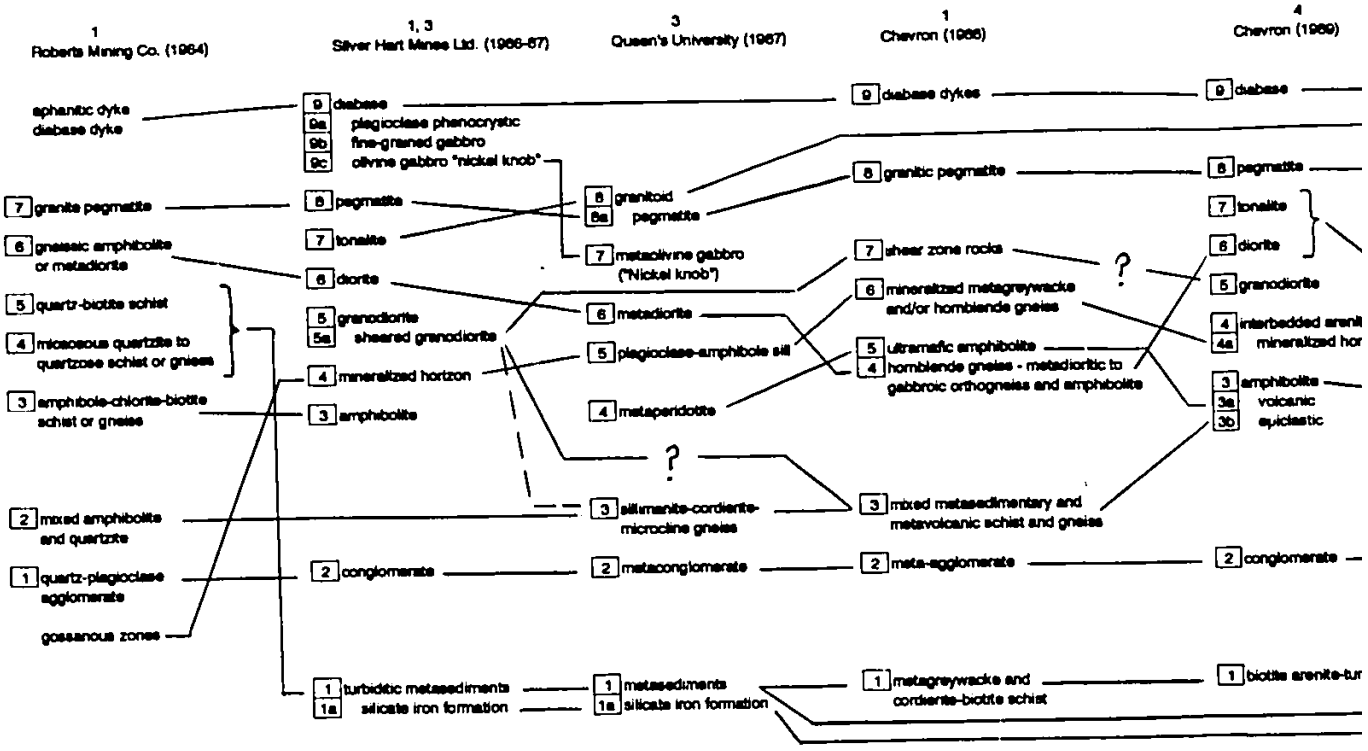

References:
1. Getzinger (1968)
2. Staargaard (1967)
3. Clode (1967)
4. Fumerton (1969)

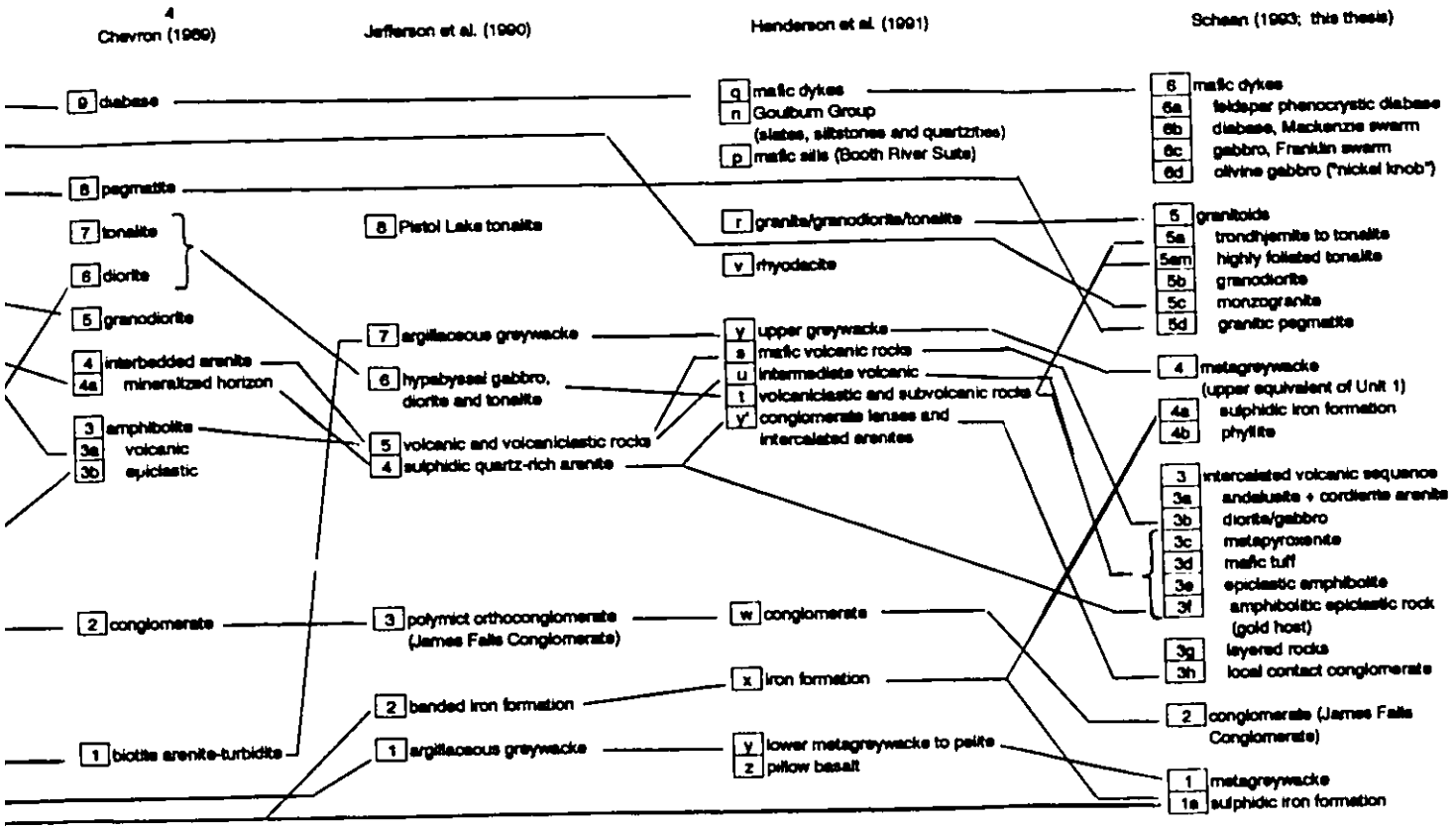
Chevron (1989)
Jefferson et al. (1990)
Henderson et al. (1991)
Schaan (1993; this thesis)
9 diabase
8 pegmatite
7 tonalite
6 diorite
5 granodiorite
4 interbedded arenite
4a mineralized horizon
3 amphibolite
3a volcanic
3b epiclastic
2 conglomerate
1 biotite arenite-turbidite
8 Pistol Lake tonalite
7 argillaceous greywacke
6 hypabyssal gabbro, diorite and tonalite
5 volcanic and volcaniclastic rocks
4 sulphidic quartz-rich arenite
3 polymict orthoconglomerate (James Falls Conglomerate)
2 banded iron formation
1 argillaceous greywacke
q mafic dykes
n Goulburn Group (slates, siltstones and quartzites)
p mafic sills (Booth River Suite)
r granite/granodiorite/tonalite
v rhyodacite
y upper greywacke
s mafic volcanic rocks
u intermediate volcanic
t volcaniclastic and subvolcanic rocks
y' conglomerate lenses and intercalated arenites
w conglomerate
x iron formation
y lower metagreywacke to pelite
z pillow basalt
6 mafic dykes
6a feldspar phenocrystic diabase
6b diabase, Mackenzie swarm
6c gabbro, Franklin swarm
6d olivine gabbro ("nickel knob")
5 granitoids
5a trondhjemite to tonalite
5am highly foliated tonalite
5b granodiorite
5c monzogranite
5d granitic pegmatite
4 metagreywacke (upper equivalent of Unit 1)
4a sulphidic iron formation
4b phyllite
3 intercalated volcanic sequence
3a andalusite + cordierite arenite
3b diorite/gabbro
3c metapyroxenite
3d mafic tuff
3e epiclastic amphibolite
3f amphibolitic epiclastic rock (gold host)
3g layered rocks
3h local contact conglomerate
2 conglomerate (James Falls Conglomerate)
1 metagreywacke
1a sulphidic iron formation

Appendix II
Host Rock Description (Unit 3f)

Systematic sampling was carried out across a trench excavated by Chevron Minerals Ltd. (Figure a and b) to characterize the succession of volcanic and volcanogenic rocks and the host unit for gold mineralization (Unit 3f). Full descriptions of each sub-unit, excluding 3f, are given in Chapter 3. The host unit is part of a stacked sequence of volcanic units defined by compositional variations. At the base of this sequence two samples taken from Unit 3e (tr11-1, tr11-2) have virtually the same mineralogy with tr11-2 being coarser than tr11-1 (reverse metamorphic grading). A noticeable increase in amphibole content in outcrop indicates the transition to metapyroxenite (Unit 3c). Gold at Turner Lake is hosted is a sulphidic (ilmenite, chalcopyrite, arsenopyrite), amphibolitic, fine-grained clastic host (Unit 3f) which overlies the metapyroxenite (Unit 3c) at this location. This unit is distinguished from the other units in the sequence in outcrop by its abundant quartz veins and paler colour (pale brownish grey vs. pale to medium greenish grey). In thin section (tr11-8) it contains 10% cummingtonite, 10 to 15% quartz and 65% plagioclase with 8% opaques. Further up in the sequence within the same unit tr11-4 contains 20% grunerite, 10% quartz and 50% plagioclase with 12% opaque minerals. Opaque minerals include ilmenite and arsenopyrite with minor chalcopyrite. The gold is present both as visible gold associated with quartz veins and has also been noted as disseminated gold in the matrix of the host rock (G. Walton, pers. comm., 1989). Quite simply, Unit 3f is a variation of Unit 3e containing less amphibole. It has been designated as a distinct sub-unit to distinguish it at the main showing

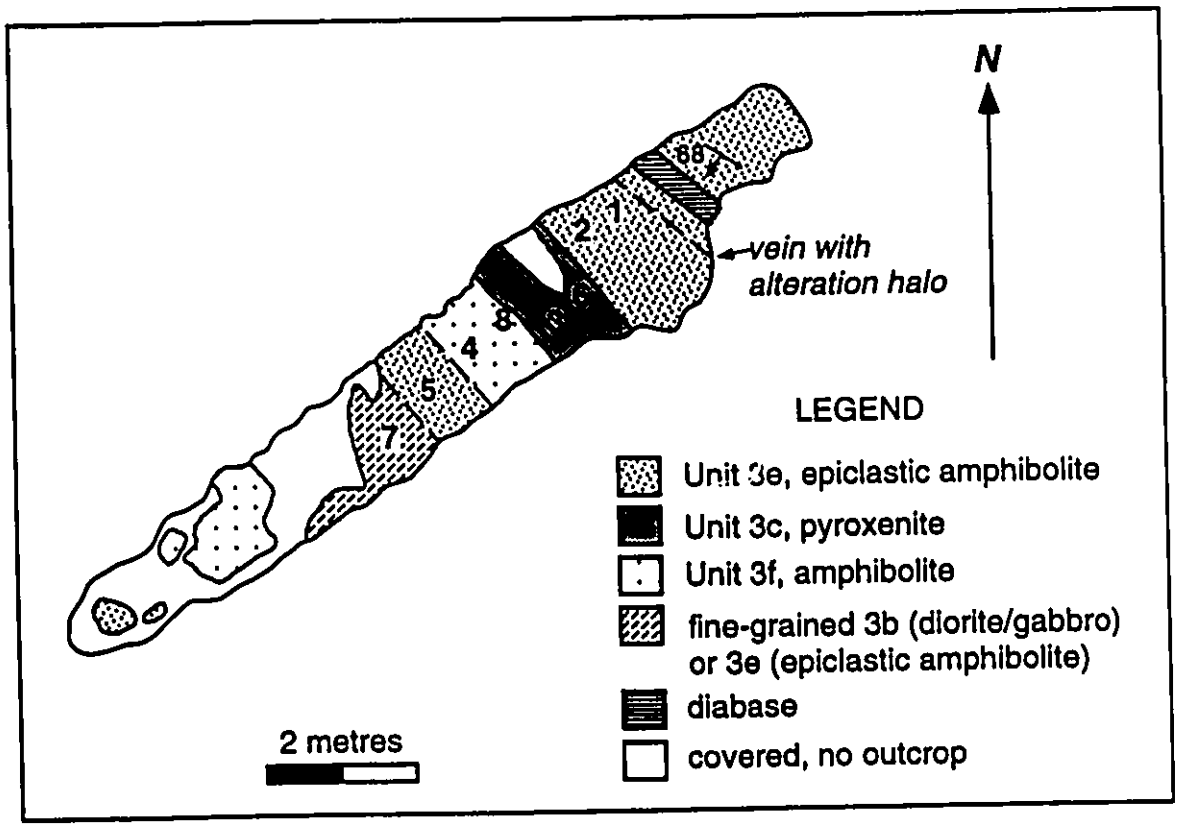

Figure a. Map of trench 11. Sample numbers indicated at location of sampling. Rock unit symbols in legend.

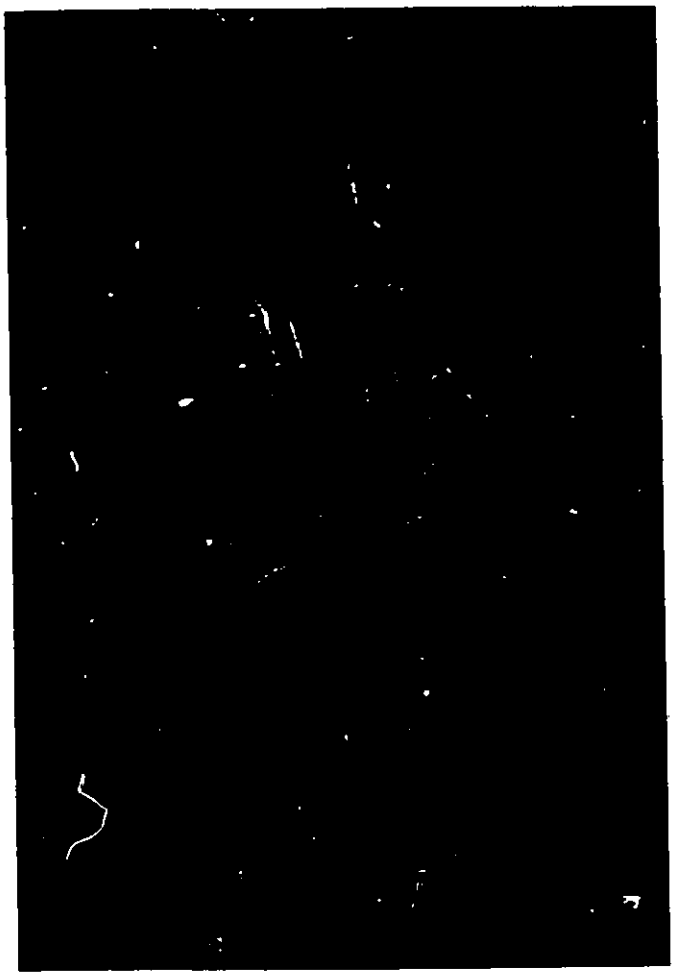

Figure b. Photograph of trench 11 at Turner Lake main showing as excavated by Chevron Minerals Ltd. (1989). View looking southwest; tops are towards the top of the photograph (ie. southwest).

(samples 89138, tr5); however, elsewhere in the map area it has not been distinguished from the other intercalated volcanic sub-units (Units 3e and d).

Contrary to Fumerton (1989), ilmenite is an abundant opaque mineral in this unit and is present in proportions up to about 10%. Fumerton reported that "...the auriferous arenites differ from other arenites in that they contain variable concentrations of pyrrhotite, arsenopyrite and gold rather than ilmenite, but both auriferous and barren arenites are primarily composed of plagioclase with some quartz veining." (Fumerton, 1989, p. I). The present study documents ilmenite as an abundant component of the sulphide mineral assemblages present both within the host and other rocks of the area. Therefore the paleoplacer model proposed by Fumerton (1989) is rejected. Furthermore there is no textural evidence of paleoplacer gold such as concentrations in heavy mineral laminae etc. All of the gold is spatially associated with quartz veins.

Roberts Mining Company had recognized that the gold mineralization is not confined to a particular host. The present study agrees with this interpretation and interprets the mineralization as stratabound (not stratiform), in a amphibolitic metaclastic host.

Appendix III. Whole rock and trace element geochemical analyses of Turner Lake samples. Total iron as Fe2O3. ppm Ti calculated from weight percent TiO2. A at top of column indicates analyses from X-Ray Assay Laboratories Inc. or Toronto, Ontario (X-Ral), 1990. B at top of column indicates analyses from X-Ral 1991.

oxide (wt. %)		A	A	A	A	A	A	A	B	B	A	A	A	B	A	A	A	A	A	A
		89012	89022	89026	89028	89034	89035	89037	89038	89054	89055	89059	89063	89069	89071	89100	89112	89115	89116	89118
		5am	3b	3b	5a	3b	5am	5c	3d	1	5c	3b	2 (cobble)	3d	3c	5b	5c	5am	3g	3a
SiO2		63.5	53.5	48.2	66.6	49.3	61.9	74.5	49.20	66.80	73.4	53.9	74.7	47.90	45.9	66.3	74.3	70.5	59.9	70.9
TiO2		0.75	1.45	0.76	0.50	0.42	0.71	0.03	0.57	0.57	0.21	1.56	0.28	0.59	0.62	0.48	0.13	0.27	0.99	0.47
Al2O3		16.2	15.9	14.7	15.3	17.6	16.4	15.2	8.19	15.00	14.8	14.5	12.5	8.75	7.72	15.9	14.4	14.8	15.9	13.1
Fe2O3**		6.88	13.2	15.6	4.7	11.5	6.73	0.37	10.5	4.90	1.3	13.9	2.45	10.40	10.4	4.69	0.95	2.89	8.50	4.48
MnO		0.11	0.18	0.19	0.08	0.16	0.10	0.06	0.18	0.05	nd	0.18	0.10	0.15	0.18	0.07	nd	nd	0.15	nd
MgO		1.41	4.01	6.74	2.22	7.91	2.81	0.15	17.60	2.35	0.51	4.45	1.17	17.40	19.0	1.84	0.45	2.65	1.81	1.99
CaO		5.10	8.13	6.87	2.26	8.72	4.81	0.66	6.55	1.82	0.97	7.42	3.9	7.14	6.75	3.42	0.58	0.58	6.93	1.72
Na2O		3.96	2.91	2.89	3.81	2.27	3.97	7.59	1.33	3.74	4.37	2.69	3.00	0.66	0.66	3.86	3.81	1.50	3.02	2.35
K2O		1.53	0.58	1.03	2.70	0.87	2.11	0.96	1.24	2.27	3.66	1.03	0.72	2.13	1.09	2.66	4.77	3.72	1.41	2.36
P2O5		0.16	0.10	0.07	0.12	0.08	0.19	0.13	0.15	0.20	0.20	0.13	0.15	0.14	0.19	0.11	0.25	0.05	< 0.39	0.09
LOI		0.70	0.31	2.08	1.85	1.23	0.47	0.54	2.54	1.47	0.62	0.54	1.00	3.00	3.93	1.08	0.77	2.08	1.31	1.93
TOTAL		100.32	100.27	99.13	100.14	100.06	100.20	100.19	98.05	99.17	100.04	100.30	99.97	98.46	98.64	100.41	100.41	99.3	100.11	99.39
element (ppm)	atomic number																			
U	3	38	207	230	73	92	117	16			85	48	27		95	86	74	174	68	30
Be	4	0	0	0	0	0	0	0			0	0	0		0	0	6	0	0	0
B	5	0	19	0	44	0	0	125			13	0	39		12	20	257	111	19	74
Sc	21	11.4	24.5	22.4	10.2	13.6	12.1	0.8			2.7	29.4	5.1		24.1	11.1	3.1	8.6	12.3	11
Ti*	22	4496	8693	4556	2997	2518	4256	180	3417	3417	1259	9352	1679	2280	3717	2878	779	1619	5935	2818
V	23	58	248	186	72	99	11	0			15	272	57		175	15	16	15	53	97
Cr	24	15	75	340	41	48	59	0	1340	145	15	55	40	1240	1370	52	8	15	14	110
Co	27	16	44	101	14	56	22	0	59	14	3	43	8	64	58	13	1	6	20	14
Ni	28	18	41	2170	36	189	43	0	648	45	7	43	17	670	543	29	7	34	7	28
Cu	29	2.8	55	3370	19	86.7	4.2	14.3	2.4	48.4	15.4	29	12.9	109	5.5	15.4	1.5	0	1.5	28.5
Zn	30	109	114	141	80.2	83.8	83.9	30.7	93.7	89.5	42.9	122	30.8	107	83.5	61.6	21.9	36.8	94.4	84.8
Ga	32	0	0	0	0	0	0	0			0	0	0		0	0	0	0	0	0
As	33	1	1	210	2	1	0	3			1	1	5		1	0	6	0	2	36
Rb	37	69	26	0	68	35	90	27	64	84	196	50	33	105	48	104	195	131	60	76
Sr	38	397	272	285	383	218	434	15	295	440	141	377	693	126	432	305	117	306	792	335
Y	39	18	39	0	0	0	11	0	13	12	0	0	20	12	0	13	14	38	37	15
Zr	40	141	93	52	150	56	152	0	73	155	87	82	88	84	56	127	55	282	186	123
Nb	41	16	21	0	22	15	11	0	17	17	23	0	0	16	11	17	0	12	25	18
Mo	42	0	0	0	0	0	0	1	7	12	2	0	0	6	0	0	0	0	0	0
Ag	47	0	0	1.6	0	0	0	0	0.5	0.5	0	0	0	0	0	0	0	0.7	1.5	0.6
Cd	48	0	0	0	0	0	0	0	1	1	0	0	0	1	0	0	0	0	0	0
Sn	50	13	0	13	0	24	0	0			0	0	0		0	28	0	12	0	0
Sb	51	1	0.4	0.5	0.2	0.3	0.4	0			0	1.0	0.8		0.5	0	0	0.2	1.6	0.2
Cs	55	5	5	5	3	9	26	0			6	11	1		6	6	7	16	6	5
Ba	56	714	180	407	802	226	659	123	309	554	448	629	295	404	444	547	459	1680	284	625
Hf	72	4	3	1	4	1	4	1			2	2	2		1	3	1	7	4	3
Ta	73	0	0	0	0	0	0	0			0	0	0		0	0	1	1	0	0
W	74	0	0	0	0	0	0	0			0	0	0		0	0	0	4	0	0
Au (ppb)	79	0	0	130	0	0	0	26			9	0	5		0	1	3	0	0	2
Pb	82	0	0	0	8	0	0	70	0	52	22	0	5	0	0	10	43	0	0	8
Bi	83	0	8	8	4	4	4	0			0	10	0		7	3	4	0	0	0
Th	90	3	2	0	6	0	4	0			9	2	9		1	4	5	14	3	6
U	92	0	0.8	0	2.5	0	1.2	3.6			7.6	0	2.0		0	1.3	6.6	3.6	0.7	1.8

oxide (ppm)		A	A	A	A	B	B	B	B	B	B	B	B	B	B	B	B	B	B	B
		89138	89139	89145	89154	tr11-1	tr11-2	tr11-3	tr11-4	tr11-5	tr11-6	tr11-7	tr11-8	90059	90064	tr5A	tr5B	90069C	90097	90098
SiO2		57.3	68.9	46.4	70.7	54.1	53.00	49.60	52.10	50.90	47.50	51.30	56.40	52.10	73.00	65.90	60.80	40.20	50.80	50.80
TiO2		1.81	0.46	0.49	0.13	1.48	1.81	0.44	2.03	1.98	0.51	1.96	1.56	1.05	0.56	1.24	1.52	0.80	0.69	0.87
Al2O3		15.7	16.2	5.41	16.9	12.80	14.20	6.28	15.20	15.50	7.42	15.50	16.40	16.40	13.40	10.80	12.70	18.70	9.66	11.40
Fe2O3		11.2	3.08	10.3	0.87	13.00	13.40	10.00	14.90	14.80	9.79	14.80	10.90	11.90	3.81	9.34	11.10	32.20	11.00	10.60
MnO		0.20	nd	0.14	nd	0.18	0.17	0.18	0.22	0.20	0.20	0.20	0.16	0.17	0.44	0.13	0.15	0.31	0.22	0.17
MgO		2.54	1.09	23.4	0.55	5.17	4.94	19.60	3.28	3.33	20.50	3.28	2.31	5.16	1.92	2.46	3.27	3.83	11.00	10.70
CaO		3.36	2.03	6.89	0.75	8.10	6.92	8.17	5.69	4.50	7.66	4.43	3.26	8.05	1.33	3.16	2.77	1.44	12.00	9.05
Na2O		6.23	5.81	0.22	5.73	2.07	3.96	0.54	4.86	4.77	0.46	4.72	6.61	2.74	3.28	3.74	4.61	0.17	1.01	1.68
K2O		0.18	1.64	0.05	3.16	0.75	0.18	0.12	0.52	1.97	0.08	1.95	0.38	0.62	1.47	0.42	0.36	1.95	0.98	1.37
P2O5		0.34	0.16	0.13	0.24	0.11	0.06	0.13	0.22	0.20	0.14	0.20	0.27	0.07	0.06	0.17	0.22	0.02	0.19	0.24
LOI		1.06	0.77	5.47	1.00	1.62	1.00	2.93	0.77	0.47	4.18	0.31	0.70	0.85	1.54	2.16	1.06	0.31	0.85	1.85
TOTAL		99.74	100.14	98.90	100.06	99.36	99.66	97.99	99.81	98.60	98.42	98.65	98.95	99.11	100.83	99.52	98.58	99.93	98.40	98.73
element (ppm)	atomic number																			
Li	3	42	84	0	188															
Be	4	0	0	0	8															
B	5	0	18	7	30															
Sc	21	20.7	4.8	27.2	3.2															
Ti*	22	9852	2758	2938	779	8873	10851	2638	12170	11750	3057	11750	9352	6295	3357	7434	9112	4796	4137	5216
V	23	83	39	120	15															
Cr	24	0	20	1830	15	106	124	1300	0	3	1470	0	6	99	137	0	0	169	683	1350
Co	27	34	6	66	4	42	45	61	49	49	59	43	30	36	13	30	36	25	39	62
Ni	28	12	18	768	13	70	74	715	29	27	736	23	15	52	24	15	15	80	282	512
Cu	29	200	5.4	7.7	2.5	44.3	40.6	0.00	32.40	39.60	0.00	36.80	11.40	20.30	54.10	96.80	170.00	9.30	1.80	149.00
Zn	30	86.4	38.0	75.0	20.6	149	145	106	163	150	113	151	143	126	81	66	71	237	126	106
Ga	32	0	0	15	0															
As	33	580	8	170	2500															
Rb	37	26	70	0	286	32	18	0	35	93	0	96	23	19	54	17	33	104	52	106
Sr	38	1530	789	357	180															
Y	39	29	0	0	0	21	19	10	34	30	11	32	40	14						
Zr	40	197	182	50	49	82	100	66	136	141	68	133	208	64	247	105	113	242	82	73
Nb	41	18	18	26	11	18	13	20	26	13	0	14	36	0	0	0	26	16	18	26
Mo	42	0	0	0	0	13	14	7	18	14	7	14	13	11	9	12	13	13	9	10
Ag	47	0.8	0.8	0	0.5	0	0	0	0	0	0	0	0	0	0	5	2	0	0	1
Cd	48	0	0	3	45	1	1	2	1	1	1	1	1	1	0	1	1	3	1	1
Sn	50	20	0	0	39															
Sb	51	0.9	0.4	4.1	1.5															
Cs	55	3	8	1	28															
Ba	56	746	931	107	620	251	140	70	327	746	43	748	756	131	584	482	667	346	267	508
Hf	72	4	4	1	2															
Ta	73	0	0	0	0															
W	74	0	0	0	9															
Au (ppb)	79	150	1	37	16	6	7	370	1100	17	340	11	48	3	22	84	9000	24	21	3
Pb	82	10	2	0	32															
Bi	83	5	0	0	0															
Th	90	3	5	0	4															
U	92	0	1.3	0	8.1															

Appendix IV. Rare earth element data from Turner Lake samples, results in ppm. Data for the Leedy Chondrite is from Masuda et al., 1973.

	element and atomic number								
sample number	La 57	Ce 58	Nd 60	Sm 62	Eu 63	Gd 64	Dy 66	Yb 70	Lu 71
89012	17.0	36	18	3.8	1.1			2.0	0.30
89022	8.1	19	11	2.8	1.0			2.0	0.30
89026	5.6	13	7	1.8	0.8			1.3	0.20
89028	25.5	49	21	3.9	1.0			1.3	0.20
89034	6.3	13	7	1.4	0.5			1.0	0.16
89035	13.2	29	13	2.8	0.9			1.2	0.18
89037	1.4	3	5	0.1	0.2			0.2	0.05
89038	14	29	15	3.5	1.0	3.4	2.7	1.3	
89054	34	64	27	5	1.6	3.8	2.8	1.2	
89055	19.6	38	16	3.1	0.6			0.4	0.05
89059	12.5	27	14	3.6	1.5			2.0	0.30
89063	22.7	41	15	2.4	0.9			0.7	0.10
89069	10	23	16	3.5	0.9	3	2.6	1.3	
89071	8.6	20	11	2.4	1.1			1.0	0.16
89100	17.5	35	15	2.9	0.9			1.1	0.17
89112	9.9	20	8	1.5	0.5			1.3	0.20
89115	54.7	107	42	7.5	1.2			2.9	0.43
89116	24.7	51	25	5.3	1.7			4.0	0.60
89118	20.3	38	15	2.5	1.1			0.9	0.14
89138	25.4	52	24	5.0	2.3			4.4	0.72
89139	27.5	52	20	3.6	0.9		1.0	0.14	
89145	5.4	13	7	1.7	0.4			0.8	0.12
89154	6.3	16	7	1.30	0.50			0.4	0.05
tr11-1	7.6	16	16	3.8	1.5	4.6	4.5	1.9	
tr11-2	7.9	17	14	4.4	1.5	4.8	4.2	1.9	
tr11-3	18	38	10	2.3	0.9	2.5	2.1	1.1	
tr11-4	18	40	22	6.1	1.9	6.4	6.5	3.9	
tr11-5	17	39	22	5.8	1.8	6.0	6.0	3.5	
tr11-6	9.5	21	13	3.1	0.8	2.8	2.3	1.2	
tr11-7	17	38	22	5.2	1.8	6.1	6.1	3.7	
tr11-8	22	46	25	6.2	1.9	7.0	7.4	4.9	
90059	5.5	12	10	2.6	1.1	3.1	3.0	1.4	
90064	36	67	22	4.5	1.1	3.3	2.4	1.3	
tr5A	14	29	16	4.0	1.3	4.3	4.2	2.7	
tr5B	18	38	20	4.9	1.5	5.5	5.3	3.0	
90069C	20	37	16	3.8	1.0	4.1	3.2	1.2	
90097	13	30	20	5.2	1.4	4.6	3.6	1.7	
90098	12	27	18	4.9	1.8	5.0	3.9	1.5	
LEEDY	0.378	0.976	0.716	0.230	0.0866	0.311	0.390	0.249	0.0387

Map 2b. Sample location map with detail from Map 2a. Sample n
followed by unit sampled.

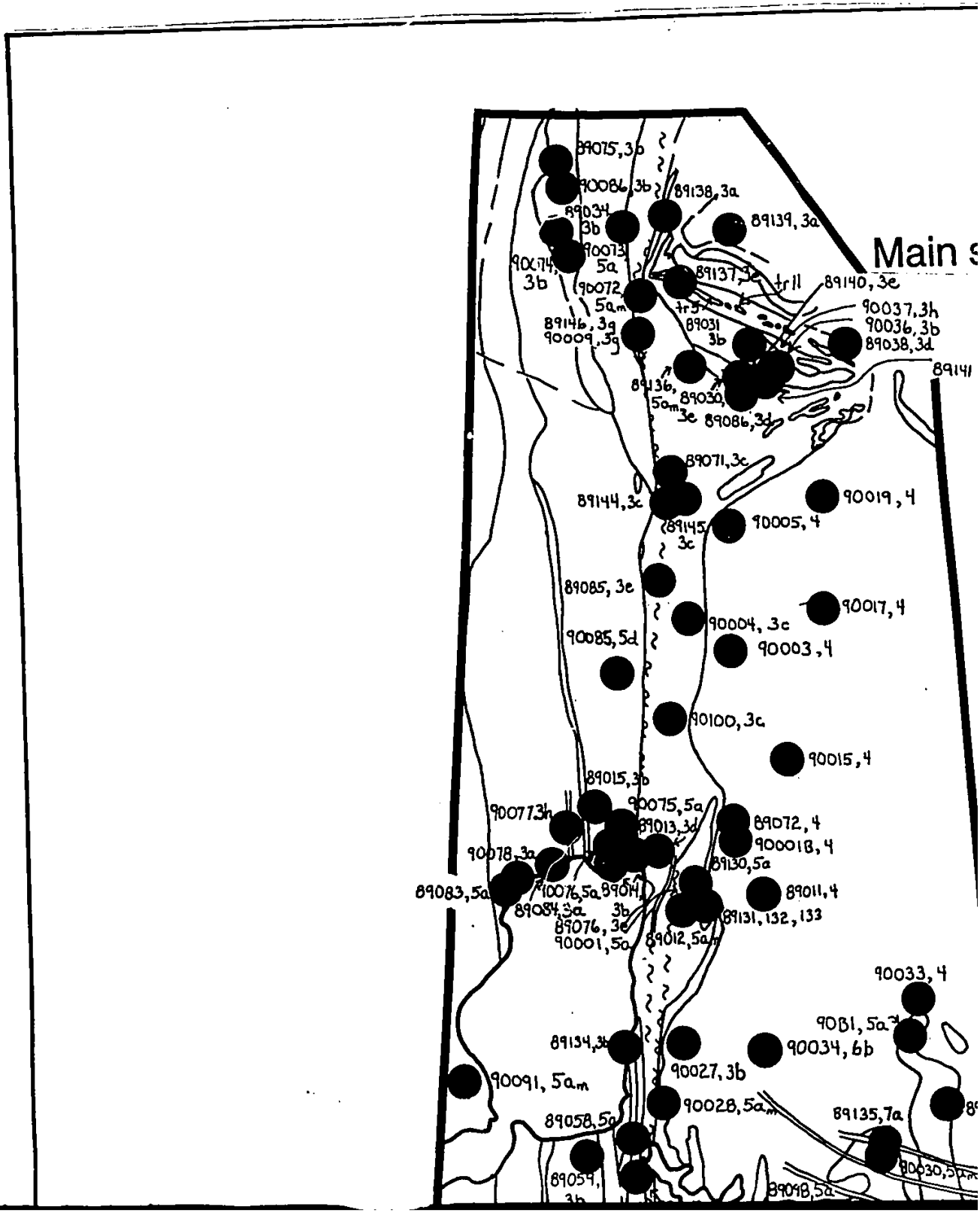

1. Sample number given

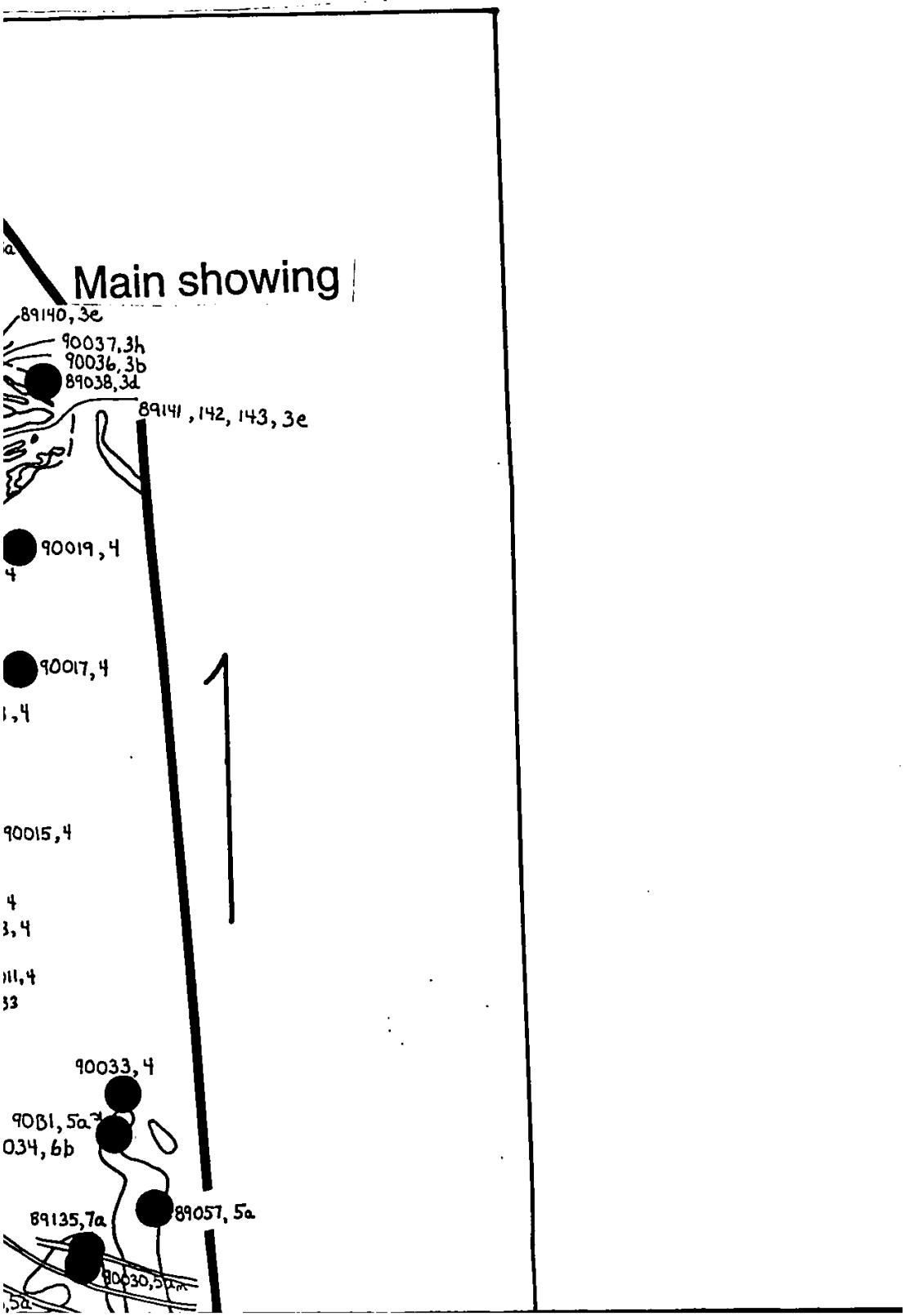

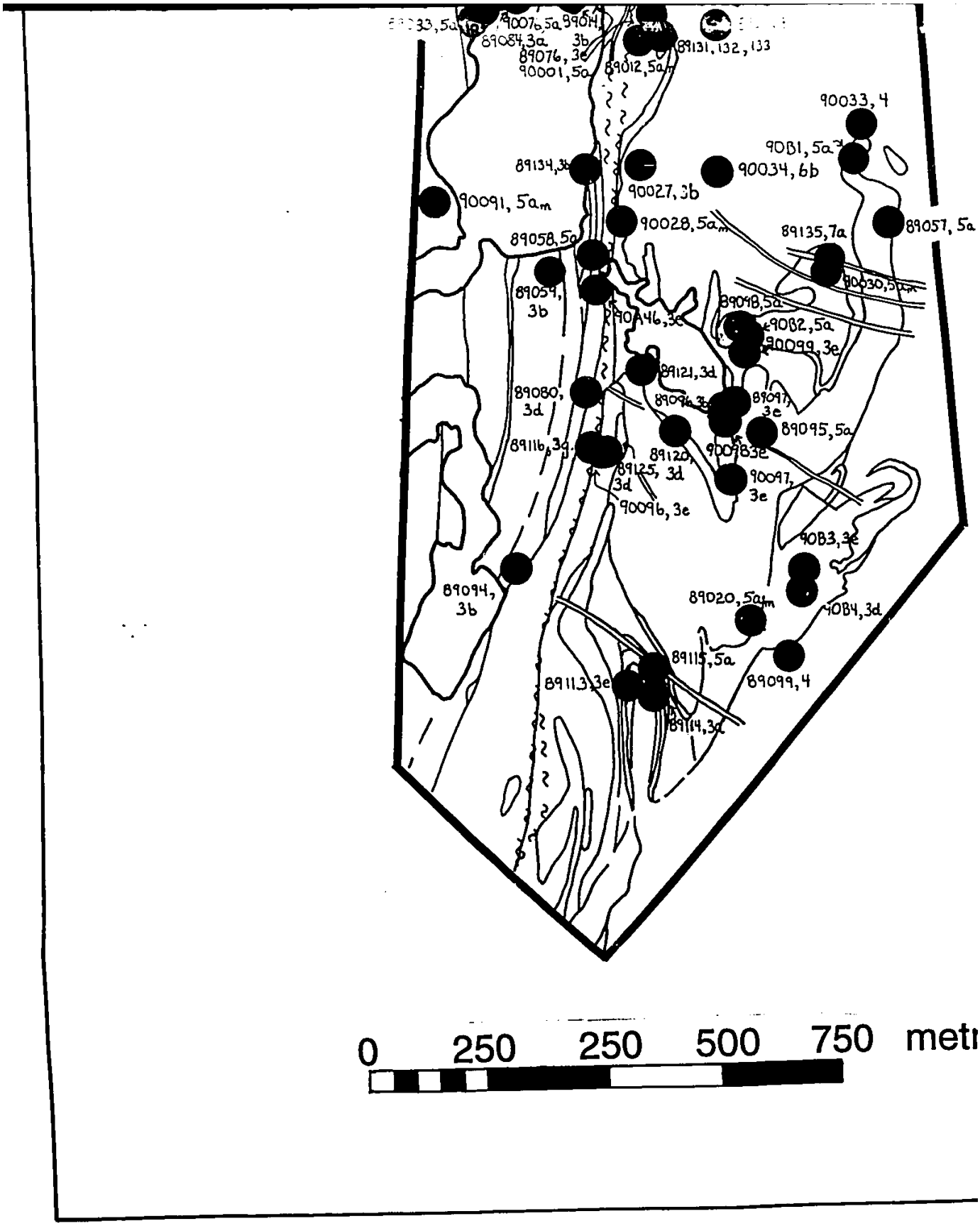
89084,3a
89076, 3e
90001, 5a
89012, 5am
89131, 132, 133
90033, 4
90081, 5a
89134, 3b
90034, 6b
90027, 3b
90091, 5am
90028, 5am
89135, 7a
89057, 5a
89058, 5a
89059, 3b
90030, 5am
89048, 5a
90046, 3e
90082, 5a
90099, 3e
89121, 3d
89080, 3d
89096, 3e
89097, 3e
89095, 5a
89116, 3d
89120, 3d
90083e
89125, 3d
90097, 3e
90096, 3e
90083, 3e
89094, 3b
89020, 5am
90084, 3d
89115, 5a
89099, 4
89113, 3e
89114, 3d
0
250
250
500
750
meti

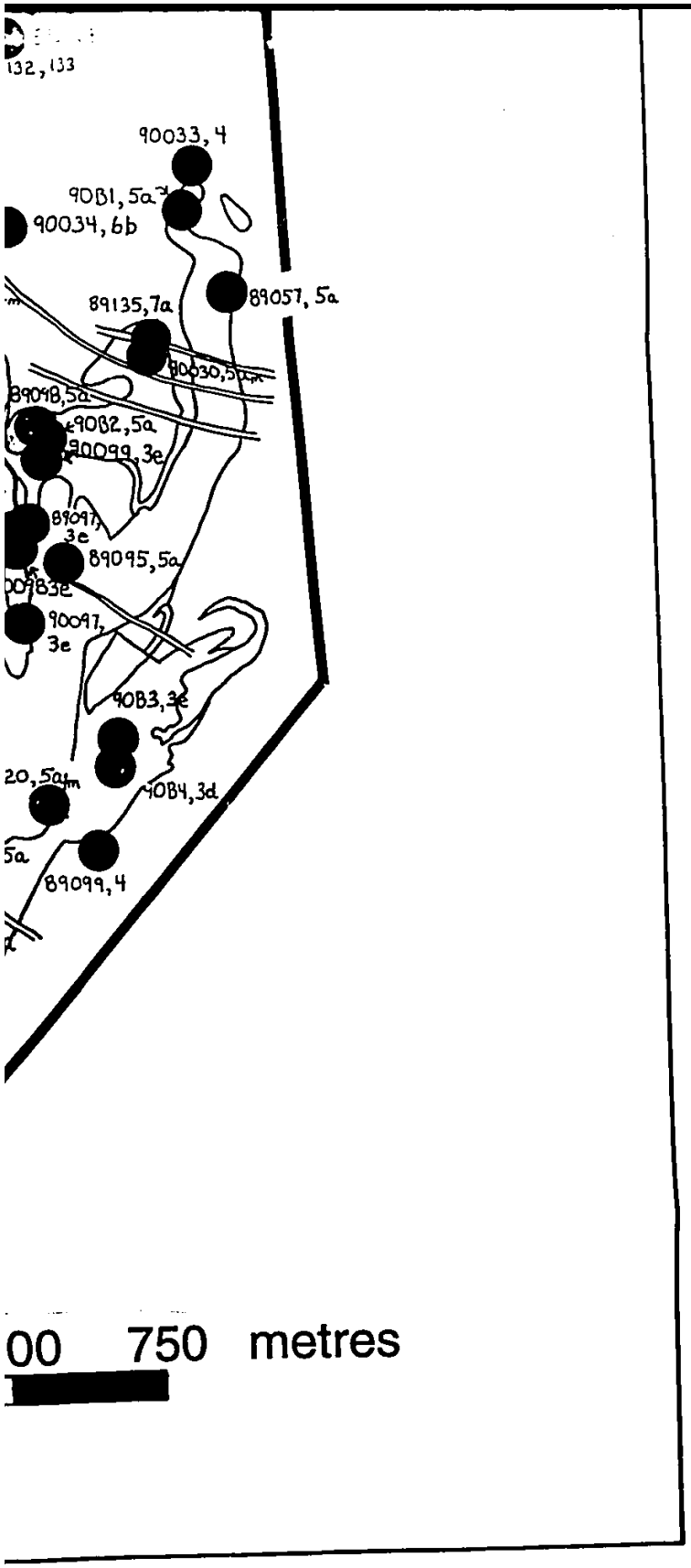
132, 133
90033, 4
90B1, 5a
90034, 6b
89135, 7a
89057, 5a
90030, 5a
89098, 5a
90B2, 5a
90099, 3e
89097, 3e
89095, 5a
90097, 3e
90B3, 3e
90B4, 3d
89099, 4
00 750 metres

EGS 1991-6 : GEOLOGY OF TU

SYMBOLS


bedding, tops known: dip known, dip unknown, overturned

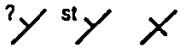
bedding, tops unknown: dip unknown, steeply dipping, vertical


S3: dip known, vertical, dip unknown

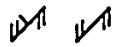
S4: dip known, vertical, dip unknown


fold axis minor fold

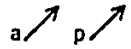
lineation: amphibole, pebble

fault


Turner Lake high strain zone


limit of mapping


outcrop*


geological boundary: defined, approximate

*indicated only where outcrop is sparse or lack of outcrop obscures contacts significantly

STRATIGRAPHY

PROTEROZOIC

Unit 6 Mafic dykes
- a. diabase; dark green ± feldspar phenocrysts.
- b. diabase; Mackenzie swarm.
- c. olivine gabbro; Franklin swarm.
- d. olivine gabbro ("Nickel Knob"); medium to coarse-grained, amphibolitized, gabbro chalcopyrite, pyrrhotite and pentlandite mineralization in Unit 4 at contact.

ARCHEAN

Unit 5 granitoid rocks
- a. variably deformed tonalite to trondhjemite; 5a, medium to coarse grained biotite ± hornblende ± muscovite trondhjemite, 5am, mylonitic tonalite with biotite clots ± hornblende.
- b. Pistol Lake biotite granodiorite; medium to coarse grained, weakly foliated

' OF TURNER LAKE AREA, PAR'

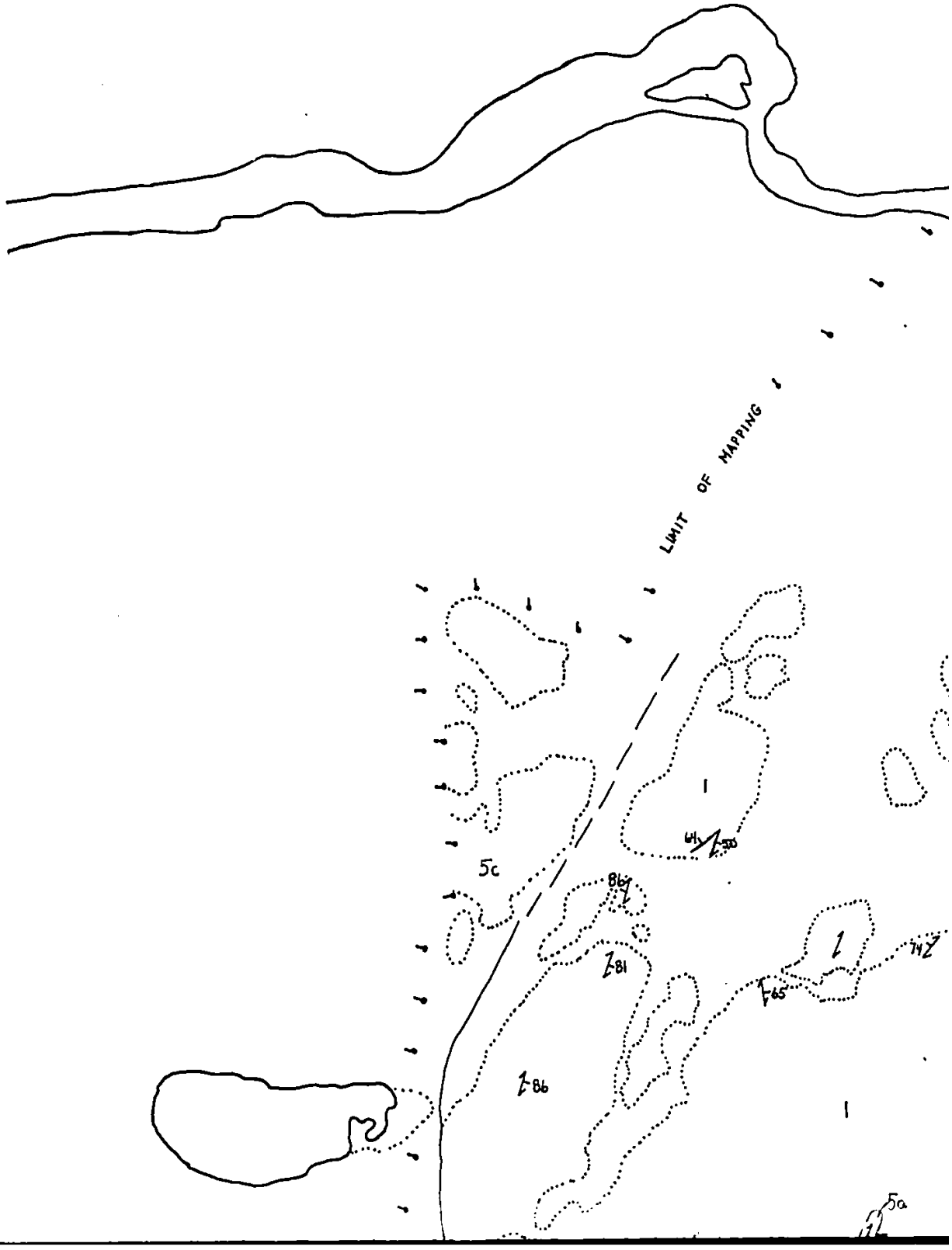

R LAKE AREA, PARTS OF NTS

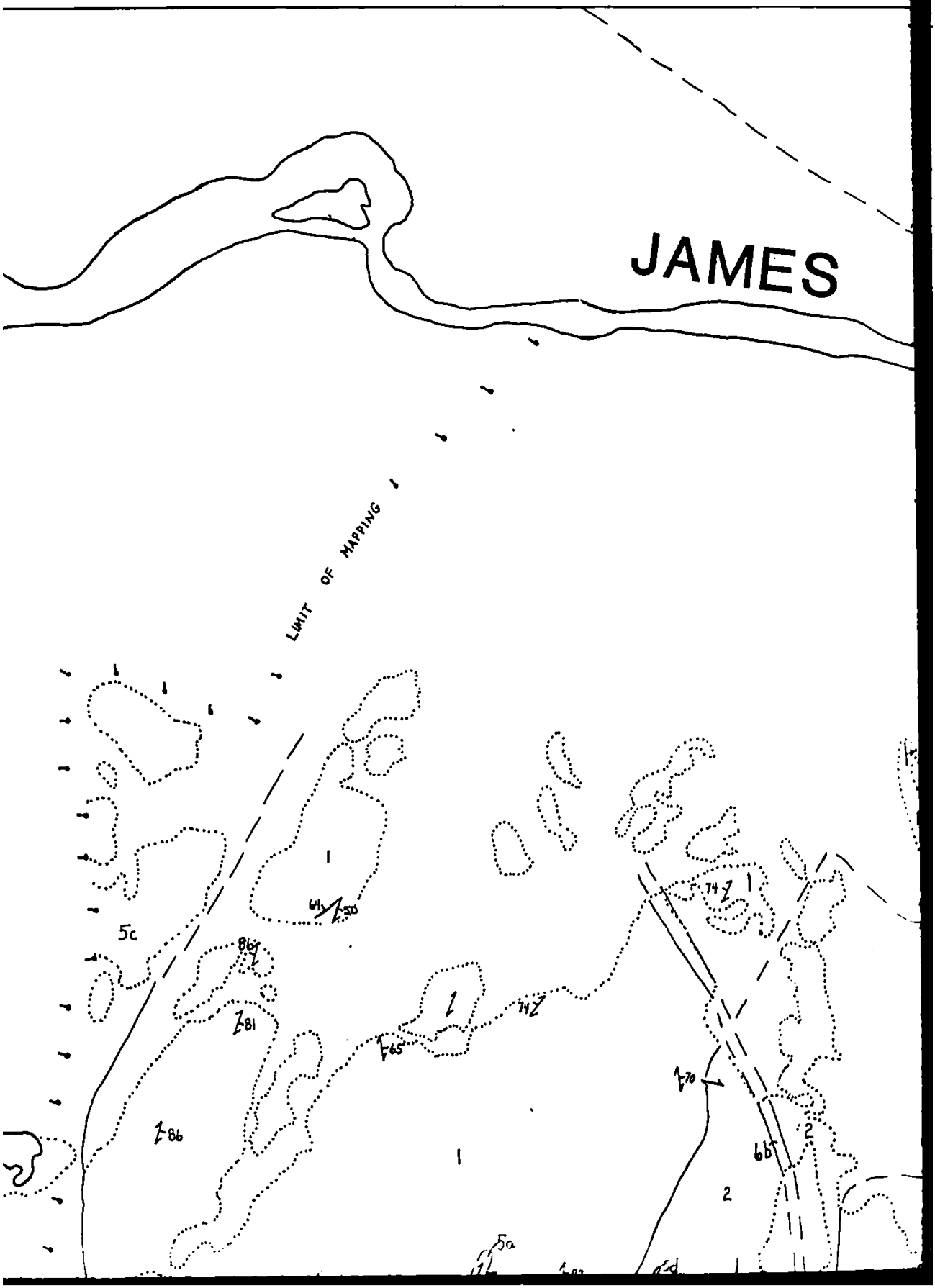

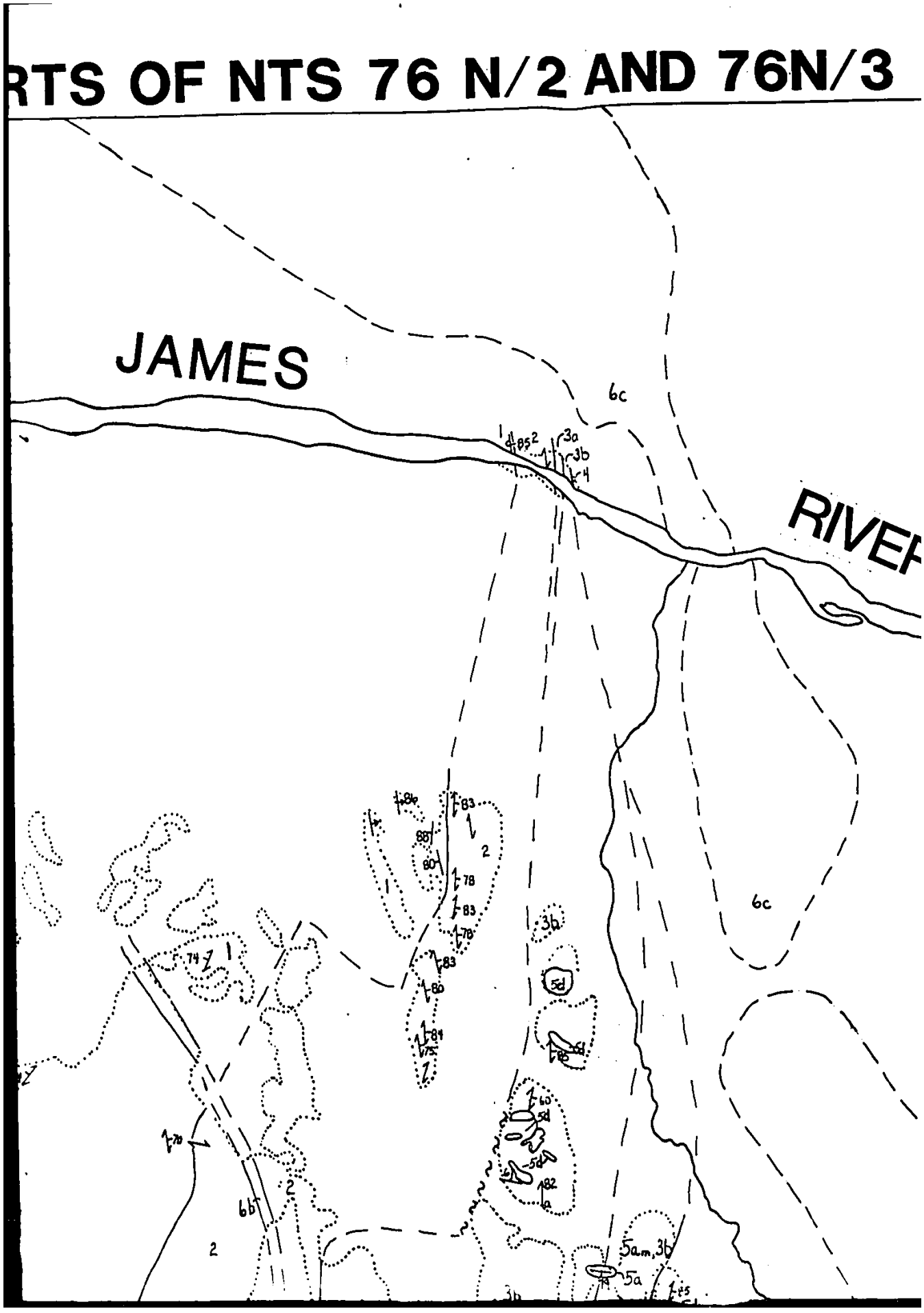
RTS OF NTS 76 N/2 AND 76N/3
JAMES
RIVER
6c
3a
3b
4
5d
5a
5am, 3b
6b
2

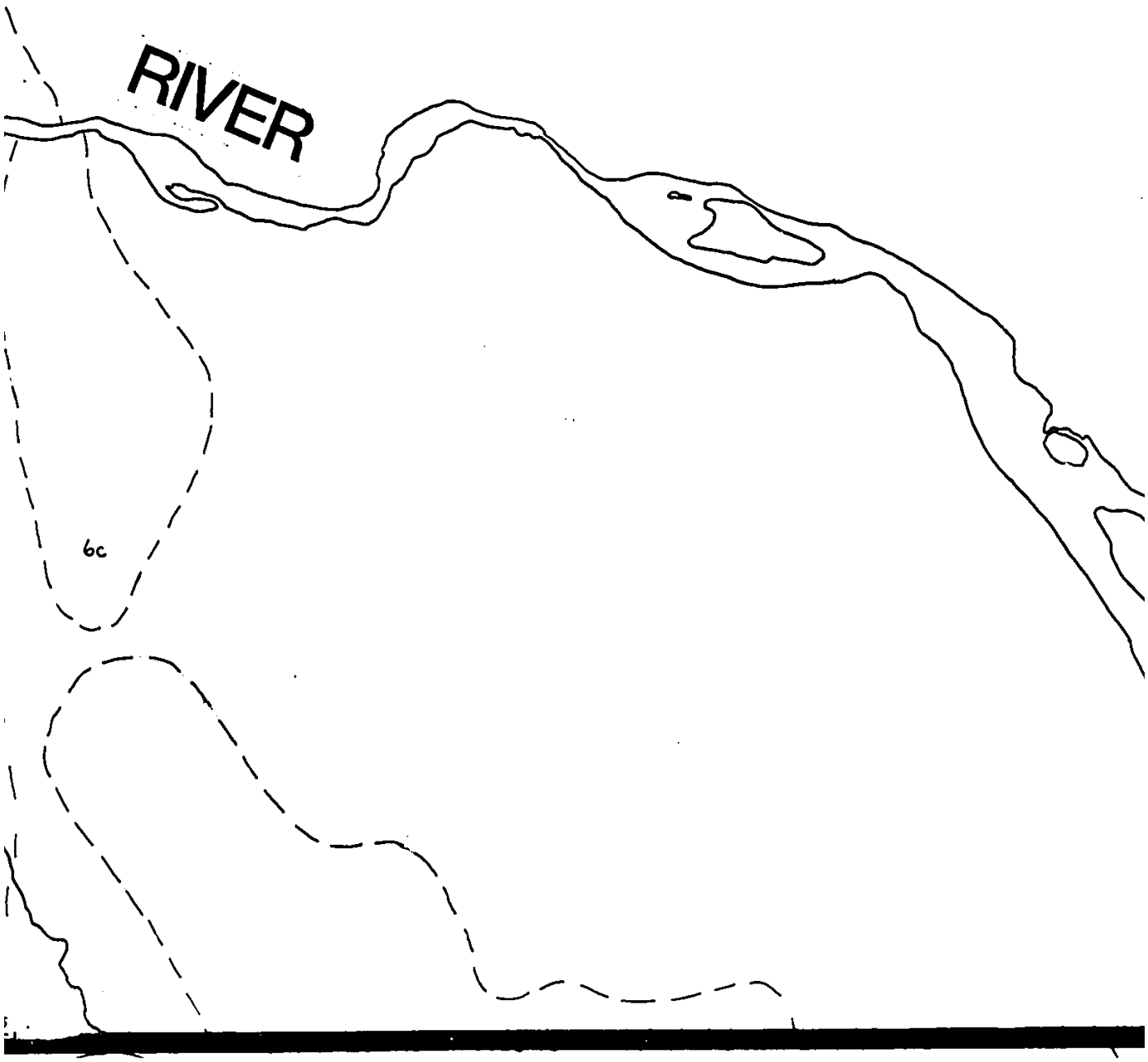
RIVER
6c

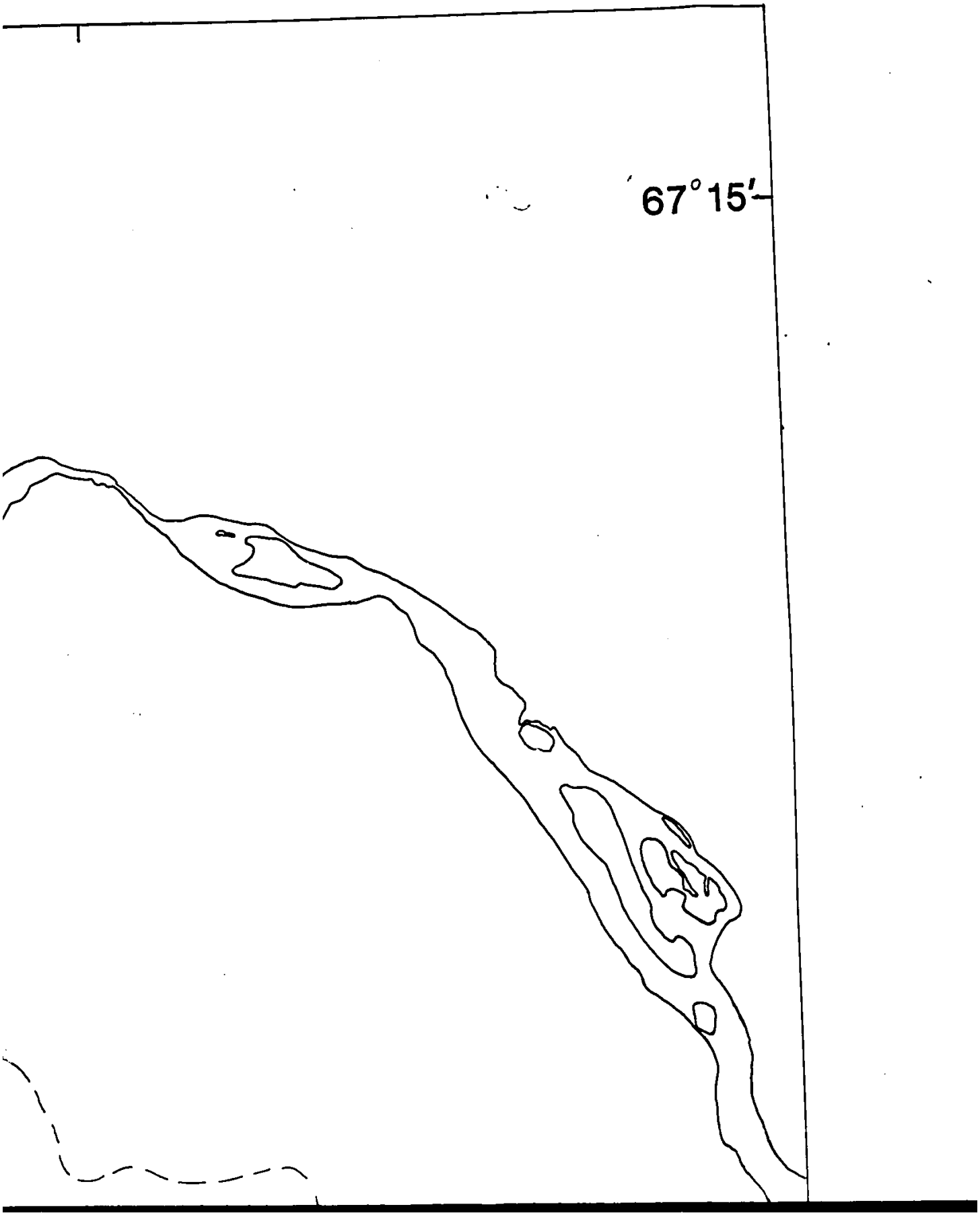
67°15'

c. olivine gabbro; Franklin swarm.
d. olivine gabbro ("Nickel Knob"); medium to coarse-grained, amphibolitized, gabbro chalcopyrite, pyrrhotite and pentlandite mineralization in Unit 4 at contact.

ARCHEAN

Unit 5 granitoid rocks
a. variably deformed tonalite to trondhjemite; 5a, medium to coarse grained biotite ± hornblende ± muscovite trondhjemite, 5am, mylonitic tonalite with biotite clots ± hornblende.
b. Pistol Lake biotite granodiorite; medium to coarse grained, weakly foliated.
c. Fish-hook Lake biotite, muscovite, monzogranite; medium to coarse grained, weakly foliated.
d. granitic pegmatite, apatite, tourmaline, muscovite bearing. Most abundant near 5c.

Yellowknife Supergroup

Unit 4 metasedimentary rocks (east), metagreywacke, thin to medium bedded cordierite ± andalusite ± fibrolite schist; quartz stringers common.
a. iron formation; thin (<50 cm), discontinuous, sulphidic.
b. phyllite; very fine grained medium to pale grey colour.

Unit 3 intercalated sequence (not necessarily in stratigraphic order)
a. andalusite ± cordierite , feldspathic, biotite arenite; cross-bedded with fine planar laminations.
b. metagabbro to diorite; discrete lenses or sheets paralleling stratigraphy.
c. metapyroxenite; massive, mafic rock with amphibole phenocrysts pseudomorphed after pyroxene in a fine grained amphibole-rich matrix.
d. mafic tuff (banded amphibolite); graded layering defined by coarseness of amphiboles (metamorphic reverse grading); contains minor feldspar.
e. tuffaceous sediment (banded amphibolite); banding defined by biotite laminations, epiclastic equivalent of Unit 3f.
f. gold host; part of sequence of Units 3d and e, sulphidic, amphibolitic, fine grained; labelled at main showing only.
g. local breccia or conglomerate within Unit 3a and between Unit 4 and 3e ± 3d and Unit 3e and 3b.

Unit 2 conglomerate (James Falls Conglomerate); polymict orthoconglomerate, locally paraconglomerate, composed of rounded to well-rounded granule to boulder-sized clasts many of which are identical in character to the rocks in the area including diorite, iron formation and greywacke clasts; matrix similar in composition to Units 1 and 4.

Unit 1 andalusite ± cordierite ± sillimanite schist; thin to medium bedded metagreywacke mustone (west).
a. sulphidic iron formation.

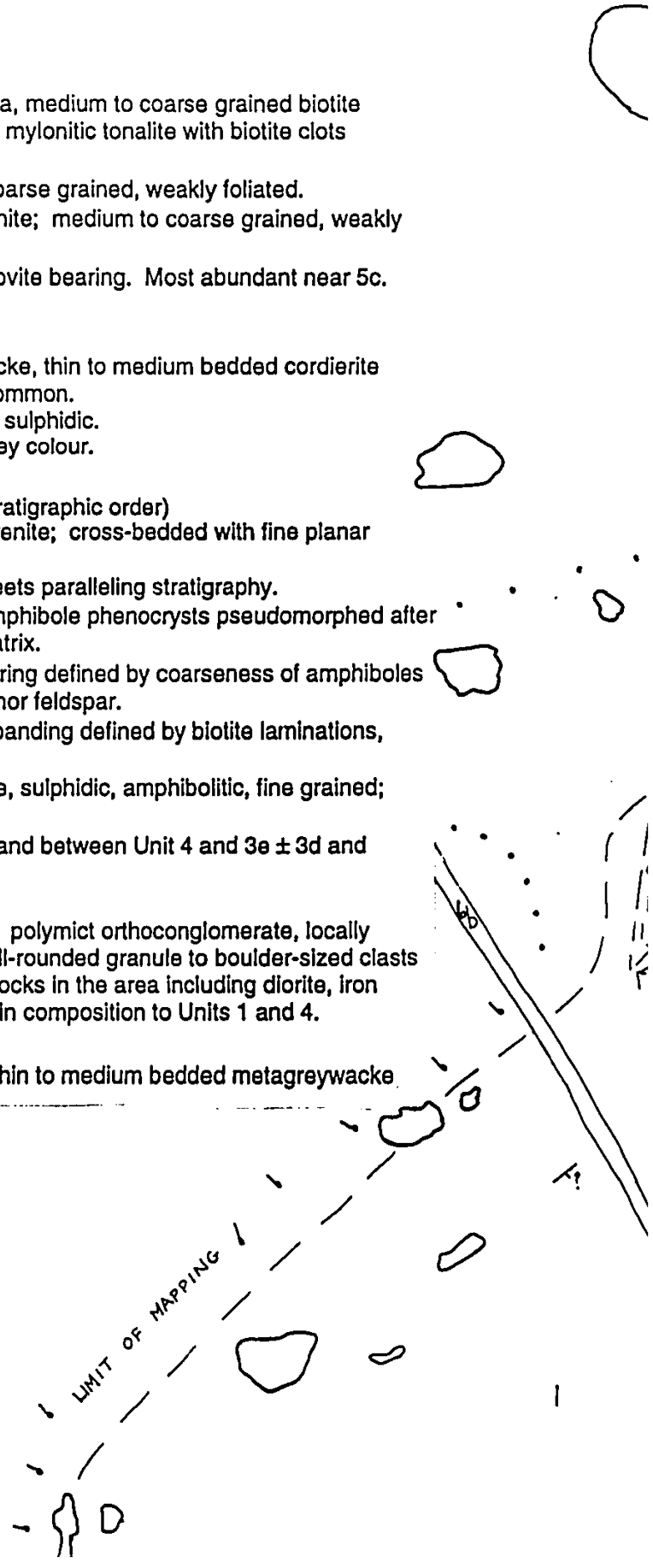


5c
6b
5a
5d
3a,5a

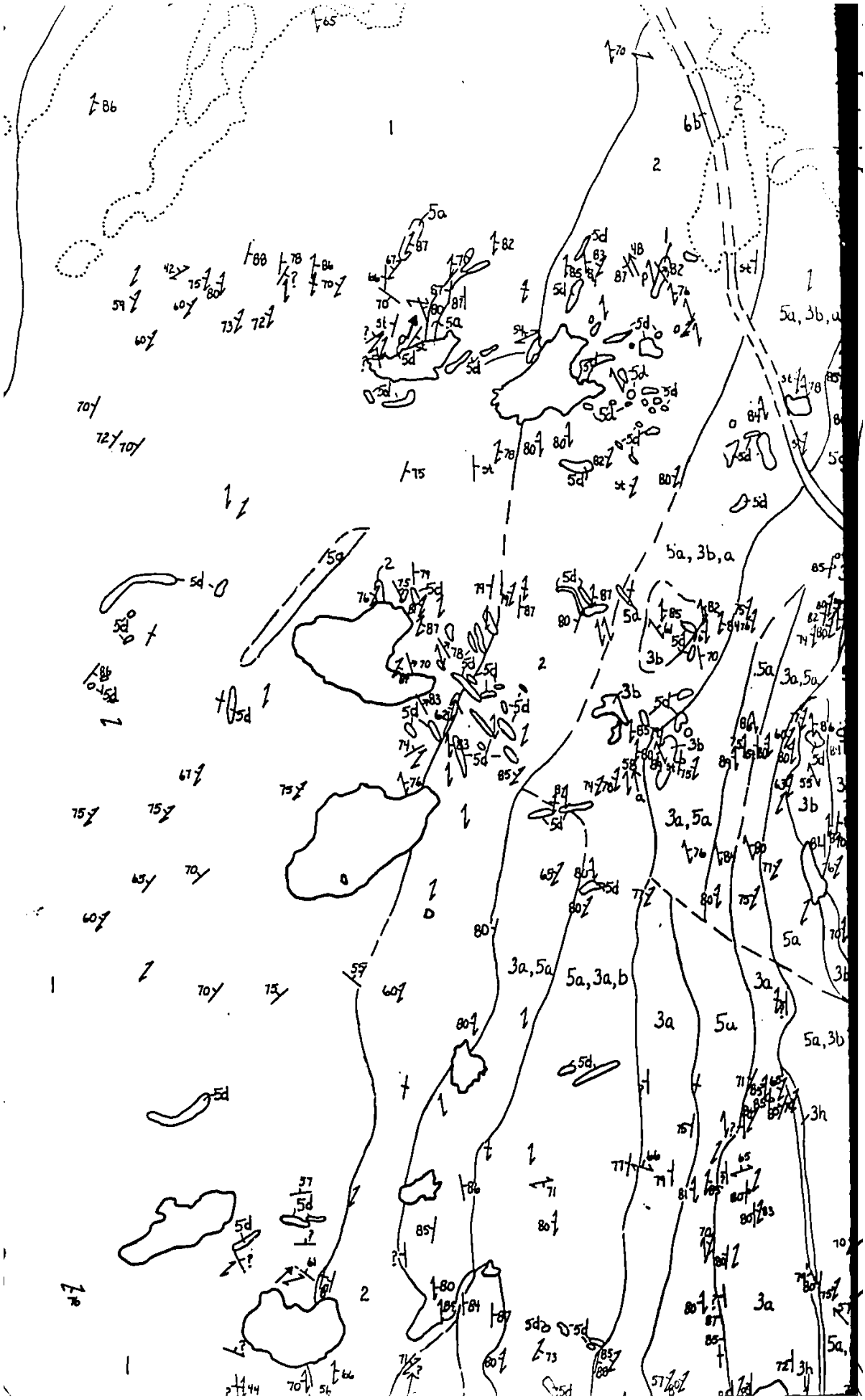
5a, 3b, a
3a, 5a
5a, 3a, b
3a
5a
3b
5d
1
2

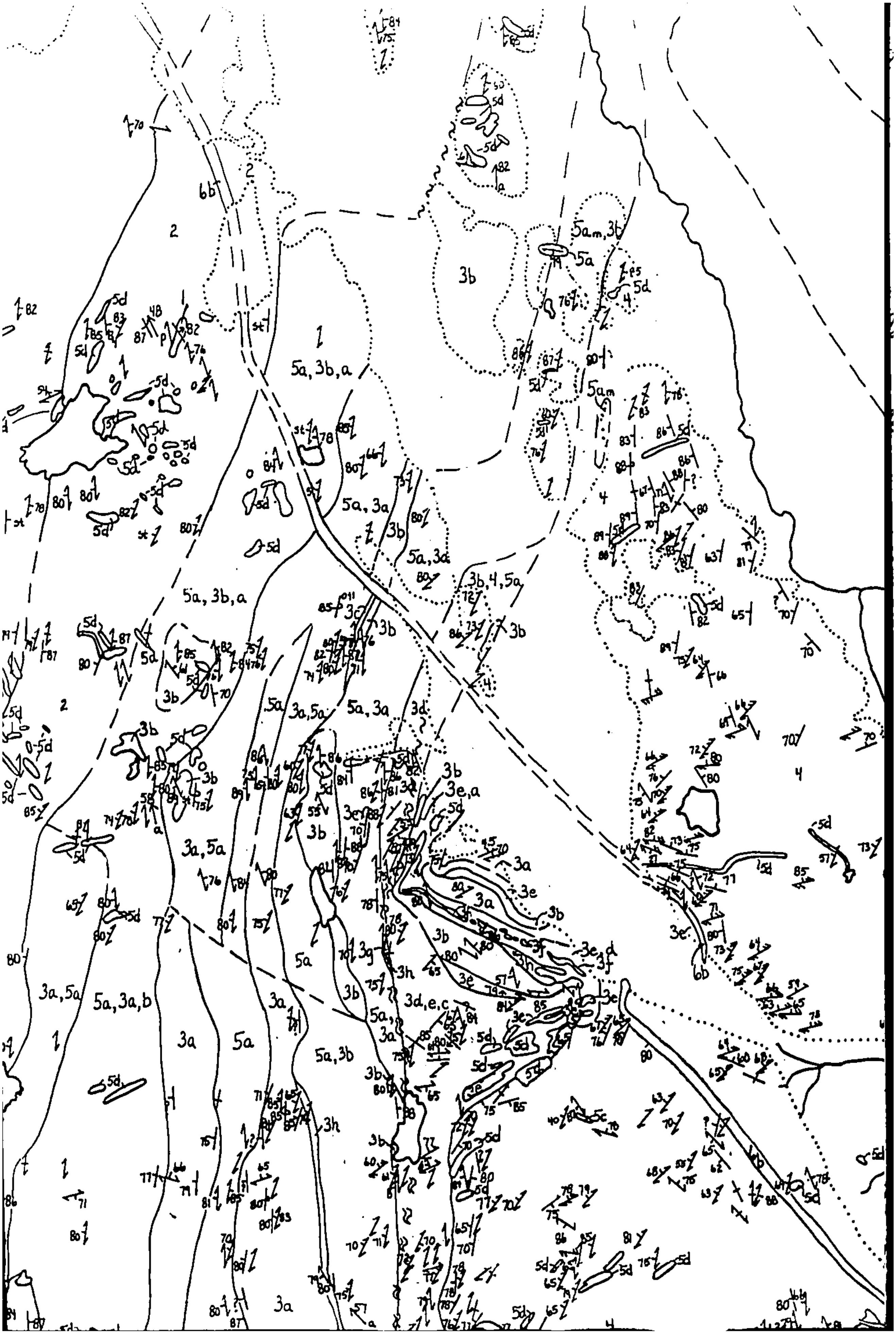
2
6b
5a,3b,a
3b
5am,3b
5a
5d
5am
4
5a,3a
3b
5a,3d
3b,4,5a
5a,3b,a
3c
3b
5a
3a,5a
5a,3a
3d
3b
3e,a
3a,5a
3b
3e
3a
3e
3b
3e,d
3f
3h
3g
3d,e,c
3a,5a
5a,3a,b
3a
5a
5a,3b
3e
6b
3h
3a
4

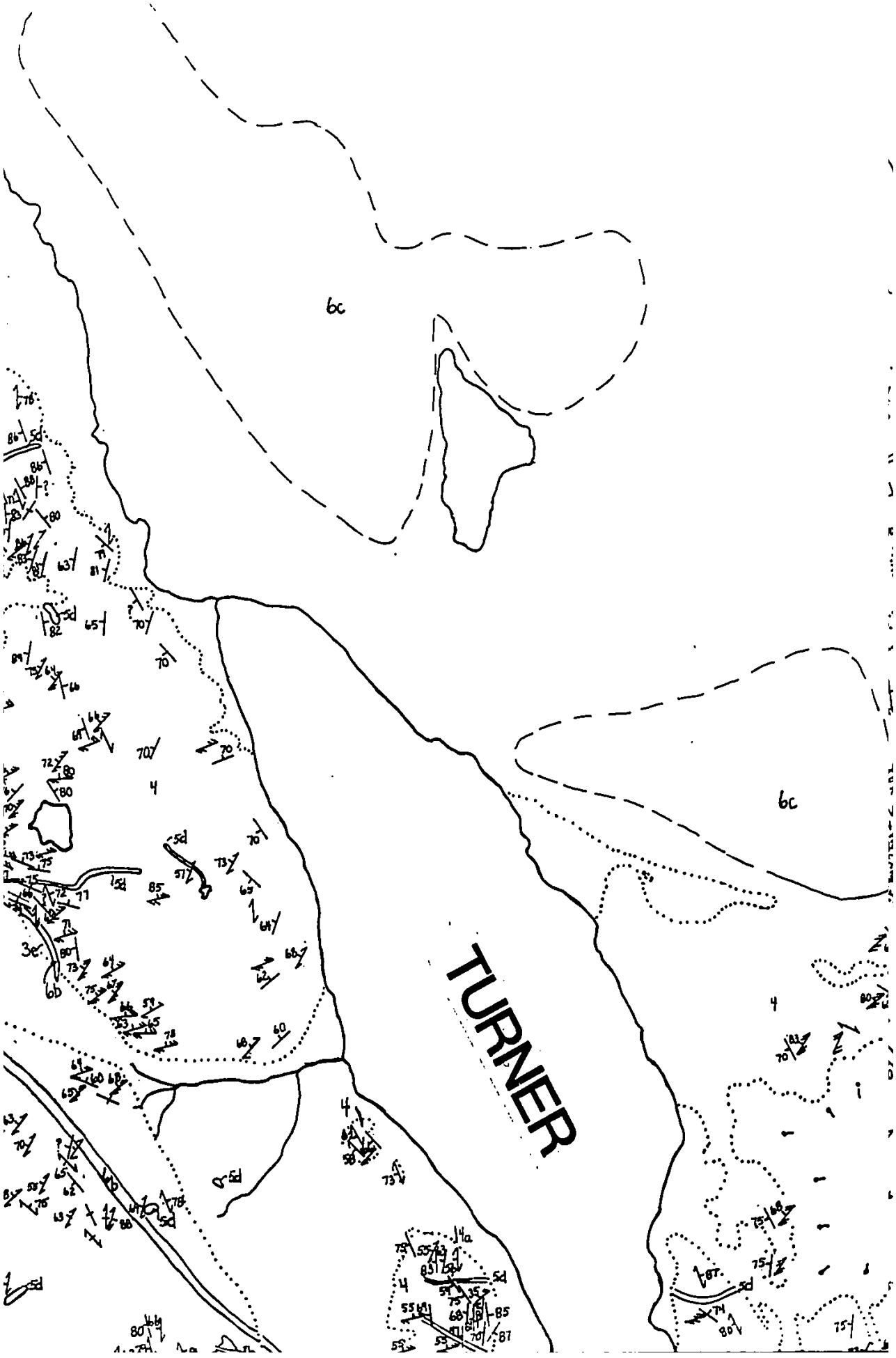
6c
6c
TURNER
4
4
4
3e
6b
5d
5d
5d
5d
5d
14a

6c
4
RNER

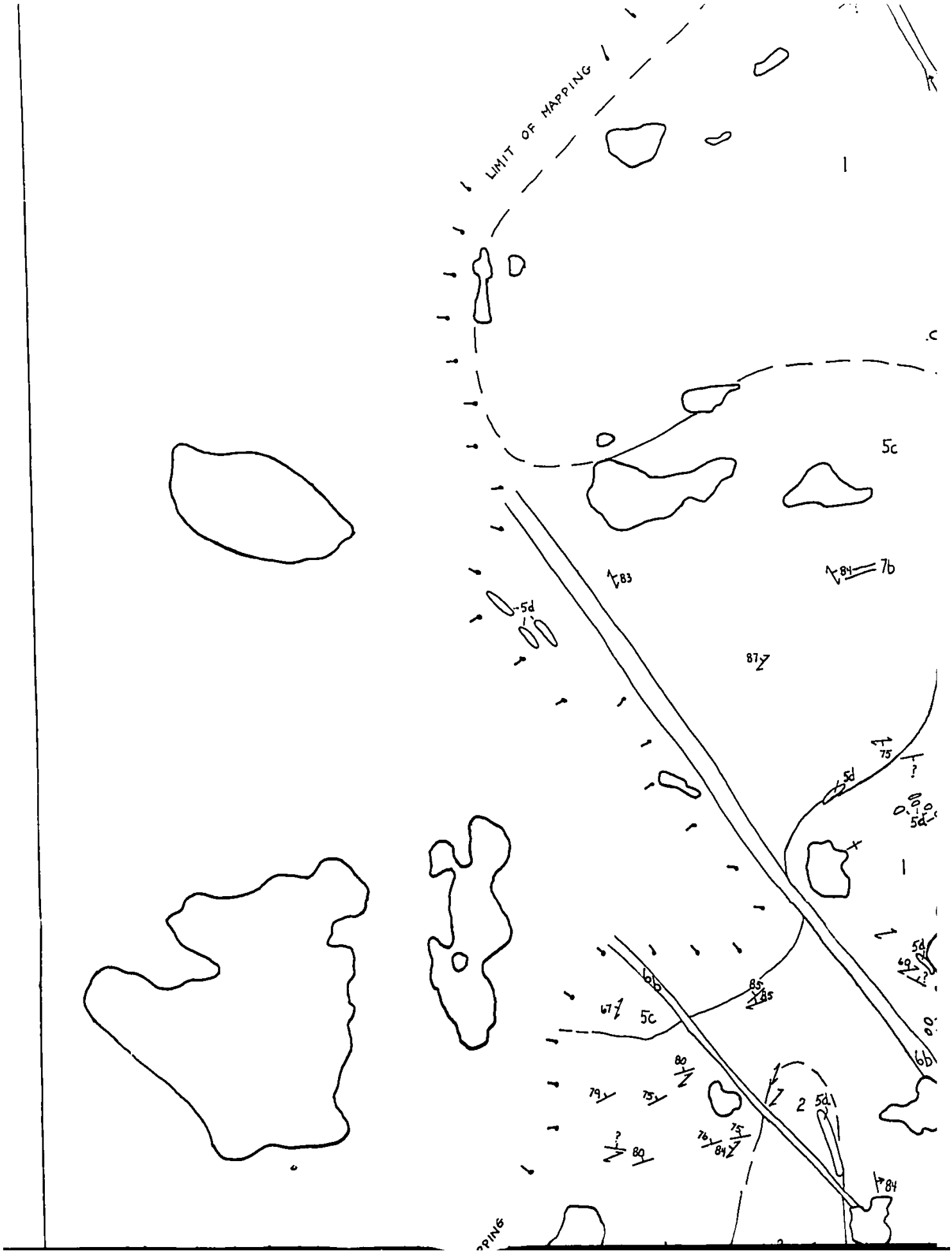
LIMIT OF MAPPING
5c
7b
5d
5d1
6b
5c
1
2


1
2
3a
3b
3a,b
5a,3a,b
5c
5d
6b
7b

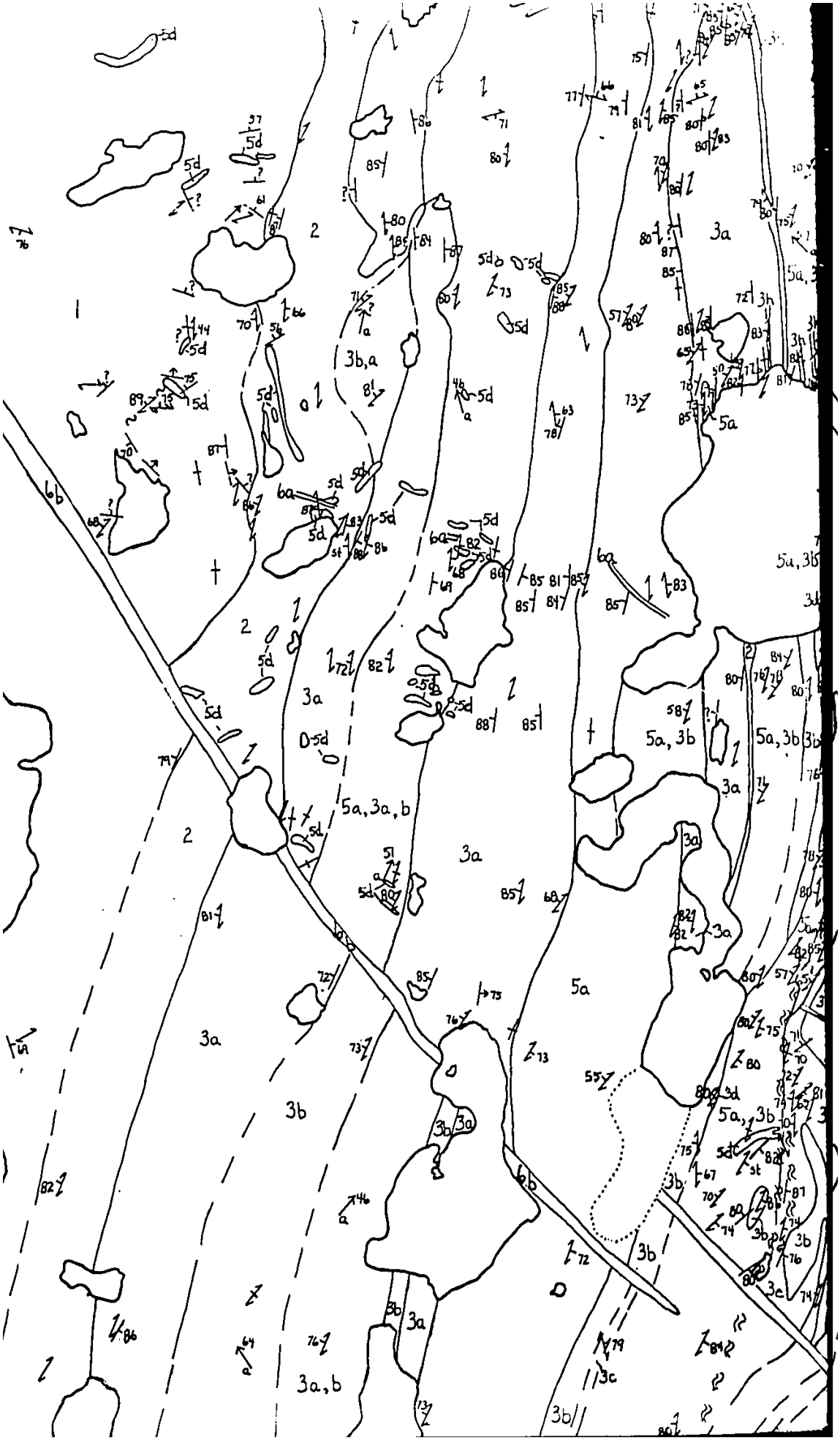
3a
3b
3b,a
5a
5a,3b
5a,3a,b
3a,b
3b1
3c
6b
6a
5d

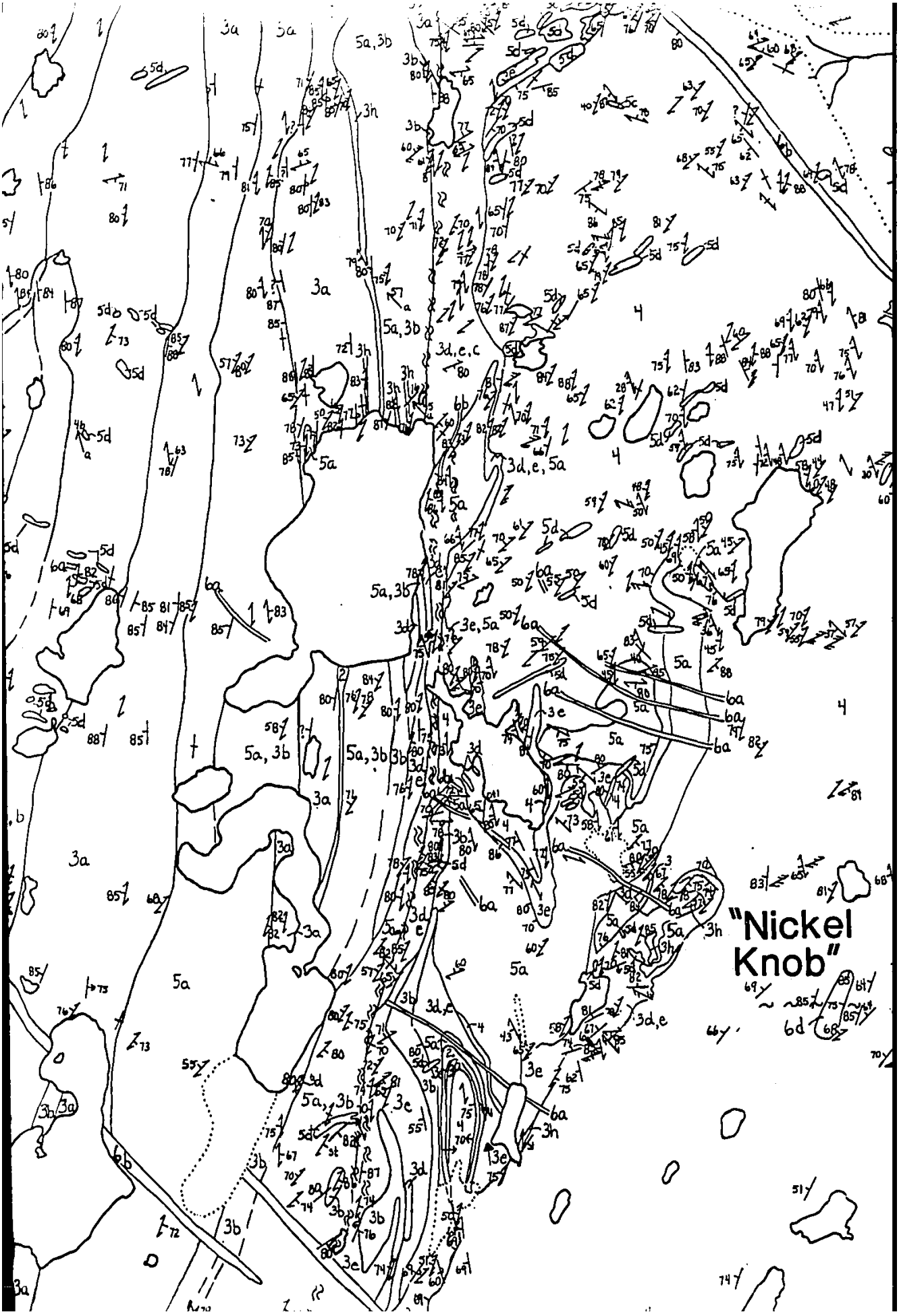
"Nickel Knob"

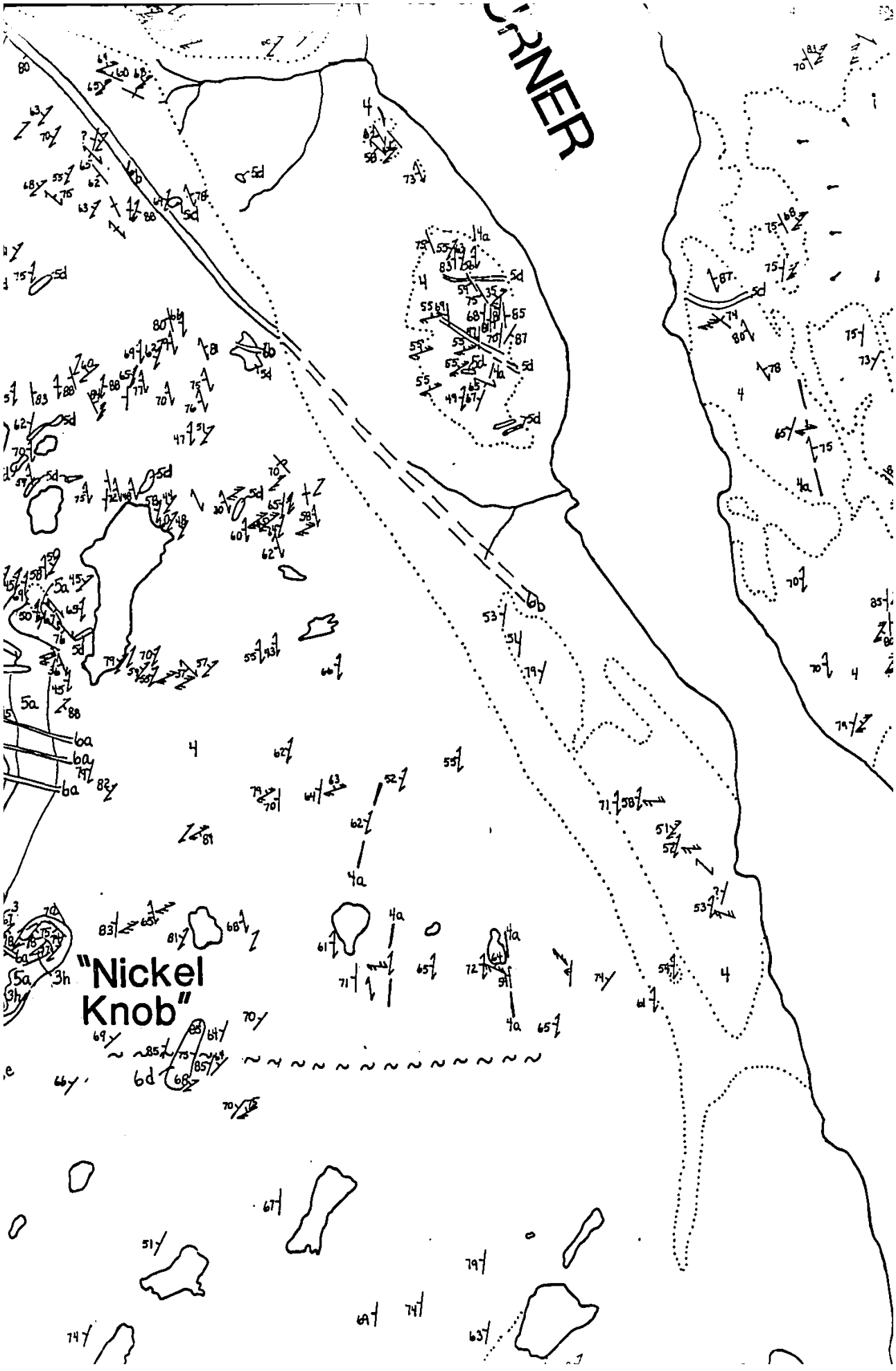
"Nickel Knob"

ER
LAKE
5d
5a
4a
4

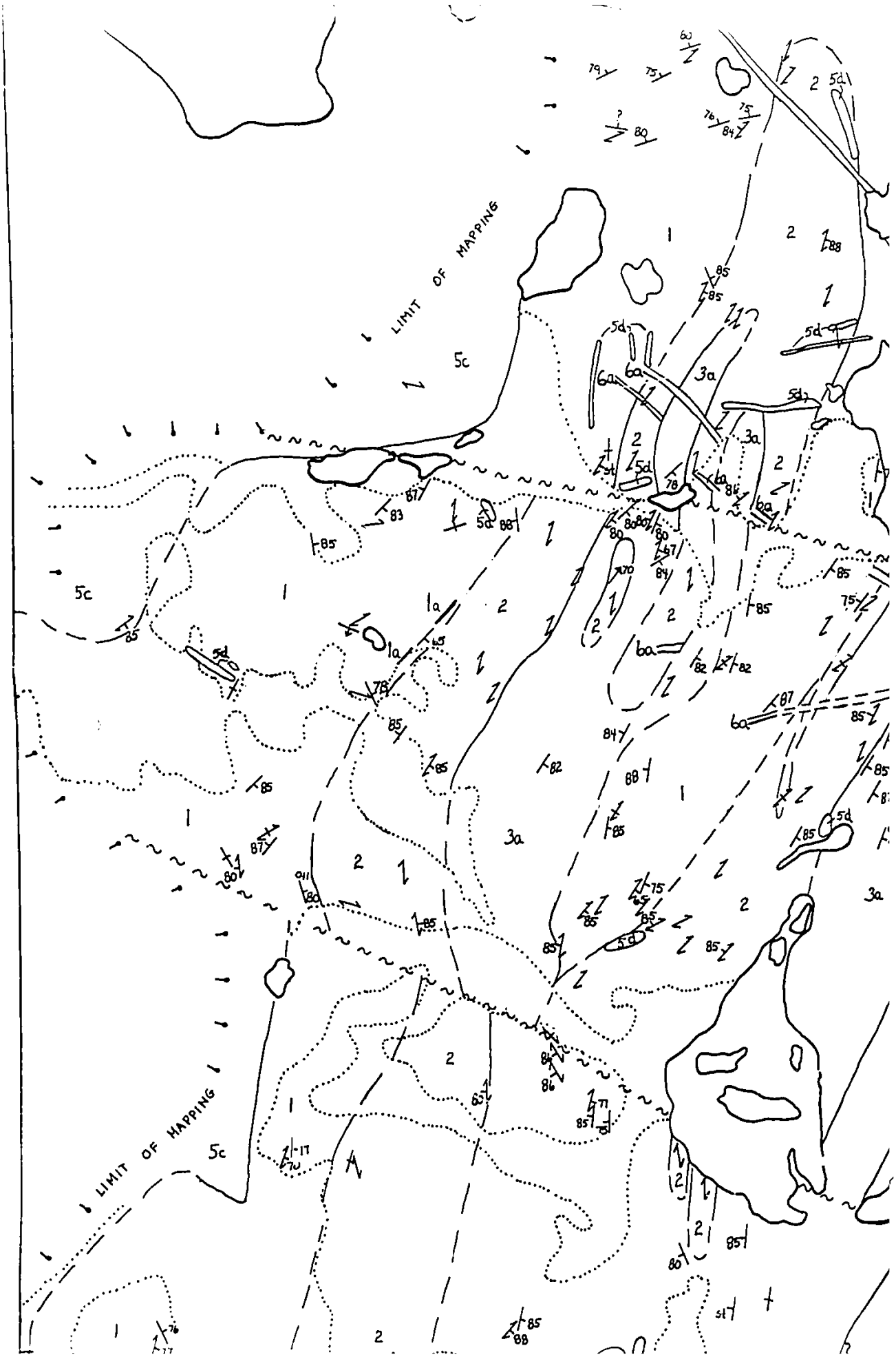
LIMIT OF MAPPING
LIMIT OF MAPPING
5c
5c
5c
1
2
3a
5d
6a
1a

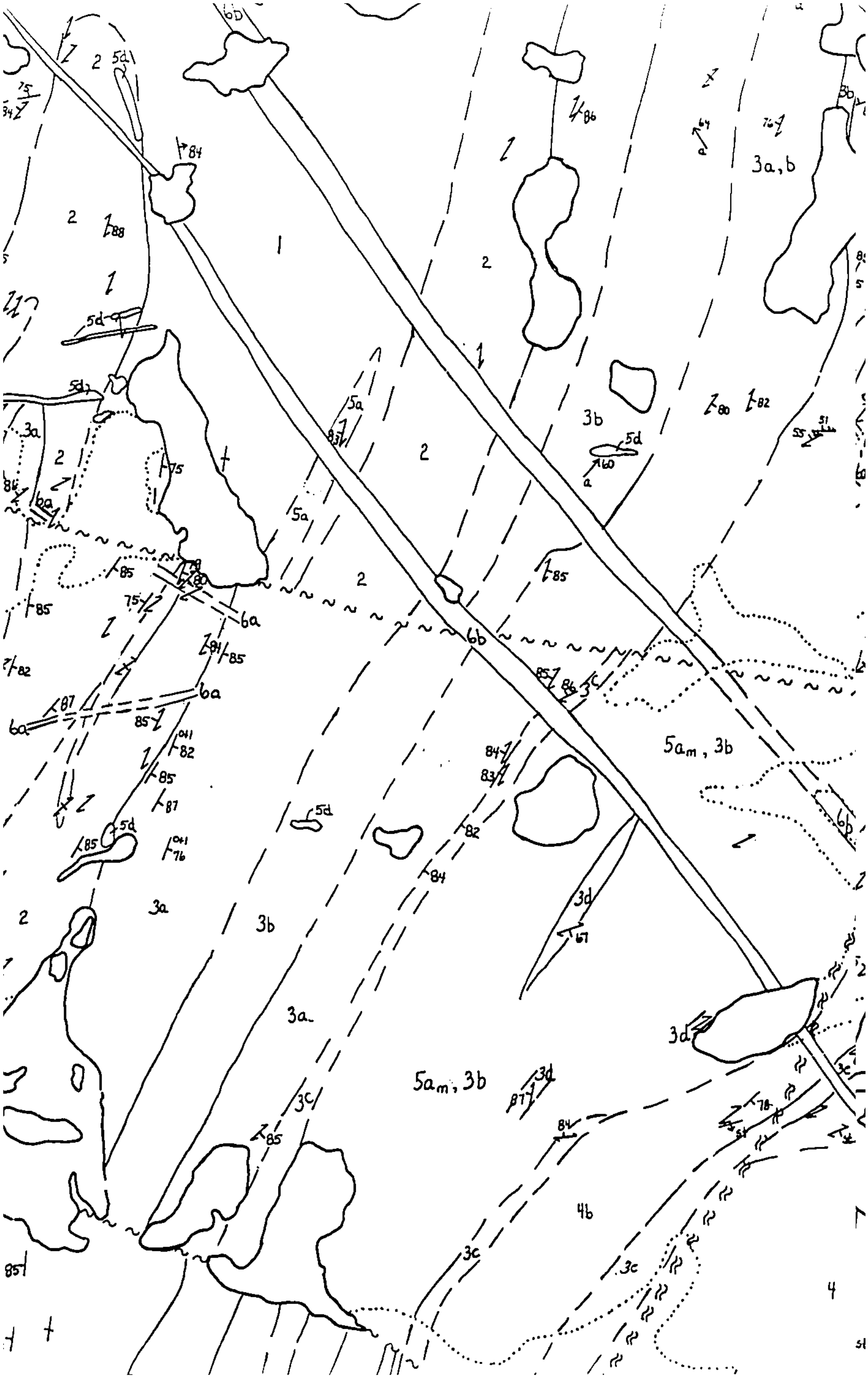

6b
2
5d
3a, b
2
1
2
5d
5a
2
3b
5d
3a
5a
2
6a
6b
6a
6a
3c
5am, 3b
5d
5d
6b
3d
2
3a
3b
3a
3d
5am, 3b
3d
3c
4b
3c
3c
4

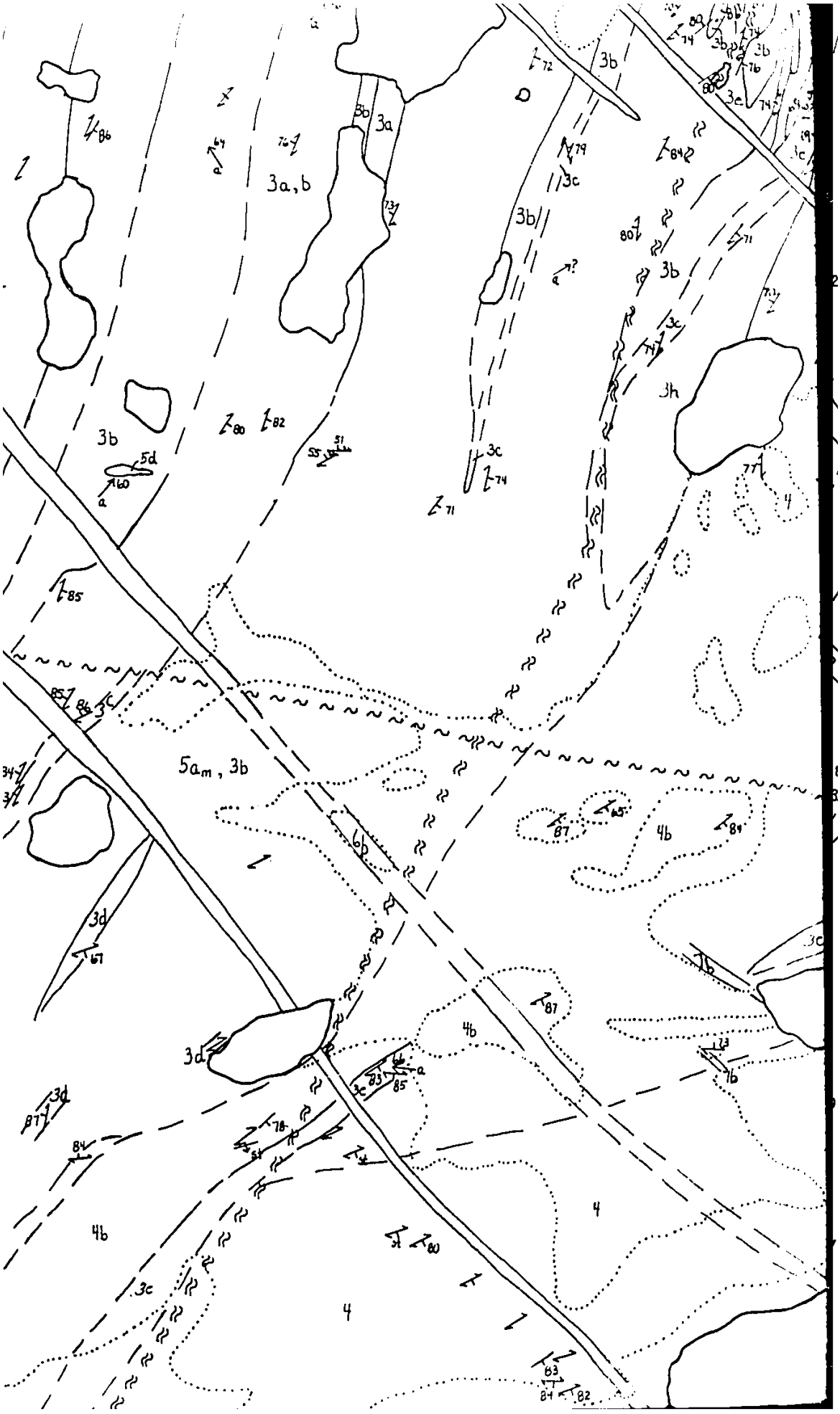
3a,b
3a
3b
3c
3d
3h
5d
5am, 3b
6b
4
4b

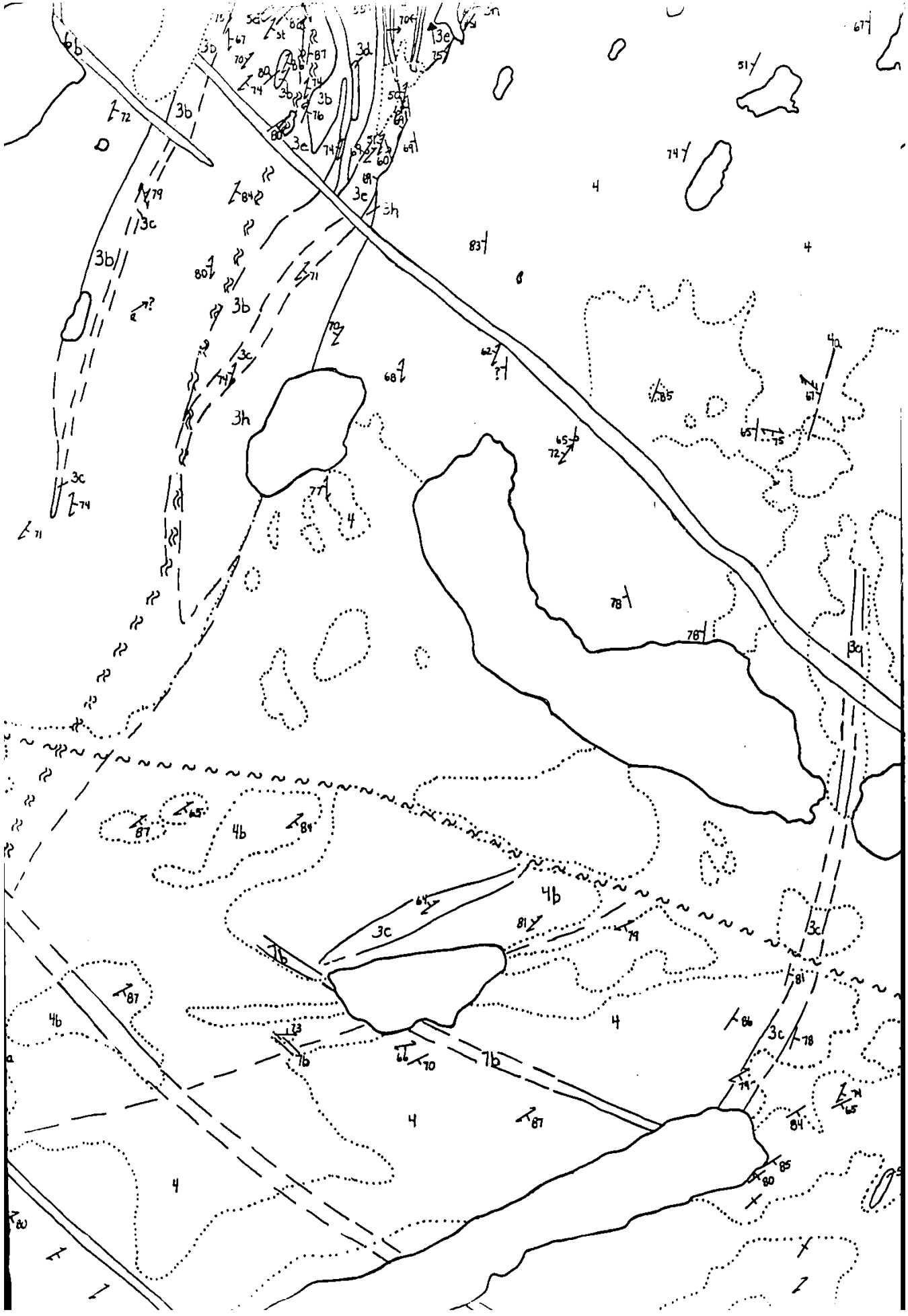
3b
3c
3d
3e
3h
4
4b
7b

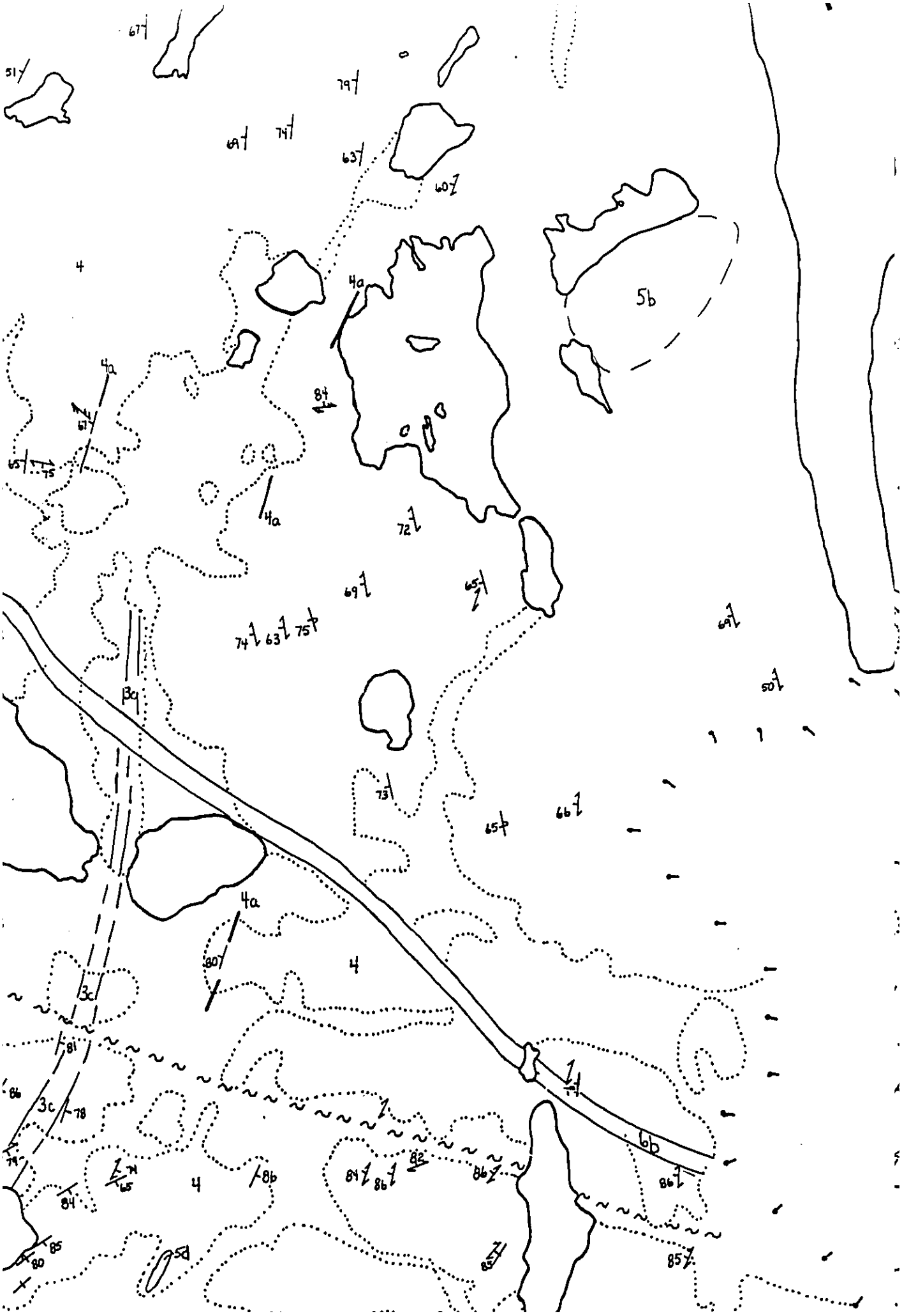
4
4a
5b
3a
3c
6b
8b

5b
6b

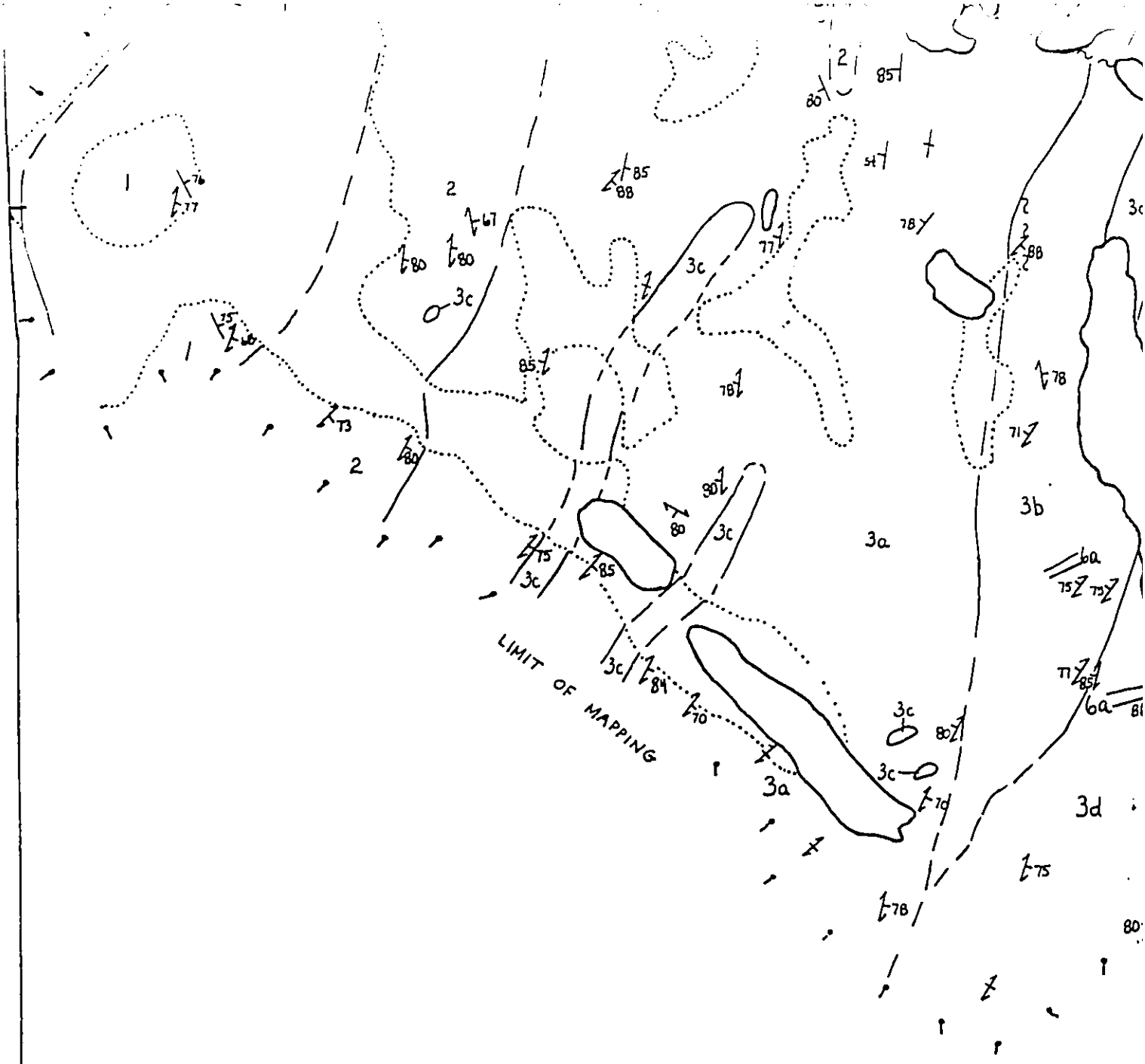
1
2
3c
3a
3b
3d
6a
LIMIT OF MAPPING

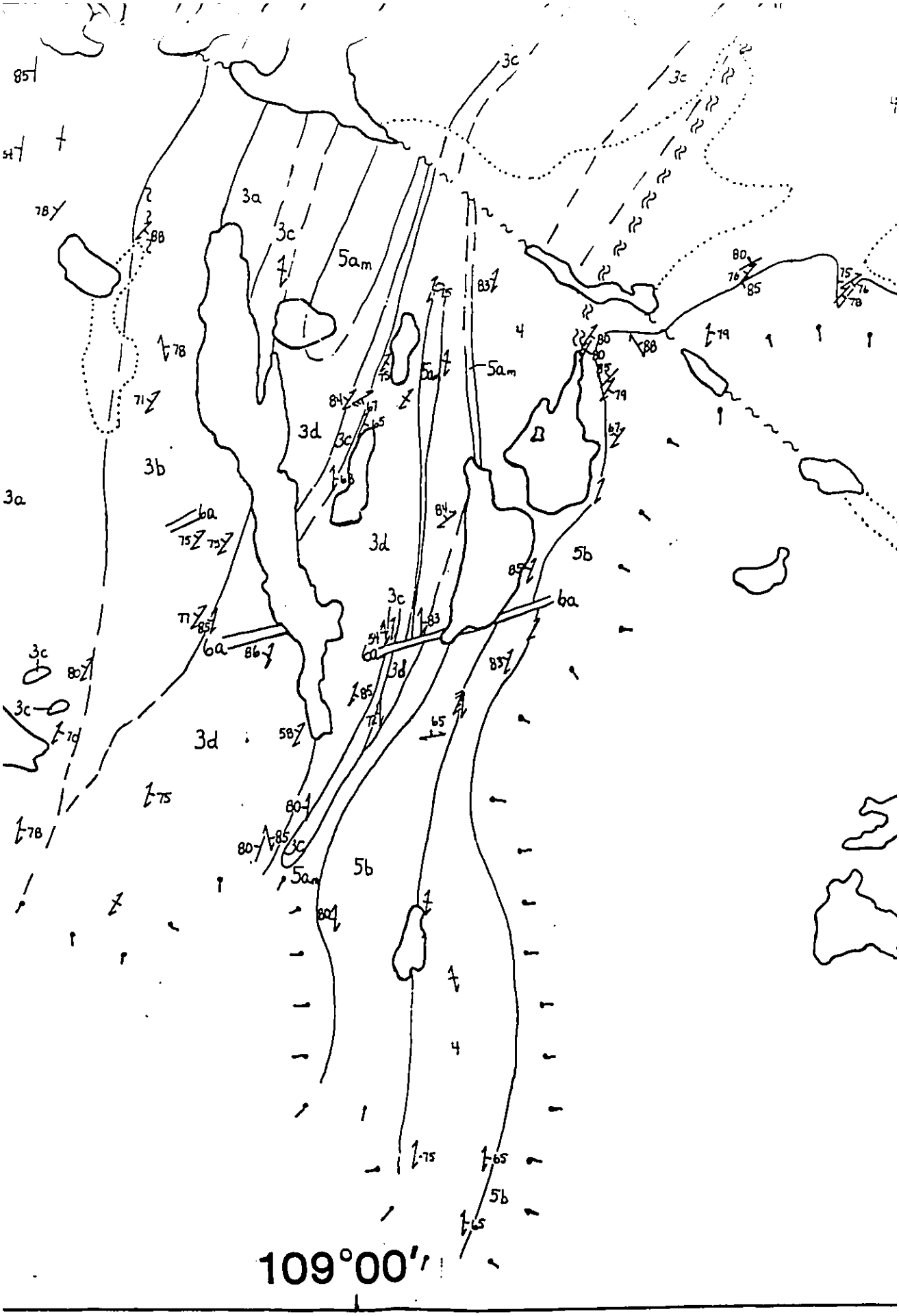
3a
3b
3c
3d
5am
5b
6a
109°00'


250 0 250 50
1 : 10,000

250 0 250 500 750 METRES

1 : 10,000

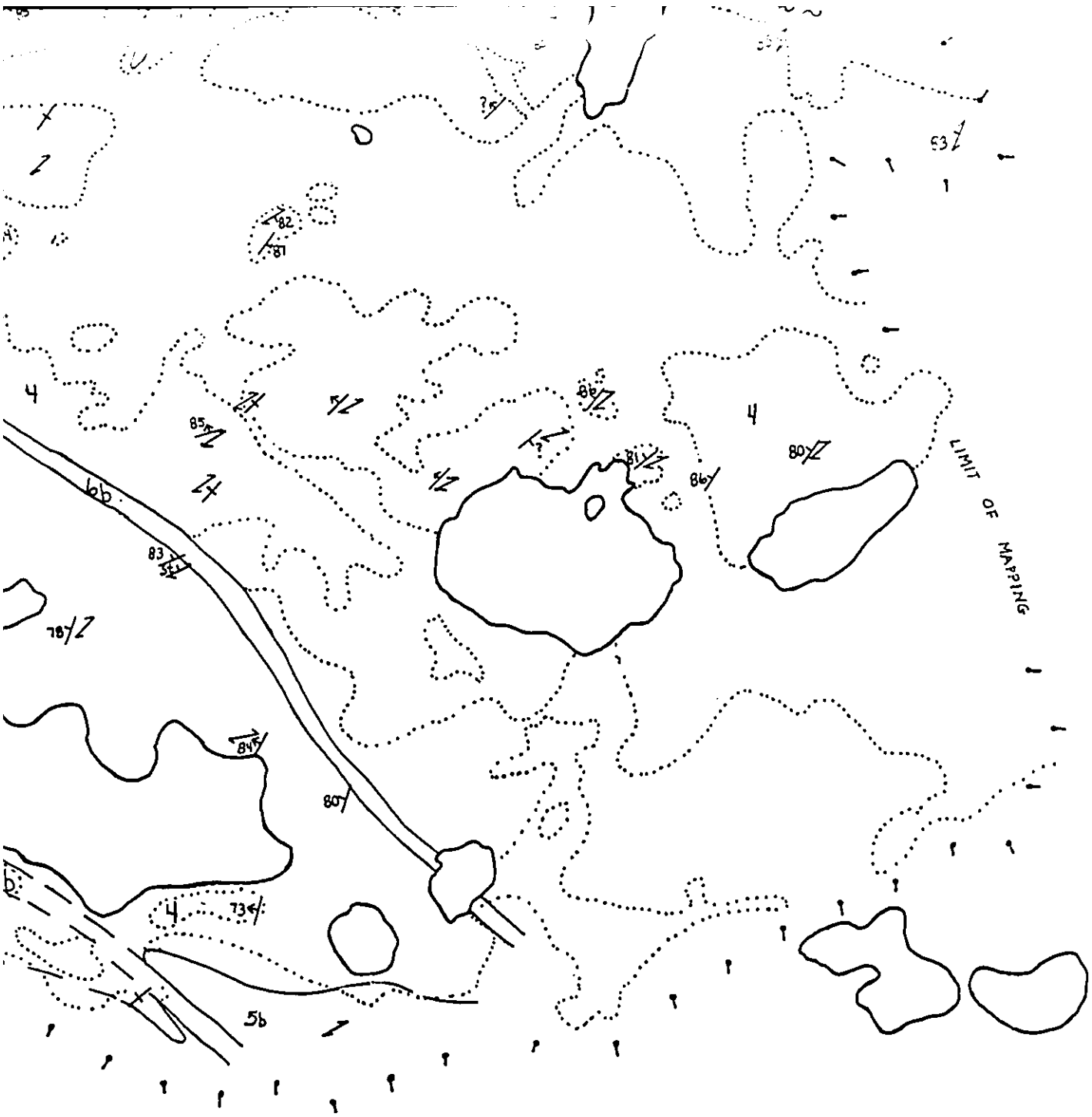

6

NWT GEOLOGY DIVISION -
Box 1500 - Yellowknif

Indian and Northern Affaire
Affairs Canada et du I

108°55'

COMPILED BY S. SCHAAN,

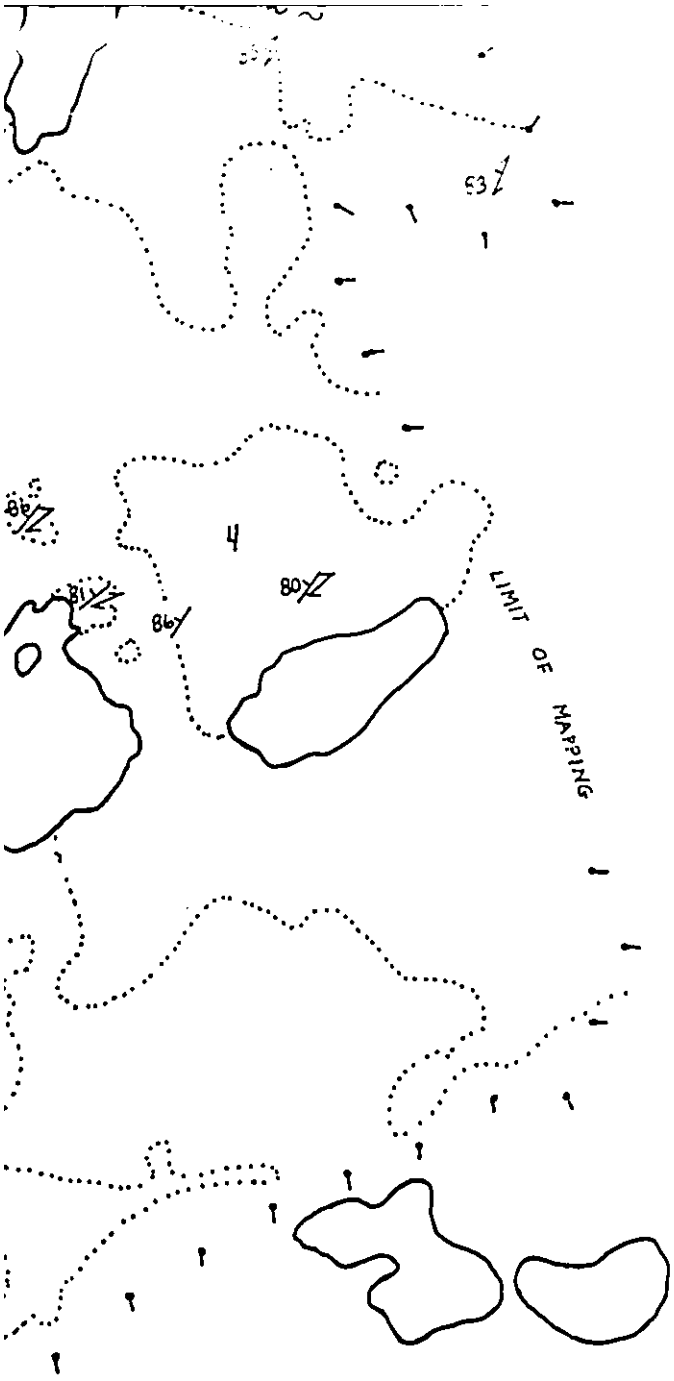

NWT GEOLOGY DIVISION – NAP
Box 1500 – Yellowknife

Indian and Northern Affairs Canada
Affaires indiennes et du Nord Canada

COMPILED BY S. SCHAAN, 1992

Map 2a. Sample location
Sample number

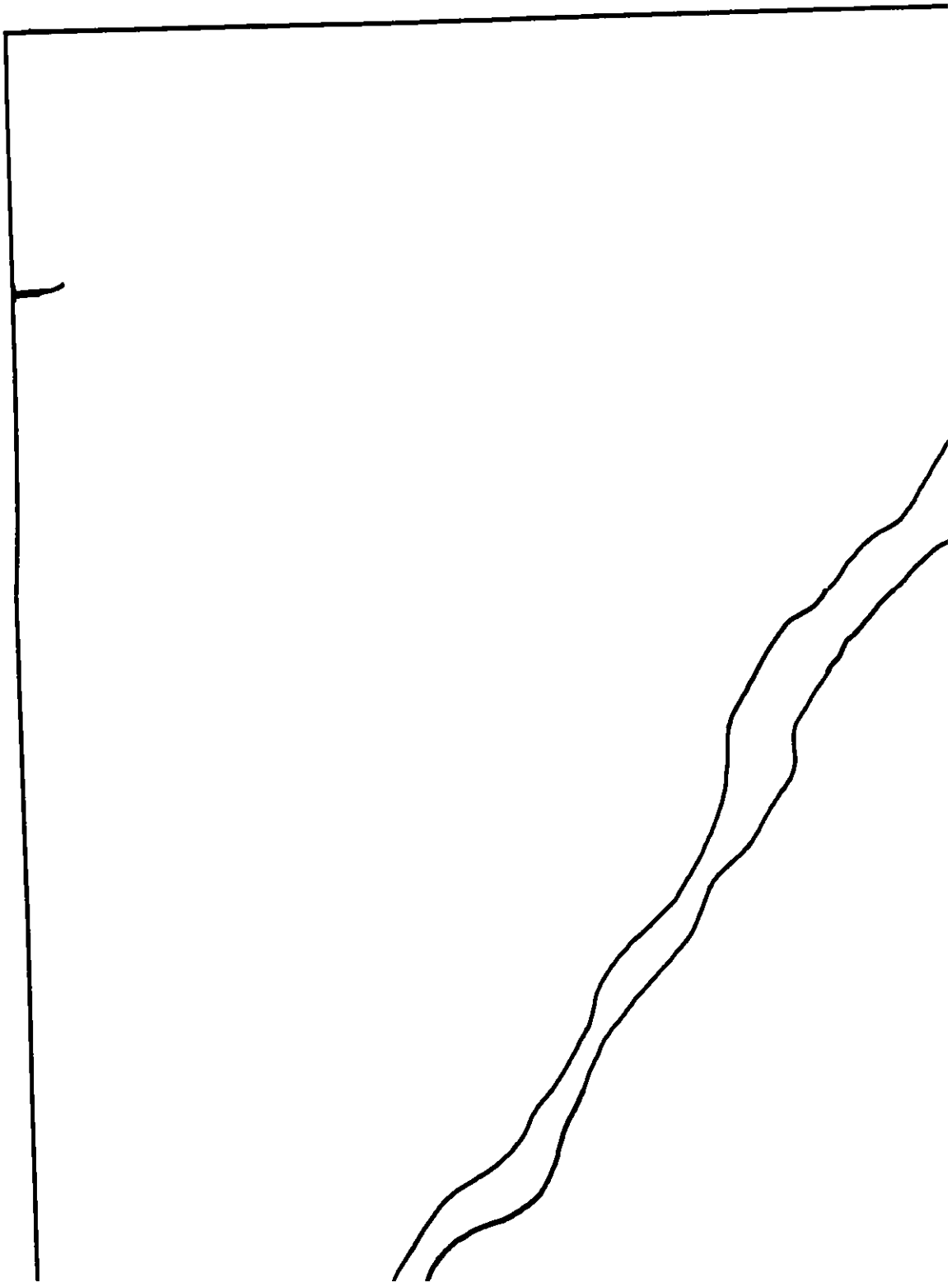

cation map for the Turner Lake are
umber is given followed by unit num

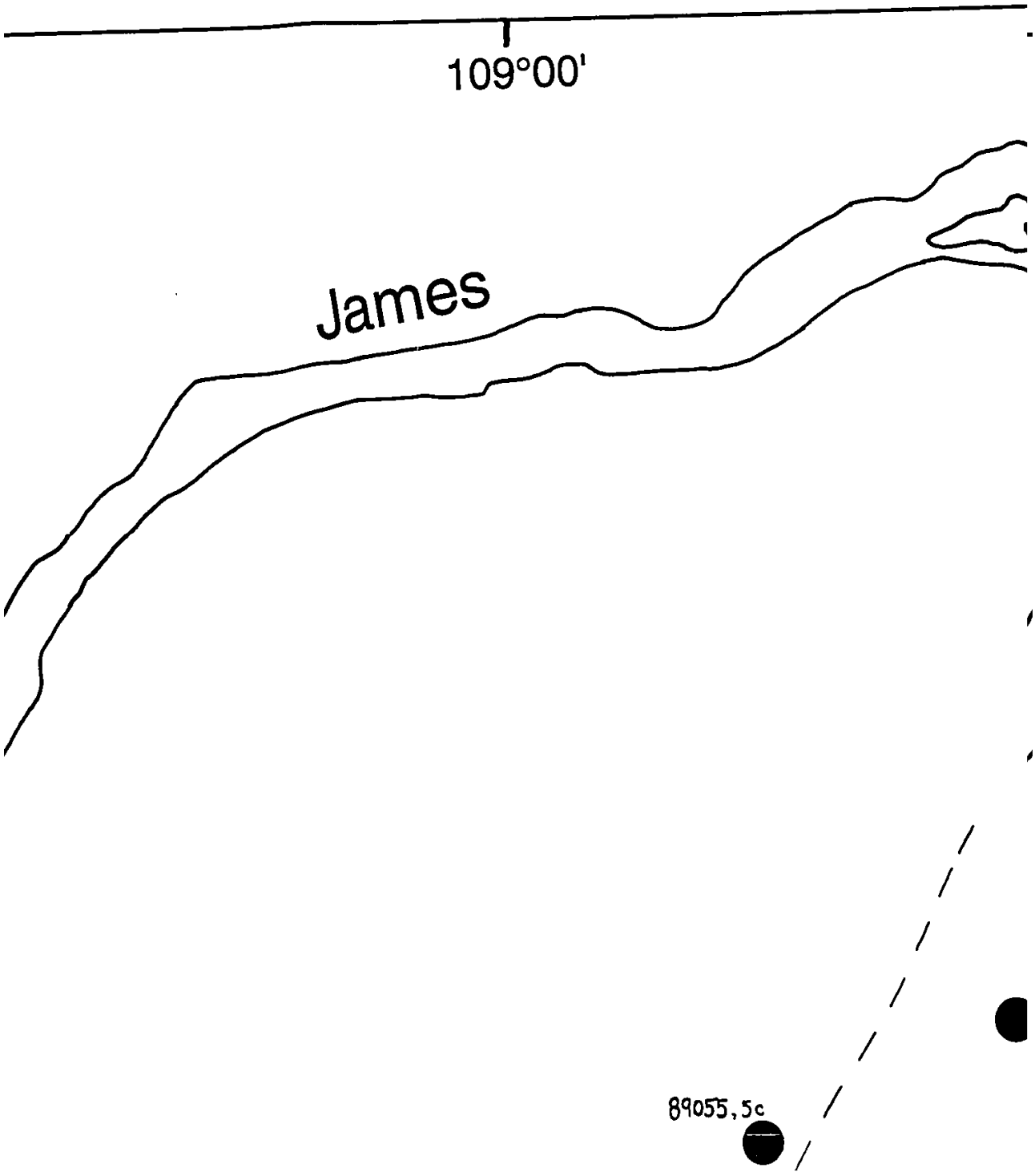

the Turner Lake area. Outline
followed by unit number sample

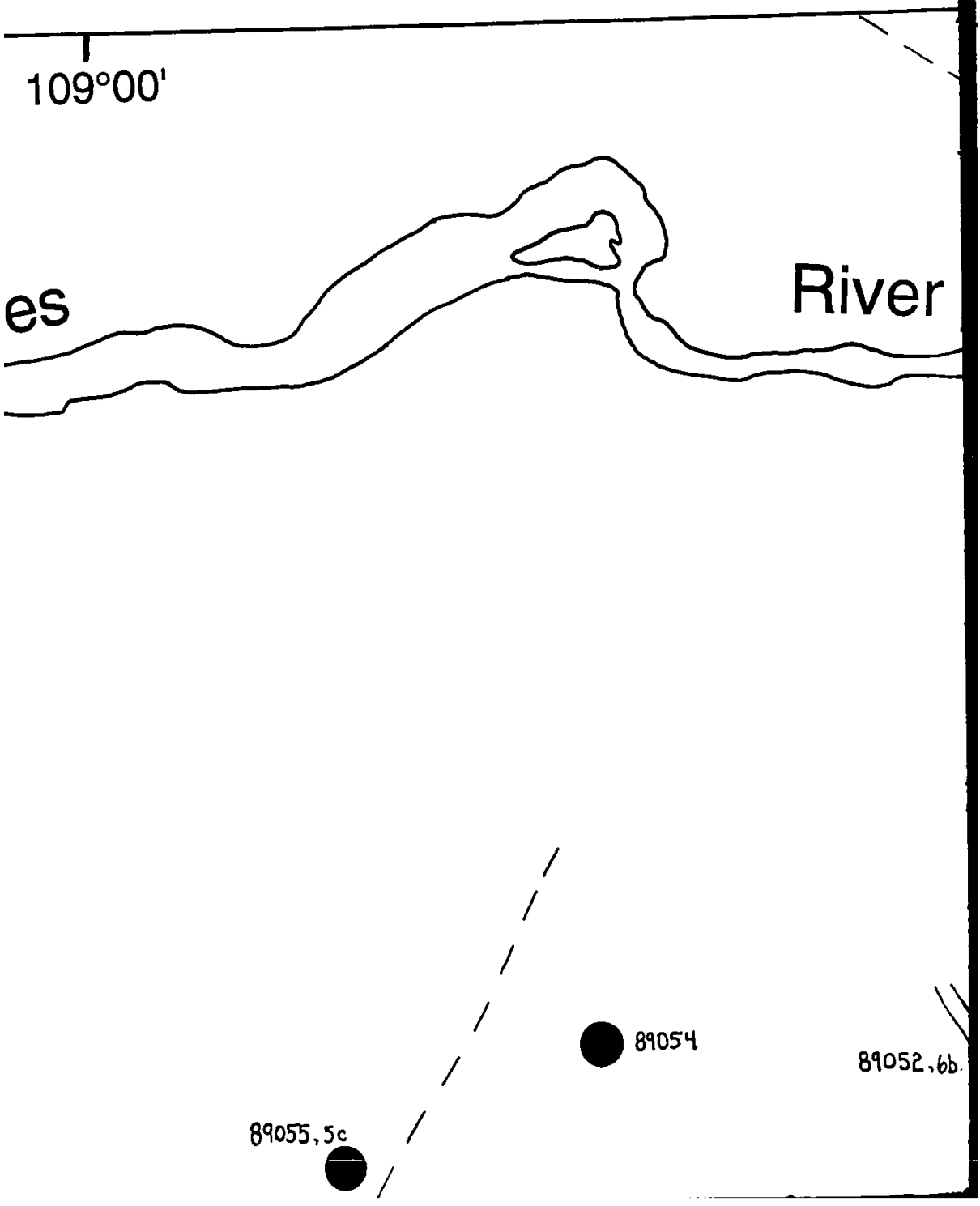

ea. Outline of map 2b is indicated.
mber sampled.

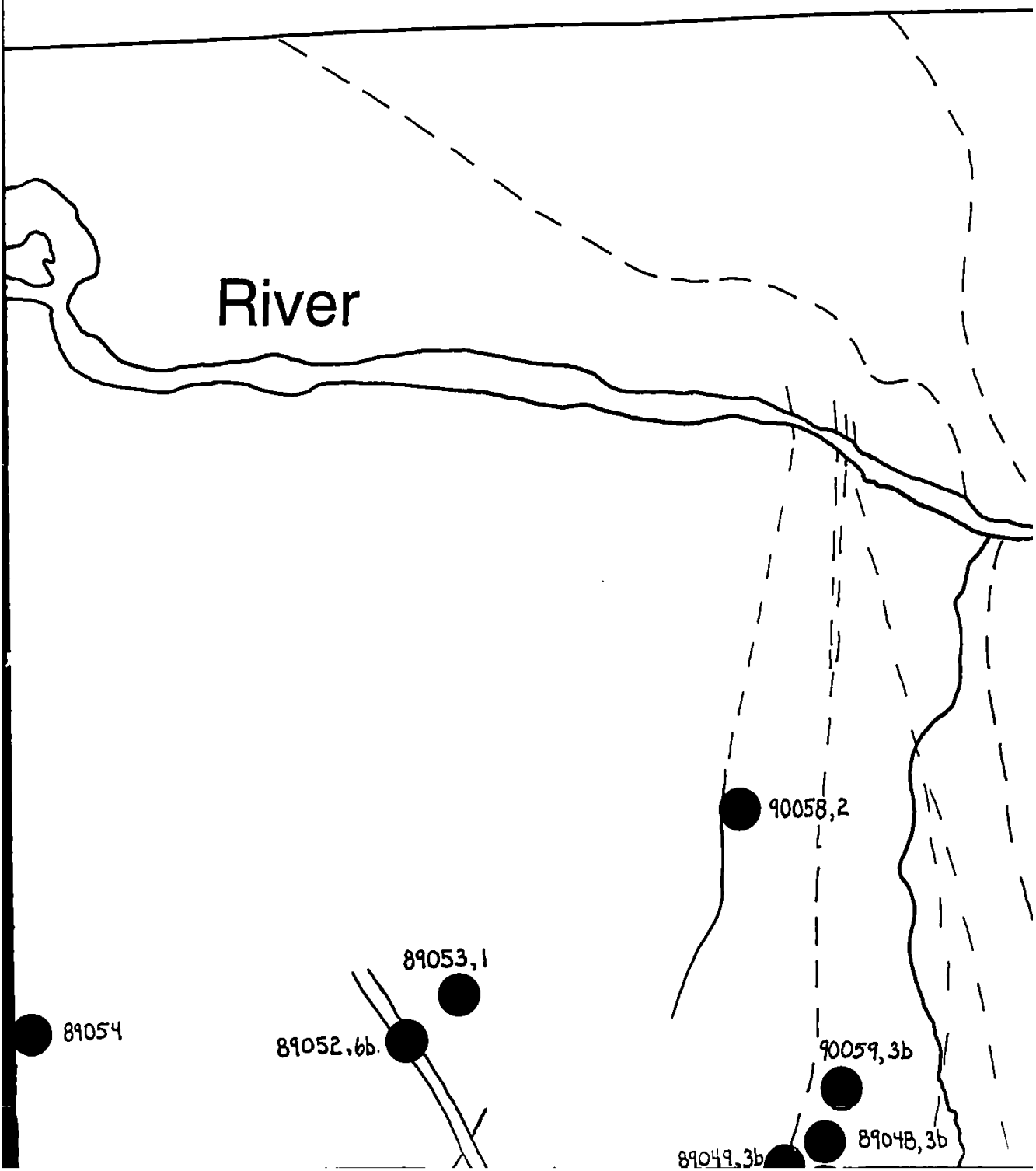

ndicated.

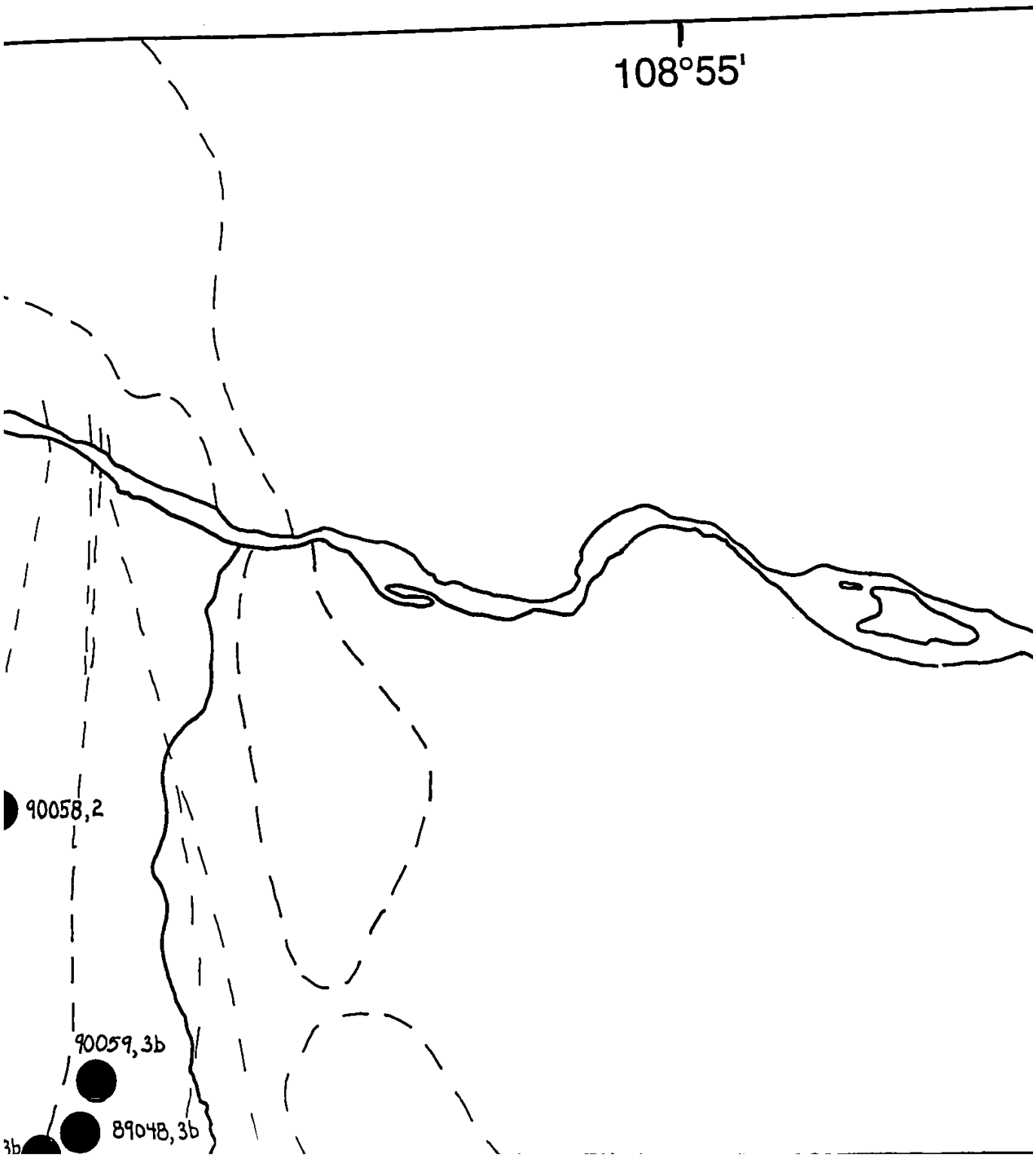

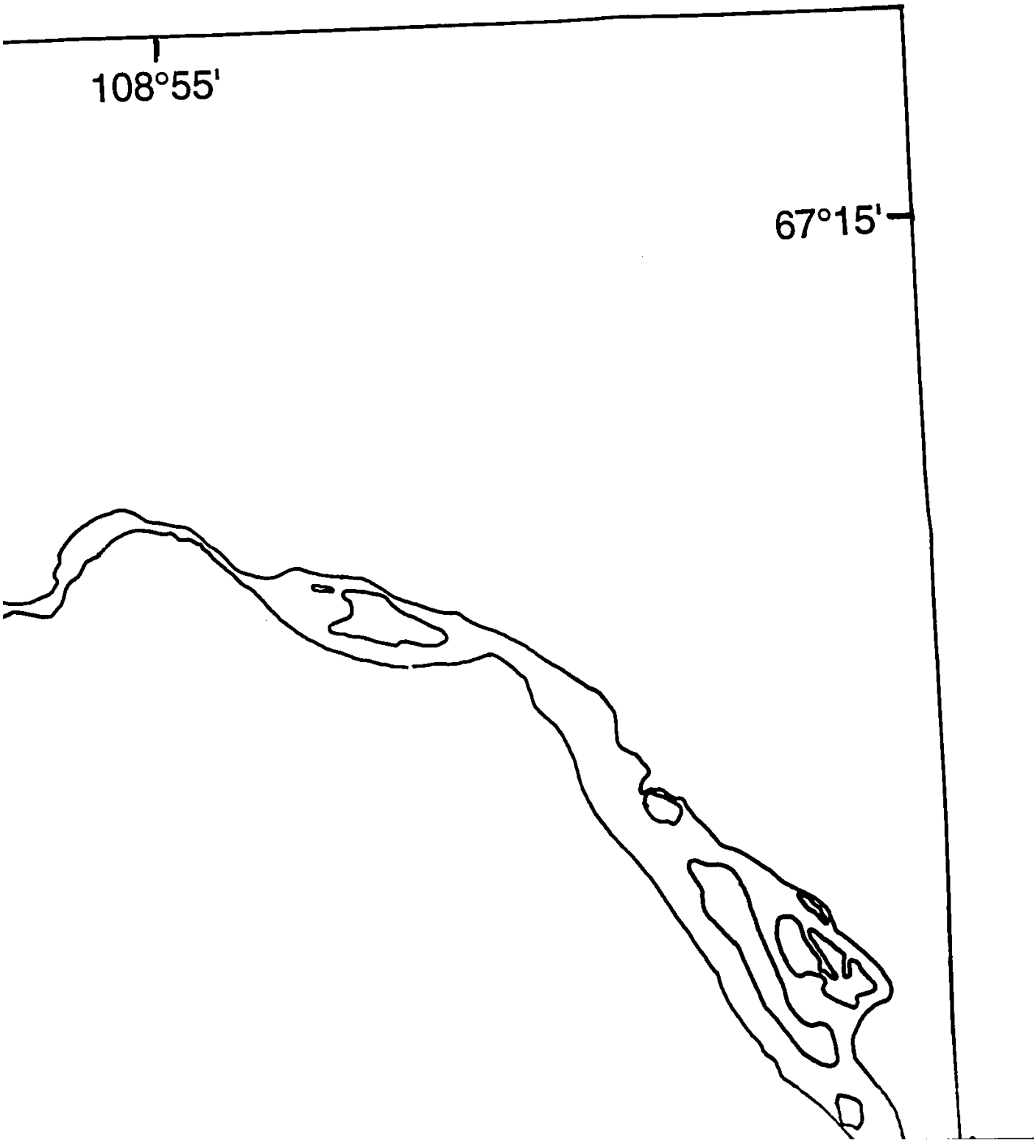
108°55'
67°15'

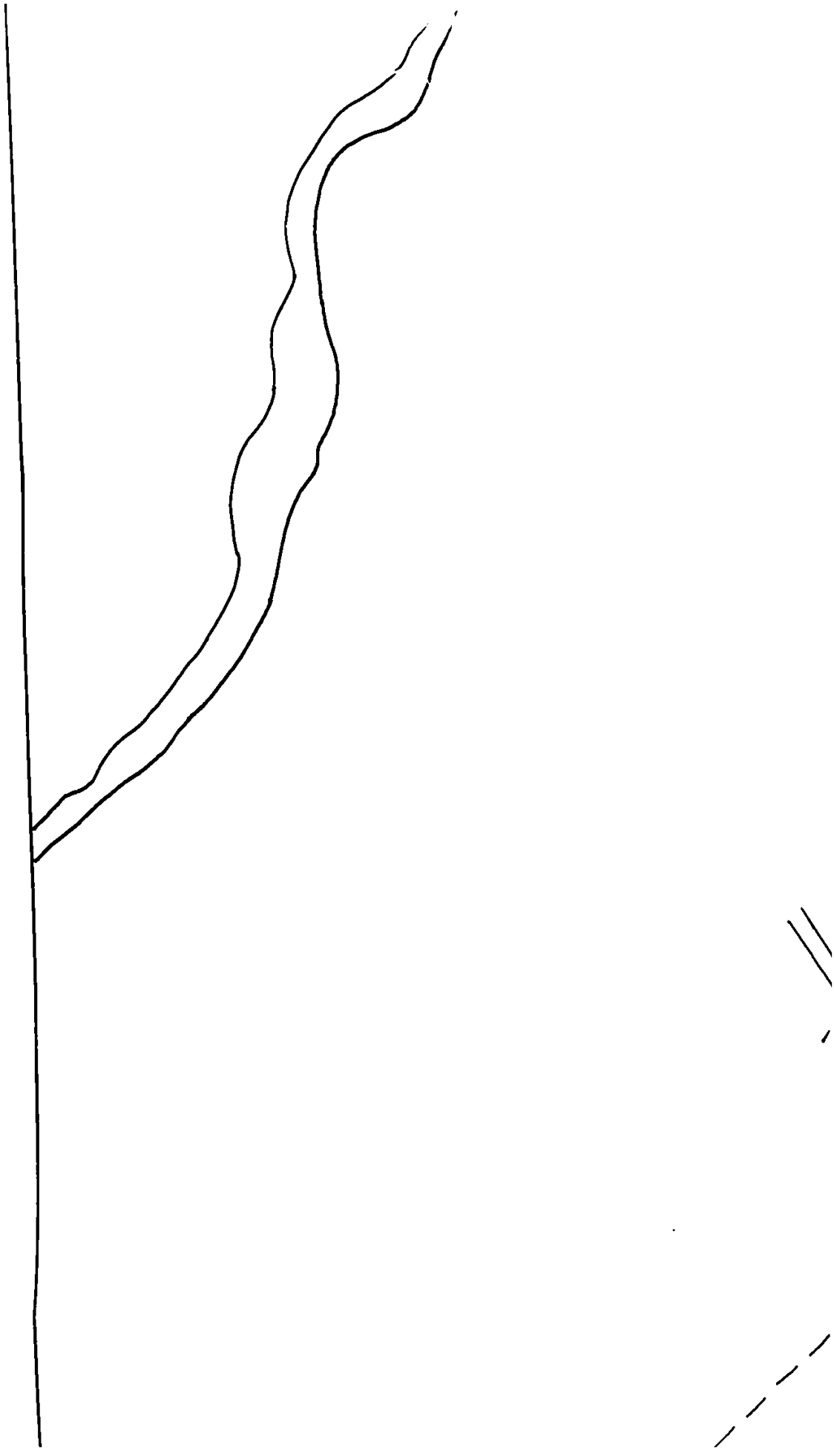

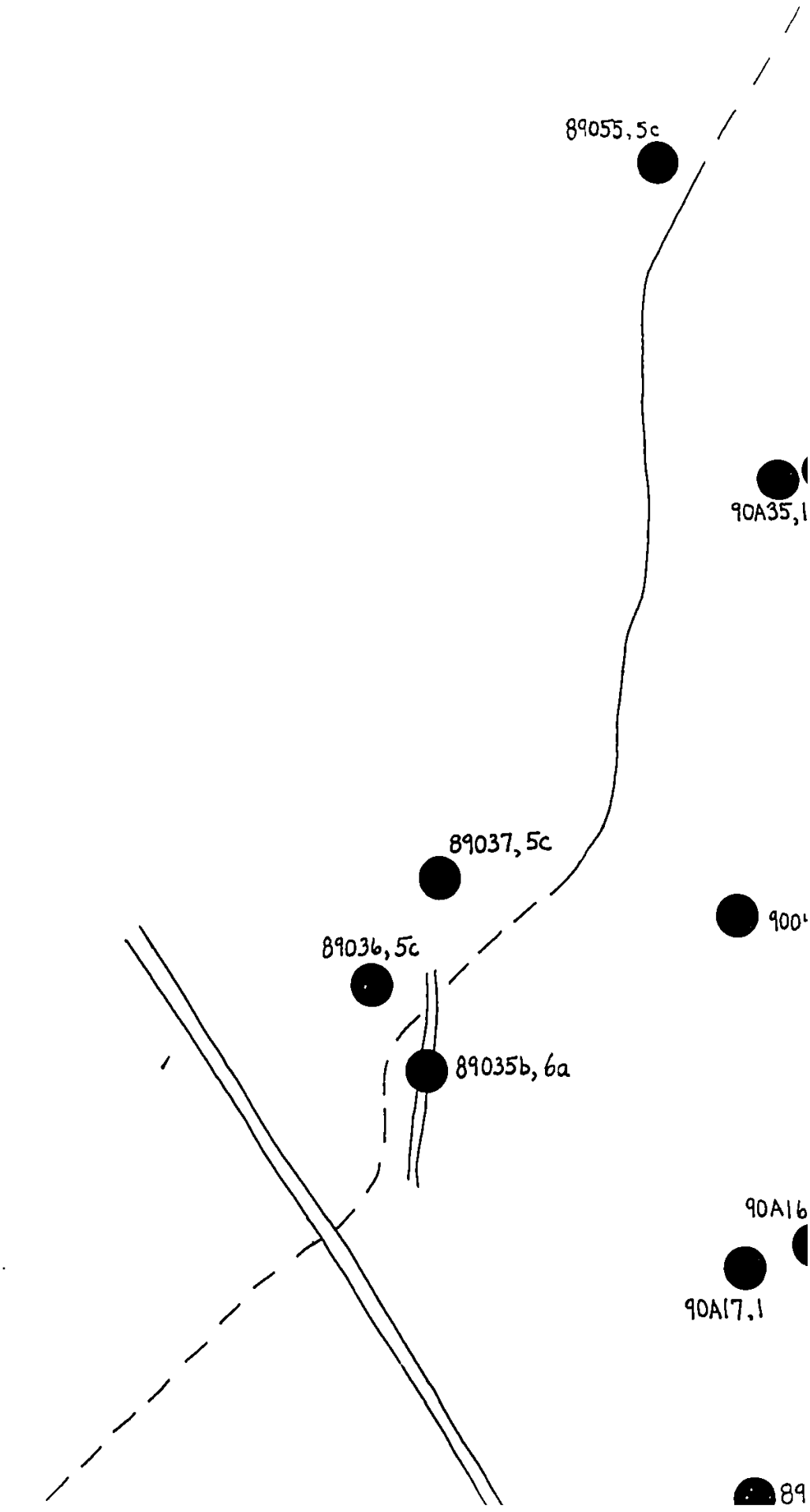
89055, 5c
90A35, 1
89037, 5c
900
89036, 5c
89035b, 6a
90A16
90A17, 1
89

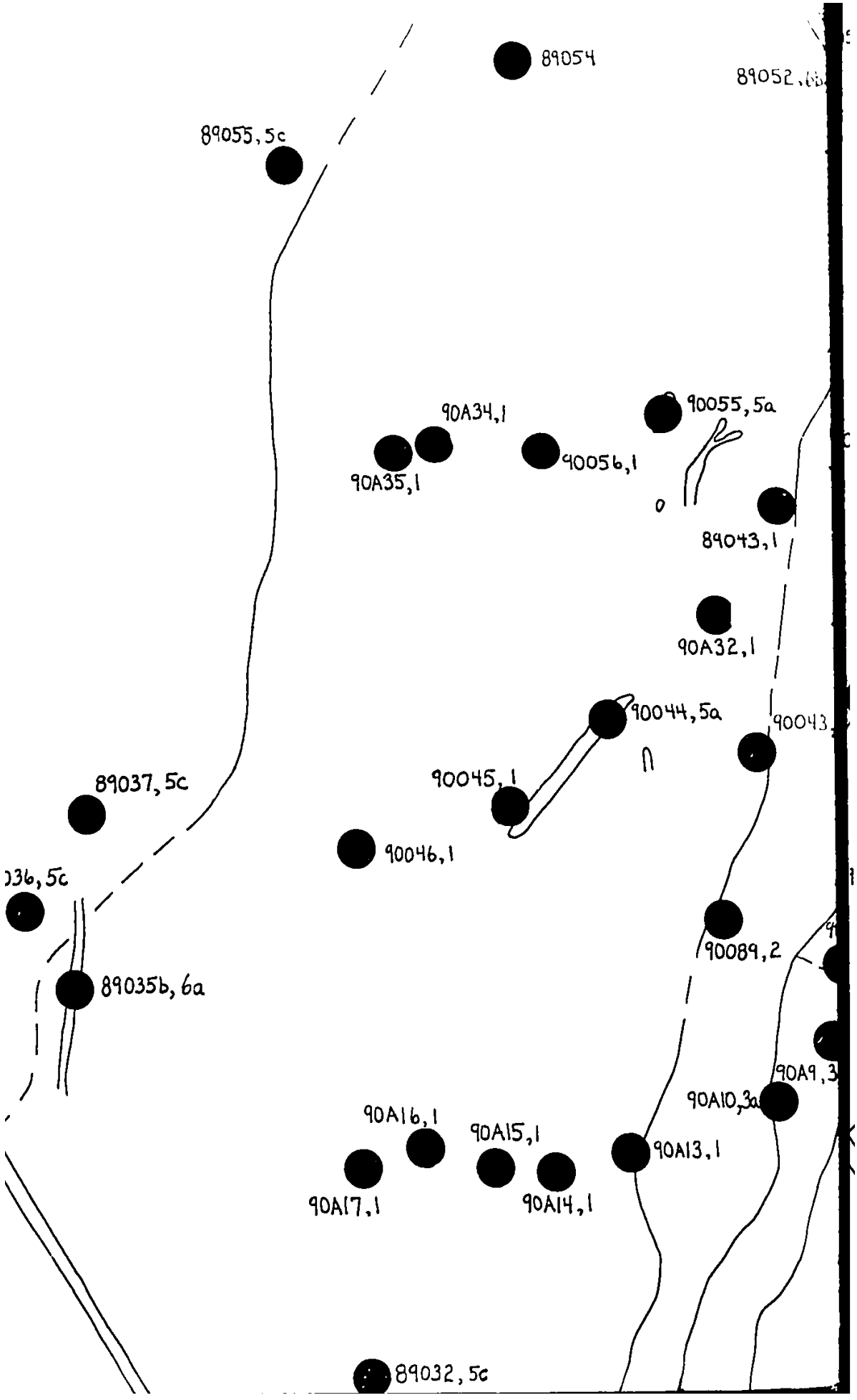
89054
89052,6
89055,5c
90A34,1
90055,5a
90A35,1
90056,1
89043,1
90A32,1
90044,5a
90043
90045,1
89037,5c
90046,1
036,5c
90089,2
89035b,6a
90A9,3
90A10,3a
90A16,1
90A15,1
90A13,1
90A17,1
90A14,1
89032,5c

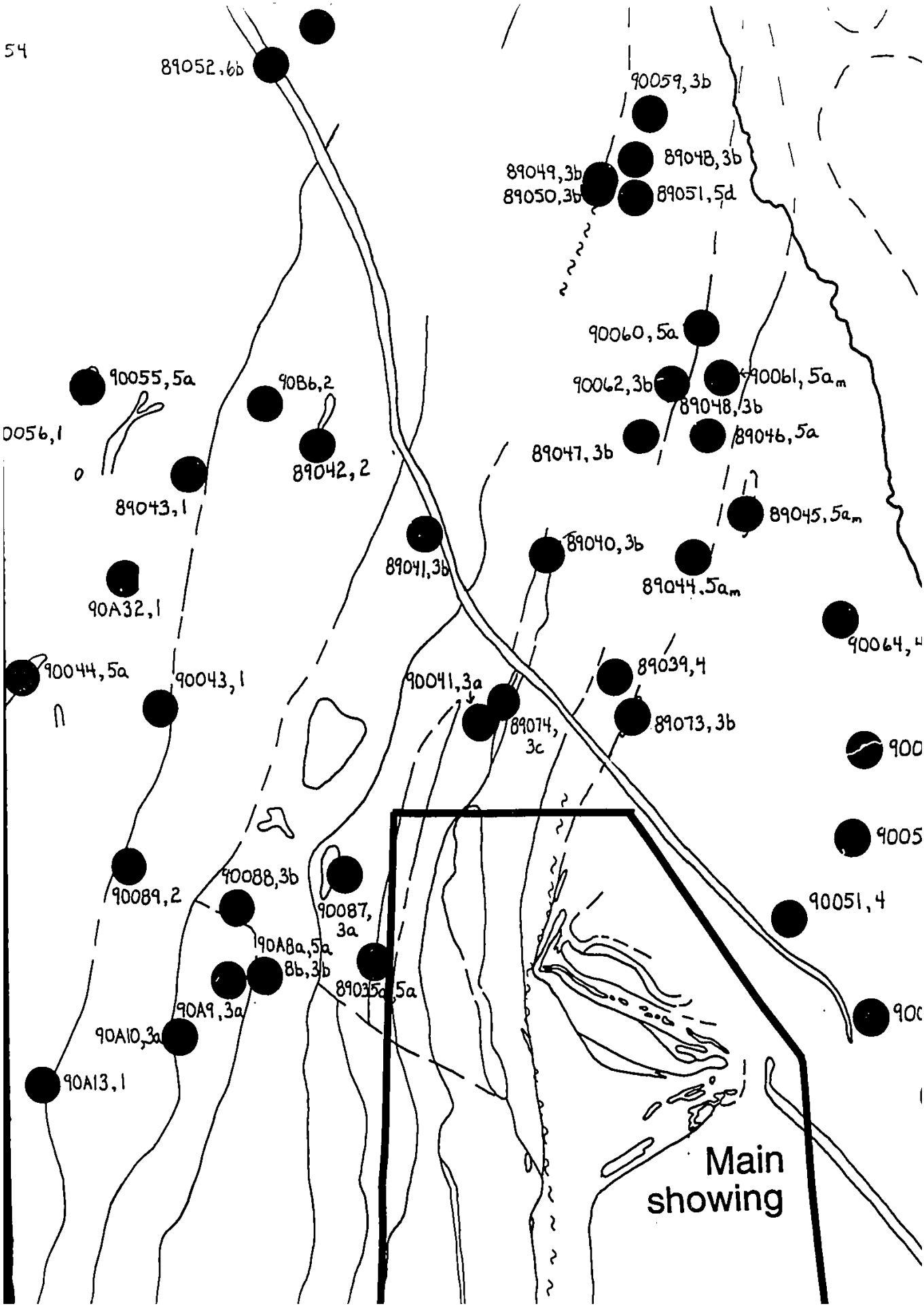
89052,6b
90059,3b
89048,3b
89049,3b
89050,3b
89051,5d
90060,5a
90062,3b
90061,5am
89048,3b
89047,3b
89046,5a
89045,5am
90055,5a
90056,1
90B6,2
89042,2
89043,1
89041,3b
89040,3b
89044,5am
90A32,1
90044,5a
90043,1
90041,3a
89039,4
89074,3c
89073,3b
90064,4
90089,2
90088,3b
90087,3a
90051,4
90A8a,5a
8b,3b
89035a,5a
90A9,3a
90A10,3a
90A13,1
Main showing

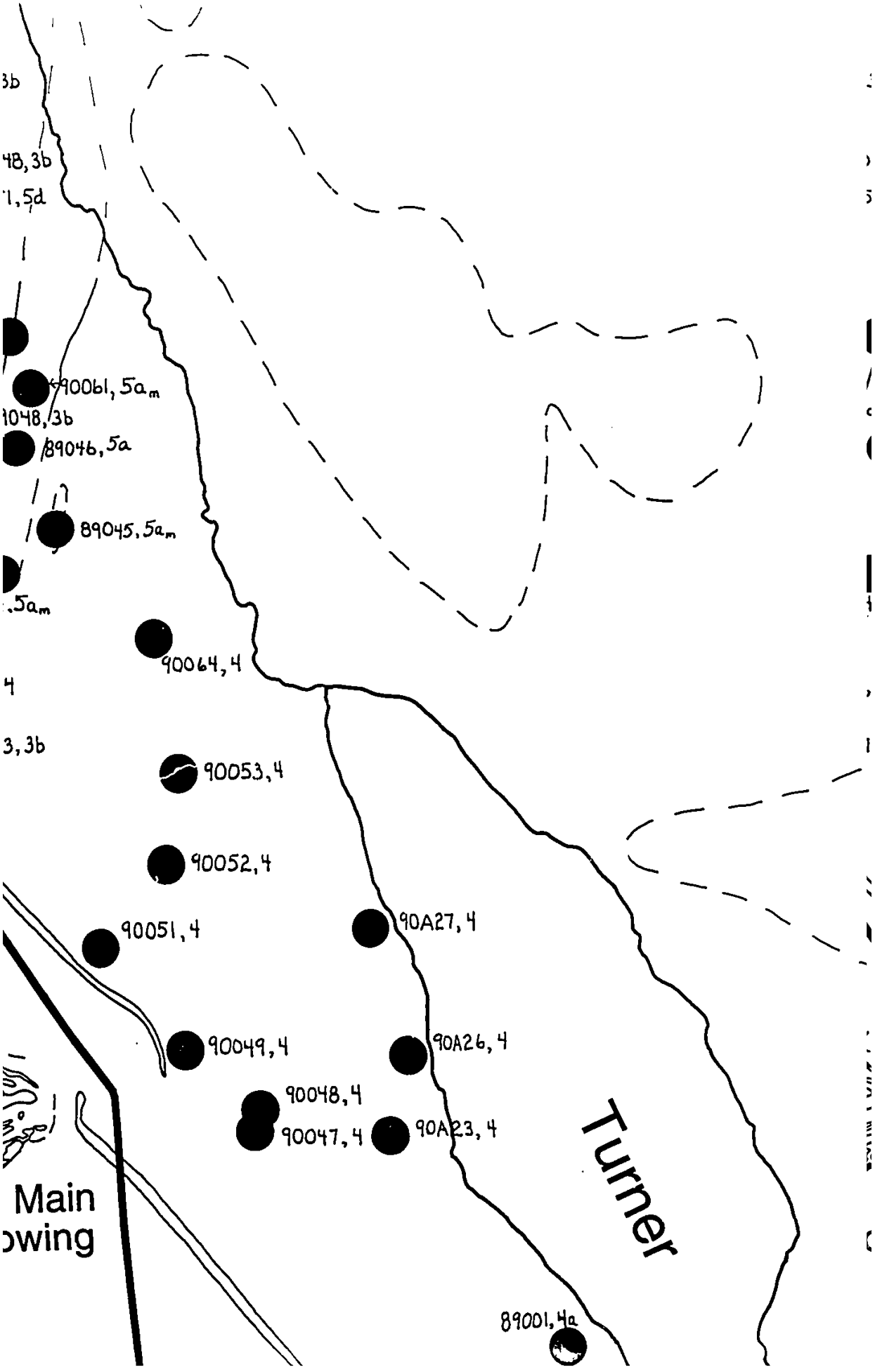
3b
48,3b
1,5d
90061, 5am
1048,3b
89046, 5a
89045, 5am
.5am
90064, 4
4
3,3b
90053, 4
90052, 4
90051, 4
90A27, 4
90049, 4
90A26, 4
90048, 4
90047, 4
90A23, 4
Main
owing
Turner
89001, 4a

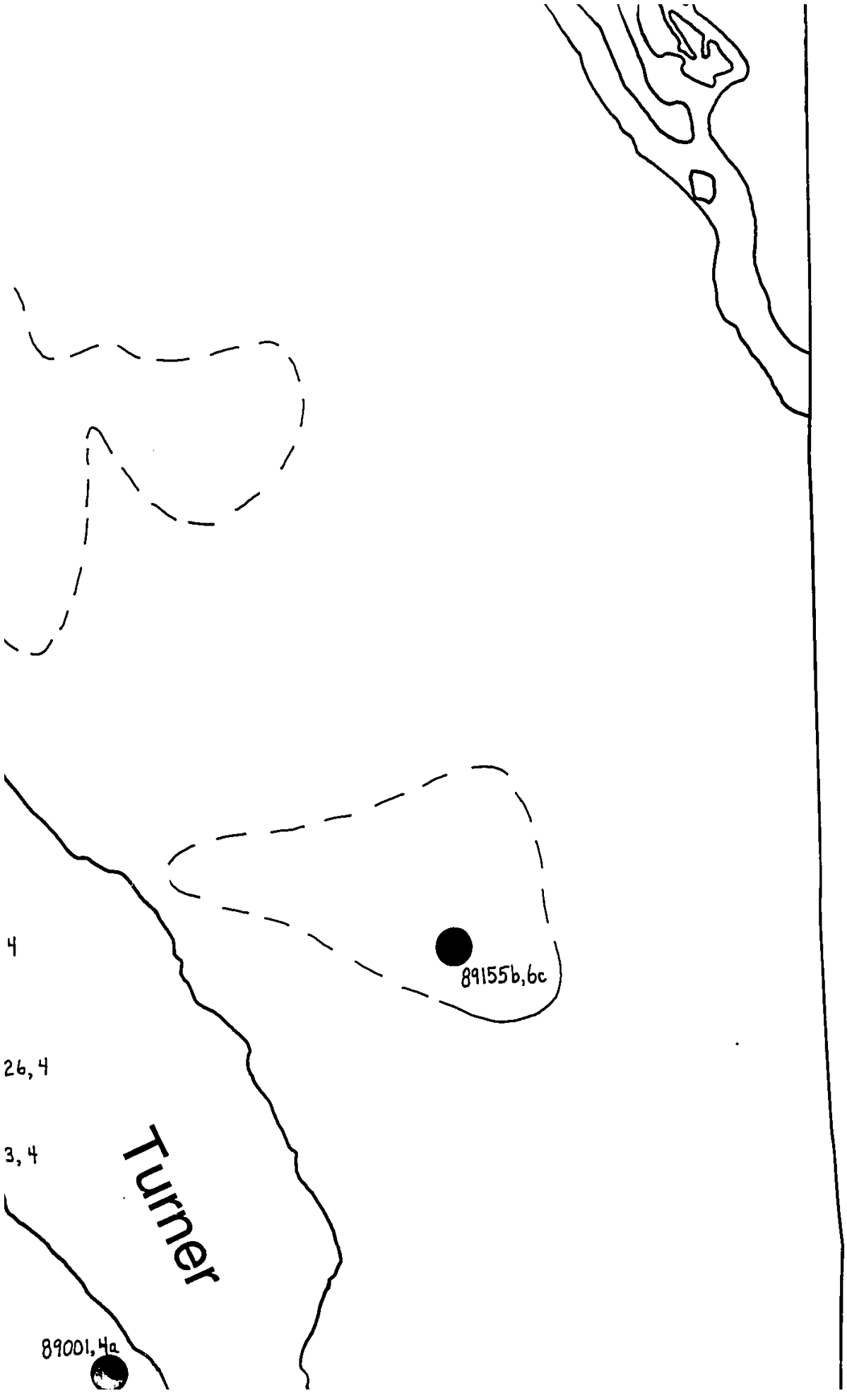
4
26, 4
3, 4
Turner
89155b, 6c
89001, 4a

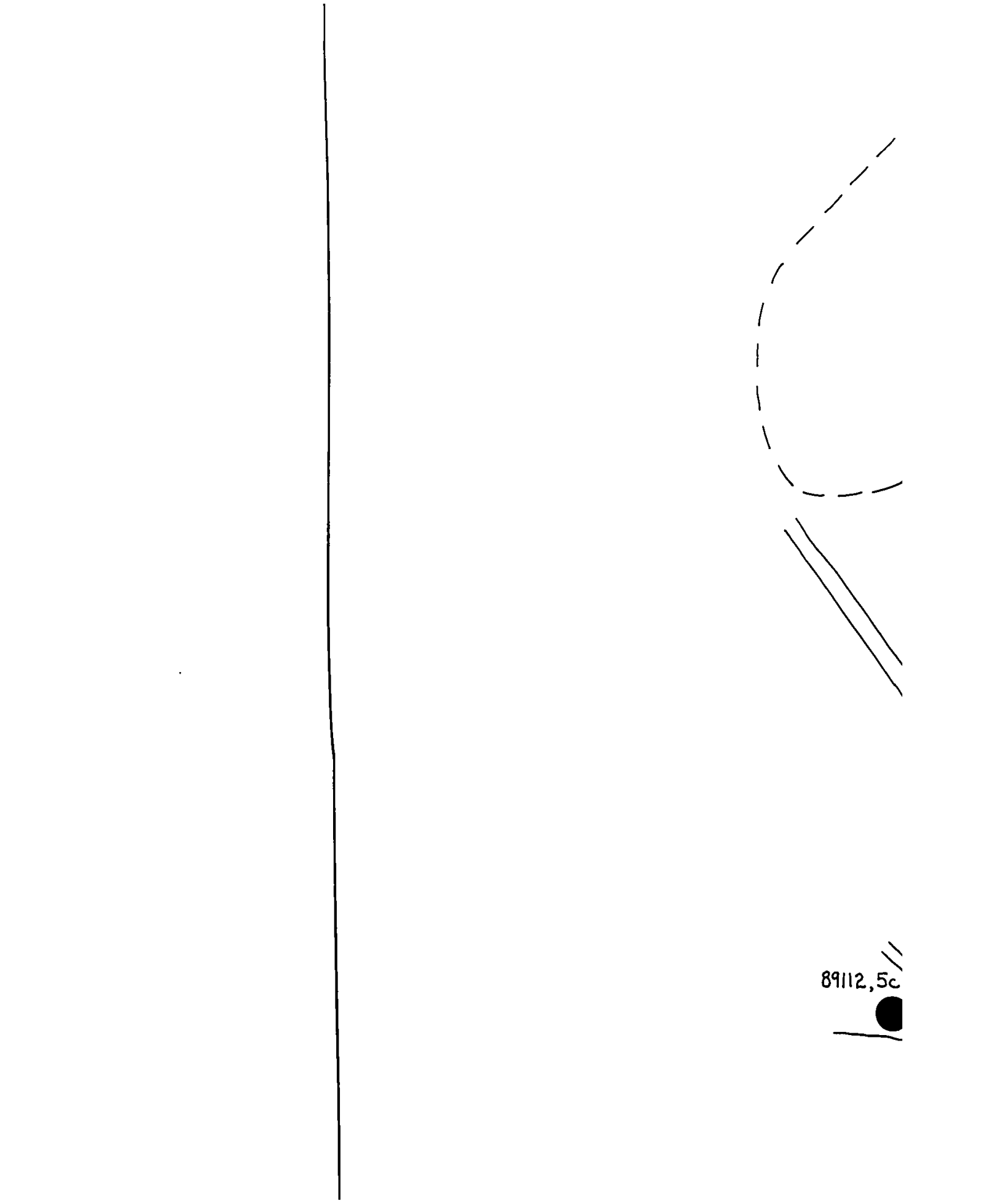
89112,5c

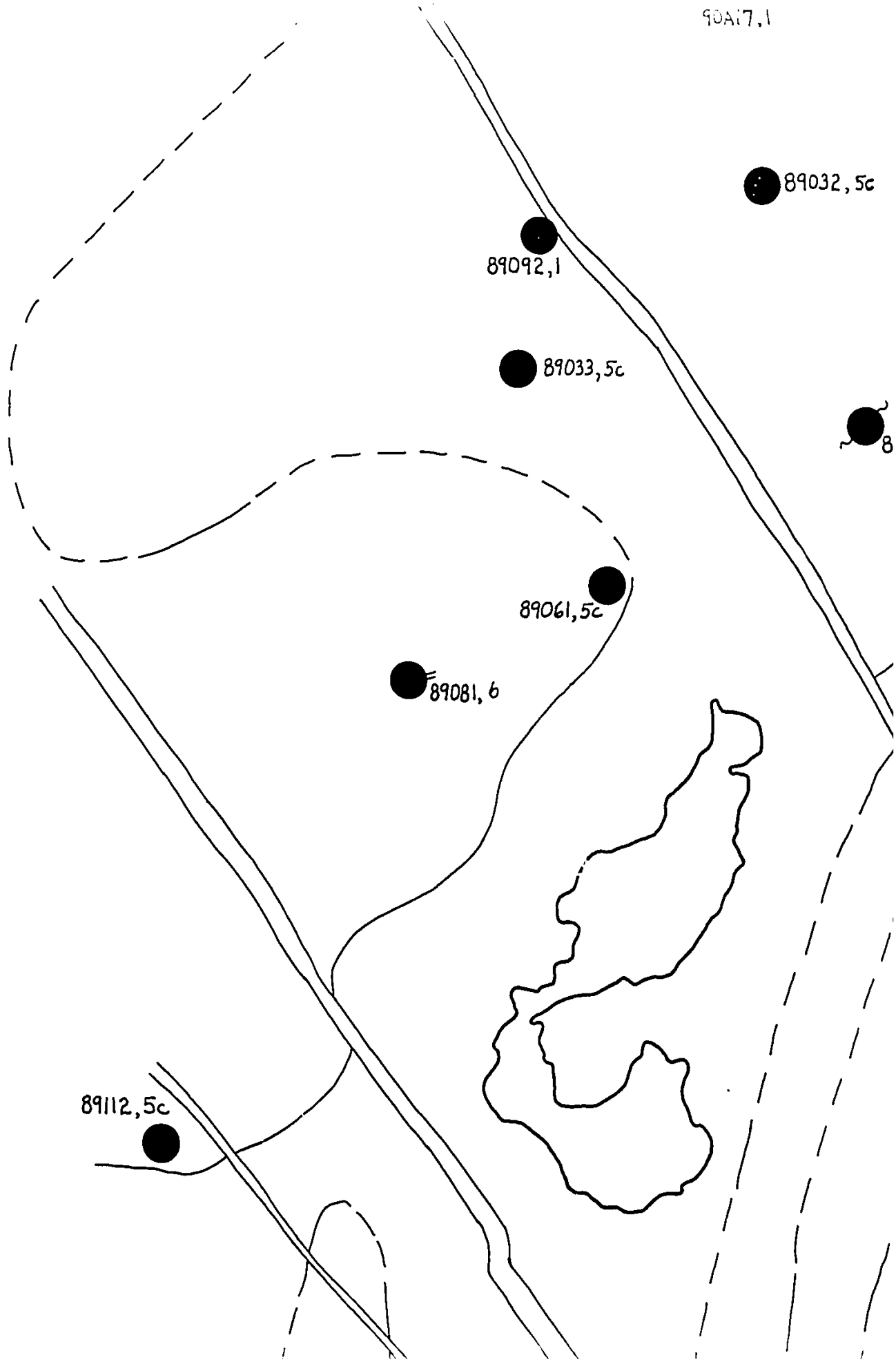
89032,5c
89092,1
89033,5c
8
89061,5c
89081,6
89112,5c

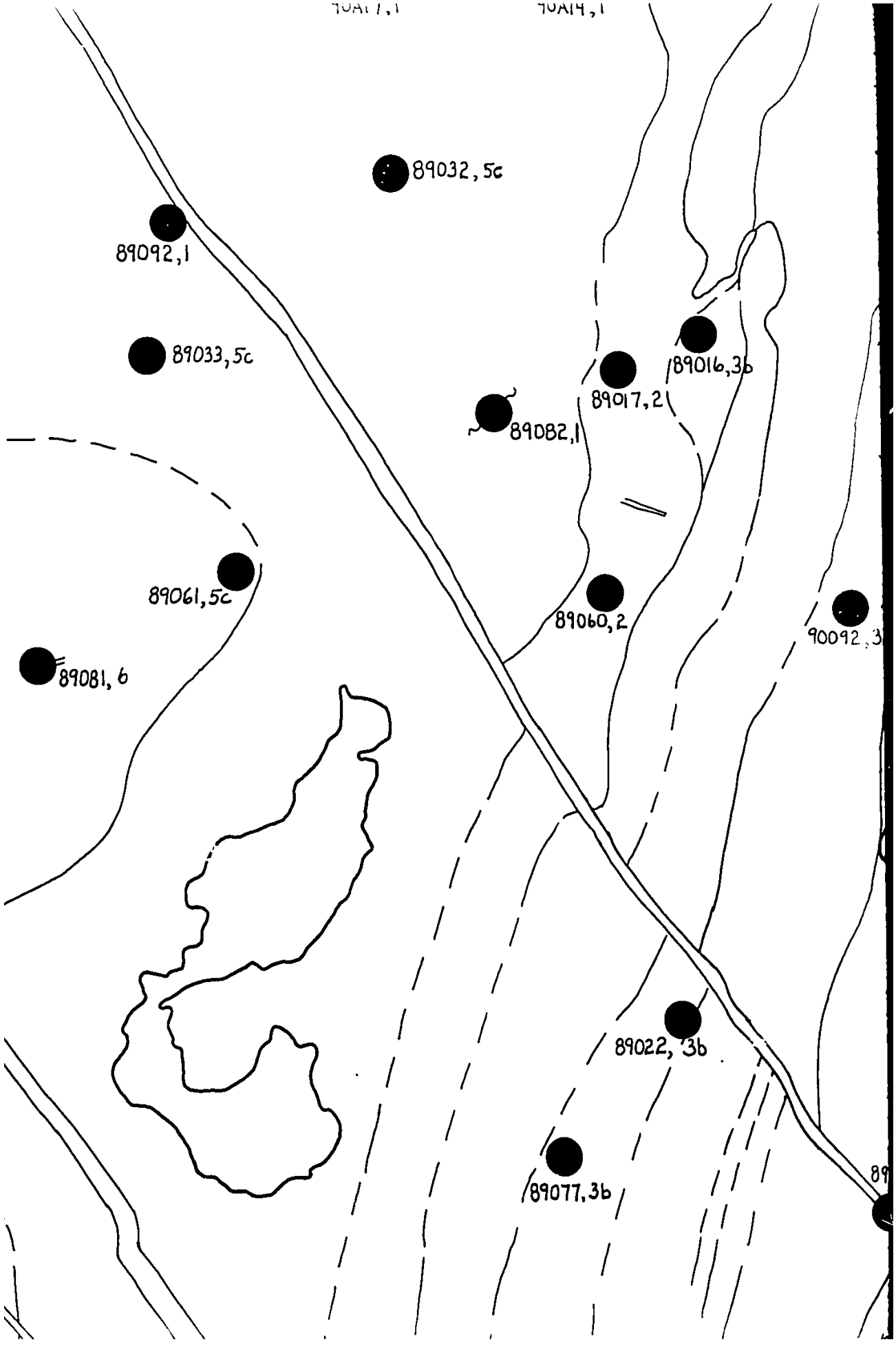
89032,5c
89092,1
89033,5c
89016,3b
89017,2
89082,1
89061,5c
89060,2
90092,3
89081,6
89022,3b
89077,3b

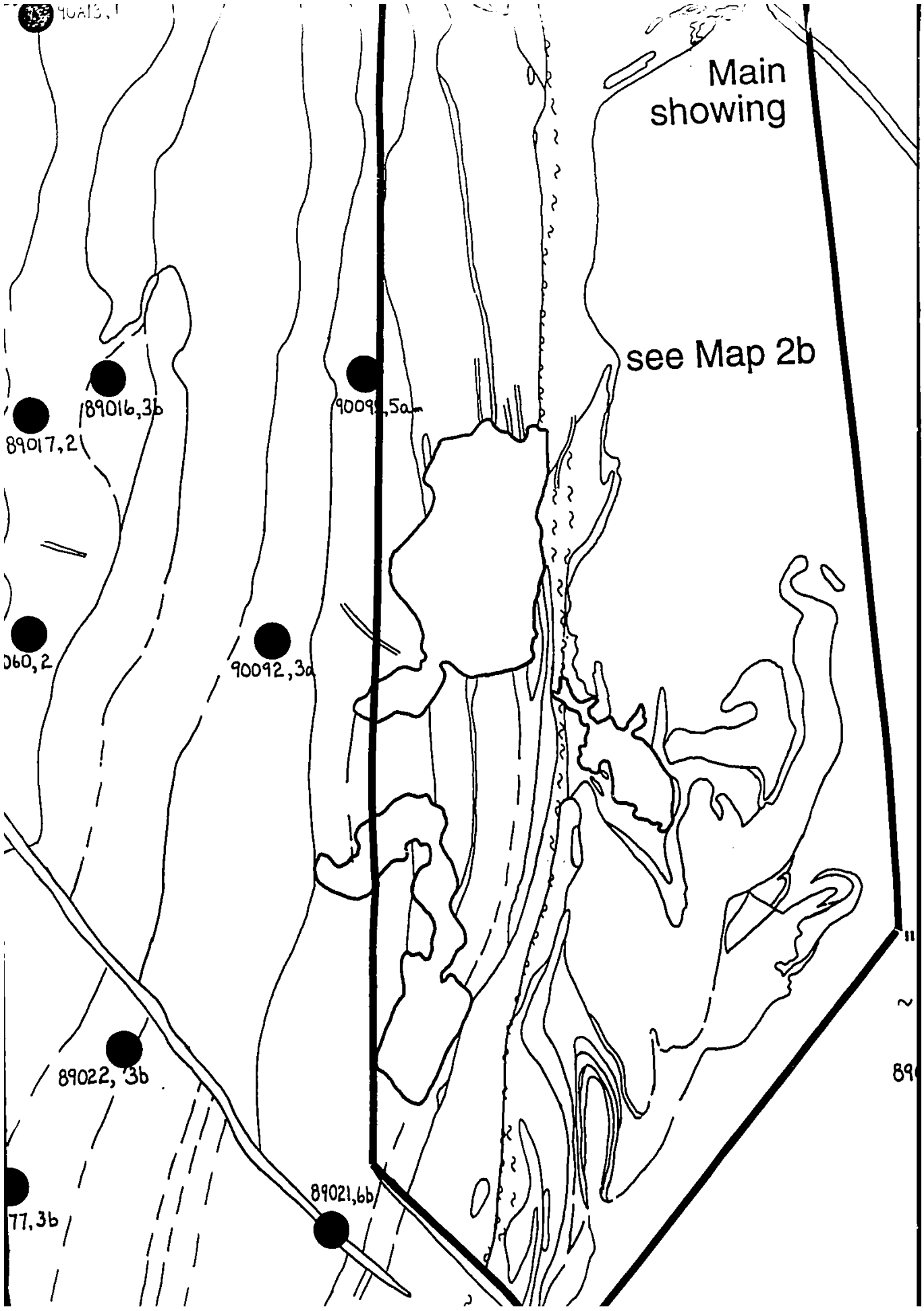
Main showing
see Map 2b
89016,3b
89017,2
90092,3a
89022,3b
89021,6b

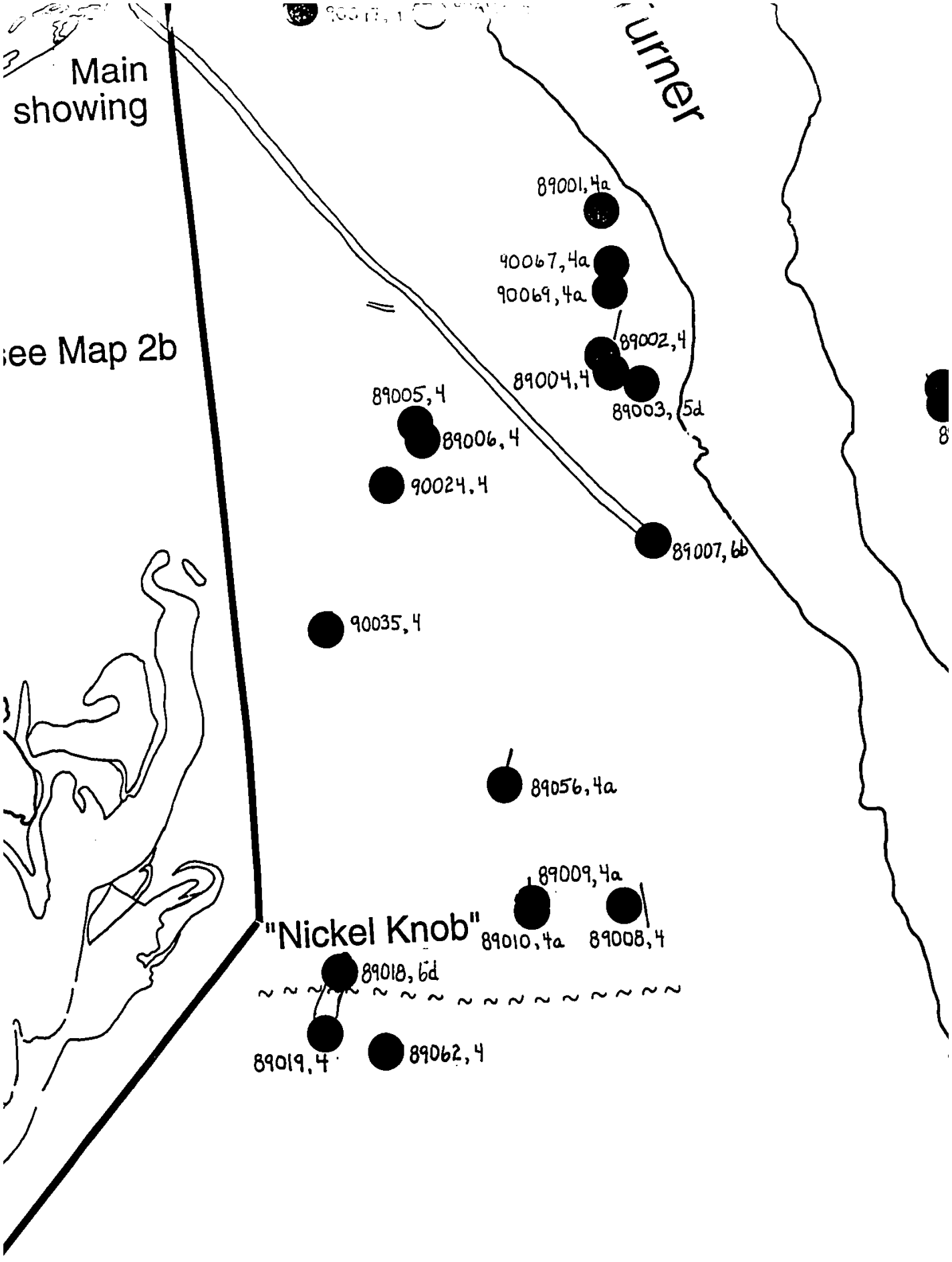
Main showing
urner
89001,4a
90067,4a
90069,4a
89002,4
89004,4
89003,5d
89005,4
89006,4
90024,4
89007,6b
90035,4
89056,4a
89009,4a
89010,4a
89008,4
"Nickel Knob"
89018,6d
89019,4
89062,4

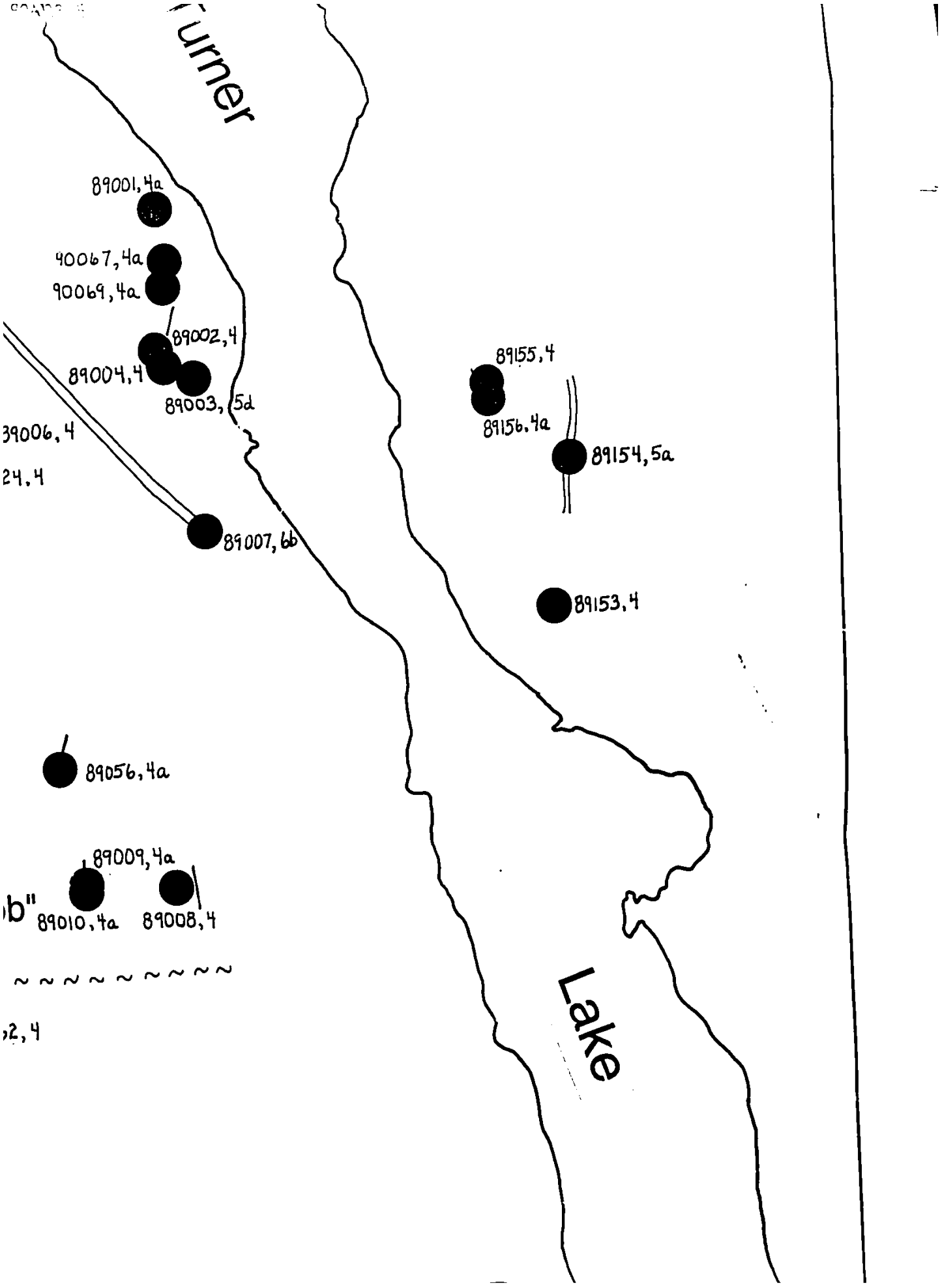
urner
89001,4a
90067,4a
90069,4a
89002,4
89004,4
89003,5d
39006,4
24,4
89007,6b
89155,4
89156,4a
89154,5a
89153,4
89056,4a
89009,4a
b"
89010,4a
89008,4
2,4
Lake

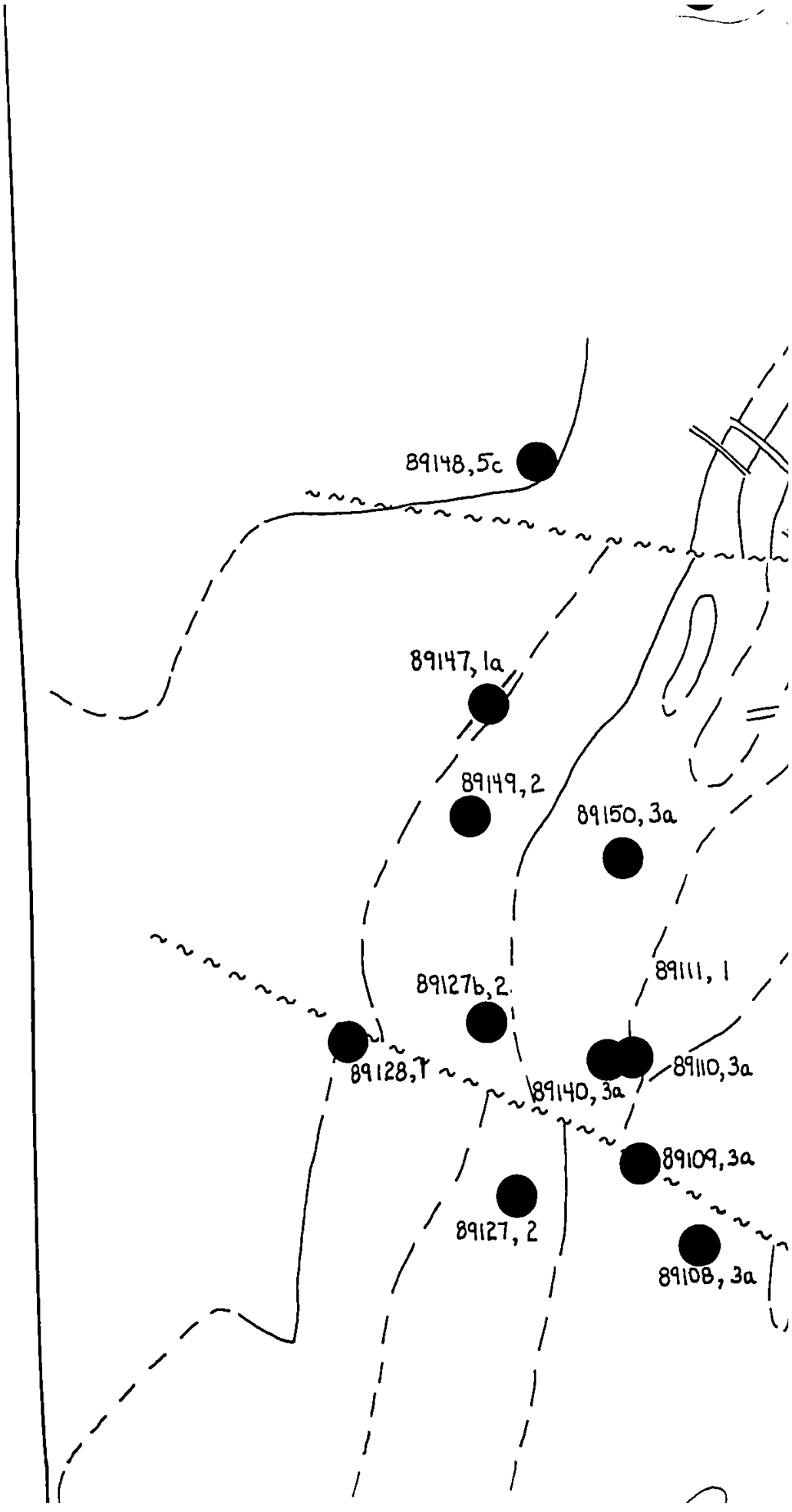
89148, 5c
89147, 1a
89149, 2
89150, 3a
89127b, 2
89111, 1
89128, 1
89140, 3a
89110, 3a
89109, 3a
89127, 2
89108, 3a

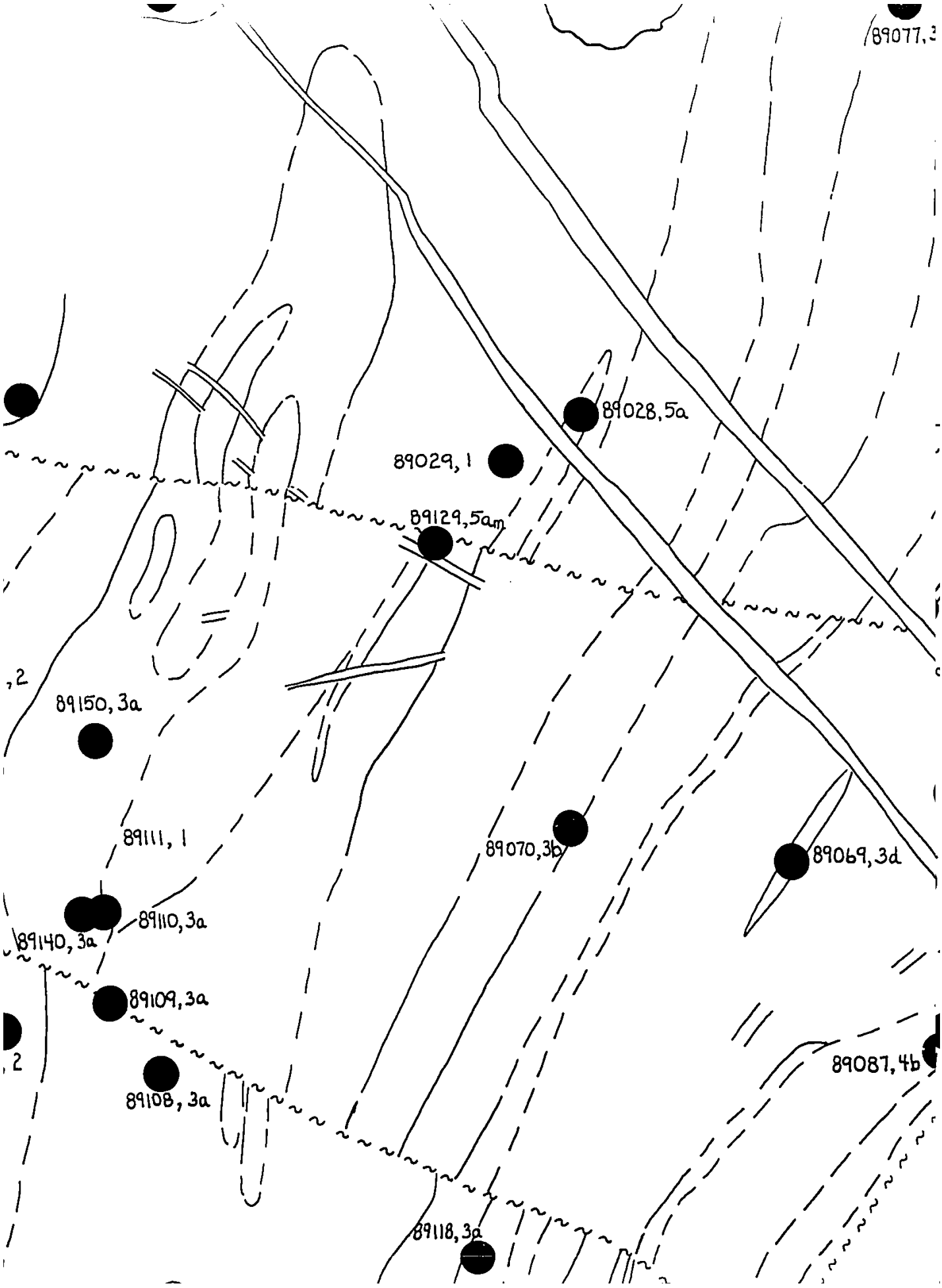
89077,3
89028,5a
89029,1
89129,5am
89150,3a
89111,1
89070,3b
89069,3d
89110,3a
89140,3a
89109,3a
89108,3a
89087,4b
89118,3a

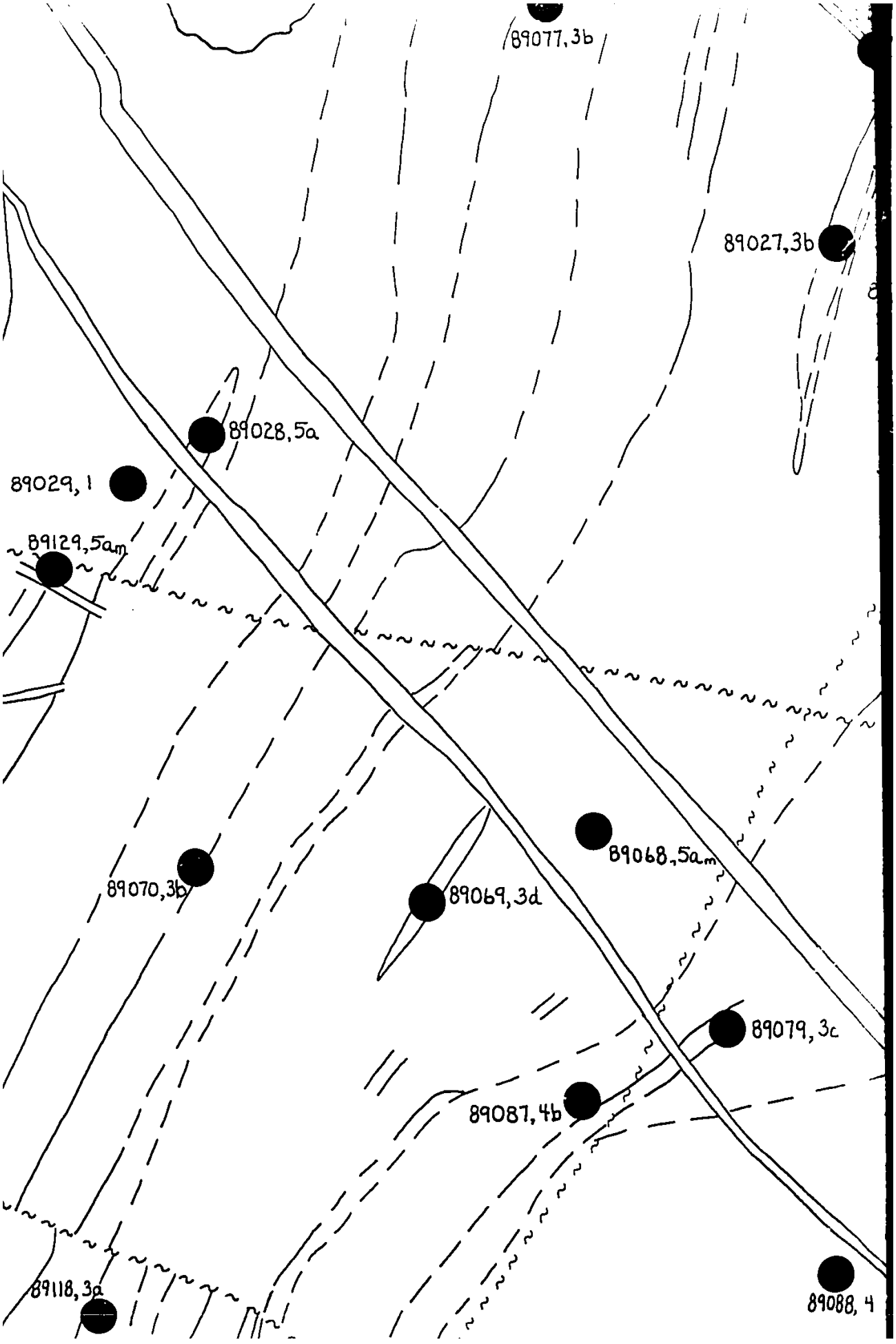
89077,3b
89027,3b
89028,5a
89029,1
89129,5am
89068,5am
89070,3b
89069,3d
89079,3c
89087,4b
89118,3a
89088,4

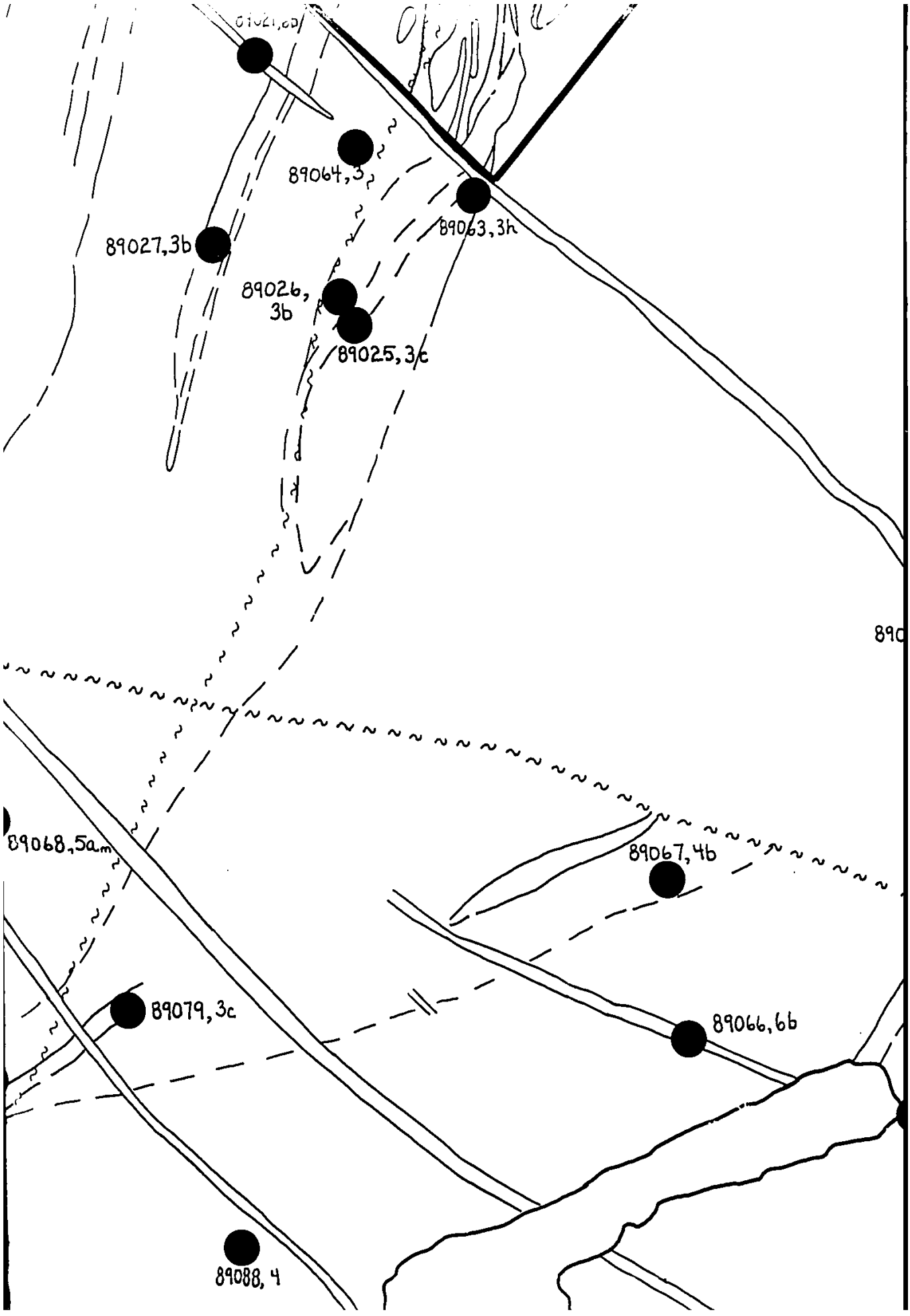
89064,3
89063,3h
89027,3b
89026,
3b
89025,3c
89068,5am
89067,4b
89079,3c
89066,6b
89088,4

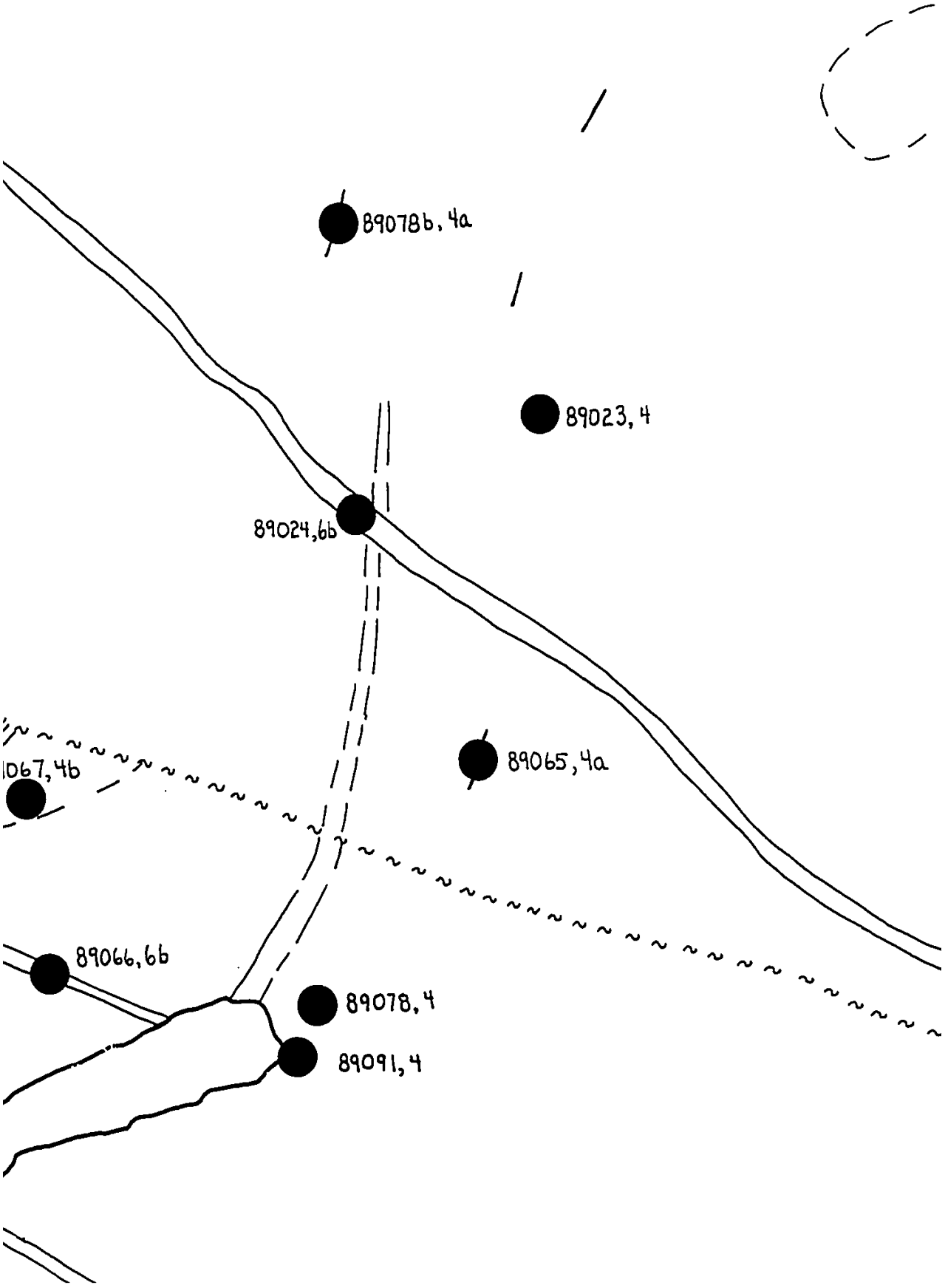
89078b, 4a
89023, 4
89024, 6b
89065, 4a
1067, 4b
89066, 6b
89078, 4
89091, 4

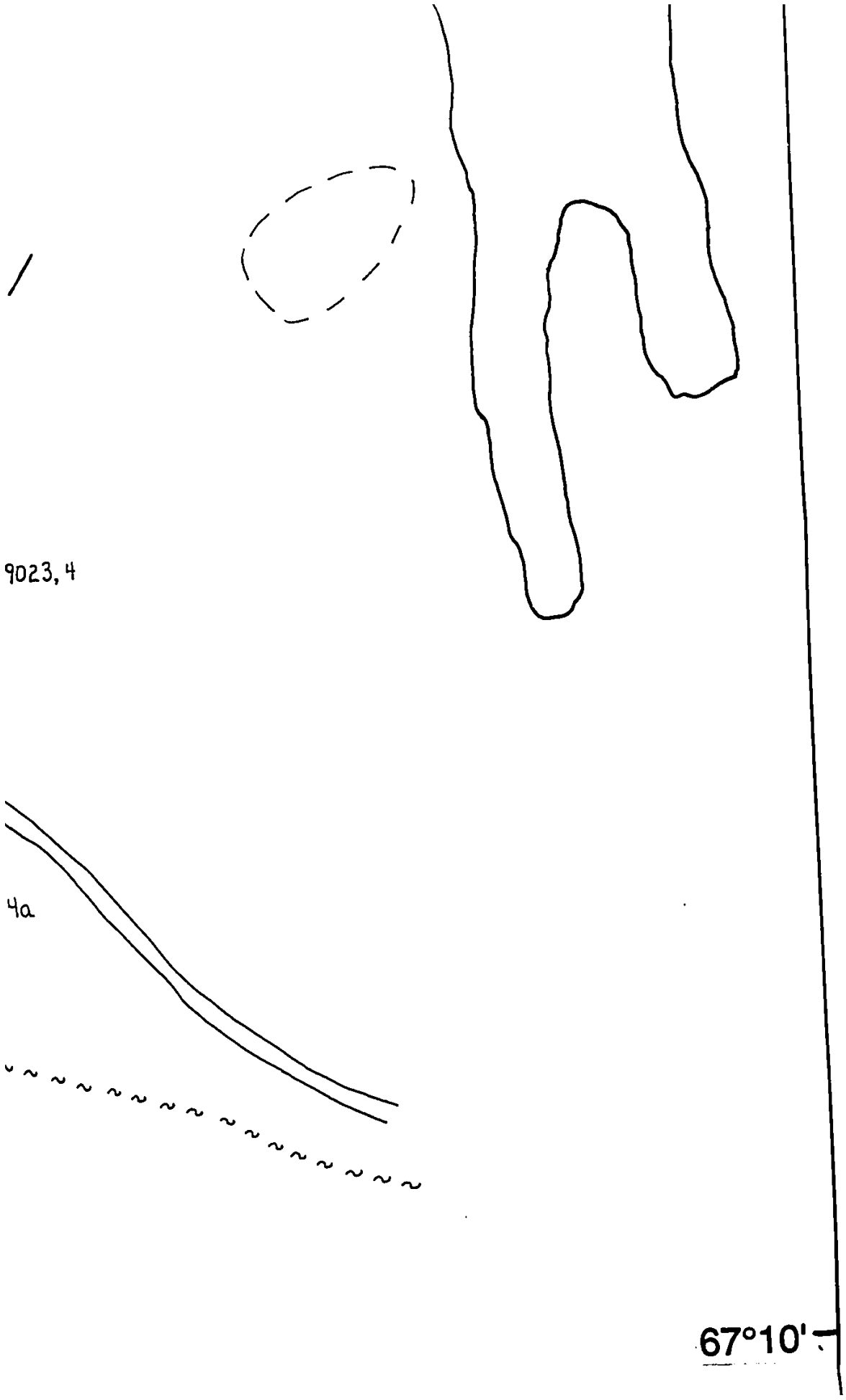
9023, 4
4a
67°10'

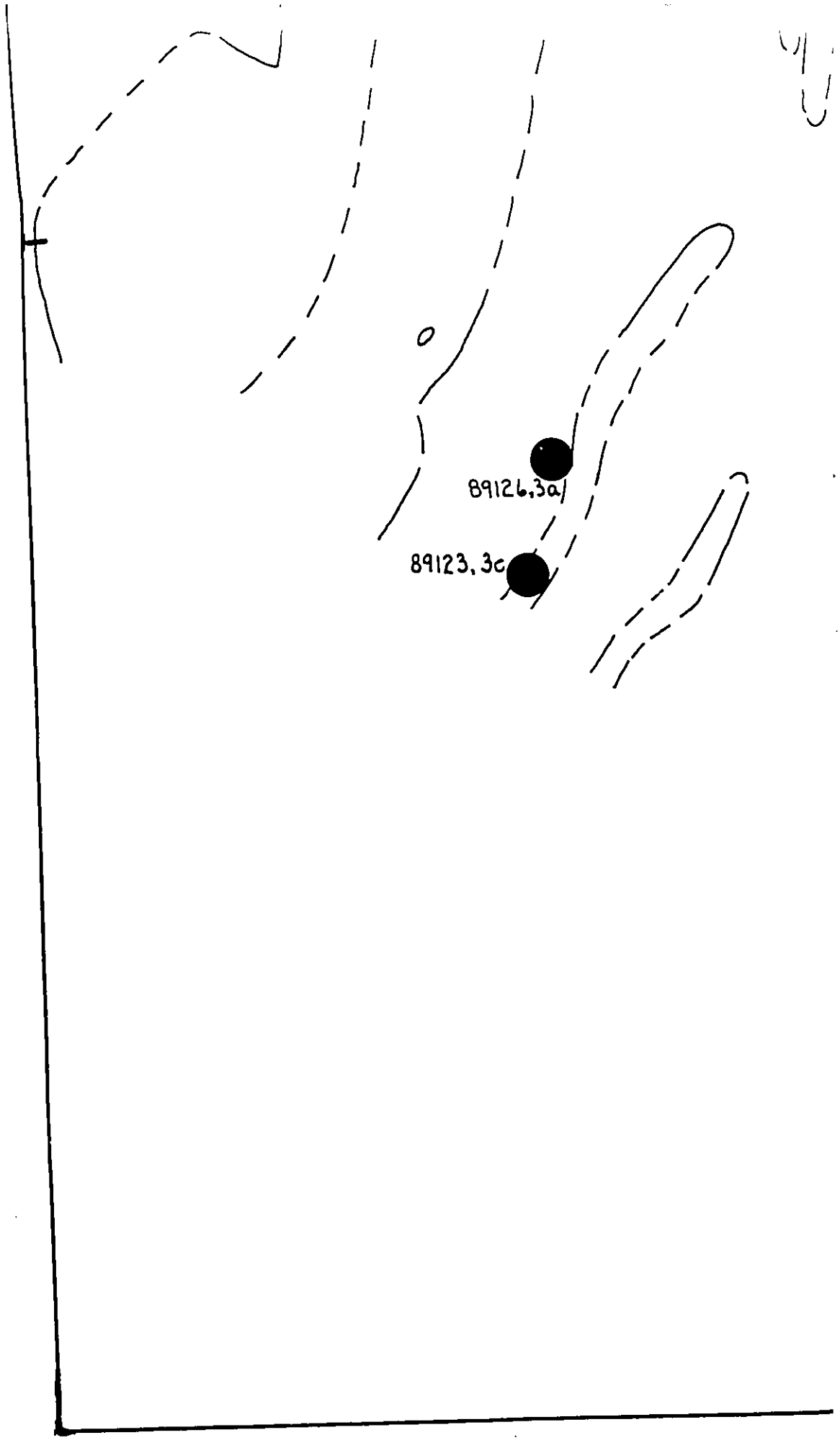
89126,3a
89123,3c

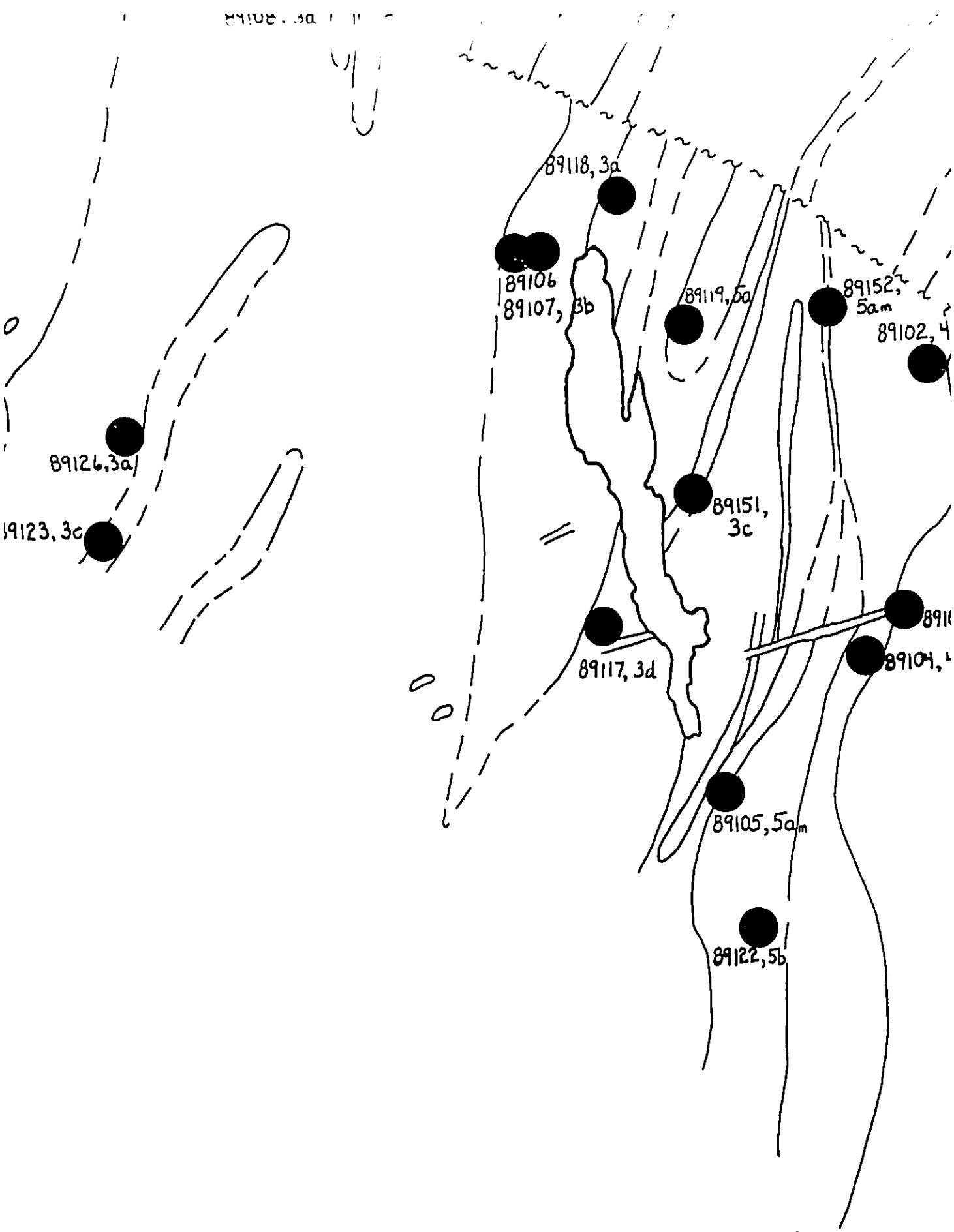
89118, 3a
89106
89107, 3b
89119, 5a
89152, 5am
89102, 4
89126, 3a
89123, 3c
89151, 3c
89117, 3d
89104,
89105, 5am
89122, 5b
109°00'

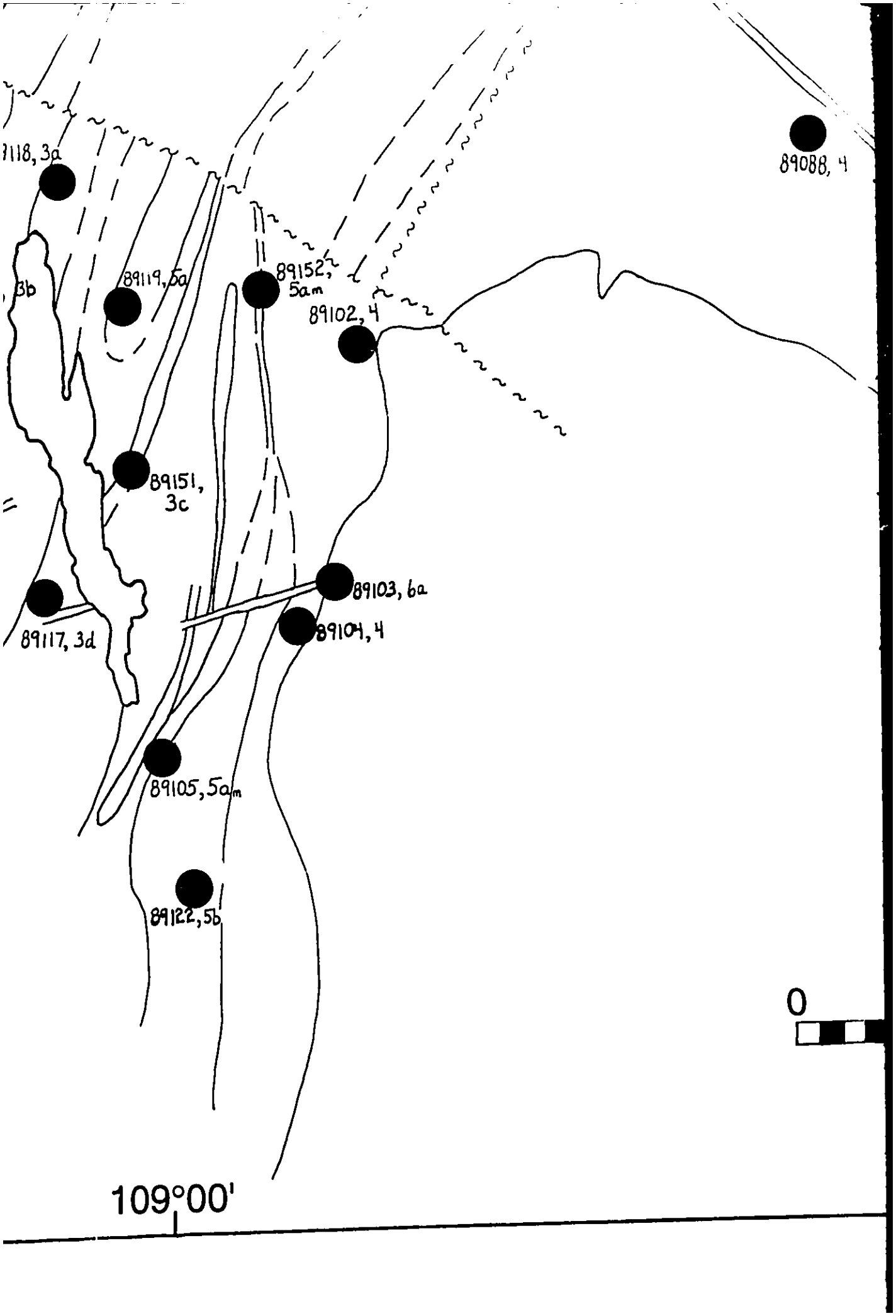
89088, 4
89118, 3a
89119, 6a
3b
89152, 5am
89102, 4
89151, 3c
89103, 6a
89104, 4
89117, 3d
89105, 5am
89122, 5b
0
109°00'

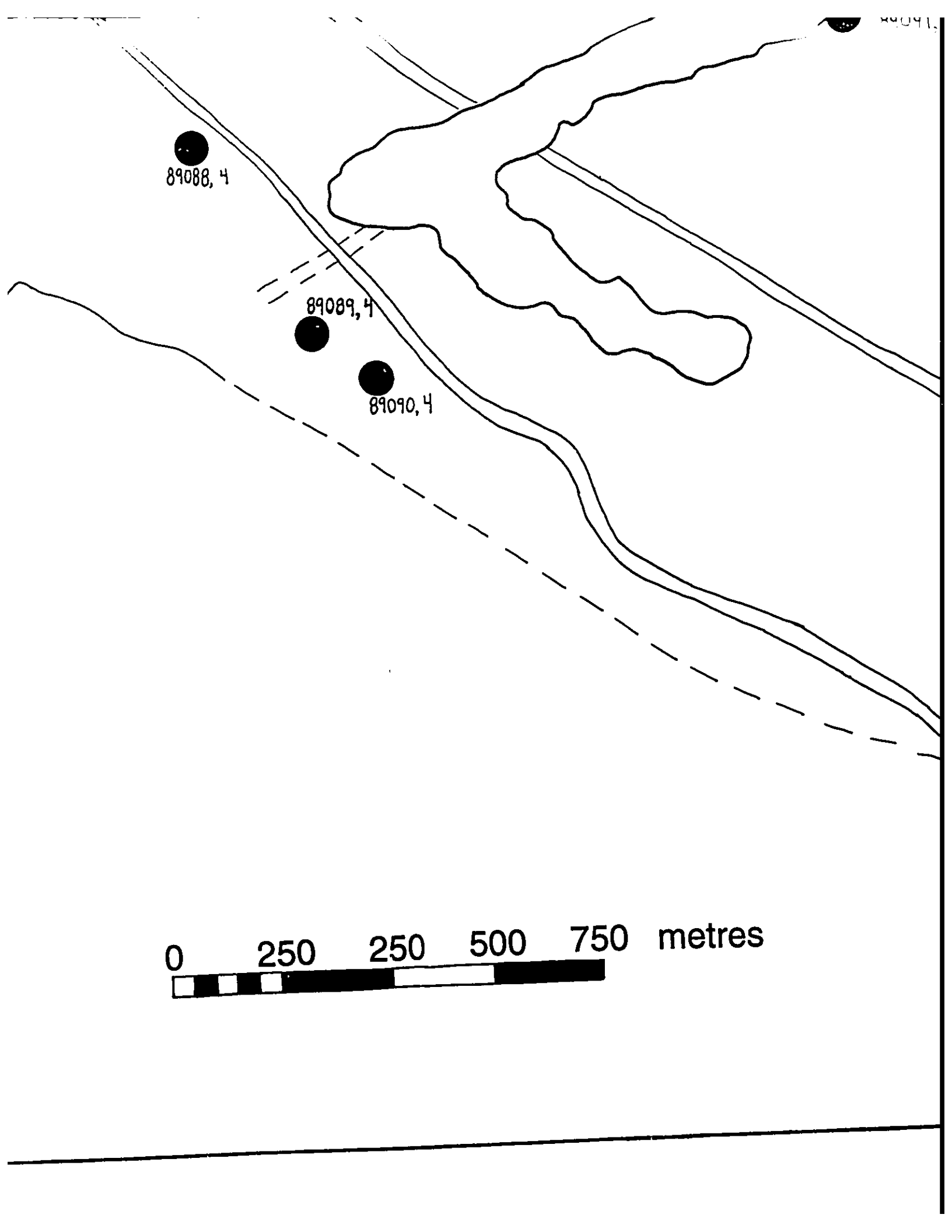
89088, 4
89089, 4
89090, 4
0
250
250
500
750
metres

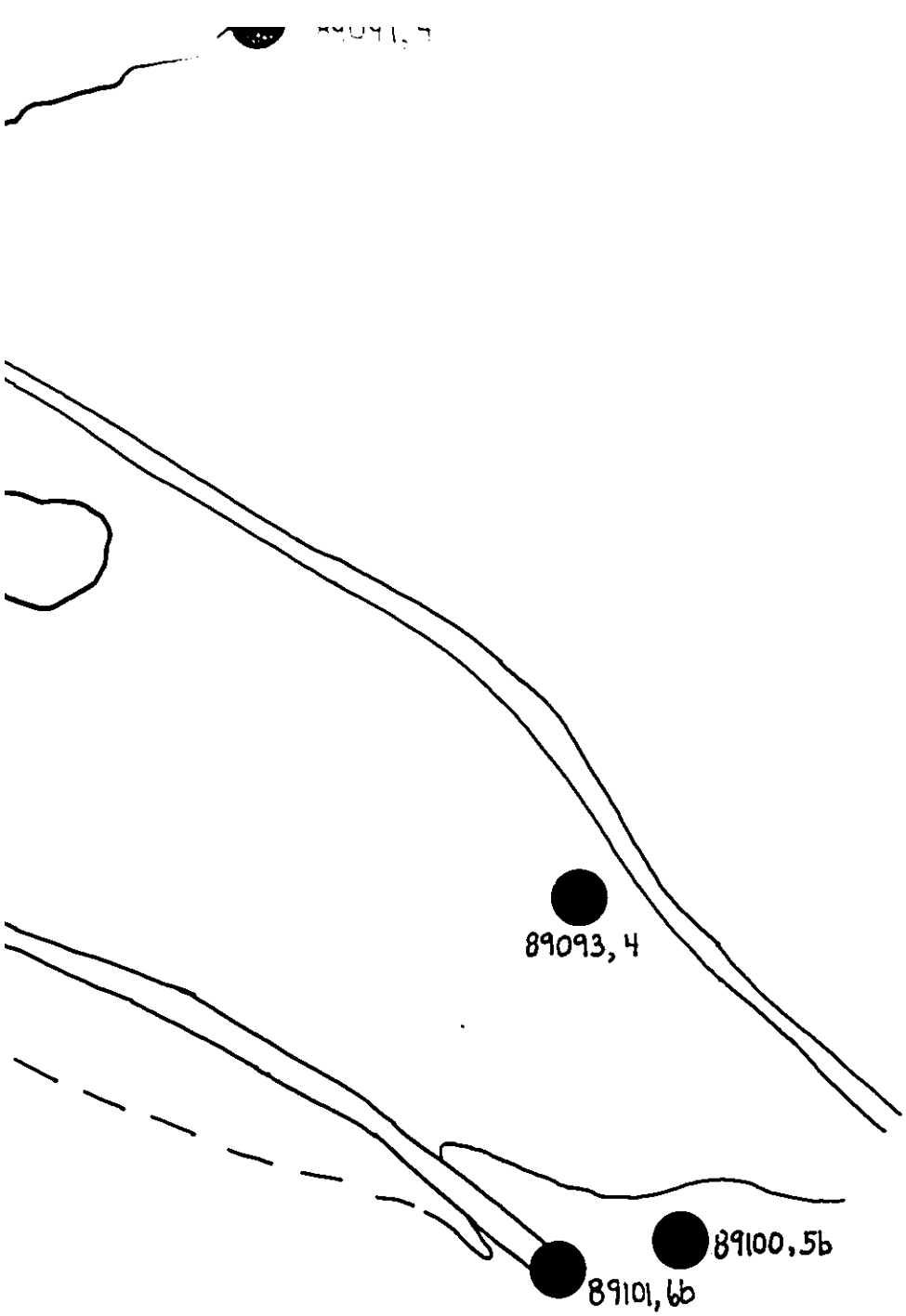

etres

108°55'

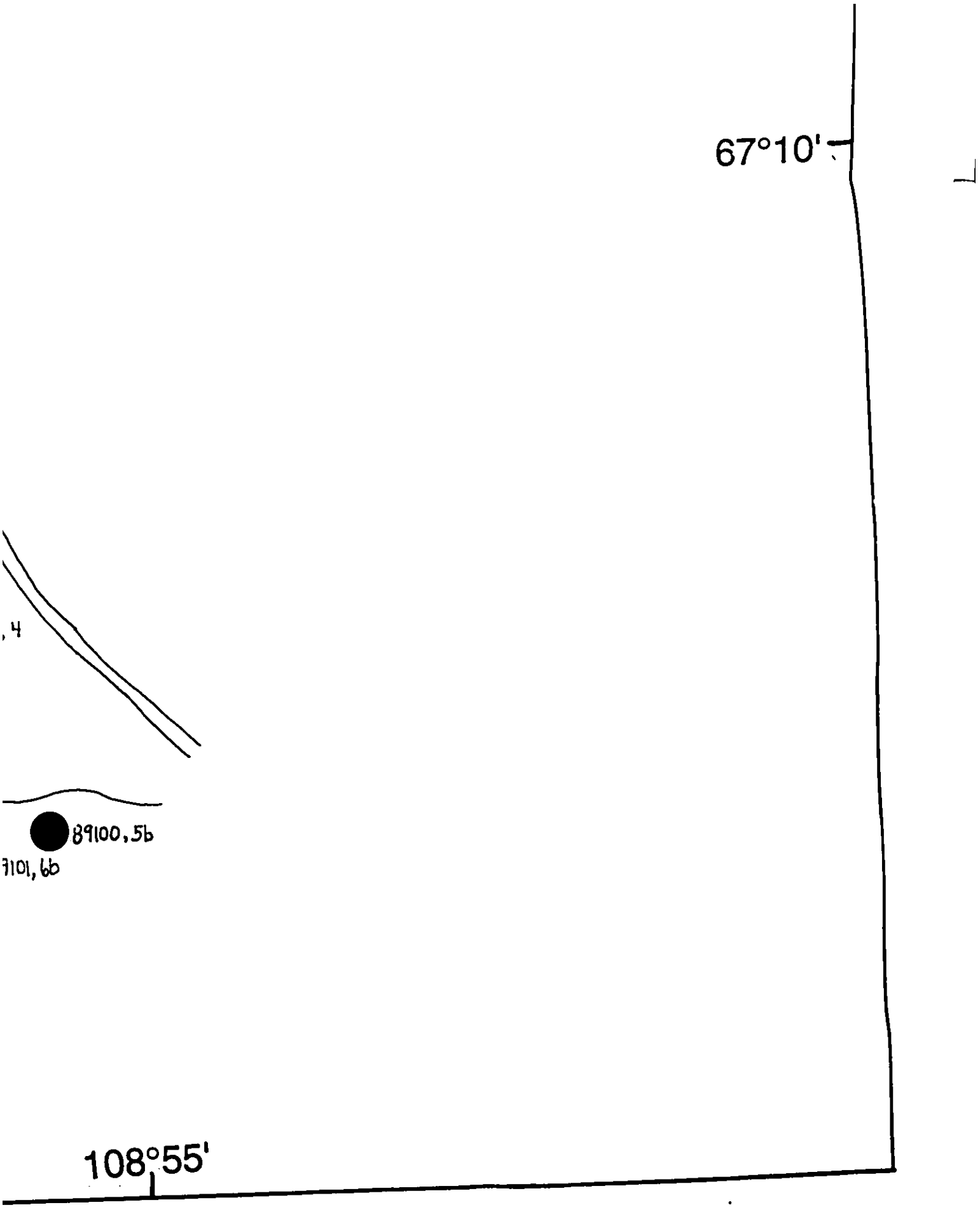
67°10'
89100,5b
7101,6b
108°55'